

**PROCESSING AND HYDROGEN  
DESORPTION PROPERTIES  
OF  
NOVEL LITHIUM BOROHYDRIDE (LiBH<sub>4</sub>)-BASED  
HYDROGEN STORAGE MATERIALS**

Kouassi Gaelle ANGUIE

A thesis submitted for the degree of Master of Philosophy  
In the Graduate School of Science and Engineering

School of Engineering and Materials

Queen Mary, University of London

2016

To my late Father:

**Anguie Jean-Marcel Elie ANGUIE**

## PREFACE

Name of candidate: Kouassi Gaelle ANGUIE

Degree for which entered: MPhil  
(MPhil / PhD / MD(Res))

Date of thesis submission: June 2016

Title of thesis: Processing and hydrogen desorption properties of novel lithium borohydride (LiBH<sub>4</sub>)-based hydrogen storage materials

Name of principal supervisor: Pr. Z. Xiao GUO (UCL)  
Pr. Mike Reece (QMUL)

Approximate word length of thesis: < 100,000

1. Please tick one box:

☒ I confirm that the above thesis does not exceed the word limit prescribed in the Regulations.

☐ I confirm that the above thesis exceeds the word limit and has received a suspension of Regulations with attached confirmation.

2. I confirm that the work presented in the thesis is my own and all references are cited accordingly (if the thesis includes any work conducted jointly please attach a statement of the part played by the candidate, certified by the supervisor). I accept that the College has the right to use plagiarism detection software to check the electronic version of the thesis.

Candidate signature: G. AKG

Date: 23/06/2016

## **ACKNOWLEDGEMENT**

I would like to thank, Pr. Z. Xiao GUO, my academic supervisor who gave me the precious opportunity to study in two of UK's best universities: QMUL and UCL. Knowing his multiple responsibilities, I am really grateful to his patient guidance and strong support throughout the four (4) years. Many thanks to Dr Kondo-Francois AGUEY-ZINSOU for his daily technical advice and support, his strong knowledge and experience benefit me and will continue during my research and development career after graduation.

I would also like to express my sincere gratitude to my sponsors: UK-SHEC and EPSRC, to the School of Engineering and Materials Science at Queen Mary University of London and the Department of Chemistry at University College London where I had very helpful support from either academic or non-academic staff. Some names include: Pr. Mike Reece, John Caufield, Jonathon Hills, Martin Vickers, Victoria Wells, Andrew Humphrey... and many other people such as my colleagues (Shahrouz Nayeboossadri, Elnaz Ajami, Negar Amini or Yiwen Wang) that were very supportive towards me.

Then, I would like to greet my family, especially, my parents for their unconditional support and certainly at last but not least my beloved children Yohann-Ebony and Ayana for giving me the strength to continue and persevere despite the countless difficulties. I dedicate this thesis to my late dad, Mr. Anguie ANGUIE who passed away 5 years ago and never saw the end of it. I hope he is proud of my achievement from where he is.

## ABSTRACT

The primary aim of this project was the development of an inorganic Lithium borohydride ( $\text{LiBH}_4$ )-based material for effective use in hydrogen storage. The objective was to find a material which would desorb a minimum of 5 wt.%  $\text{H}_2$  under mild conditions. To do so,  $\text{LiBH}_4$  has been investigated and the possibility to destabilise it so that it could release a maximum of its hydrogen content without losing boron, which is a requirement for reversible hydrogen storage. Why  $\text{LiBH}_4$ ? Lithium borohydride has one of the greatest hydrogen content (18.5 wt.%) among hydride materials. Nevertheless, the compound is very stable, hence the desorption temperature is too high for practical considerations. Hopefully, some interesting results have been reported by previous studies and opened the way for possible improvement mainly in terms of lowering the desorption temperature. The impact of chemical additions such as transition metal chlorides and ammonium chloride ( $\text{NH}_4\text{Cl}$ ) to its thermostability has been assessed.  $\text{NH}_4\text{Cl}$  has a number of advantages compared to transition metal chlorides since it contains hydrogen, is less heavy and is a precursor to ammonia borane ( $\text{NH}_3\text{BH}_3$ ), another promising material for solid-state hydrogen storage applications. Mass spectrometry and thermal analysis of mixtures of  $\text{LiBH}_4$  and  $\text{NH}_4\text{Cl}$  indicate that contrary to the results obtained with the addition of transition metal chlorides where a significant amount of  $\text{B}_2\text{H}_6$  escapes from the mixture upon heating, sole release of hydrogen may be obtained. Moreover, the onset hydrogen desorption may be as low as  $65^\circ\text{C}$  for ( $\text{LiBH}_4 + \text{NH}_4\text{Cl}$ ) mixtures, similarly to the one observed for ( $2\text{LiBH}_4 + \text{ZnCl}_2$ ) mixtures. In the case of  $\text{NH}_4\text{Cl}$ -added mixtures, the proportion of  $\text{H}_2$  released is much higher, around 2 wt.% at this temperature. Also, sole release of up to 6 wt. % hydrogen may be achieved at temperatures as low as  $150^\circ\text{C}$ , which is a huge improvement compared to pure  $\text{LiBH}_4$ , transition metal chlorides added mixtures and even  $\text{NH}_3\text{BH}_3$ . This whole study shows the clear potential for using B-N-H compounds as high-capacity hydrogen storage applications.

## **LIST OF CHAPTERS AND SUB-CHAPTERS**

COVER.....	0
PREFACE.....	0
ACKNOWLEDGEMENT S.....	1
ABSTRACT.....	2
LIST OF CONTENTS.....	3
LIST OF CHAPTERS AND SUB-CHAPTERS.....	3
LIST OF FIGURE CAPTIONS.....	8
LIST OF TABLES.....	19
LIST OF EQUATIONS.....	22
CHAPTER 1    General introduction .....	29
CHAPTER 2    Overview of hydrogen storage.....	39
2.1    Hydrogen storage issues and methods.....	40
2.1.1    Hydrogen Storage Challenges for on-board applications.....	40
2.1.2    Hydrogen storage methods.....	42
2.1.2.1    Gaseous hydrogen.....	42
2.1.2.2    Liquid hydrogen.....	46
2.1.2.3    Hydrogen in solids.....	49
2.2    Research on complex hydrides.....	65
2.2.1    Alانات.....	65

2.2.1.1	Sodium alanate, $\text{NaAlH}_4$ .....	66
2.2.1.2	Lithium alanate, $\text{LiAlH}_4$ .....	66
2.2.1.3	Other alanates: $\text{Mg}(\text{AlH}_4)_2$ and $\text{KAlH}_4$ .....	67
2.2.2	Amides-based complex systems.....	68
2.2.2.1	Lithium amide, $\text{LiNH}_2$ .....	68
2.2.2.2	Association with metal hydrides.....	69
2.2.2.3	Association with complex hydrides: alanates and borohydrides.....	71
2.2.3	Borohydrides.....	72
2.2.3.1	Background information.....	72
2.2.3.2	Preparation and synthesis.....	75
2.2.3.3	Properties and applications of borohydride compounds.....	87
2.2.3.4	Borohydrides for hydrogen storage applications.....	89
2.2.4	Amine-borane systems.....	98
2.2.4.1	Ammonia borane (AB).....	98
2.2.4.2	Diammoniate of diborane (DADB).....	102
2.2.4.3	Borazole (also known as borazine, BZ).....	103
2.2.4.4	Other volatile B-N-H compounds.....	105
CHAPTER 3	Experimental methods.....	107
3.1	Sample preparation.....	108
3.1.1	Materials.....	108
3.1.2	Pre-treatment of powder mixtures.....	109
3.1.3	Mechanical milling.....	110

3.2	Sample characterisation.....	112
3.2.1	TG-DTA-MS.....	112
3.2.2	X-Ray Diffraction.....	120
3.2.3	SEM-EDS.....	122
3.2.4	FT-IR.....	125
CHAPTER 4	Experimental results: thermal and structural study.....	129
4.1	Decomposition of pristine lithium borohydride, $\text{LiBH}_4$ .....	130
4.2.1	Dehydrogenation properties using TG-DTA-MS.....	130
4.2.2	Structural and morphological properties using XRD, FT-IR and SEM/EDS.....	133
4.2	Decomposition of $\text{LiBH}_4$ associated with fourth-period metal chlorides.....	136
4.2.1	Experimental design.....	137
4.2.2	Effect of milling from structural and morphological properties using XRD, FT-IR and SEM/EDS results.....	139
4.2.3	Dehydrogenation properties using TG-DTA-MS .....	148
4.2.3.1	2:1 molar ratio of $\text{LiBH}_4$ to $\text{ZnCl}_2$ .....	150
4.2.3.2	3:1 molar ratio of $\text{LiBH}_4$ to $\text{TiCl}_3$ .....	152
4.2.3.3	2:1 molar ratio of $\text{LiBH}_4$ to $\text{NiCl}_2$ .....	153
4.2.3.4	3:1 molar ratio of $\text{LiBH}_4$ to $\text{CrCl}_3$ .....	154
4.3	Hydrogen desorption from complex mixtures ( $\text{LiBH}_4 + x\text{NH}_4\text{Cl}$ ) and ( $\text{NH}_3\text{BH}_3 + y\text{NH}_4\text{Cl}$ ).....	157
4.3.1	Experimental design.....	158



4.3.2	Effect of milling and heat treatment from structural and morphological properties using XRD, FT-IR and SEM/EDS.....	160
4.3.3	Dehydrogenation properties using TG-DTA-MS.....	162
4.3.3.1	1:1 molar ratio of $\text{LiBH}_4$ to $\text{NH}_4\text{Cl}$ .....	166
4.3.3.2	1:2 molar ratio of $\text{LiBH}_4$ to $\text{NH}_4\text{Cl}$ .....	170
4.3.3.3	1:3 molar ratio of $\text{LiBH}_4$ to $\text{NH}_4\text{Cl}$ .....	174
4.3.3.4	1:1 and 1:2 molar ratios of $\text{NH}_3\text{BH}_3$ to $\text{NH}_4\text{Cl}$ .....	178
4.3.3.5	Carbon additions to $\text{LiBH}_4\text{-NH}_4\text{Cl}$ and $\text{NH}_3\text{BH}_3\text{-NH}_4\text{Cl}$ compositions.....	182
CHAPTER 5	General discussion.....	192
5.1	Dehydrogenation from as-received lithium borohydride $\text{LiBH}_4$ .....	194
5.2	Dehydrogenation from $(n\text{LiBH}_4 + \text{MCl}_n)$ .....	202
5.2.1	Summary of results.....	203
5.2.2	Comparative discussion .....	207
5.2.2.1	<i>For <math>\text{ZnCl}_2</math> addition</i> .....	207
5.2.2.2	<i>For <math>\text{TiCl}_3</math> addition</i> .....	209
5.2.2.3	<i>For <math>\text{NiCl}_2</math> addition</i> .....	212
5.2.2.4	<i>For <math>\text{CrCl}_3</math> addition</i> .....	215
5.2.2.5	Summary of comparative discussions for chloride additions to $\text{LiBH}_4$ .....	217

5.3	Dehydrogenation from ( $\text{LiBH}_4 + x\text{NH}_4\text{Cl}$ ) and from ( $\text{NH}_3\text{BH}_3 + y\text{NH}_4\text{Cl}$ ).....	220
5.3.1	Summary of results.....	220
5.3.1.1	$\text{LiBH}_4$ -based systems.....	222
5.3.1.2	$\text{NH}_3\text{BH}_3$ -based systems.....	227
5.3.1.3	Carbon additions.....	228
5.3.2	Comparative discussion.....	231
5.3.2.1	For $\text{NH}_4\text{Cl}$ addition to $\text{LiBH}_4$ .....	231
5.3.2.2	For $\text{NH}_4\text{Cl}$ addition to $\text{NH}_3\text{BH}_3$ .....	238
5.3.2.3	Summary of comparative discussions for $\text{NH}_4\text{Cl}$ addition to $\text{LiBH}_4$ and $\text{NH}_3\text{BH}_3$ .....	241
CHAPTER 6	Conclusions.....	243
CHAPTER 7	Future work.....	248
APPENDICES.....		250
Appendix 1	Patent application.....	251
Appendix 2	Poster.....	266
REFERENCES.....		267

## LIST OF FIGURE CAPTIONS

### Chapter 1: General Introduction

<b>Figure 1.1</b> World energy consumption by fuel type 1990-2035, 1 Btu= 1055.056 J, taken from <i>World Energy Outlook 2010</i> (the Energy Information Administration, [Web 1]).....	30
<b>Figure 1.2</b> Hydrogen, primary energy sources, energy converters and applications. Courtesy of European Commission special report on <i>Hydrogen energy and Fuel Cells</i> ([Web 2]).....	31
<b>Figure 1.3</b> Relative Proportion of Sources of Hydrogen in 2000 and 2007 ([Web 3]).....	32
<b>Figure 1.4</b> An illustration of an individual fuel cell, courtesy of the Global Energy Network Institute [Web 8].....	34
<b>Figure 1.5</b> left, Mercedes-Benz (Daimler AG) Citaro to join TFL's New Hydrogen powered bus fleet on route RV1 [Web 11] and right: Intelligent Energy, London Taxis International, TRW Conekt and Lotus Engineering partnership Hydrogen black cab in London, UK [Web 12].....	35

**Chapter 2: Literature review**

<b>Figure 2.1</b> Schematic of a typical compressed hydrogen composite tank, <i>Quantum Technologies</i> , [1].....	44
<b>Figure 2.2</b> Schematic of a hollow Glass microsphere for hydrogen storage, [Web 18].....	45
<b>Figure 2.3</b> Prototype of a two-cell conformable tank, Thiokol Propulsions, [Web 20].....	45
<b>Figure 2.4</b> Schematic of a typical cryogenic hydrogen tank, the Linde Group, [Web 21].....	47
<b>Figure 2.5</b> Hydrogen spill-over applied to MOFs [32].....	54
<b>Figure 2.6</b> Family tree of hydriding alloys and complexes, Sandrock [35].....	56
<b>Figure 2.7</b> Schematic model of metal structure with H atoms in the interstices between the metal atoms and H <sub>2</sub> molecules at the surface. Schlappbach and Züttel [36].....	57
<b>Figure 2.8</b> Schematic of phase transitions in most of the metal hydrides, David [37].....	58
<b>Figure 2.9</b> Molecular processes during hydrogen uptake, David [37].....	59
<b>Figure 2.10</b> Hydrogen capacities for various stores, Fuel cell program from the Department of Energy, USA [Web 23].....	64

<b>Figure 2.11</b> Crystal structure of $\text{LiNH}_2$ ; red (large), green (middle) and blue (small) spheres represent Li, N, H atoms, respectively. (Miwa <i>et al.</i> [59] , Shevlin <i>et al.</i> [60])....	68
<b>Figure 2.12</b> Comparisons in the ammonia level during TG analysis, Taken from Shaw <i>et al.</i> [67].....	70
<b>Figure 2.13</b> Low (a) and high (b) temperature structures of $\text{LiBH}_4$ determined from X-Ray diffraction, red (large), green (middle) and blue (small) spheres represent Li, B and H atoms, respectively (Miwa <i>et al.</i> [59], Shevlin <i>et al.</i> [60]).....	84
<b>Figure 2.14</b> Thermal desorption spectra of pure $\text{LiBH}_4$ (Brampton <i>et al.</i> [Web 24]).....	92
<b>Figure 2.15</b> (a): The desorption temperature $T_d$ as a function of the Pauling electronegativity $P$ . Inset shows the correlation between $T_d$ and estimated $\Delta H_{\text{des}}$ from eq. 2.19 (b): Powder x-ray diffraction profiles of purchased $\text{MBH}_4$ where $M=\text{Li, Na, and K}$ , and prepared $M(\text{BH}_4)_n$ where $M=\text{Mg, Zn, Sc, Zr, and Hf}$ by mechanical milling (Nakamori <i>et al.</i> [134]).....	94
<b>Figure 2.16</b> XRD patterns of $\text{Ca}(\text{BH}_4)_2$ before dehydrogenation (a), after dehydrogenation at $320^\circ\text{C}$ (b) and after dehydrogenation at $500^\circ\text{C}$ , taken from Mao <i>et al.</i> [145] .....	95
<b>Figure 2.17</b> Graphic synopsis of the decomposition pathway of $\text{Mg}(\text{BH}_4)_2$ , taken from Soloveichik <i>et al.</i> [150].....	96
<b>Figure 2.18</b> Thermogravimetric curves of $\text{Mg}(\text{BH}_4)_2$ with or without additives such as: $\text{TiCl}_3$ , $\text{TiO}_2$ , $\text{TiB}_2$ , $\text{TiH}_2$ and Ti with a mass ratio of 2 to 1, Taken from Li <i>et al.</i> [Web 25].....	97
<b>Figure 2.19</b> Synthetic procedures by Shore, Parry and co-workers [152][155].....	100

<b>Figure 2.20</b> The proposed thermal dehydrogenation mechanism of AB, Taken from Wang <i>et al.</i> [159].....	101
<b>Figure 2.21</b> Structural similarities between diammoniate of diborane (left) and ammonia borane (right).....	102
<b>Figure 2.22</b> DSC curves (a) and MS curves (b) for hydrogen (m/z 2) and borazine (m/z 80) at a heating rate of 1°C.min <sup>-1</sup> .....	103
<b>Figure 2.23</b> The thermal decomposition of AB under hydrogen release and formation of volatile compounds: aminoborane and borazole and polymeric intermediates, PAB and PIB, .....	106
<b>Figure 2.24</b> Heterocyclic structure of borazole B <sub>3</sub> N <sub>3</sub> H <sub>6</sub> .....	107
 <b>CHAPTER 3: Experimental methods</b>	
<b>Figure 3.1</b> Glove box <i>Saffron Scientific Equipment Ltd</i> .....	110
<b>Figure 3.2</b> SPEX milling machine inside the argon filled glove box.....	111
<b>Figure 3.3</b> <i>Setaram Setsys</i> 16/18TG/DTA facility (a) combined with MS (b).....	112
<b>Figure 3.4</b> Schematic of a thermogravimetric apparatus, taken from [Web 27].....	113
<b>Figure 3.5</b> Typical TGA curves with characteristic effects: a) thermal decomposition with the formation of gaseous reaction products, b) multi-step decomposition, c) explosive decomposition with recoil effect, taken from Widmann [169].....	114

<b>Figure 3.6</b> Schematic illustration of a DTA single cell.....	115
<b>Figure 3.7</b> Typical DTA curve with characteristic effects, O: offset, B: baseline, EX: exothermic event, EN: endothermic event, taken from [Web 28].....	116
<b>Figure 3.8</b> Schematic illustration of a mass spectrometer, taken from [Web 29].....	118
<b>Figure 3.9</b> Example of TG-DTA-MS figures for pure $\text{LiBH}_4$ taken from Orimo <i>et al.</i> [170].....	119
<b>Figure 3.10</b> Schematic illustration of a X-RAY diffractometer.....	120
<b>Figure 3.11</b> <i>STOE STADI-P</i> diffractometer.....	121
<b>Figure 3.12</b> Example of XRD patterns for chlorides-added $\text{LiBH}_4$ systems (a) before dehydrogenation and (b) after dehydrogenation taken from Zhang <i>et al.</i> [171].....	122
<b>Figure 3.13</b> Schematic illustration of a Scanning Electron microscope, taken from [Web 30].....	123
<b>Figure 3.14</b> Typical EDS spectrum.....	124
<b>Figure 3.15</b> Example of SEM morphologies for $\text{LiBH}_4$ -based systems (a): after dehydrogenation and (b): after rehydrogenation on taken from Fang <i>et al.</i> [172].....	125
<b>Figure 3.16</b> Schematic illustration of a Fourier Transformation Infrared Spectroscope, taken from [Web 31].....	126
<b>Figure 3.18</b> Examples of FT-IR spectra – Asymmetric bending, symmetric bending, and asymmetric stretching modes of $[\text{BH}_4]^-$ are labelled as $\nu_4$ , $\nu_2$ and $\nu_3$ respectively taken from Youn Lee <i>et al.</i> [173].....	127

## **CHAPTER 4: Experimental results: thermal and structural study**

<b>Figure 4.1</b> MCD scans as a function of cycle temperature.....	131
<b>Figure 4.2</b> 3D representation of $H_2$ ( $m/z=2$ ) measurements as a function of cycle temperatures.....	132
<b>Figure 4.3</b> Simultaneous DTA, TG and MS of pure $LiBH_4$ – Heating rate: $5^\circ C.min^{-1}$ to a maximum temperature of $550^\circ C$ .....	132
<b>Figure 4.4</b> XRD diffraction pattern of as-received pure $LiBH_4$ : experimental curve and fitted peaks on top.....	134
<b>Figure 4.5</b> SEM images of pure $LiBH_4$ after 5 minutes milling at low (a) and high (b) magnifications.....	134
<b>Figure 4.6</b> Periodic table highlighting selected metals at fourth period in the periodic table forming chlorides added to $LiBH_4$ taken from [Web 32].....	138
<b>Figure 4.7</b> FT-IR profiles of $2LiBH_4+ZnCl_2$ ball milled for 1 (a) and 5 (b) minutes after ball milling representing different bond environments.....	141
<b>Figure 4.8</b> SEM images a: pure $LiBH_4$ after 5 minutes milling b: ( $LiBH_4:TiCl_3=3:1$ ) after 5 minutes milling c: ( $LiBH_4:CrCl_3=3:1$ ) after 5 minutes milling d: ( $LiBH_4:NiCl_2=2:1$ ) after 5 minutes milling.....	142
<b>Figure 4.9</b> SEM images a: pure $LiBH_4$ after 5 minutes milling b: ( $LiBH_4:CrCl_3=3:1$ ) after 5 minutes milling c1 and c2: ( $LiBH_4:TiCl_3=3:1$ ) after 5 minutes milling d1 and d2: ( $LiBH_4:NiCl_2=2:1$ ) after 5 minutes milling.....	143



<b>Figure 4.10</b> SEM-EDS profiles of (a): pure $\text{LiBH}_4$ , (b1) and (b2): ( $\text{LiBH}_4\text{:TiCl}_3=3\text{:}1$ ) after 5 minutes milling.....	144
<b>Figure 4.11</b> SEM-EDS profiles of (a): pure $\text{LiBH}_4$ , (b1) and (b2): ( $\text{LiBH}_4\text{:NiCl}_2=2\text{:}1$ ) after 5 minutes milling.....	145
<b>Figure 4.12</b> XRD data of $\text{CrCl}_3$ -added $\text{LiBH}_4$ as-milled for 5 minutes (a) and 15 minutes (b).....	147
<b>Figure 4.13</b> Total mass desorbed when heated up to $300^\circ\text{C}$ as a function of milling time.....	148
<b>Figure 4.14</b> DTA-TG-MS analyses of $\text{LiBH}_4$ and $n\text{LiBH}_4 + \text{MCl}_n$ ( $\text{M}=\text{Zn, Ti, Ni, Cr}$ ) at a heating rate of $5^\circ\text{C}\cdot\text{min}^{-1}$ .....	149
<b>Figure 4.15</b> TG-DTA-MS profiles of ( $\text{LiBH}_4\text{:ZnCl}_2=2\text{:}1$ ) after 15 minutes milling.....	151
<b>Figure 4.16</b> TG-DTA-MS profiles of ( $\text{LiBH}_4\text{:TiCl}_3=3\text{:}1$ ) after 5 minutes milling.....	153
<b>Figure 4.17</b> TG-DTA-MS profiles of ( $\text{LiBH}_4\text{:NiCl}_2=2\text{:}1$ ) after 5 minutes milling.....	154
<b>Figure 4.18</b> TG-DTA-MS profiles of ( $\text{LiBH}_4\text{:CrCl}_3=3\text{:}1$ ) after 5 minutes milling.....	155
<b>Figure 4.20</b> Powder X-ray diffraction patterns of pure $\text{NH}_4\text{Cl}$ (a), pure $\text{LiBH}_4$ (b), ( $\text{LiBH}_4\text{:NH}_4\text{Cl}=1\text{:}1$ ) not milled (c), ( $\text{LiBH}_4\text{:NH}_4\text{Cl}=1\text{:}1$ ) after 1 minute milling (d), ( $\text{LiBH}_4\text{:NH}_4\text{Cl}=1\text{:}2$ ) after 5 minutes milling (e), ( $\text{LiBH}_4\text{:NH}_4\text{Cl}=1\text{:}3$ ) after 1 minute milling (f).....	160

<b>Figure 4.21</b> SEM-EDS profiles of mixtures of LiBH <sub>4</sub> and NH <sub>4</sub> Cl mechanically milled for 1 minute.....	162
<b>Figure 4.22</b> DTA profiles of pure LiBH <sub>4</sub> and pure NH <sub>4</sub> Cl).....	163
<b>Figure 4.23</b> DTA profiles of mixtures of LiBH <sub>4</sub> and NH <sub>4</sub> Cl with different molar ratio 1:1 (i), 1:2 (ii), and 1:3 (iii) and several thermal events around 65°C (A), 100°C (B), 145°C (C), 185°C (D), 195°C (E <sub>1</sub> ), 210°C (E <sub>2</sub> ), 235°C (F), 280°C (G).....	164
<b>Figure 4.26</b> Thermal desorption profiles of a sample with a 1:1 molar ratio of LiBH <sub>4</sub> to NH <sub>4</sub> Cl after 1 minute of milling (a): high range of MS 10 <sup>-9</sup> order (b): low range of MS 10 <sup>-12</sup> order.....	167
<b>Figure 4.27</b> Thermal desorption profiles of a sample with a 1:1 molar ratio of LiBH <sub>4</sub> to NH <sub>4</sub> Cl after 5 minutes of milling (a): high range of MS 10 <sup>-9</sup> order (b): low range of MS 10 <sup>-12</sup> order.....	168
<b>Figure 4.28</b> Thermal desorption profiles of a sample with a 1:1 molar ratio of LiBH <sub>4</sub> to NH <sub>4</sub> Cl after 10 minutes of milling (a): high range of MS 10 <sup>-9</sup> order (b): low range of MS 10 <sup>-12</sup> order.....	169
<b>Figure 4.29</b> Thermal desorption profiles of a sample with a 1:2 molar ratio of LiBH <sub>4</sub> to NH <sub>4</sub> Cl after 1 minute of milling (a): high range of MS 10 <sup>-9</sup> order (b): low range of MS 10 <sup>-12</sup> order.....	171

**Figure 4.30** Thermal desorption profiles of a sample with a 1:2 molar ratio of  $\text{LiBH}_4$  to  $\text{NH}_4\text{Cl}$  after 5 minutes of milling (a): high range of MS  $10^{-9}$  order (b): low range of MS  $10^{-12}$  order.....171

**Figure 4.31** Thermal desorption profiles of a sample with a 1:2 molar ratio of  $\text{LiBH}_4$  to  $\text{NH}_4\text{Cl}$  after 10 minutes of milling (a): high range of MS  $10^{-9}$  order (b): low range of MS  $10^{-12}$  order.....173

**Figure 4.32** Thermal desorption profiles of a sample with a 1:3 molar ratio of  $\text{LiBH}_4$  to  $\text{NH}_4\text{Cl}$  after 1 minute of milling (a): high range of MS  $10^{-9}$  order (b): low range of MS  $10^{-12}$  order.....175

**Figure 4.33** Thermal desorption profiles of a sample with a 1:3 molar ratio of  $\text{LiBH}_4$  to  $\text{NH}_4\text{Cl}$  after 5 minutes of milling (a): high range of MS  $10^{-9}$  order (b): low range of MS  $10^{-12}$  order.....176

**Figure 4.34** Thermal desorption profiles of a sample with a 1:3 molar ratio of  $\text{LiBH}_4$  to  $\text{NH}_4\text{Cl}$  after 10 minutes of milling (a): high range of MS  $10^{-9}$  order (b): low range of MS  $10^{-12}$  order.....177

**Figure 4.35** Thermal desorption profiles of a sample with a 1:1 molar ratio of  $\text{NH}_3\text{BH}_3$  to  $\text{NH}_4\text{Cl}$  after 1 minute of milling (a): high range of MS  $10^{-10}$  order (b): low range of MS  $10^{-12}$  order.....179

**Figure 4.36** Thermal desorption profiles of a sample with a 1:1 molar ratio of  $\text{NH}_3\text{BH}_3$  to  $\text{NH}_4\text{Cl}$  after 5 minutes of milling (a): high range of MS  $10^{-10}$  order (b): low range of MS  $10^{-12}$  order.....180

<b>Figure 4.37</b> Thermal desorption profiles of a sample with a 1:2 molar ratio of $\text{NH}_3\text{BH}_3$ to $\text{NH}_4\text{Cl}$ after 1 minute of milling (a): high range of MS $10^{-10}$ order (b): low range of MS $10^{-12}$ order.....	181
<b>Figure 4.38</b> Thermal desorption profiles of a sample with a 1:2:5 mol % molar ratio of $\text{LiBH}_4$ to $\text{NH}_4\text{Cl}$ and C after 1 minute of milling (a): high range of MS $10^{-10}$ order (b): low range of MS $10^{-12}$ order.....	183
<b>Figure 4.39</b> Thermal desorption profiles of a sample with a 1:2:5 mol % molar ratio of $\text{LiBH}_4$ to $\text{NH}_4\text{Cl}$ and C after 5 minutes of milling (a): high range of MS $10^{-10}$ order (b): low range of MS $10^{-12}$ order.....	184
<b>Figure 4.40</b> Thermal desorption profiles of a sample with a 1:3:5 mol % molar ratio of $\text{LiBH}_4$ to $\text{NH}_4\text{Cl}$ and C after 1 minute of milling (a): high range of MS $10^{-10}$ order (b): low range of MS $10^{-12}$ order.....	186
<b>Figure 4.41</b> Thermal desorption profiles of a sample with a 1:3:5 mol % molar ratio of $\text{LiBH}_4$ to $\text{NH}_4\text{Cl}$ and C after 5 minutes of milling (a): high range of MS $10^{-10}$ order (b): low range of MS $10^{-12}$ order.....	187
<b>Figure 4.42</b> Thermal desorption profiles of a sample with a 1:1:5 mol % molar ratio of $\text{NH}_3\text{BH}_3$ to $\text{NH}_4\text{Cl}$ and C after 1 minute of milling (a): high range of MS $10^{-9}$ order (b): low range of MS $10^{-10}$ order.....	188
<b>Figure 4.43</b> Thermal desorption profiles of a sample with a 1:1:5 mol % molar ratio of $\text{NH}_3\text{BH}_3$ to $\text{NH}_4\text{Cl}$ and C after 5 minutes of milling (a): high range of MS $10^{-9}$ order (b): low range of MS $10^{-11}$ order.....	189

<b>Figure 4.44</b> Thermal desorption profiles of a sample with a 1:2:5 mol % molar ratio of $\text{NH}_3\text{BH}_3$ to $\text{NH}_4\text{Cl}$ and C after 1 minute of milling (a): high range of MS $10^{-9}$ order (b): low range of MS $10^{-11}$ order.....	190
--	-----

## Chapter 5: General Discussion

<b>Figure 5.1</b> Possible decomposition paths of as-received $\text{LiBH}_4$ .....	201
---	-----

<b>Figure 5.2</b> Influence of the electronegativity on the hydrogen liberation temperature during the formation of borides of transition metals .....	205
--	-----

<b>Figure 5.3:</b> Influence of the electronegativity on the hydrogen liberation temperature during the formation of borides of transition metals.....	213
--	-----

<b>Figure 5.4:</b> TG mass loss of different mixtures of $\text{LiBH}_4$ as a function of the amount of $\text{NH}_4\text{Cl}$ , Step 2: 80-140°C.....	225
--	-----

<b>Figure 5.5:</b> TG-DTA-MS data for the decomposition of ammonium borohydride, $\text{NH}_4\text{BH}_4$ , taken from Karkamkar <i>et al.</i> [208].....	233
---	-----

<b>Figure 5.6:</b> Yield of borazine as a function of $\text{NH}_4\text{Cl}$ proportion (data extracted from Mikheeva <i>et al.</i> [161]).....	235
---	-----

<b>Figure 5.7:</b> Isothermal measurements of main DSC peaks (data extracted from Wolf <i>et al.</i> [167]).....	240
--	-----

## LIST OF TABLES

### Chapter 1: General Introduction

N/A

### Chapter 2: Literature review

<b>Table 2.1</b> D.O.E. hydrogen storage revised technical targets for on-board hydrogen storage [Web 14].....	41
<b>Table 2.2</b> Hydrogen storage properties of intermetallic compounds according to the online database of the I.E.A. [38].....	60
<b>Table 2.3</b> Different types of complex hydrides and their gravimetric density.....	62
<b>Table 2.4</b> Examples of M-N-H systems, M=Li, Mg, Li-Mg, Ca, Lu [77].....	71
<b>Table 2.5</b> Mixed complex hydrides, Lu <i>et al.</i> [77].....	72
<b>Table 2.6</b> Main elements forming simple metal Borohydrides and metal borohydride complexes, James <i>et al.</i> [96].....	77
<b>Table 2.7</b> Formation of borohydrides from the elements, Goerrig [101].....	79
<b>Table 2.8</b> Some example of thermodynamic properties, James and Wallbridge [96].....	82
<b>Table 2.9</b> Vibrational frequencies of some tetrahydroborates – part 1, James and Wallbridge [96].....	83

<b>Table 2.10</b> Vibrational frequencies of other tetrahydroborates – part 2, various sources [96].....	83
--	----

### **Chapter 3: Experimental methods**

<b>Table 3.1</b> Main characteristics of selected chemicals.....	109
<b>Table 3.2</b> Nature of DTA peaks involved in typical processes.....	116
<b>Table 3.3</b> The 3 smaller areas of the IR region.....	127
<b>Table 3.4</b> Example of vibrational frequencies of relevant borohydrides from various sources.....	128

### **Chapter 4: Experimental results**

<b>Table 4.1</b> Ion masses and tentative identification for $\text{LiBH}_4$ mass spectra.....	130
<b>Table 4.2</b> Properties of starting materials and possibly formed metal borohydrides.....	139
<b>Table 4.3</b> Properties of starting materials and details of mechanical milling treatment.....	149
<b>Table 4.4</b> Detected masses during the dehydrogenation of binary compositions.....	165

**Chapter 5: General discussion**

<b>Table 5.1</b> Calculated thermodynamic functions for the different probable reactions between $\text{LiBH}_4$ and $\text{CrCl}_3$ , taken from Volkov <i>et al.</i> [203].....	216
<b>Table 5.2</b> Summary of TG and MS results – Step 1 – 30-80°C (peaks at 50 and/or 70°C).....	223
<b>Table 5.3</b> Summary of TG and MS results – Step 2 – 80-140°C (peak at 95°C).....	224
<b>Table 5.4</b> Summary of TG and MS results – Step 3 – 140-185°C and 185-225°C (peaks at 165°C and 195°C).....	226
<b>Table 5.5</b> Summary of TG and MS results for mixtures of $\text{NH}_3\text{BH}_3$ and $\text{NH}_4\text{Cl}$ – Steps 1, 2 and 3.....	227
<b>Table 5.6</b> Summary of TG and MS results for Carbon-added $\text{LiBH}_4$ -based mixtures – Steps 1, 2 and 3.....	229
<b>Table 5.7</b> Summary of TG and MS results for Carbon-added $\text{NH}_3\text{BH}_3$ -based mixtures – Steps 1, 2 & 3.....	230
<b>Table 5.8</b> Different steps during decomposition of ammonium borohydride, $\text{NH}_4\text{BH}_4$ , taken from Karkamkar <i>et al.</i> [208].....	234



## LIST OF EQUATIONS

### Chapter 1: General Introduction

N/A

### Chapter 2: Literature review

**Eq. 2.1a**  $3\text{NaAlH}_4 \rightarrow \text{Na}_3\text{AlH}_6 + 2\text{Al} + 3\text{H}_2$  .....66

**Eq. 2.1b**  $\text{Na}_3\text{AlH}_6 \rightarrow 3\text{NaH} + \text{Al} + 3/2\text{H}_2$  .....66

**Eq. 2.2a**  $3\text{LiAlH}_4 \rightarrow \text{Li}_3\text{AlH}_6 + 2\text{Al} + 3\text{H}_2$ .....66

**Eq. 2.2b**  $\text{Li}_3\text{AlH}_6 + 2\text{Al} \rightarrow 3\text{LiH} + 3\text{Al} + 3/2\text{H}_2$ .....66

**Eq. 2.3**  $\text{NH}_2 + 2\text{LiH} \leftrightarrow \text{Li}_2\text{NH} + \text{H}_2$  .....69

**Eq. 2.4**  $2\text{LiNH}_2 \rightarrow \text{Li}_2\text{NH} + \text{NH}_3$  .....70

**Eq. 2.5**  $\text{LiH} + \text{NH}_3 \rightarrow \text{LiNH}_2 + \text{H}_2$  .....70

**Eq. 2.6**  $\text{M}'\text{BH}_4 + \text{M}''\text{X}_n \rightarrow \text{M}''(\text{BH}_4)_n + \text{M}'\text{X}$  .....76

X= Br, Cl, I, or F forming a metal halide when bonded to a metal

**Eq. 2.7**  $\text{MH}_n + n/2\text{B}_2\text{H}_6 \rightarrow \text{M}(\text{BH}_4)_n$  .....76

<b>Eq. 2.8</b> $\text{MH}_n + \text{B}(\text{OCH}_3)_3 \rightarrow \text{MBH}_n(\text{OCH}_3)_3$ .....	77
--	----

<b>Eq. 2.9</b> $4\text{MBH}_n(\text{OCH}_3)_3 \rightarrow \text{M}(\text{BH}_4)_n + 3\text{MB}_{(4-n)/3}(\text{OCH}_3)_4$ .....	77
---	----

M=Li, K or Na

<b>Eq. 2.10</b> $4\text{MH} + (\text{C}_2\text{H}_5)_2\text{O} \cdot \text{BF}_3 \rightarrow 3\text{MF} + \text{MBH}_4 + (\text{C}_2\text{H}_5)_2\text{O}$ .....	77
--	----

<b>Eq. 2.11</b> $\text{H}_2\text{B}(\text{NH}_3)_2(\text{BH}_4)_n + \text{M} \rightarrow \text{M}(\text{BH}_4)_n + 1/2\text{H}_2 + \text{H}_2\text{BNH}_2 + \text{NH}_3$ .....	80
--	----

<b>Eq. 2.12</b> $a\text{MX} + 2/3an\text{B}_2\text{H}_6 \rightarrow a\text{M}(\text{BH}_4)_n + \text{BX}_a$ (X=OCH <sub>3</sub> , OC <sub>2</sub> H <sub>5</sub> ) .....	80
--	----

<b>Eq. 2.13</b> $\text{M}(\text{BH}_4)_n \rightarrow \text{M} + n\text{B} + 2n\text{H}_2$ .....	81
---	----

<b>Eq. 2.14</b> $\ln\left(\frac{P_{eq}}{P_0}\right) = \frac{\Delta H}{RT} - \frac{\Delta S}{R}$ .....	81
---	----

where  $P_0$  is the standard pressure i.e., 1.013 bar),  $T$  is the absolute temperature and  $R$  is the gas constant.

<b>Eq. 2.15a</b> $\text{LiBH}_4 \rightarrow \text{LiBH}_{4-\varepsilon} + (\varepsilon/2)\text{H}_2$ .....	91
--	----

<b>Eq. 2.15b</b> $\text{LiBH}_{4-\varepsilon} \rightarrow \text{LiBH}_2 + (1-\varepsilon/2)\text{H}_2$ .....	91
--	----

<b>Eq. 2.15c</b> $\text{LiBH}_{4-\varepsilon} \rightarrow \text{LiBH}_2 + (1-\varepsilon/2)\text{H}_2$ .....	91
--	----

<b>Eq. 2.16</b> $\text{MCl}_n + n\text{LiBH}_4 \rightarrow \text{M}(\text{BH}_4)_n + n\text{LiCl}$ .....	91
--	----

<b>Eq. 2.17</b> $\text{LiBH}_4 + 1/2\text{MgH}_2 \leftrightarrow \text{LiH} + 1/2\text{MgB}_2 + 2\text{H}_2$ .....	94
--	----

<b>Eq. 2.18</b>	$\text{Ca}(\text{BH}_4)_2 \leftrightarrow 1/3\text{CaB}_6 + 2/3\text{CaH}_2 + 10/3\text{H}_2$	95
<b>Eq. 2.19a</b>	$\text{Mg}(\text{BH}_4)_2 \rightarrow 1/6\text{MgB}_{12}\text{H}_{12} + 5/6\text{MgH}_2 + 13/6\text{H}_2$	96
<b>Eq. 2.19b</b>	$1/6\text{MgB}_{12}\text{H}_{12} + 5/6\text{MgH}_2 + 13/6\text{H}_2 \rightarrow \text{MgH}_2 + 2\text{B} + 3\text{H}_2$	96
<b>Eq. 2.19c</b>	$\text{MgH}_2 + 2\text{B} + 3\text{H}_2 \rightarrow \text{Mg} + 2\text{B} + 4\text{H}_2$	97
<b>Eq. 2.20a</b>	45% yield $\text{LiBH}_4 + \text{NH}_4\text{Cl} \rightarrow \text{LiCl} + \text{NH}_3\text{BH}_3 + \text{H}_2$ Diethyl ether	99
<b>Eq. 2.20b</b>	45% yield $\text{LiBH}_4 + (\text{NH}_4)_2\text{SO}_4 \rightarrow \text{Li}_2\text{SO}_4 + 2\text{NH}_3\text{BH}_3 + 2\text{H}_2$ Diethyl ether	99
<b>Eq. 2.20c</b>	45% yield $\text{DADB} + \text{NH}_4\text{Cl} \rightarrow [\text{H}_2\text{B}(\text{NH}_3)_2]\text{Cl} + \text{NH}_3\text{BH}_3 + \text{H}_2$ Diethyl ether/NH <sub>3</sub>	99
<b>Eq. 2.20d</b>	~80-91% yield $\text{DADB} \rightarrow 2\text{NH}_3\text{BH}_3$ Polyether/B <sub>2</sub> H <sub>6</sub>	100
<b>Eq. 2.20e</b>	70% yield $(\text{CH}_3)_2\text{OBH}_3 + \text{NH}_3 \rightarrow \text{NH}_3\text{BH}_3 + (\text{CH}_3)_2\text{O}$ Dimethyl ether	100
<b>Eq. 2.21</b>	$n\text{H}_3\text{BNH}_3 (\text{l}) \rightarrow (\text{H}_2\text{BNH}_2)_n (\text{s}) + n\text{H}_2 (\text{g}) \quad (107-117^\circ\text{C})$	100
<b>Eq. 2.22</b>	$(\text{H}_2\text{BNH}_2)_n (\text{s}) \rightarrow (\text{HBNH})_n (\text{s}) + n\text{H}_2 (\text{g}) \quad (150^\circ\text{C})$	101

<b>Eq. 2.23</b> $(\text{HBNH})_n (\text{s}) \rightarrow n\text{BN} (\text{s}) + n\text{H}_2 (\text{g}) (500-1400^\circ\text{C})$ .....	101
<b>Eq. 2.24</b> $3\text{NH}_4\text{Cl} + 3\text{LiBH}_4 \rightarrow \text{B}_3\text{N}_3\text{H}_6 (\text{borazole}) + 3\text{LiCl} + 9\text{H}_2$ .....	104
<b>Eq. 2.25</b> $\text{NH}_4\text{Cl} + \text{LiBH}_4 \rightarrow \text{H}_3\text{N.BH}_3 (\text{ammonia borane}) + \text{LiCl} + \text{H}_2$ .....	104
<b>Eq. 2.26</b> $\text{NH}_4\text{Cl} + \text{LiBH}_4 \rightarrow \text{NH}_4.\text{BH}_4 (\text{ammonium borohydride}) + \text{LiCl}$ .....	105
<b>Eq. 2.27</b> $\text{NH}_4\text{Cl} + \text{LiBH}_4 \rightarrow \text{NH}_3.\text{BH}_3 (\text{ammonia borane}) + \text{LiCl} + \mathbf{H}_2$ .....	105
<b>Eq. 2.28</b> $\text{NH}_4\text{Cl} + \text{LiBH}_4 \rightarrow \text{NH}_2.\text{BH}_2 (\text{aminoborane}) + \text{LiCl} + \mathbf{2H}_2$ .....	105
<b>Eq. 2.29</b> $\text{NH}_4\text{Cl} + \text{LiBH}_4 \rightarrow 1/3(\text{B}_3.\text{N}_3.\text{H}_6) (\text{borazole}) + \text{LiCl} + \mathbf{3H}_2$ .....	105

### Chapter 3: Experimental methods

<b>Eq. 3.1</b> $\lambda = 2d_{hkl} \sin \theta_{hkl}$ .....	120
where h, k and l are the Millar indices of a set of planes.	
<b>Eq. 3.2</b> $A = \log_{10}(1/T) = -\log_{10} T = -\log I / I_o$ .....	127

## **Chapter 4: Experimental results**

N/A

## **Chapter 5: General Discussion**

**Eq. 5.1**  $\text{LiBH}_4 \rightarrow \text{LiH} + 1/2\text{B}_2\text{H}_6 \rightarrow \text{LiH} + \text{B} + 3/2\text{H}_2$  .....197

**Eq. 5.2**  $\text{LiBH}_4 \rightarrow \text{LiH} + \text{B} + 3/2\text{H}_2$   $T_d=220-500^\circ\text{C}$ .....198

**Eq. 5.3**  $\text{LiBH}_4 \rightarrow \text{'LiBH}_2\text{' + H}_2 \rightarrow \text{LiH} + \text{B} + 3/2\text{H}_2$  .....198

**Eq. 5.4**  $\text{LiBH}_4 \rightarrow 1/6\text{Li}_2\text{B}_{12}\text{H}_{12} + 5/6\text{LiH} + 13/12\text{H}_2 \rightarrow \text{LiH} + \text{B} + 3/2\text{H}_2$  .....198

**Eq. 5.5**  $10\text{LiBH}_4 \rightarrow 10\text{LiH} + 5\text{B}_2\text{H}_6$  (220-300°C).....199

**Eq. 5.6**  $2\text{LiBH}_4 + 5\text{B}_2\text{H}_6 \rightarrow \text{Li}_2\text{B}_{12}\text{H}_{12} + 13\text{H}_2$  (280-300°C).....199

**Eq. 5.7**  $\text{LiBH}_4 \rightarrow 5/6\text{LiH} + 1/12\text{Li}_2\text{B}_{12}\text{H}_{12} + 13/12\text{H}_2$  (220-300°C).....199

**Eq. 5.8**  $\text{B}_2\text{H}_6 \rightarrow 2\text{B} + 3\text{H}_2$  (300-400°C).....200

**Eq. 5.9**  $\text{Li}_2\text{B}_{12}\text{H}_{12} \rightarrow 2\text{LiH} + 12\text{B} + 5\text{H}_2$  (400-550°C).....200

<b>Eq. 5.10</b>	$n_2.M_1Cl_{n1} + n1.M_2(BH_4)_{n2} \rightarrow n_2.M_1(BH_4)_{n1} + n1.M_2Cl_{n2}$	.....202
-----------------	---	----------

<b>Eq. 5.11</b>	% ionic character = $100*(1-e^{-0.25*(X_a-X_b)^2})$ where $X_a$ and $X_b$ are the higher and lower electronegativities respectively.....	205
-----------------	--	-----

<b>Eq. 5.12a</b>	$2LiBH_4 + ZnCl_2 \rightarrow ZnH_2 + 2LiBH_3Cl$	(RT).....209
------------------	--	--------------

<b>Eq. 5.12b</b>	$2LiBH_4 + ZnCl_2 \rightarrow Zn(BH_4)_2 + 2LiCl$	(RT-110°C).....209
------------------	---	--------------------

<b>Eq. 5.12c</b>	$ZnH_2 \rightarrow Zn + H_2$	(120°C).....209
------------------	------------------------------	-----------------

<b>Eq. 5.12d</b>	$Zn(BH_4)_2 \rightarrow Zn + B_2H_6 + H_2$	(220°C) .....209
------------------	--	------------------

<b>Eq. 5.12e</b>	$LiBH_3Cl \rightarrow LiCl + 1/2B_2H_6$	(220°C) .....209
------------------	---	------------------

<b>Eq. 5.13a</b>	$3LiBH_4 + TiCl_3 \rightarrow Ti(BH_4)_3 + 3LiCl$	(RT).....211
------------------	---	--------------

<b>Eq. 5.13b</b>	$Ti(BH_4)_3 \rightarrow TiH_2 + 3B + 5H_2$	(60-90°C).....211
------------------	--	-------------------

<b>Eq. 5.13c</b>	$LiBH_4 \rightarrow LiH + B + 3/2H_2$	(60-90°C).....211
------------------	---------------------------------------	-------------------

<b>Eq. 5.13d</b>	$TiH_2 + B \rightarrow TiB_2 + H_2$	(220-300°C).....211
------------------	-------------------------------------	---------------------

From Eq. 5.13b, c and d,

<b>Eq. 5.13e</b>	$2LiBH_4 + TiCl_3 + LiH \rightarrow TiB_2 + 3LiCl + 4.5H_2$	(RT-300°C).....211
------------------	---	--------------------

<b>Eq. 5.14a</b>	$NiCl_2 + 2LiBH_4 \rightarrow Ni(BH_4)_2 + 2LiCl$	(RT).....214
------------------	---	--------------

<b>Eq. 5.14b</b>	$Ni(BH_4)_2 \rightarrow Ni + 2B + 4H_2$	(70°C).....214
------------------	---	----------------

<b>Eq. 5.14c</b>	$3Ni(BH_4)_2 \rightarrow Ni_3B + 9/2H_2 + 5/2B_2H_6$	(150°C).....214
------------------	--	-----------------

<b>Eq. 5.15a</b>	$6LiBH_4 + 2CrCl_3 = 6LiCl + 3B_2H_6 + 3H_2 + 2Cr$ .....	216
------------------	--	-----

**Eq. 5.15b**  $3\text{LiBH}_4 + \text{CrCl}_3 = 3\text{LiCl} + \text{CrB}_2 + \text{B} + 6\text{H}_2$  .....216

**Eq. 5.15c**  $3\text{LiBH}_4 + \text{CrCl}_3 = 3\text{LiCl} + 6\text{H}_2 + 3\text{B} + \text{Cr}$  .....216

**Eq. 5.16a**  $6\text{CrCl}_3 + 15\text{LiBH}_4 \rightarrow 5\text{Cr}(\text{BH}_4)_3 + 10\text{LiCl} + \text{Li}_5\text{CrCl}_8$  (RT) .....217

**Eq. 5.16b**  $\text{LiBH}_4 + \text{Li}_5\text{CrCl}_8 \rightarrow 6\text{LiCl} + \text{Cr} + \text{H}_2$  (100-170°C).....217

**Eq. 5.16c**  $\text{Cr}(\text{BH}_4)_3 \rightarrow \text{CrB}_2 + \text{B} + 6\text{H}_2$  (180-300°C).....217

# **Chapter 1.    Introduction**



Hydrogen offers a clean and sustainable alternative to fossil fuels in a modern world in which almost every aspect of human life is associated with their use. In fact, energy consumption from sustainable energy sources such as wind or solar electricity is rapidly growing; however, the overall contribution can almost be neglected compared to the one from fossil fuels. In order to support the growing demand for fossil fuels, new reserves need to be discovered and there is a fear that someday, we will inevitably run out of them.

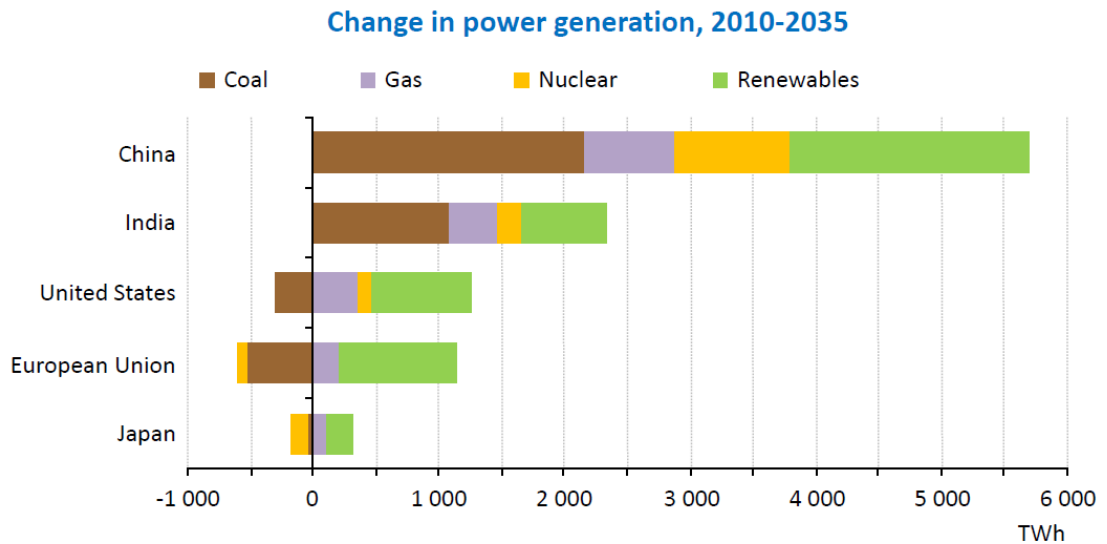


**Figure 1.1:** World energy production by fuel type and by country 2010-2035, 1  
TWh=  $3600 \cdot 10^{12}$  J

Taken from *World Energy Outlook 2012* (the Energy Information Administration, [Web 1])

Hydrogen has a number of advantages compared to fossil fuels. Firstly, hydrogen is the lightest and the most abundant element on the earth. However, less than 1 % is present as molecular hydrogen gas, the largest portion is chemically bound to form  $H_2O$  in water and some is bound to liquid or gaseous hydrocarbons. Secondly, compared to the other fuel carriers such as natural gas or gasoline, it has, on

a weight basis, a high energy density partly due to its low molecular weight. Indeed, in a hydrogen molecule, the electron is accompanied by only one proton, and the energy gain per electron is very high. As a result, the chemical energy per unit mass of hydrogen ( $39.4 \text{ kWh}\cdot\text{kg}^{-1}$ ) is almost three times ( $\sim 2.6$ ) larger than that of other chemical fuels, e.g. liquid hydrocarbons ( $13.1 \text{ kWh}\cdot\text{kg}^{-1}$ ). But, at the same time, the energy per unit volume is 4 times lower. Finally, carbon emission is avoided but even though the main product of hydrogen burning to air is water, some nitrogen compounds can be formed and may have to be controlled.

Hydrogen can be generated from a variety of sources e.g. solar and nuclear energy and is also relevant to all the energy sectors such as: Transport, Buildings and Industry as it can be directly converted into heat, or into electricity (via fuel cells).

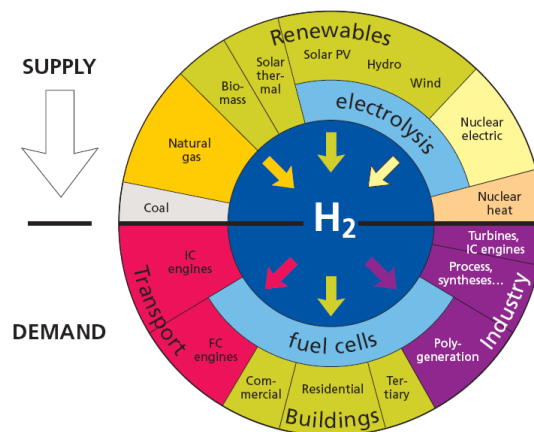


**Figure 1.2:** Hydrogen, primary energy sources, energy converters and applications. Courtesy of European Commission special report on *Hydrogen energy and Fuel Cells* ([Web 2])

Hydrogen production is a large and growing industry. Nevertheless, the world hydrogen production is not monitored [Web 3], but was estimated at around 500

million cubic meters in 2003 with a growth rate of 10% per year. According to the National Hydrogen Association [Web 4], about 60 % of the production is used as feedstock for ammonia production and subsequent use in fertilizers. Petroleum refining consumes around 23 % for the removal of sulphur from low-grade heavy oils into more valuable products. Around 9 % is used to manufacture methanol, and the remainder is for chemical, metallurgical and space purposes. Around 96 percent of it is derived from fossil fuels. Electrolysis still has minimal impact and is used to produce hydrogen when extremely high hydrogen purity is needed. In the year 2000, crude oil was the dominant fossil fuel to produce hydrogen (55 %) but in the most recent figures (2007), natural gas has become the dominant fuel (49 %).

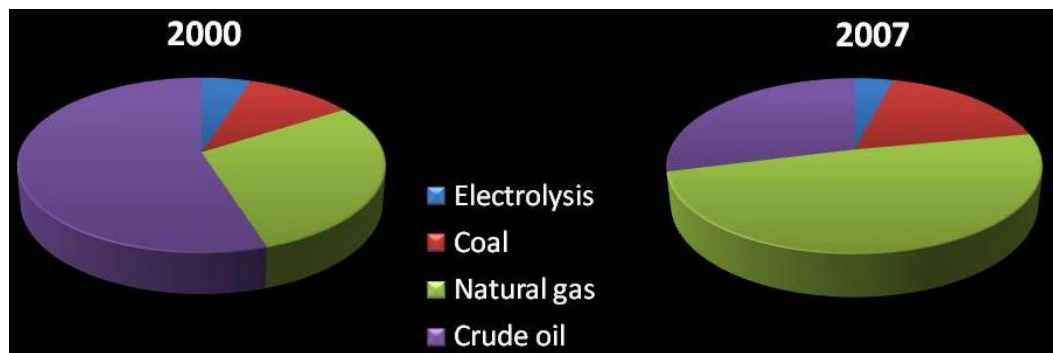


**Figure 1.3:** Relative Proportion of Sources of Hydrogen in 2000 and 2007 ([Web 3])

At present, 90 hydrogen production routes have been reported [Web 5] that can be divided into four categories: biological, chemical, electrochemical and thermal technologies. Each technology is in a different stage of development but almost all the technologies are using an electrolyser or a reformer. They are the technologies of choice in the current and near term [1]. In the medium to long term, fossil fuel-based technologies associated with the capture of the CO<sub>2</sub> released, could be the next step. In the long term, direct production of hydrogen without the use of fossil fuels but

using renewable energies might be the only alternative in order to reduce mechanical, transfer and electrical losses.

Indeed, the main process used to form pure hydrogen is steam reforming of fossil fuels (see Figure 1.3) such as: natural gas (49 %), oil (29 %), or coal (18 %). The generic formula is:  $C_nH_m + nH_2O \rightarrow nCO + (n+m/2).H_2$ . This would remain the most economical way as long as fossil fuels are available relatively cheaply and in large quantities and hydrogen is only required in small quantities.

A small part (see Figure 1.3) is produced by water electrolysis. The generic formula is:  $2H_2O + \text{energy} \rightarrow 2H_2 + O_2$ . If fossil fuels are used to generate the electricity, there is no advantage over using the fossil fuels directly as there are still carbon dioxide emissions and as well as a considerable loss of energy. Therefore, the large scale use of hydrogen depends heavily on using renewable energies or nuclear energy. The process itself has to be improved in order to lower the excess amount of energy ( $4.5\text{-}5 \text{ kWh.m}^{-3}.H_2$  in most industrial electrolyzers) needed to split pure water, thus the cost since electricity is known to be one of the most expensive forms of energy [2]. This can be done [Web 6] by adding an electrolyte and using electrocatalysts but up to now, the proton reduction catalyst used is a very expensive metal: platinum. Recently, a new molecular molybdenum-oxo complex [3] has been shown to catalyze the generation of hydrogen from neutral buffered water. It would not require organic additives into the electrolyte and would be seventy times cheaper than platinum, which can significantly reduce the production costs.

The use of hydrogen as an energy carrier such as electricity is only justified when there are reasons not to use the primary source directly, which is particularly relevant to vehicular applications.

Moreover, hydrogen can be used as a fuel directly in an internal combustion engine [Web 7], not much different from the engines used with gasoline. It converts the chemical energy into thermal energy and then to electrical energy, the overall efficiency is only 40% or less, and considerable energy is wasted during the energy transfer process. However, if this is done by converting the hydrogen energy into electrical energy in fuel cells, and then, this energy is used for driving an electrical motor, the efficiency can be very much increased, up to 80 % since a fuel cell and electric motor combination is not directly limited by the Carnot efficiency of an internal combustion engine. Fuel cells are different from conventional electrochemical cell batteries in that they consume reactant from an external source, which must be replenished.

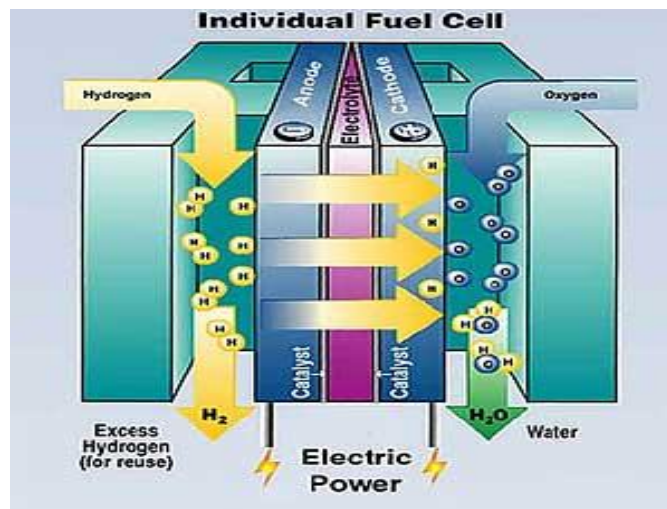
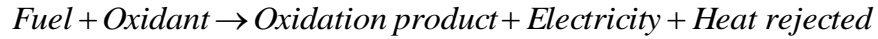


**Figure 1.4:** An illustration of an individual fuel cell, courtesy of the Global Energy Network Institute [Web 8]

A fuel cell [Web 9] is an energy conversion device that converts chemical energy into electrical energy with a high efficiency. A hydrogen fuel cell uses hydrogen as its fuel and oxygen (usually from air) as its oxidant. Typical fuel cell

consists of an electrolyte material sandwiched in between two thin electrodes (porous anode and cathode). Hydrogen molecules separate into hydrogen ions, protons and electrons due to the presence of a catalyst on the anode.

The overall reaction occurring in fuel cells could be described by:



Hydrogen powered fuel cells can be applied for cars and buses, as well as residential power stations, mobile phones and computers. There are a number of prototype cars e.g. *Mercedes-Benz F800 Concept* and buses e.g. *Daimler A.G. Citaro* based on fuel cell technology developed by motor car manufacturers [Web 10].

In 2003, three fuel cell buses were introduced by Transport for London [Web 11] as part of the Cleaner Urban transport for Europe (CUTE) trial for a two-year trial on Route 25 and then, extended until 2007 on route RV1 and due to start again in 2011 (see Figure 1.5). In 2010, a hydrogen-powered black cab (see Figure 1.5) was introduced [Web 12] and by 2012, a fleet of 20 taxis should be in service in London.



**Figure 1.5:** left, Mercedes-Benz (Daimler AG) Citaro to join TFL's New Hydrogen powered bus fleet on route RV1 [Web 11] and right: Intelligent Energy, London Taxis International, TRW Conekt and Lotus Engineering partnership Hydrogen black cab in London, UK [Web 12]

Compared to a traditional combustion engine, a fuel cell is a favourable energy conversion device mainly because of its high efficiency and clean emission. However, the high capital cost for fuel cells is by far the largest factor contributing to the limited market penetration of fuel cell technology.

Although hydrogen is one of the most promising energy options of future, much work still needs to be carried out in order to achieve such promised benefit. In the United Kingdom, United Kingdom Sustainable Hydrogen Energy Consortium (UK-SHEC) [Web 13] has been established in 2003 as part of the EPSRC SUPERGEN initiative to encourage the development of sustainable power generation and supply.

The research has been divided into 5 themes: hydrogen production, hydrogen storage, social and economic Implications, interdisciplinary research and capacity building. Technical research in hydrogen energy concentrates on three aspects: hydrogen production, hydrogen distribution and storage. There are some other issues such as safety, environmental concerns and costs that are equally important, which need to be addressed.

One of the main problems is to handle and transport hydrogen safely [Web 7] because hydrogen has one of the widest explosive/ignition mix range with air of all the gases. This makes the use of hydrogen particularly dangerous in enclosed areas such as tunnels or underground parking. Moreover, pure hydrogen-oxygen flames burn in the ultraviolet colour range and are nearly invisible to the naked eye. Hydrogen is odourless and leaks cannot be detected by smell. Higher hydrogen codes and standards need to be implemented such as early leak detection with hydrogen

sensors. Also, hydrogen pipelines and tanks could be subject to additional problems such as embrittlement as the small molecules of hydrogen tend to leak easily and the release of hydrogen into a confined space such as a garage is very dangerous due to the risks of explosion.

There are other concerns with regards to the possible environmental effects of hydrogen production, storage and utilisation [Web 7]. At the production stage, most of hydrogen produced is derived from fossil fuel reforming which leads to higher emissions of carbon dioxide. Also, if hydrogen is directly used as a fuel in an ICE, the engine may produce nitrous oxides and other pollutants as air input into the combustion cylinder is approximately 78 % nitrogen. The  $N_2$  molecule has a very weak binding energy of around  $946 \text{ kJ.mol}^{-1}$  and the reaction with hydrogen has sufficient energy to break this bond and produce unwanted components such as nitric acid ( $HNO_3$ ) and hydrogen cyanide gas (HCN), both are very toxic. Compared to hydrocarbons and their emissions of pollutants, it would seem that even though hydrogen would produce noxious by-products, the impact would be less damaging as hydrocarbons contains more hydrogen. Fortunately, hydrogen as a fuel for fuel cells does not produce greenhouse gas emissions, but water. Therefore, the use of hydrogen can clean air in much polluted cities.

Setting up a hydrogen economy would require a huge investment in the infrastructure to store and distribute hydrogen to vehicles; however, the existing petrol stations could be used. Since most hydrogen is derived from natural gas, the pricing of the two is very closely linked. Despite the pressure of the financial crisis, the hydrogen market has remained relatively resilient because hydrogen is mainly used



for other applications such as in refineries to purify low-grade crude oils and for the production of ammonia for agricultural applications.

In summary, the issues still faced by hydrogen are not advocating for its use in large scale at near to medium term but there is still hope on a long term basis. Indeed, hydrogen is beneficial but the problem with its storage is primordial.

Due to the above issues that have been highlighted, the main objectives of this study are to: to identify a new suitable system based on a new chemical hydride i.e.  $\text{LiBH}_4$  capable of satisfying the onboard requirements and consecutively, to design experimental set-up in order to conduct a systematic investigation of the dehydrogenation properties of the best compositions.

The thesis is divided into four chapters. The first part will deal with the literature review on the thematic of hydrogen storage, while the second chapter will present the experimental set-up elaborated in the laboratory as well as the different characterisations methods used. The third section presents the experimental results and the relevant individual discussions for the most promising systems presented in the thesis whereas the last parts will deal with the general discussion, conclusions from the whole study and the future work.

## **Chapter 2.    Overview of Hydrogen Storage Methods**

This section of the thesis will tackle the hydrogen storage methods. The three states in which you can find hydrogen are directly related to the 3 types of storage methods currently under scrutiny. The following section is about identifying the hydrogen storage issues and describing the different methods currently being envisaged.

## 2.1 Hydrogen storage issues and methods

Hydrogen energy systems still face a lot of technical and economical barriers that must be first overcome. The technical challenges are the real time production, the safe and convenient storage and the efficient combustion of hydrogen. The main economical challenge is the cost of hydrogen production. As it has been mentioned in the general introduction, all the production processes involve a loss of energy and therefore, are not 100% energy-efficient. Thus, improvements must be made in hydrogen production but also in all the other aspects of the hydrogen economy, i.e., transport, storage and utilisation technologies. However, storage seems to be one of the main bottlenecks that need to be addressed before even thinking of a possible hydrogen economy.

### 2.1.1 Hydrogen Storage Challenges for on-board applications

There are various practical targets for hydrogen storage. One widely accepted set of system targets were developed through the FreedomCAR and Fuel Partnership, collaboration between U.S. Department of Energy (D.O.E.), Council for Automotive Research (U.S.C.A.R.), five major car companies and two electric utility companies

[Web 14]. These targets are for a system rather than a material in order to include hydrogen use in both ICEs and fuel cells. The storage system includes the weight of the tank, temperature and pressure control equipment. The targets are set for a 5-kg storage system without impacting the driver and passenger spaces for a driving range of at least 300 miles (around 500 km). In 2009, the on-board Hydrogen Storage System Targets have been revised to reflect feedback knowledge gained in hydrogen-fueled vehicles. Since the original release of the targets, they have been primarily focused on developing technologies in order to get sufficient information to allow the auto industry to make decisions about the marketability of hydrogen fuel cell-powered vehicles by 2015. But, in 2009, there has been a shift of direction towards the promotion of shorter-term technologies for reducing petroleum use in ICEs to the detriment of fuel cell vehicles even though it is been suggested that a sustained support for a balanced portfolio of shorter-term and longer-term options should be encouraged.

**Table 2.1:** D.O.E. hydrogen storage revised technical targets for on-board hydrogen storage  
[Web 14]

Target	2010 (old*)	2015 (old*)
System Gravimetric density (wt%)	4.5 (6)	5.5 (9)
System Volumetric Density ( $\text{kg.m}^{-3}$ )	28 (45)	40 (81)
System Fill time (min)	4.2 (3)	3.3 (2.5)
Fueling rate ( $\text{kg.min}^{-1}$ )	1.2 (1.67)	1.5 (2.0)
Storage System Cost ( $\text{\$.H}_2\text{.kg}^{-1}$ )	TBD (133)	TBD (67)

*\*previous targets before the major revision in 2009*

In order to achieve system-level capacities, the gravimetric and volumetric capacities of the material alone must be higher than the system-level targets.

### 2.1.2 Hydrogen storage methods

Current hydrogen storage methods involve compressed hydrogen gas tanks, liquid hydrogen tanks, cryogenic compressed hydrogen, high-surface-area adsorbents, metal hydrides and chemical hydrogen storage materials. All except the latter constitutes “reversible” hydrogen storage systems because hydrogen regeneration could take place by simple change of pressure and/or temperature. There are some well-established technologies and more technologies under active research with advantages and disadvantages that have been summed up in the following paragraphs. The present study is an attempt to tackle the main limitations observed in previous studies with an innovative approach. Elam *et al.* [4] described in details the International Energy Agency’s requirements and targets. The IEA has implemented different tasks within cooperating groups of scientists on a particular topic of interest [Web 15]. During the study, tasks 17 (2001-2006) and 22 (2006-2009 and extended until 2012) were of great interest. The following paragraphs detail the three principal forms of Hydrogen storage under gas, liquid and solid forms [5].

#### 2.1.2.1 Gaseous hydrogen

Hydrogen may be compressed and stored in a high pressure gas cylinder for pressures up to 700 bar. Increasing gas pressure improves the energy density of hydrogen which increases from 120-142 MJ.m<sup>-3</sup> to 1700 kJ.m<sup>-3</sup>, leading to smaller, but

not lighter, container tanks. More recently, carbon fibre-reinforced composites are tested as tank materials to stand high pressures and are much lighter. Also, cryogas, gaseous hydrogen cooled to near cryogenic temperatures, is another alternative that can be used to increase the energy density by volume of gaseous hydrogen. Finally, a more novel method to store hydrogen gas at high pressures is the use of glass microspheres [5]. Car manufacturers such as Honda have demonstrated gaseous hydrogen methods [Web 16]. The following sections provide more details of four of the most promising methods to store hydrogen gas under high pressure.

### **Steel, composite and cryogas tanks**

The most common method to store hydrogen in gaseous form is in steel tanks. In fact, tanks are made of materials with a very high tensile strength, a low density, and without any affinities with hydrogen, typically, stainless steel. Because hydrogen is a small, energetic molecule, it tends to diffuse through any liner material intended to contain it, e.g. materials without carbon grain-boundary segregation, leading to the embrittlement of its container. That is why materials easily subject to embrittlement should not be used, such as high strength steels (ferritic, martensitic and bainitic steels), titanium and its alloys and some nickel-based alloys. Instead, austenitic stainless steels, copper or aluminium alloys are largely immune to hydrogen effects at ambient temperatures. As for composite tanks, there are several advantages. Their low weight meets key targets. Composite tanks require no internal heat exchange and may be usable for cryogas. They consist of three layers: an inner polymer liner, overwrapped with a carbon-fibre composite and an outer layer of an aramid-material capable of avoiding mechanical and corrosion damage [5].

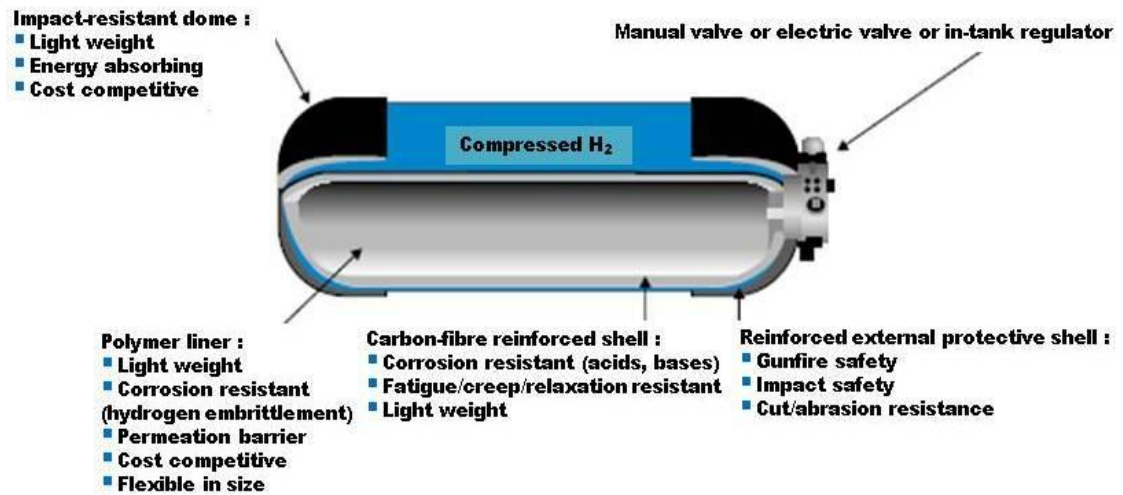


**Figure 2.1:** Schematic of a typical compressed hydrogen composite tank, *Quantum Technologies*, [1]

Another approach into cryo-compressed tanks is based on the fact that, at a fixed pressure and volume, gas tank volumetric capacity increases as the tank temperature decreases [Web 17]. Thus, by cooling a tank from room temperature to liquid nitrogen temperature ( $-196^{\circ}\text{C}$  or  $77\text{K}$ ), its volumetric capacity will increase by a factor of four, although system volumetric capacity will be less than this due to the increased volume required for the cooling system.

For all these three techniques, the main disadvantages are the large physical volume required and the fact that the ideal cylindrical shape is difficult to conform to the available space especially in vehicles. Moreover, achieving higher pressures (up to 800 bar) necessitates a greater use of external energy to power the compression. Indeed, according to Zhou *et al.* [6], the isothermal compression of hydrogen from 1 bar to 800 bar consumes energy of  $2.21 \text{ kWh.kg}^{-1}$ ; in a real compression work, consumption is even higher because the compression is not isothermal.

Research & Development (R&D) is needed on material embrittlement, the development of stronger and low-cost construction materials, e.g. carbon fibres and the development of techniques to recover the compression energy during vehicle operation.

### **Glass microspheres**

A less common method to store hydrogen gas is the use of glass microspheres [1]. Hollow glass spheres are filled with hydrogen at high pressure (350-700 bar) and high temperature (300°C) by permeation in a high-pressure vessel. Next, the microspheres are cooled down to room temperature and transferred to the vehicle tank. Finally, they are heated up to 200-300°C for a controlled release of hydrogen.

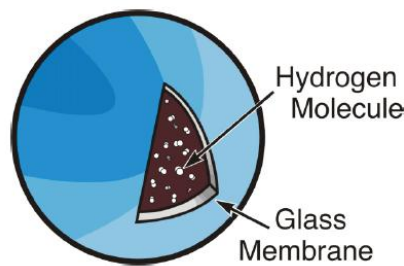


**Figure 2.2:** Schematic of a hollow Glass microsphere for hydrogen storage, [Web 18]

A clear advantage is the potentiality of a safe onboard storage and also it can be used in conformable tanks [Web 19].



**Figure 2.3:** Prototype of a two-cell conformable tank, Thiokol Propulsions, [Web 20]



The hydrogen storage density has been demonstrated to be 5.4 wt % at a pressure of x bar. Nevertheless, it shows some disadvantages. The main drawback is that the spheres slowly leak hydrogen at ambient temperature. The second disadvantage is the high temperature requirement. R&D is needed to ensure stronger glasses are developed and an optimal H<sub>2</sub> permeability is achieved.

Gaseous hydrogen remains the most established method to store hydrogen in specially-designed tanks along with liquid Hydrogen.

#### 2.1.2.2 Liquid Hydrogen

Alternatively, high volumetric density liquid hydrogen may be used. However, liquid hydrogen is cryogenic and requires extremely cold temperatures (-253°C at an atmospheric pressure). Another option includes storing hydrogen as a constituent in other liquids, such as anhydrous NH<sub>3</sub> [5].

#### **Cryogenic liquid hydrogen**

It has a density of 70.8 kg.m<sup>-3</sup> at normal boiling point which is -253°C. The theoretical gravimetric density is 100 wt % and only 20 wt % of this can be reached in practical systems. The corresponding volumetric densities are: 80 kg.m<sup>-3</sup> in theory and 30 kg.m<sup>-3</sup> in practice. It means that the energy densities are much higher than the ones from compressed hydrogen but about 30-40 % are lost in the production step. As the critical temperature is -240°C and the critical pressure is 13 bar (above these pressure

and temperature, hydrogen is gaseous), liquid hydrogen containers are open systems to prevent strong overpressure.

Therefore, heat transfer through the container leads directly to the loss of hydrogen. Larger containers have a smaller surface to volume ratio than small containers, so the loss of hydrogen is smaller. Moreover, another drawback is the necessity to use super-insulated cryogenic containers as the liquid storage tank must be reinforced (compressing constraints) but also insulated (chilling constraints) because the liquefaction process involves pressurising and cooling steps. Ice may form around the tank and help corrode it further if the insulation fails.

The challenges of liquid hydrogen storage are the energy efficiency of the liquefaction process and the thermal insulation of the cryogenic storage tank in order to limit the boil-off of hydrogen. So, insulation for liquid hydrogen tanks is usually expensive and delicate. Thus, applications are limited to the air and space where extra-costs have a limited impact.

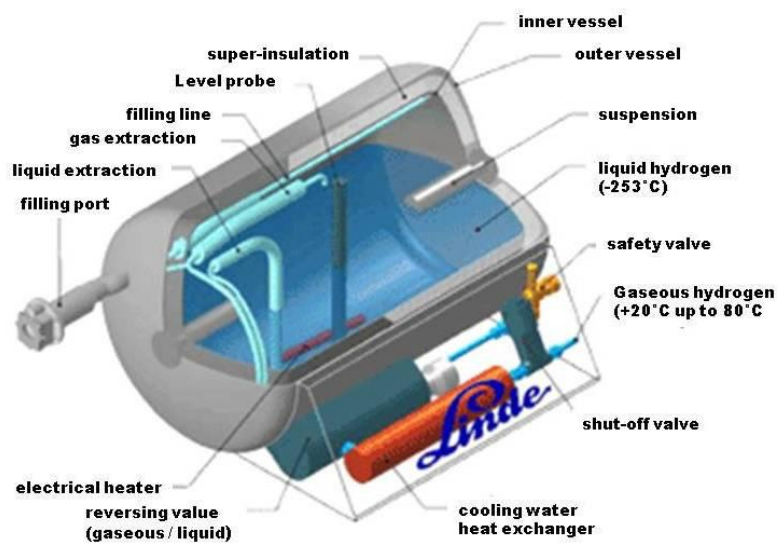


**Figure 2.4:** Schematic of a typical cryogenic hydrogen tank, the *Linde Group*, [Web 21]

The main advantage with liquid hydrogen is the high storage density that can be achieved at relatively low pressures. Liquid Hydrogen has been demonstrated in vehicles especially by BMW, producing BMW Hydrogen 7 vehicles [Web 22]. R&D is needed especially for more efficient liquefaction, lower cost and better insulated containers and an automated boil-off capture and reliquefaction.

### **Anhydrous ammonia NH<sub>3</sub>**

Ammonia provides high theoretical hydrogen gravimetric and volumetric densities of respectively, 17.7 wt % and 105 kg.m<sup>-3</sup>. It has mild pressurisation and cryogenic constraints [5], [Web 17]. It can also be stored as a liquid at ambient temperature and pressure when mixed with water. It is the second most commonly produced chemical in the world. Ammonia (NH<sub>3</sub>) releases H<sub>2</sub> in an appropriate catalytic reformer through the equation:  $NH_3 \rightarrow \frac{1}{2}N_2 + \frac{3}{2}H_2$  at temperatures between 650°C and 1000°C, using nickel catalysts. It could be used for on-board catalytic cracking of vaporized NH<sub>3</sub> to provide N<sub>2</sub> and H<sub>2</sub> for fuel cells (FC) or else, it could be directly burned in a modified ICE. However, ammonia is a toxic gas at normal temperature and pressure and has a potent odour. There must be a dissociation system for fuel cell applications as the residual NH<sub>3</sub> could be potentially poisonous for the fuel cells (especially the PEMFC).

R&D is still needed to develop highly efficient cracking catalysts and a thorough purification system to avoid residual NH<sub>3</sub>.

In general, it can be concluded that the handling and transport of liquid hydrogen, which may involve highly toxic chemicals or extreme temperatures, requires a safe and well-organised industrial infrastructure. The build-up of such infrastructure could be quite costly and would integrate other applications such as stationary applications and aviation transport.

#### 2.1.2.3 Hydrogen in solids

Storage of hydrogen in solid materials has the potential to be a safe and energy-efficient medium for vehicular and stationary applications. They can be divided into two categories: Carbon and other high-surface area materials such as zeolites, MOFs, and clathrate hydrate and Rechargeable hydrides.

#### **Adsorption by Carbon and other HSA materials**

This approach consists in adsorbing molecular hydrogen into a solid storage material such as:

- **Carbon structures** (e.g. fullerenes, single or multi-walled nanotubes or activated carbon) ;
- **Non-carbon structures** (e.g. zeolites with different pore architecture and composition or metal-organic framework) ;
- **Miscellaneous structures** (e.g. boron nitride (BN) nanostructures, clathrates or polymeric adsorbers).

According to the International Union of Pure and Applied Chemistry (IUPAC), the classification of the pores is as follows:

- Micropores are the pores with an internal diameter less than 2 nm;

- Mesopores are the pores with an internal between 2 and 50 nm;
- Macropores are the pores with an internal diameter greater than 50 nm.

It is quite usual to see in the literature the term nanopores as this implies pores of the nanometre size. In the last few years, carbon-based nanoporous materials such as activated carbons, single-walled carbon nanotubes and metal-organic frameworks have been proposed as the most promising adsorbents for hydrogen storage applications. Hydrogen densities similar to liquid hydrogen can be achieved with appropriate adsorption media. Hydrogen adsorption at solid surfaces is closely related to the applied pressure and the temperature. The variation of attractive surface forces as a function of distance from the surface indicates whether Van der Waals type weak physisorption (physical adsorption) of molecular hydrogen ( $H_2$ ) occurs, or whether dissociation and chemisorptions (chemical adsorption) of atomic hydrogen (H) takes place.

- *Carbon-based materials*

Elemental carbon can form a variety of structures: graphitic carbon; activated carbon; carbon nanofibers; carbon fullerenes and carbon nanotubes. One of the first investigations of the adsorption of hydrogen on high-surface-area carbon (coconut-shell charcoal) was reported in a paper by Kidnay and Hiza [7] in 1967. They focused on the behaviour of adsorbents from a cryogenic engineering perspective. Numerous works have been carried out mainly on activated carbon, graphitic nanofibers and single-walled carbon nanotubes. Firstly, activated carbon has been proposed as a storage medium for hydrogen. A density of about 40 % of liquefied hydrogen was

reported by Chahine and Bose [8] to be adsorbed at 5 MPa using densified activated carbon with a high surface area and a high bulk density. However, a temperature of -196°C (77K) was required to achieve this level of performance. Thus, this thermal management issue has prompted work on other carbon structures that could adsorb hydrogen in significant quantity at milder temperatures. As reported in a review by Dillon [9]-[10], carbon nanofibers in one hand and carbon nanotubes on the other hand have been extensively studied before 2001 but everybody agrees [11] the spectacular initial storage capacities [12]-[13],[15], reported few years ago have not been reproducible and that they might have been the result of measurement errors. Systematic studies have been initiated to highlight the main issues [16]-[18]. Under ambient conditions, practical hydrogen storage capacities inferior to 3 wt % have been found in a variety of nanostructured carbon materials; this is well short of DOE targets. However, there is still hope as some encouraging results have been obtained with a promising method which consists in the dissociation of hydrogen followed by spillover [19]. Also, several studies have shown interesting enhancements in hydrogen uptake by doping transition metals on carbon structures. Calculations predict a possible hydrogen uptake of up to 7 wt % with a suitable structure such as carbon nanotubes with a defect-modulated titanium doping reported by Shevlin and Guo [20]. The task for the future is to synthesize modelled carbon materials [21].

R&D is still required to develop a carbon sample and activation procedure that can be used as an international standard in the field, study carbon-metal composites capable of catalysing H<sub>2</sub> dissociation and spillover and continue theoretical modelling studies of H on carbon surfaces and in bulk.

- ***Other materials: Zeolites, MOFs and clathrate hydrates***

Besides the carbon materials, other materials such as zeolites, metal Organic Frameworks (MOFs) and clathrate hydrates have been investigated for hydrogen storage.

Firstly, Dyer [22] described zeolites as a large class of highly crystalline aluminosilicate materials defined by a network of linked cavities and pores of molecular dimensions that gives rise to their molecular sieving properties. Zeolites were before the development of coordination polymers such as MOFs the crystalline materials with the highest specific surface reported to be  $900 \text{ m}^2.\text{g}^{-1}$  for zeolite Y. The work of Weitkamp *et al.* [23] in 1995 was among the first ones on zeolites specifically for hydrogen storage applications. They investigated zeolites with different pore architectures and compositions e.g. A, X and Y in the temperature range from  $25^\circ\text{C}$  to  $200^\circ\text{C}$  and pressure range from 0.25 to 10 MPa. The results suggest that zeolites containing sodalite cages in their structure are particularly suitable for hydrogen uptake, with the highest  $\text{H}_2$  storage capacity of 0.08 wt % for a sample loaded at  $200^\circ\text{C}$  and 10 MPa. Since, several structures have been investigated and a maximum of 1.8 wt % of adsorbed hydrogen has been found for a zeolite NaY at  $-196^\circ\text{C}$  and 1.5 MPa by Langmi *et al.* [24]. Not surprisingly, it had been found that the maximum hydrogen uptake occurs at liquid nitrogen temperature of  $-196^\circ\text{C}$ , because hydrogen molecules are not particularly active at  $-196^\circ\text{C}$  as they are at room temperature. Therefore, it is difficult for these hydrogen molecules to escape after being compressed into the small channels in the zeolite. Adsorption data for ambient temperature, which seems more realistic for onboard storage in cars, are relatively scarce. For a composite material

consisting of the lithium form of low-silica X (LSX) zeolite [25], platinum on activated carbon catalyst and specially generated carbon bridges between the two solid phases, a sorption capacity of 1.6 wt% has been reached at room temperature (25°C) and a pressure of 10 MPa, this is the highest hydrogen uptake reported for zeolites as hydrogen stores. Cryogenic condition is certainly one of the necessary requirements for a higher hydrogen uptake in zeolites, but will inevitably increase the cost of hydrogen storage applications, similar to the issues with liquid hydrogen storage. From 2008 onwards, no publications have been done on hydrogen storage applications for zeolites.

MOFs are a new class of crystalline materials with a low density, a high specific surface area and a structural stability. Hirscher and co-workers [26] described MOFs as one of the most interesting adsorbents for hydrogen storage applications. In 1999, Li *et al.* [27] used carboxylate rigid organic ligands to aggregate metal ion clusters which have been found to be ideal to form extended and very stable frameworks. In 2003, the first investigations of hydrogen storage in MOFs were reported for MOF-5 (see Fig 2.6) [28]. This showed that, at -196°C (77K) MOFs can store more hydrogen than any other crystalline microporous materials. The low adsorption temperature and the reversibility of the process indicate clearly that it is a very similar process to that of physisorption in zeolites for instance. These first investigations generated a lot of interest and initiated numerous reports especially on MOF-5 and IRMOF-1 (isorecticular MOF) which have been extensively studied due to its high specific area and the simple and cheap chemical constituents. The high hydrogen uptake values of MOF-5 of 1 wt% at room temperature and 4.5 wt% at -196°C (77K) and 0.8 bar obtained in 2003 [28] have been confirmed later on but at least 2 other independent



laboratories [29]-[30]. Even, a maximum of 7 wt % has been reported by Lin *et al.* [31] for copper co-ordination framework materials with a high BET specific surface area of 3000-4700 m<sup>2</sup>.g<sup>-1</sup>. In this series of materials, the density of the adsorbed hydrogen decreased with increasing pore size while the amount adsorbed increased. This suggests that there is an optimum pore size for hydrogen adsorption. There are now several reported MOFs which has more than 6 wt % H<sub>2</sub> storage capacity at -196°C (77K) and moderate pressures (<80 bar) e.g. MOF-177.

However, MOFs show high moisture sensitivity and challenging low H<sub>2</sub>-storage capacity at room temperature. To improve room-temperature uptake [32], there is a need to modify MOFs in order to strengthen the hydrogen binding with frameworks because the preference for low temperature adsorbing can be explained by the fact that hydrogen interaction with the surfaces of materials is a weak dispersion like the one observed in other microporous materials.

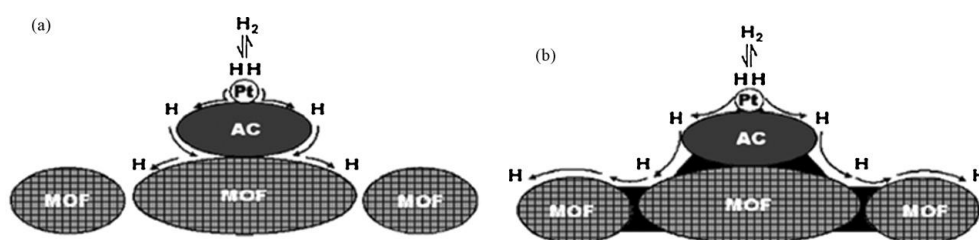


**Figure 2.5:** Hydrogen spill-over applied to MOFs [32]

Another type of hydrogen storage materials has been exhibited, namely the clathrate hydrogen hydrates. Clathrate hydrates are best known for their ability to encapsulate methane, which is assumed to be present in this form in vast amounts on the ocean floor. In such gas hydrates, the water molecules form cages in which guest molecules such as methane can be trapped. Some years ago, it was discovered by Mao

*et al.* [33] that hydrogen molecules could also be encapsulated in clathrate structures at high pressures of about 2000 bar and a temperature of  $-24^{\circ}\text{C}$  to form a pure  $\text{H}_2$ -clathrate compound. Storage of  $\text{H}_2$  in this type of material is carried out by capturing the hydrogen in  $\text{H}_2\text{O}$  cages. Hydrogen-bonded  $\text{H}_2\text{O}$  frameworks can generate polyhedron cages around guest molecules to form solid clathrate hydrates. Lee *et al.* [34] studied the clathrates to find practical conditions in which they can be used as hydrogen storage materials and found that, when THF is added to the mixture, the pressure can be lowered considerably. However it still remains a challenge to employ hydrogen hydrates as practical hydrogen storage materials. The synthesis process is very slow because their formation is controlled by diffusion through a bulk solid phase. Permanent cooling which is necessary to keep hydrogen hydrates stable may become an issue because, if the cooling fails, the material will release large amounts of hydrogen in a rather short time, which may lead to safety problems. The main advantage of adsorption for hydrogen storage is that hydrogen can be stored at ambient temperature under low pressure, which is much safer than the compressed-gas in tank hydrogen storage. The relatively low cost of the materials provides economical benefits. However, the strong dependence on the low temperature for high hydrogen uptake is the main drawback for hydrogen adsorption. Apart from adsorption, another type of interaction can be exploited for hydrogen storage applications: absorption/desorption.

### Absorption/Desorption via rechargeable hydrides

Research on absorption/desorption of hydrogen via hydrides has been going on for decades and has been compiled in a huge database. A summary of this database held by the IEA HIA is provided in the following figure. The alloy side of the tree represents compounds where H is usually bound in interstitial sites in a metallic state. From this category, Mg and Mg-based compounds have proved to be very promising. The right side is a representation of the complexes which have recently provided encouraging results and may offer hope.

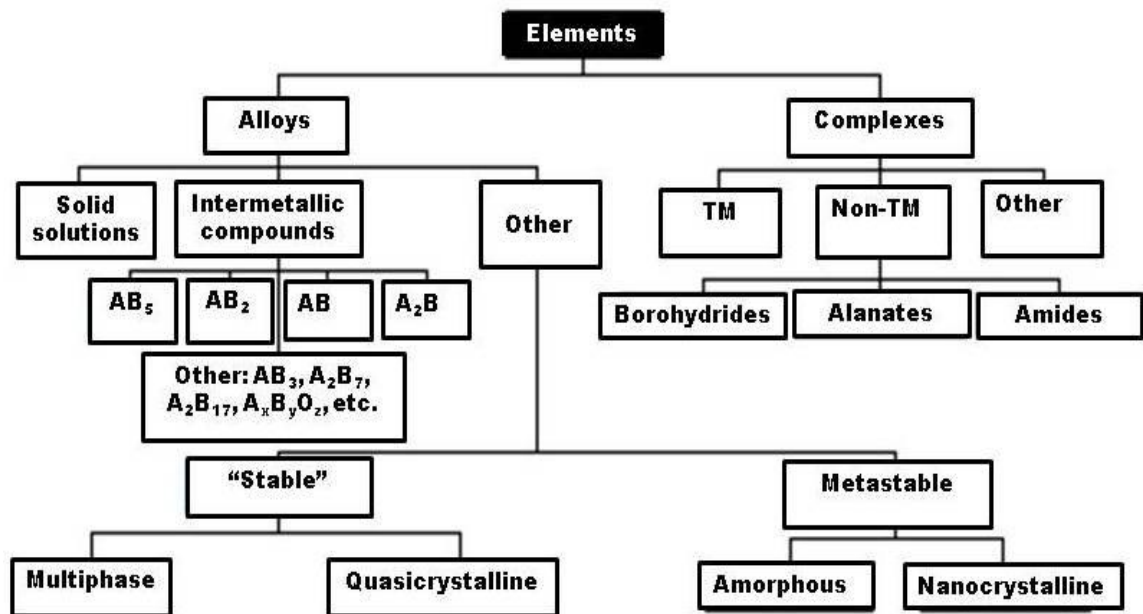
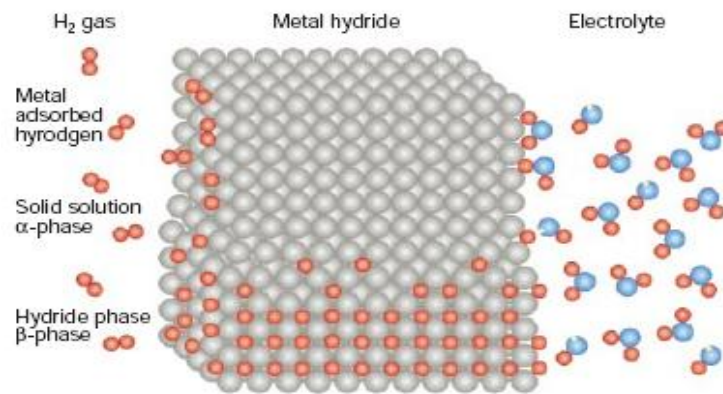


**Figure 2.6:** Family tree of hydriding alloys and complexes, Sandrock [35]

- ***Absorption/Desorption via metal hydrides***

Many solid materials like metals and alloys are capable of reversibly absorbing large amounts of hydrogen. Charging can be made using either molecular hydrogen  $H_2$  or H atoms coming from an electrolyte as schematised in the next figure. Before absorption, molecular hydrogen is dissociated into two H atoms at the surface and in the desorption process, the two atoms recombine to  $H_2$ .



*Hydrogen atoms are from physisorbed hydrogen molecules on the left-hand side and from dissociation of water molecules on the right-hand side*

**Figure 0.7:** Schematic model of metal structure with H atoms in the interstices between the metal atoms and  $H_2$  molecules at the surface. Schlapbach and Züttel [36]

The host metal initially dissolves some hydrogen as a solid solution ( $\alpha$ -phase). As the hydrogen pressure and the concentration of hydrogen in the metal increases, interactions between hydrogen atoms become locally important and nucleation and growth of the hydride, known as the  $\beta$ -phase, occur. Due to the phase transition upon hydrogen absorption, metal hydrides have the very useful property of absorbing large amounts of hydrogen at a constant pressure, i.e. the pressure does not increase with the amount of hydrogen absorbed as long as the phase transition occurs. The

characteristics of the hydrogen absorption and desorption can be tailored by partial substitution of the constituent elements in the host lattice.

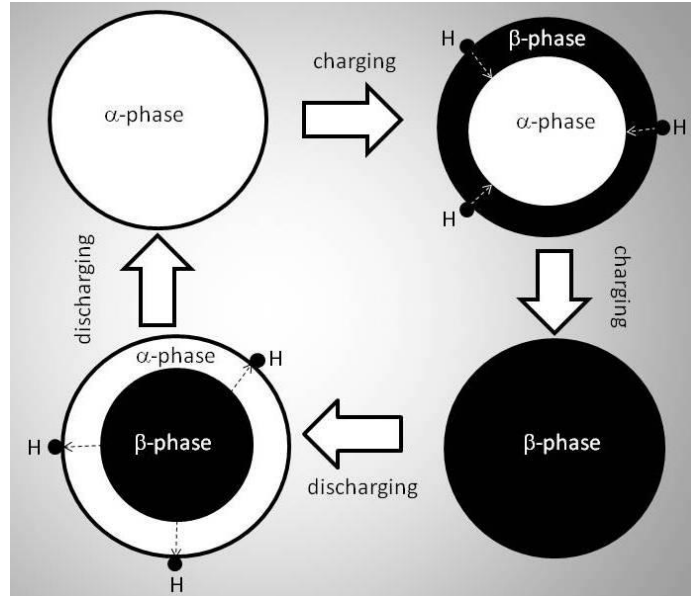


**Figure 2.8:** Schematic of phase transitions in most of the metal hydrides, David [37]

The main interaction when a hydrogen molecule approaches the metal surface is due to the Van der Waals forces leading to the physisorbed state ( $E_{\text{phys}} \approx 10 \text{ kJ.mol}^{-1} \text{H}_2$ ), approximately at a distance of one molecular radius ( $\approx 0.2 \text{ nm}$ ) from the metal surface. Due to the weak interaction, a significant physisorption is only observed at low temperatures ( $< 0^\circ\text{C}$ ). This kind of interaction is too weak to hold more hydrogen molecules. Most absorption occurring on the surface is one of the reasons for the low capacity of physisorption systems.

In fact, the initial penetration of H is slightly linked to surface structure, morphology and purity. In most cases, there is an oxide barrier at the grain surface inducing an incubation period. Hence, the dissociation of hydrogen molecules is more difficult to be achieved at the grain boundaries. This step is kinetically limiting the

hydrogenation reaction. This can be quantified by measuring the pressure variations as a function of time. Three steps are identified: incubation, absorption and equilibrium. To decrease the time of incubation, using additives seems to be a good solution. Particles of additives segregate at the grain boundaries playing a catalytic role for the hydrogen molecule dissociation. By this way, absorption occurs earlier.

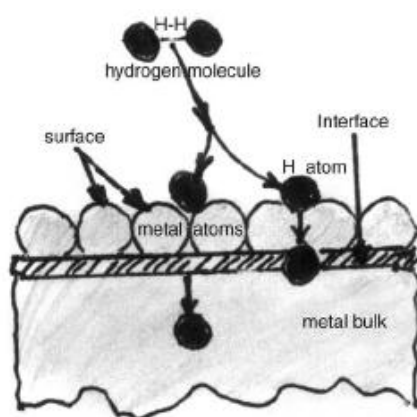


**Figure 2.9:** Molecular processes during hydrogen uptake, David [37]

Several families of intermetallic compounds are interesting for hydrogen storage. They all consist of an element with a high affinity to hydrogen, the A-element and an element with a low affinity to hydrogen, the B-element. The latter is often nickel as nickel is an excellent catalyst for the hydrogen dissociation. The electropositive elements are the most reactive ones i.e. scandium, yttrium, the lanthanides, the actinides, and the members of the titanium and vanadium groups.

**Table 2.2:** Hydrogen storage properties of intermetallic compounds according to the online database of the I.E.A. [38]

Type	Metal	Hydride	Crystallographic Structure	Gravimetric density (wt % H <sub>2</sub> )	P (bar)	T (°C)
elemental	Pd	PdH <sub>0.6</sub>	Pm3m	0.56	0.02	25
AB	FeTi	FeTiH <sub>2</sub>	Pm3m	1.89	5	30
AB <sub>2</sub>	ZrV <sub>2</sub>	ZrV <sub>2</sub> H <sub>6.5</sub>	Fd3m	3.01	10 <sup>-9</sup>	50
AB <sub>2</sub>	TiV <sub>2</sub>	TiV <sub>2</sub> H <sub>4</sub>	b.c.c.	2.6	10	40
A <sub>2</sub> B	Mg <sub>2</sub> Ni	Mg <sub>2</sub> NiH <sub>4</sub>	P6222	3.59	1	282
AB <sub>5</sub>	LaNi <sub>5</sub>	LaNi <sub>5</sub> H <sub>6</sub>	P6/mmm	1.37	2	25

*A is an element with high affinity to hydrogen and B is an element with low affinity to hydrogen.*

One of the most interesting properties of the metal hydrides is the extremely high volumetric density of the hydrogen atoms present in the host lattice. Intermetallic hydrides reach a volumetric hydrogen density of 115 kgH<sub>2</sub>.m<sup>-3</sup> e.g. LaNi<sub>5</sub> to form LaNi<sub>5</sub>H<sub>6</sub>. Metal hydrides are very effective to store large amounts of hydrogen in a safe and compact way. All the reversible hydrides working around ambient temperature and atmospheric pressure consist of transition metals; therefore the gravimetric hydrogen density is limited to less than 3 wt % H<sub>2</sub>. For instance, the gravimetric density of LaNi<sub>5</sub>H<sub>6</sub> is only 1.4 wt % H<sub>2</sub>. Recent attention turned to the hydrides formed by light weight metals, and Mg became and still is the focus. Magnesium hydride, MgH<sub>2</sub>, has a high theoretical H<sub>2</sub> capacity of 7.7 wt % combined with good reversibility [39]. But, the initial experimental results [40] showed a high operating temperature of around 300°C due to the high thermodynamic stability of MgH<sub>2</sub>, which is too high for practical onboard applications.

Many efforts have been devoted in recent years to reduce desorption temperature and to fasten the re/dehydrogenation reactions. To achieve this, researchers [41] tried to change the microstructure of the hydride by ball-milling or mechanical alloying with

elements such as Zn, Al, Fe, Ag, In or Cd which reduce the stability of the hydrides and also by using appropriate catalysts such as transition metals (e.g. Pd or Pt) or oxides (e.g.  $\text{TiO}_2$ ,  $\text{V}_2\text{O}_5$ ,  $\text{Cr}_2\text{O}_3$ ,  $\text{Mn}_2\text{O}_3$ ,  $\text{Fe}_3\text{O}_4$  or  $\text{CuO}$ ) to facilitate the dissociation and recombination of hydrogen molecules at the surface of the magnesium particles and therefore improve kinetics by accelerating the gas-solid reaction. Although many efforts have been devoted to the Mg-based hydrides in recent years, it remains a challenge to explore the properties of other appropriate light weight metal hydrides.

- *Absorption/Desorption via complex hydrides*

Finally, complex hydrides form a category of hydrogen storage materials which have attracted growing interest. Actually, the groups I, II and III of light elements such as Li, Mg, B, Al, N build a large variety of metal hydrogen complexes. They are all saline materials in which hydrogen is covalently bonded to central atoms in “complex” anions in contrast to interstitial hydrides. These are especially interesting because of their light weight and the number of hydrogen atoms per metal atom which is in many cases 2. This kind of complexes shows the highest volumetric density:  $150 \text{ kgH}_2\cdot\text{m}^{-3}$  with for example  $\text{Al}(\text{BH}_4)_3$ , and the highest gravimetric density known today for a chemical hydrogen material: 21 wt %  $\text{H}_2$  with  $\text{Be}(\text{BH}_4)_2$ . The main difference of the complex hydrides to the above described metal hydrides is the transition to an ionic or covalent compound of the metals upon hydrogen absorption. Unlike the metal hydrides, hydrogen in complex hydrides is released via a cascade of decomposition steps and each step reaction calls for different conditions. The current barriers stem from the high pressure and temperature conditions needed in order to form the hydride and to release the hydrogen. Therefore, there is a huge difference between the



theoretical capacity and the practically attainable capacity. Similarly to the metal hydrides, the challenge stands in the capacity to explore the properties of new and appropriate light weight hydride compounds.

**Table 2.3:** Different types of complex hydrides and their gravimetric density

Anion group	Hydrides	Capacity (wt % H <sub>2</sub> )
[NH <sub>2</sub> ] <sup>-</sup>	LiNH <sub>2</sub>	8.79
	Mg(NH <sub>2</sub> ) <sub>2</sub>	7.17
	NaNH <sub>2</sub>	5.18
[BH <sub>4</sub> ] <sup>-</sup>	LiBH <sub>4</sub>	18.54
	Al(BH <sub>4</sub> ) <sub>3</sub>	16.94
	Mg(BH <sub>4</sub> ) <sub>2</sub>	14.96
	Ca(BH <sub>4</sub> ) <sub>2</sub>	11.58
	NaBH <sub>4</sub>	10.68
	Ti(BH <sub>4</sub> ) <sub>3</sub>	8.60
	Zr(BH <sub>4</sub> ) <sub>3</sub>	6.58
	Fe(BH <sub>4</sub> ) <sub>3</sub>	8.14
[AlH <sub>4</sub> ] <sup>-</sup>	LiAlH <sub>4</sub>	10.64
	Mg(AlH <sub>4</sub> ) <sub>2</sub>	9.36
	Ca(AlH <sub>4</sub> ) <sub>2</sub>	7.91
	NaAlH <sub>4</sub>	7.48
	Ti(AlH <sub>4</sub> ) <sub>3</sub>	8.60

In summary, hydrogen can be stored in different forms in tanks as a cryogenic liquid or a compressed gas. Liquid hydrogen presents some advantages and disadvantages comparatively to gaseous hydrogen. The main advantage is the high density of liquid hydrogen which allows the storage of greater quantities of hydrogen than in the gaseous state. Another advantage is its storage at low pressure. Nevertheless, the major drawbacks on top of the cost and energy consumption are the

losses due to evaporation. BMW and General Motors (GM) are the main automotive companies working with liquid hydrogen and all other companies such as Daimler Chrysler, Ford, Honda, Toyota and Nissan/Renault think more seriously on gaseous hydrogen initially at 350 bar with the future development of tanks at 700 bar. Apart from tanks of gaseous or liquid hydrogen, hydrogen can be stored on the surfaces of solids by adsorption or within solid materials making it possible to store larger quantities of hydrogen in smaller volumes at low pressure and at temperatures closer to room temperature. It is also possible to achieve volumetric storage densities greater than liquid hydrogen because the hydrogen molecule is dissociated into atomic hydrogen within the metal hydride lattice structure. Finally, hydrogen can be strongly bound within molecular structures, as chemical compounds containing hydrogen atoms.

The following figure compares the volumetric and gravimetric H<sub>2</sub> density of the main storage options and shows that up to now, no current technology meets the targets. There is room for improvement for complex hydrides.

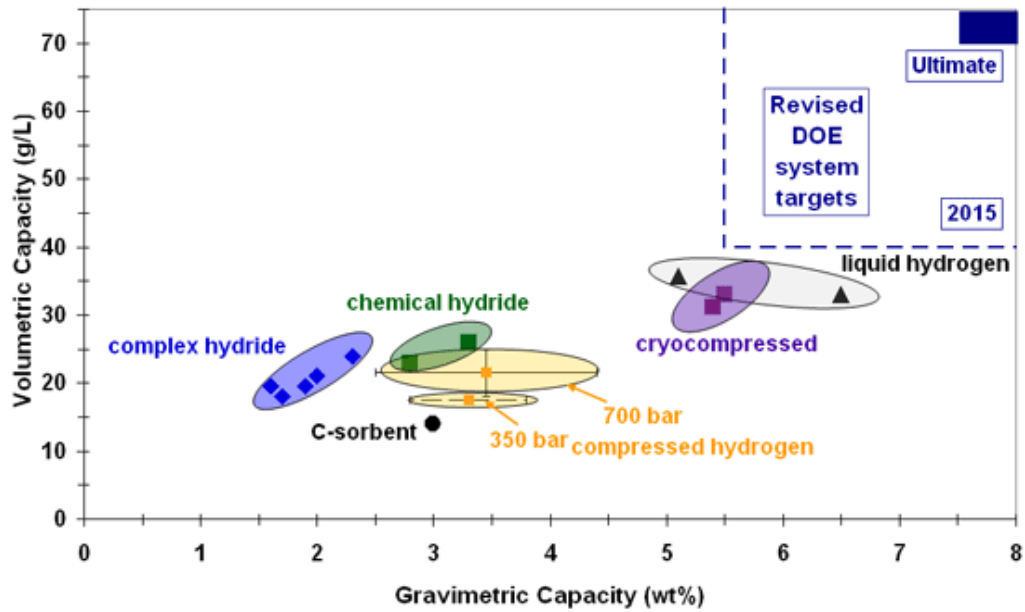


**Figure 2.10:** Hydrogen capacities for various stores, Fuel cell program from the Department of Energy, USA [Web 23]

For this present study, a hydrogen capacity of 5 wt % has been chosen for the material gravimetric density as our own target and this has strongly orientated the study towards the complex hydrides as within this category, several materials have this potential in terms of theoretical gravimetric capacities. Indeed, gaseous and liquid hydrogen are impractical for vehicular applications due to safety issues and volumetric constraints whereas hydrogen in physisorbed materials and metal hydrides, despite decades of extensive research have not exhibited any promising features in terms of high gravimetric hydrogen density, adequate hydrogen dissociation energetic, reliability and low cost, a combination necessary for commercial vehicular applications. Therefore, storing hydrogen in complex hydrides holds much more promise than the other storage methods and that is the main reason why a thorough description is done in the following sub-chapter.

## 2.2 Research on complex hydrides

Complex hydrides are considered as chemical hydrogen storage materials. They use light elements such as nitrogen, boron or aluminium to chemically bind hydrogen. In these chemical hydrogen storage materials, hydrogen is ‘discharged’ by a series of chemical reactions and the hydrogen is ‘recharged’ by a chemical processing pathway. This makes them unique compared to the previously described metal hydrides or carbon adsorbents where the hydrogen release and uptake is controlled by temperature and pressure. In the following paragraphs, alanates, amide-based systems and amine-boranes are described briefly whereas, borohydrides are described more thoroughly.

### 2.2.1 Alanates

The term “alanates” or “aluminumhydrides” refers to a family of compounds containing hydrogen and aluminium. Since the pioneering work of Bogdanovic *et al.* [42] on Ti-catalyzed  $\text{NaAlH}_4$  in 1996, catalysed alanates have offered a renewed potential. Their main attractive feature is their easy accessibility. Sodium and lithium alanates are commercially available while magnesium alanate can be processed easily [43]. In fact, studies involving complex hydrides of aluminium have been restricted, in the first time, to sodium aluminium hydride with a small amount of work reported involving lithium aluminium hydride. But now, there is a number of other alanates which are being explored for hydrogen storage applications.

2.2.1.1 Sodium alanate, NaAlH<sub>4</sub>

The decomposition occurs in two stages:



Firstly, Bogdanovic and coworkers [44] discovered that the addition of transition-metal-based catalysts to NaAlH<sub>4</sub> enhanced not only the dehydriding and rehydriding kinetics from [45] (cited from [46]) 17.5 MPa hydrogen pressure at 270°C for 3 hours to 15.2 MPa hydrogen pressure at 170°C for 3 hours but also lowered considerably the decomposition temperature from 200°C to only 150°C. Many other research groups focused their activity in understanding the mechanisms involved in catalyzed sodium alanates. Among them, Zaluska *et al.* [47], Walters *et al.* [48], and Gross *et al.* [49] may be cited. These groups confirmed that solid-state addition of catalysts to NaAlH<sub>4</sub> via high-energy ball milling was an impressive way to enhance kinetics and to lower desorption temperature.

2.2.1.2 Lithium alanate, LiAlH<sub>4</sub>

In the same view, numerous researchers have now studied the hydriding/dehydriding properties of LiAlH<sub>4</sub>. The study of lithium alanate shows that the decomposition also occurs in three (3) stages:



It has been demonstrated that the decomposition of  $\text{LiAlH}_4$  can be catalysed by the milling of  $\text{TiCl}_4$  with  $\text{LiAlH}_4$  forming an intermediate nano- or microcrystalline phase,  $\text{AlTi}_3$  [50], eliminating the first step and lowering the decomposition temperature of the second step [51]. The effect of many other catalysts has been put to the test but it appears that Ni [52] and  $\text{NiCl}_2$  [53] are the most effective ones lowering (for the latter) the dissociation temperature by  $50^\circ\text{C}$ . Also, it has been proved [54] that it is possible to achieve reversibility of the second step but not the first.

#### 2.2.1.3 Other alanates: $\text{Mg}(\text{AlH}_4)_2$ and $\text{KAlH}_4$

In addition to the extensively studied  $\text{NaAlH}_4$  and  $\text{LiAlH}_4$ , researchers such as Fichtner *et al.* [43] and Wang *et al.* [55] reported interesting hydriding capabilities of  $\text{Mg}(\text{AlH}_4)_2$  and Ti-doped  $\text{Mg}(\text{AlH}_4)_2$  respectively. They found reasonable dehydrogenation rates and a high hydrogen capacity but strictly no reversibility. As for  $\text{KAlH}_4$ , Morioka *et al.* [56] demonstrated reversible hydrogen capability but the dissociation temperature reported was too high (above  $300^\circ\text{C}$ ) and more recently, Ares *et al.* [57] demonstrated a significant reduction in desorption temperature upon doping by  $\text{TiCl}_3$  by  $50^\circ\text{C}$ .

The successful research around alanates, mainly from the point of view of lowering the dissociation temperature as well as kinetics, allows us to think that the methods could be transposed to other complex hydrides of higher hydrogen content such as amides-based systems, borohydrides and amine-boranes.

## 2.2.2 Amides-based systems

The association of amides and other hydride compounds exhibits exciting reversible hydrogen capacity [58] as opposed to amides alone.

### 2.2.2.1 Lithium amide, $\text{LiNH}_2$

Lithium amide,  $\text{LiNH}_2$  is a member of the alkali metal amides family. It is an important reagent in organic synthesis. Lithium amide and other alkali metal amides play a prominent role in the development of chemistry.  $\text{LiNH}_2$  is a body-centred-cubic (bcc) tetragonal structure as shown in Figure 2.11, below with lattice parameters:  $a=5.034 \text{ \AA}$  and  $c=10.256 \text{ \AA}$ .

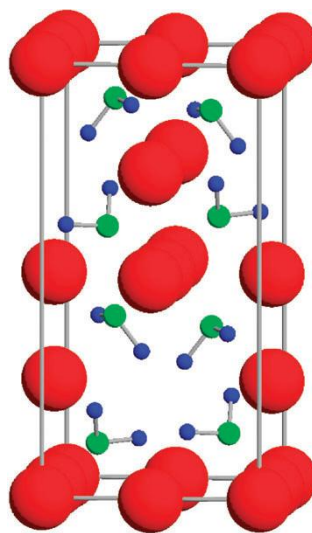


**Figure 2.11:** Crystal structure of  $\text{LiNH}_2$ ; red (large), green (middle) and blue (small) spheres represent Li, N, H atoms, respectively. (Miwa *et al.* [59] , Shevlin *et al.* [60])

Pure  $\text{LiNH}_2$  decomposes to lithium imide ( $\text{Li}_2\text{NH}$ ) and ammonia ( $\text{NH}_3$ ) at temperatures above  $200^\circ\text{C}$ . Nevertheless, it has been reported by Chen *et al.* [61] that the association with  $\text{LiH}$  would release hydrogen instead of ammonia.

#### 2.2.2.2 Association with metal hydrides

$\text{Li-N-H}$  system for hydrogen storage was also reported by Hu *et al.* [62][63]. They demonstrated that  $\text{Li-N-H}$  could be used as a reversible hydrogen storage medium with a theoretical capacity up to 10.6 wt %. It has been generally agreed that the following reaction occurs with a theoretical reversible capacity of 6.5 wt %:



The addition of  $\text{LiH}$  to  $\text{LiNH}_2$  in the dehydriding process reduces the highly supposed  $\text{NH}_3$  contamination. Also, as  $\text{LiH}$  decomposes at a very high temperature, the addition of  $\text{LiNH}_2$  to  $\text{LiH}$  was reported to dramatically decrease the desorption temperature. So, the release and uptake of hydrogen occur at milder conditions. Despite the huge interest in  $\text{LiNH}_2$ - $\text{LiH}$  mixtures, there are several problems such as: the high dissociation temperature above  $200^\circ\text{C}$ , the slow release kinetics and the release of ammonia during reaction with  $\text{LiH}$ . To understand the involved reactions, researchers have proposed two possible mechanisms. Chen *et al.* [61] claimed that the dehydrogenation process between  $\text{LiH}$  and  $\text{LiNH}_2$  proceeds by a direct molecule-molecule reaction attributable to the strong affinity between  $\text{H}^{\delta+}$  in  $\text{LiNH}_2$  and  $\text{H}^{\delta-}$  in  $\text{LiH}$ . On the other hand, Ichikawa *et al.* [64] showed experimentally that the hydrogen



desorption reaction between LiH and LiNH<sub>2</sub> is based on the intermediate reaction that involves the formation of ammonia gas as follows:



This ammonia-mediated reaction model has since been confirmed by Song *et al.* [65] using first-principles calculations but also experimentally by Yao *et al.* [66] and Shaw *et al.* [67].

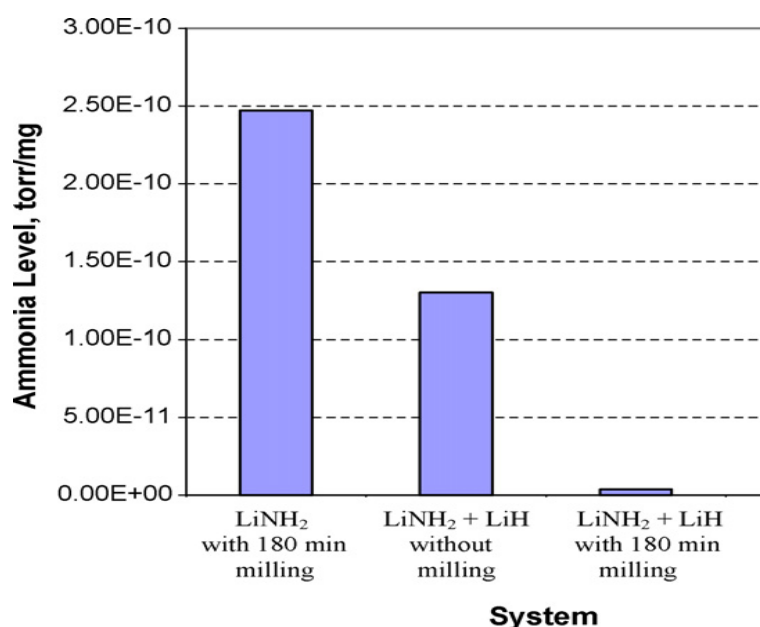


**Figure 2.12:** Comparisons in the ammonia level during TG analysis, Taken from Shaw *et al.* [67]

As the binding for amide systems is understood [60] to be ionic, the method thought to decrease the bond strength is to decrease the charge on the cations, e.g. by replacing Li by Mg or Ca. This is the strategy adopted by several groups such as Nakamori *et al.* [68], Chen *et al.* [69], Aoki *et al.* [70], Janot *et al.* [71], Chen *et al.* [72] and Xiong *et al.* [73]), Nakamori *et al.* [74] and Leng *et al.* [75]-[76]. The dehydrogenation temperatures and the hydrogen capacity of some of these systems are listed in Table

2.4 below showing comparable results to the ones obtained initially with Li-N-H systems.

**Table 2.4:** Examples of M-N-H systems, M=Li, Mg, Li-Mg, Ca, Lu [77]

Metal hydride	Reaction with metal amide	Desorption products	Desorption temperature (°C)	Hydrogen capacity (wt. %)	Source
LiH	LiH + LiNH <sub>2</sub>	Li <sub>2</sub> NH	150-430	6.5	[61] [69]
	2LiH + Mg(NH <sub>2</sub> ) <sub>2</sub>	Li <sub>2</sub> Mg(NH) <sub>2</sub>	200	5.6	[46]
	8LiH + 3Mg(NH <sub>2</sub> ) <sub>2</sub>	Li <sub>2</sub> NH-Mg <sub>3</sub> N <sub>2</sub>	< 500	7	[46]
	4LiH + Mg(NH <sub>2</sub> ) <sub>2</sub>	Li <sub>3</sub> N-Mg <sub>3</sub> N	<500	9.2	[46]
MgH <sub>2</sub>	MgH <sub>2</sub> + 2LiNH <sub>2</sub>	Li <sub>2</sub> Mg(NH) <sub>2</sub>	-	4.5	[78]
	MgH <sub>2</sub> + LiNH <sub>2</sub>	LiMgN	-	6.1	[79]
	2MgH <sub>2</sub> + Mg(NH <sub>2</sub> ) <sub>2</sub>	Mg <sub>3</sub> N <sub>2</sub>	200	7.4	[68]
CaH <sub>2</sub>	CaH <sub>2</sub> + 2LiNH <sub>2</sub>	CaNH-Li <sub>2</sub> NH	140	4.5	[80]
	CaH <sub>2</sub> + Ca(NH <sub>2</sub> ) <sub>2</sub>	CaNH	500	2.1	[81]

In conclusion, it can be said that simple metal hydrides are successfully destabilised by combining with metal amides.

#### 2.2.2.3 Association with complex hydrides: alanates and borohydrides

Based on these works on M-N-H systems in which mixtures of amide and binary hydrides were revealed to be capable of releasing hydrogen due to Coulombian attraction between H<sup>δ+</sup> in amide and H<sup>δ-</sup> in hydrides, several new systems were reported as potential candidate materials such as: Li-Al-N-H systems (Lu *et al.* [82], Kojima *et al.* [83] and Xiong *et al.* [84]) and Li-B-N-H systems (Pinkerton *et al.* [85]-[86], Meisner *et al.* [87] and Aoki *et al.* [88]). These systems generally consist of

mixtures of complex metal hydrides and metal amides. Some examples are shown in Table 2.5 below.

**Table 2.5:** Mixed complex hydrides, Lu *et al.* [77]

Complex hydride	Reaction with metal amide	Desorption products	Desorption temperature (°C)	Hydrogen capacity (wt %)
LiAlH <sub>4</sub>	LiAlH <sub>4</sub> + LiNH <sub>2</sub>	Li <sub>2</sub> NH-Al	85-320	-
	2LiAlH <sub>4</sub> + LiNH <sub>2</sub>	Li <sub>3</sub> AlN <sub>2</sub> H <sub>4</sub>	165	5
LiBH <sub>4</sub>	LiBH <sub>4</sub> + 2LiNH <sub>2</sub>	Li <sub>4</sub> BH <sub>4</sub> (NH <sub>2</sub> ) <sub>3</sub>	-	4.5
	LiBH <sub>4</sub> + LiNH <sub>2</sub>	Li <sub>4</sub> BH <sub>4</sub> (NH <sub>2</sub> ) <sub>3</sub>	500	2.1

In conclusion, amide-based systems offer an excellent potential but further improvements are still needed in order to meet the practical requirements. Moreover, the ammonia formed as a by-product should be reduced or eliminated to avoid contamination of the fuel cell. Besides the mixtures of hydrides-amides, another class of materials, the borohydrides, has been considered for hydrogen storage applications. It is reviewed in more detail as it forms a base of the different systems investigated for this particular thesis.

### 2.2.3 Borohydrides

They generally contain greater amounts of hydrogen than alanates and amides-based mixtures. In fact, metal borohydrides are the highest hydrogen containing compounds among complex hydrides.

### 2.2.3.1 Background information

The terms “Tetrahydroborate” or “Borohydride” refer to either the compounds containing a metal and a hydroborate group,  $[BH_4^-]$  or more generally to the compounds containing boron and hydrogen. Due to a desire for uniformity and clarity, the IUPAC has recommended the name tetrahydroborate even if the term borohydride is widely known and will definitely be used in this document. A brief history will be presented followed by the description of the main classes of borohydrides.

#### **Brief history**

The chemistry of such compounds is not very old: it has only about 80 years in history. It was started in Germany in 1920s by the works of A. Stock, a major pioneer in the chemistry of boron hydrides [88]. In 1933, A. Stock studied the reaction of diborane with sodium amalgam. It has been shown afterwards in 1949 by J. S. Kasper [90] that the product of this reaction contains sodium borohydride. This original work on boron hydride compounds was continued and developed by H. I. Schlesinger and his co-workers in early 1940s who reviewed the first metal borohydrides and proposed all the main methods of synthesis of compounds of aluminium [91], beryllium [92] and lithium [93]. Their works have not lost their value and technological importance until now.

The preparation of the magnesium compound in 1950 by Wiberg *et al.* [94] and then, the preparations of the sodium and potassium compounds by Schlesinger *et al.* [95] in 1953 followed. Since then, metal borohydrides and their derivatives have been extensively studied and numerous reviews such as the extensive review of James and Wallbridge [96] in 1979 are available and up-dating the previous ones. More recently

in 2004, Bulychev [97] revealed in his review that in the USSR, the borohydrides have been extensively studied in 1950s and 1960s by scientists such as E.M. Fedneva, V.I. Mikheeva, K.N. Semenenko and more recently by U. Mirsaidov and their works were entirely supported by military departments intended to use borohydride substances as components for rocket propellants.

### **Classification of borohydrides**

Among borohydride compounds, different groups can be cited:

- Group A: formed by alkali metal borohydrides, they are part of the simpler anion family  $MBH_4$  ( $M=Li, Na, K, Rb$  and  $Cs$ ); they are ionic, white, crystalline, high-melting point solids that are sensitive to moisture but not to oxygen.
- Group B: formed by alkaline-earth metal borohydrides; they are intermediate between ionic and covalent.
- Group C: formed by Group IIIB, Group IVB and transition metal borohydrides; they are covalently bonded and are either liquids or sublimable solids. [98]-[99]

Apart from simple metal borohydride, another type of borohydrides has been developed: the borohydride complexes. Makhaev [100] described them as coordination compounds containing the simplest hydroborate anion  $BH_4^-$  as a ligand. Before this review work, another important review has been done by Marks and Kolb [98] on the borohydride complexes of covalent transition metals, lanthanides and actinides.

The borohydrides are a class of materials that is diversified and if they are to be used for hydrogen storage applications, it is important to explore the methods of synthesis as very few of them are commercially available at present and the availability and low cost are key features for commercial vehicular applications

**Table 2.6:** Main elements forming simple metal Borohydrides and metal borohydride complexes, James *et al.* [96]

<u>Li</u>	<u>Be</u>												
<u>Na</u>	<u>Mg</u>												
<u>K</u>	<u>Ca</u>	Sc											
<u>Rb</u>	<u>Sr</u>	Y											
<u>Cs</u>	<u>Ba</u>	La										<u>Al</u>	
		Ac	<u>Ti(III)</u>	V	Cr	[Mn]	[Fe]	[Co]	Ni	[Cu]	<u>Zn</u>	[Ga]	
			<u>Zr(IV)</u>	Nb	Mo		Ru			[Ag]	[Cd]	[In]	[Sn]
			<u>Hf(IV)</u>		W					[Au]		<u>Tl(I)</u>	Pb

{ A    B
{ C

*The elements underlined form simple hydroborates  $M(BH_4)_n$  which are stable or decompose only slowly at ambient temperatures ; those not underlined have only been isolated with other groups, in addition to the hydroborate group and form complexes ; Those in brackets form compounds which have been reported to be unstable at room temperature but may be isolated at lower temperatures.*

### 2.2.3.2 Preparation and synthesis

The literature dealing with the general preparation of borohydride compounds is very extensive and sometimes complicated. These compounds can be prepared using a large variety of reactions that has been described in exhaustive reviews: the review from James and Walbridge [96] which details particularly salt-like ionic borohydrides and the review from Marks and Kolb [98] whose main focus is on covalent metal tetrahydroborates to cite only those ones. Only  $LiBH_4$ ,  $NaBH_4$ , and  $KBH_4$  are commercially available. To allow characterisation of pure compounds, synthesis of other borohydrides have been essentially made using convenient procedures at the laboratory scale. Here are some examples of efficient methods to synthesize solvent-free simple and pure borohydrides, ie.  $Mg(BH_4)_2$  [105]-[106],  $Ca(BH_4)_2$  [107] and  $Zn(BH_4)_2$  [108]-[109].

**Preparation from metathetic reactions**

Metathetic reactions which usually employ alkali metal borohydrides and the appropriate metal halide (bromide, iodide, chloride, and fluoride) were originally found to improve the preparations of aluminium and beryllium compounds [104] and these reactions have remained a useful and general method for the preparations of borohydride compounds. These are the reactions involving the transfer of a hydroborate group from an element to another.



X= Br, Cl, I, or F forming a metal halide when bonded to a metal

**Preparations from metal hydrides**

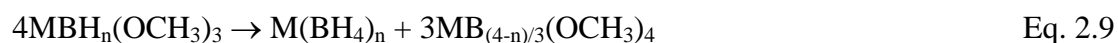
This is the most frequently used method. The metal hydride may be used to convert the boron compound to diborane in situ or the latter reagent may be used directly.

- ***Diborane:*** the direct reaction with the corresponding metal hydride in ethereal solvents under suitable conditions produces high yields of the borohydrides.



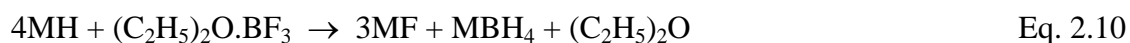
M: desired cation metal

- ***Alkoxyboron compounds:*** the most convenient for laboratory preparations; the metal hydride is reacted with trimethyl borate in the absence of solvent in first instance to yield the corresponding trimethoxyhydroborate which then disproportionates at low temperatures in a solvent.



M=Li, K or Na

- **Boron halides and their derivatives:** Boron trifluoride etherate reacts with an excess of a simple anion alkali hydride in ether at 120-130°C to form the corresponding hydroborate in high yield.



The ether may be removed from the hydroborate by pumping at 33°C under vacuum.

One possible preparation process starts from boron hydrides  $\text{MH}_n$  (M=Na, K) which are available. The disadvantage of this process is that the rate of substitution is low owing to the insolubility of the secondary product MX, so that complex grinding of the components is generally necessary. Furthermore, it is difficult to separate off M and/or X completely, so that only impure  $\text{LiBH}_4$  qualities can be obtained.

The diborane that forms escapes via the gas phase, is optionally purified and is introduced in a second reactor into a suspension of LiH in a solvent (e.g. diethyl ether). This method permits the preparation of pure solutions of  $\text{LiBH}_4$  in anethereal solvent.

A disadvantage is the production of gaseous diborane as an intermediate. This has extremely high reactivity (spontaneously inflammable in air) and toxicity (MWC 0.1 ppm). The process can therefore be carried out on a commercial scale only if



extremely controlled conditions are observed, and complex measures are necessary for monitoring possible diborane emissions and eliminating them in the event of an accident. In order to avoid this disadvantage, it is possible to choose a process in which diborane reacts further in the same reaction vessel without being isolated, or in which no diborane is formed at all, e.g. the reaction of lithium hydride with boron trifluoride in diethyl ether. Although this process can result in good yields when the reaction is carried out under pressure, diborane is still formed as an intermediate; diborane is only very sparingly soluble in the diethyl ether, and diborane emissions are therefore still to be expected. Furthermore, the use of diethyl ether as solvent is a problem owing to its high volatility and ready flammability.

For this reason, it is desirable to prepare  $\text{LiBH}_4$  solutions in a simple manner using solvents which are better to handle, e.g. THF or THF derivatives. Solutions of  $\text{LiBH}_4$  in THF are known as such, they are generally prepared by dissolving solid  $\text{LiBH}_4$  in THF. For all the synthetic methods, very little concrete information is made available such as, for example, relating to the course of the reaction, reaction yields or product purity.

### **Direct synthesis from the elements**

The solvent-free direct synthesis of some alkali and alkali-earth metal borohydrides from elements has been reported in the literature in a patent by D. Goerrig [101] in 1960. The hydrogenation of the corresponding metal or metal hydride together with elemental boron is carried out at a temperature between 350 and 1000°C and a pressure between 3 and 15 MPa. But, in the examples, the temperature of 620-650°C and the hydrogen pressure of 15 MPa are applied to allow effective

hydrogenation. Goerrig also claimed that such a method is generally applicable to alkali and alkali-earth metals.

**Table 2.7:** Formation of borohydrides from the elements, Goerrig [101]

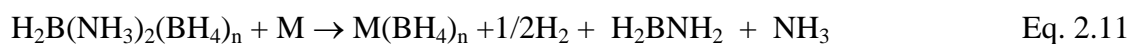
Starting materials	Molar ratio B:M or B:MH <sub>n</sub>	Hydrogenation Conditions (°C/ MPa H <sub>2</sub> )	Yield (%)
K	48:52	650/15	96
Li	45:55	650/15	84.3
NaH	45:55	650/15	81.1
Mg	60:40	620/15	30.1
BaH <sub>2</sub>	62.5:38.5	650/15	58

Recently in 2008, these results have been demonstrated experimentally by Zuttel's group [102]-[103] at EMPA in Switzerland for the direct synthesis of LiBH<sub>4</sub> from elemental Li and B at P=15 MPa and T=600-700°C. From this, it can be assumed that the best conditions to reach the reversibility of LiBH<sub>4</sub> from the elements are still too high and other pathways need to be found. Direct formation from the elements (that is to say from lithium metal and boron as well as hydrogen) is possible in principle but requires extreme conditions e.g., 150 MPa H<sub>2</sub> and 650°C). Such conditions require extraordinarily expensive apparatuses; in addition, elemental boron is not available cheaply.

### **Preparation by miscellaneous methods**

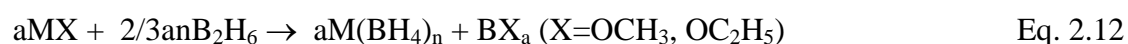
- ***Preparation from alkali metals:***

The direct reaction of an alkali metal with the diammoniate of diborane in liquid ammonia:



- ***Preparation from metal alkoxides:***

A solution of a metal alkoxide  $\text{M}(\text{OR})_n$  is treated with diborane. This type of reactions offer the advantage of being very rapid but there is a need to maintain large quantities of diborane in the system.



- ***Preparation from tetrahydroaluminates*** by either a simple replacement of the borohydride units by tetrahydroaluminate ligands or the reaction of the hydroaluminate with diborane. Although  $\text{Al}(\text{BH}_4)_3$  is an undesirable by-product.

Following the methods of synthesis, it is useful to explore the main properties and their exploitation in the different applications.

### 2.2.3.3 Properties and applications of borohydride compounds

A good knowledge of the key thermodynamic and structural properties of the borohydride compounds are an important feature in the road to establishing this class of materials as hydrogen stores.

#### **Thermodynamic properties of borohydrides**

Scifinder software [110] has been used to find the different CAS registration numbers. What can be pointed out is that, firstly, very few thermodynamic data has been published in the open literature. Also, thermodynamic constants such as the

standard enthalpy of formation ( $\Delta H_f$ , reverse of Eq. 2.6) may differ from one review to another and the values must be taken with extreme precaution.



Also, the heat of dehydrogenation is a very important parameter of hydrogen storage materials. That is desirable that this value is about 40 kJ.mol<sup>-1</sup>H<sub>2</sub> to provide a reasonable equilibrium hydrogen pressure at 80-120°C.

The enthalpy of formation  $\Delta H_f$  and enthalpy of dehydrogenation  $\Delta H_{des}$  of the corresponding borohydride  $M(BH_4)_n$  may not have the same absolute value because the dehydrogenation of borohydrides is a multi-step process involving the formation of the corresponding metal hydride or boride. Also, there is an almost linear correlation between desorption temperature and estimated  $\Delta H_{des}$  using Van't Hoff plot.

$$\ln\left(\frac{P_{eq}}{P_0}\right) = \frac{\Delta H}{RT} - \frac{\Delta S}{R} \quad \text{Eq. 2.14}$$

where  $P_0$  is the standard pressure i.e., 1.013 bar),  $T$  is the absolute temperature and  $R$  is the gas constant.

The slope of the straight line is proportional to  $\Delta H$  and the axis intercept is proportional to  $\Delta S$ . Therefore, the enthalpy and entropy are roughly estimated from the Van't Hoff plot; the equilibrium pressure  $P_{eq}$  at each temperature is designated as the pressure value at the median of dehydrogenation capacity. These values can be compared to the standard enthalpies and entropies of reaction assumed from density functional theory (DFT) calculations.

Indeed, the direct calorimetric measurements of reactive and volatile borohydride compounds are very challenging; therefore, calculations of thermodynamics have been widespread using density functional theory (DFT).

**Table 2.8:** Some example of thermodynamic properties (James [96])

Property	LiBH <sub>4</sub>	NaBH <sub>4</sub>	Be(BH <sub>4</sub> ) <sub>2</sub>	Mg(BH <sub>4</sub> ) <sub>2</sub>	Ca(BH <sub>4</sub> ) <sub>2</sub>	Al(BH <sub>4</sub> ) <sub>3</sub>
<b>CAS n°</b>	16949-15-8	16940-66-2	17440-55-6	16903-37-0	17068-95-0	16962-07-5
<b>Desorption products</b>	LiH-B	NaH-B	Be-B	Mg-B	CaH <sub>2</sub> -CaB <sub>6</sub>	Al-B
<b>Melting point, °C</b>	268	505	-	-	-	-64.5
<b>*Obs. decomp temp (calc.), °C</b>	470 (402)	595 (609)	123	323	360	150
<b>ΔH<sub>des</sub>, kJ.mol<sup>-1</sup></b>	75	90	27	40	75.5	6

*\*Observed decomposition temperature and in brackets, the calculated one*

The DFT calculations have a good correlation with experimental data as long as the crystal structure of the compounds is known.

### **Structural properties of borohydrides**

There is a relative diversity in the known structures of the borohydrides. These structures have been determined using different diffraction methods such as X-ray diffraction, synchrotron or neutron powder diffraction or vibrational spectroscopy such as Infrared (IR) and Raman (R) spectroscopy.

In particular, Infrared spectroscopy is very useful as to some extent, the relationship between the various types of structures in the borohydrides is reflected in the infrared spectra of the different compounds.

The spectra of a wide variety of borohydride systems have been reported and several of these reports have been related to establishing whether the hydroborate group was present in the system as a discrete ion  $[BH_4^-]$  or was bonded to the metal atom either by hydrogen bridge or in some other related way.

**Table 2.9:** Vibrational frequencies of some tetrahydroborates – part 1, James and Wallbridge [96]

Compound	Spectral activity	Frequency (cm <sup>-1</sup> )			
		<b>B-H<sub>1</sub> stretching mode</b>	<b>B-H<sub>2</sub> deformation mode</b>	<b>Bridge stretching (expansion)</b>	<b>Bridge stretching (symmetry)</b>
<b>LiBH<sub>4</sub></b>	IR, R	2290	1094	-	-
<b>NaBH<sub>4</sub></b>	IR, R	2290	1120	-	-
<b>KBH<sub>4</sub></b>	IR, R	2280	1115	-	-
<b>Al(BH<sub>4</sub>)<sub>3</sub></b>	IR, R	2549	1116	1850	1600
<b>Zr(BH<sub>4</sub>)<sub>4</sub></b>	IR, R	2584	1223	2198	-
<b>Hf(BH<sub>4</sub>)<sub>4</sub></b>	IR, R	2581	1228	2207	-

**Table 2.10:** Vibrational frequencies of other tetrahydroborates – part II, Various sources

Compound	Source	Spectral information	Frequency (cm <sup>-1</sup> )	
			<b>Stretching vibrations</b>	<b>Bending vibrations</b>
<b>Mg(BH<sub>4</sub>)<sub>2</sub></b>	[104][122]	IR, R	2230-2296-2390	1126-1261
<b>Ca(BH<sub>4</sub>)<sub>2</sub></b>	[124]	R	2200-2500	1000-1400
<b>Zn(BH<sub>4</sub>)<sub>2</sub></b>	[108]	IR	2084-2307-2454	1108-1396

So far, a lot of controversial results have been produced on the structure of borohydride compounds. Among the simple metal borohydrides, the alkali metal borohydrides have been investigated in depth [111]. Their solid-state structures contain relatively mobile tetrahedral  $[BH_4^-]$  units, the ordering of which tends to induce structural phase transitions.

In  $LiBH_4$ , for example, there is an endothermic phase transition ( $4.18 \text{ kJ.mol}^{-1}$ , [112]) when the temperature increases to 380K ( $107^\circ\text{C}$ ) from ordered orthorhombic to disordered hexagonal structure. However, no phase transition has been reported at low temperatures.

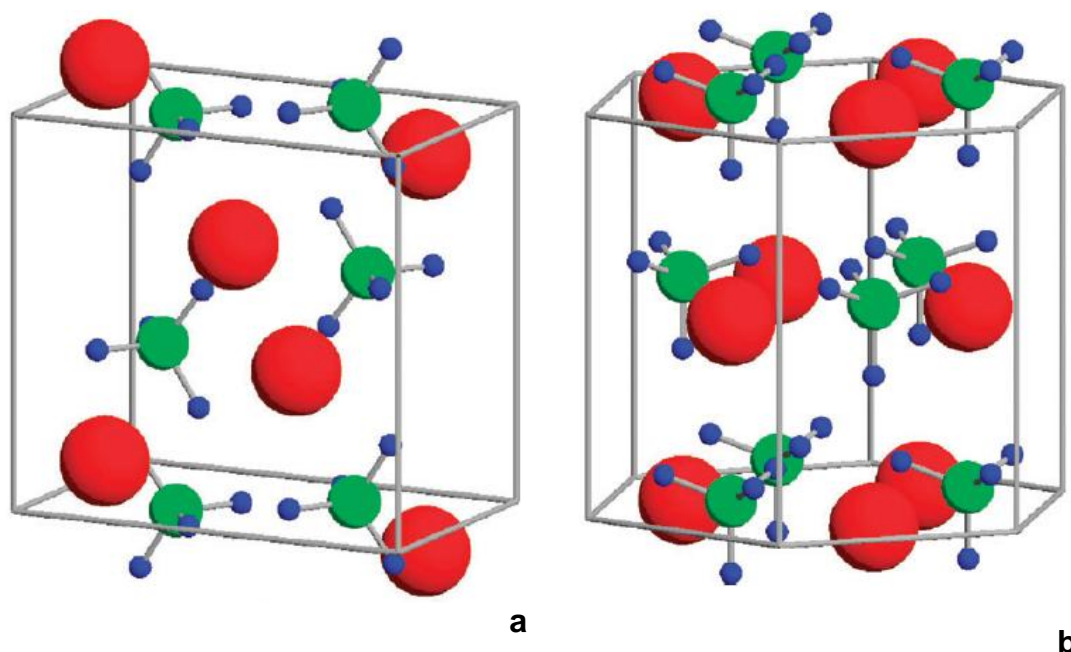


**Figure 2.13:** Low (a) and high (b) temperature structures of  $LiBH_4$  determined from X-Ray diffraction, red (large), green (middle) and blue (small) spheres represent Li, B and H atoms, respectively. (Miwa *et al.* [59], Shevlin *et al.* [60])

The room temperature structures of  $MBH_4$  ( $M=Na, K, Rb, Cs$ ) all have cubic symmetry and contain orientationally disordered tetrahedral  $[BH_4^-]$  units. Unlike in

the  $\text{LiBH}_4$  crystal structure, on cooling, the  $[\text{BH}_4^-]$  units tend to form a more ordered structure.

The structure of RT  $\text{NaBH}_4$  was found [113] to be of a NaCl-type and was determined by neutron diffraction. It shows a similar transition from ordered RT-phase into more ordered LT-phase at 190K (-83°C) but its RT-phase has cubic symmetry and its LT-phase a tetragonal symmetry [114].

Furthermore, a similar structural change from cubic into tetragonal symmetry was observed in  $\text{KBH}_4$  at 65-70K (-208/-203°C) but the difference is only in the relative positions of the H atoms. It should be noted that one of the main means to find out if there is a phase change in a compound is by measuring the thermal conductivity  $\kappa$  as a function of either the temperature or the pressure. Anomalies in the data are a clear indication of a phase transition.

Several studies have indicated that Rb and Cs compounds also form lower symmetry structures at 35-44K (-238/-229°C) and 22-27K (-251/-246°C) respectively but these have not been identified yet despite several attempts, maybe because these two compounds attract less interest than the other alkali metal congeners.

Of these compounds, Li [115] and Na [116] have been well investigated under pressure. Many controversial studies have been made on the theoretical prediction of high pressure structure of  $\text{LiBH}_4$  since the only detailed experimental study by Pistorius [117]. These studies have been reviewed in detail by a Swedish research group led by Sundqvist [118] but no predictions or experiments could be in good agreement to each other.



Also, the ambient pressure cubic phase of  $\text{NaBH}_4$  transforms into a tetragonal  $P-4_21c$  near 63 kbar and then into an orthorhombic  $Pnma$  phase above 89 kbar and up to 300 kbar.

Currently, several groups are working on the preparation and structure determination of class B and class C (please refer to Table 2.6 for details on the classification) metal borohydrides such as  $\text{Mg}(\text{BH}_4)_2$ ,  $\text{Ca}(\text{BH}_4)_2$ ,  $\text{Zn}(\text{BH}_4)_2$  and  $\text{Al}(\text{BH}_4)_3$  on the other hand. There was very little structural data on these borohydrides until recently because of the difficulty in obtaining crystalline products of sufficient quality.

The literature data on the synthesis and structural properties of  $\text{Mg}(\text{BH}_4)_2$  are contradictory likely because of the presence of different solvates and the difficulty in removing the solvent molecules without causing the decomposition. The first report on the crystalline structure of unsolvated  $\text{Mg}(\text{BH}_4)_2$  was made by Konoplev and Bakulina [119] in 1971 using XRD and stating that there was a transition at  $186^\circ\text{C}$  from tetragonal LT phase into a cubic HT phase stable. Also, many other structural predictions have been made since but there were all different. Recently, high resolution synchrotron X-ray powder synchrotron combined with the preparation of a highly crystalline product performed by Her *et al.* [120] showed another picture of the polymorphic transformation occurring at 453K ( $180^\circ\text{C}$ ) from a hexagonal LT phase into an orthorhombic HT phase stable to 613K ( $340^\circ\text{C}$ ). All reports are only in good agreement concerning the temperature of the transition around  $180^\circ\text{C}$  and the instability of the high temperature phase above  $300^\circ\text{C}$  as reported by a communication from Riktor *et al.* [121] on in-situ synchrotron diffraction studies. More efforts should be made towards the preparation of highly pure crystalline and unsolvated  $\text{Mg}(\text{BH}_4)_2$  in order to get a definitive structural characterisation.

The structure of the LT phase was confirmed to be hexagonal by a very recent work led by Cerny *et al.* [122] using synchrotron X-ray and neutron diffraction. They exhibited a very complex crystal structure for the hexagonal LT phase very similar to that of  $\text{Ca}(\text{BH}_4)_2$ . As for  $\text{Ca}(\text{BH}_4)_2$ , the analogue of  $\text{Mg}(\text{BH}_4)_2$ , it has been found to undertake a polymorphic transformation around 440K (167°C). The LT phase has been reported to be orthorhombic by Kedrova and Malsetva [123] in 1977. This assertion was confirmed almost 30 years later by Miwa *et al.* [124] but no information was available on the supposed HT phase. In 2009, Filinchuk *et al.* [125] observed three polymorphs of  $\text{Ca}(\text{BH}_4)_2$  in the temperature range 30-600°C which are of orthorhombic-F<sub>2</sub>dd, tetragonal-I4<sub>2</sub>d and tetragonal-P<sub>4</sub>.

Up to now, the crystal structure of  $\text{Zn}(\text{BH}_4)_2$  has not been elucidated yet and structural information is not available at present. Finally,  $\text{Al}(\text{BH}_4)_3$  has been shown [126][127] to have two structural phases: there is a transition from liquid  $\text{Al}(\text{BH}_4)_3$ , the orthorhombic  $\beta$  phase into monoclinic  $\alpha$  phase at 180-195K (-93°C/-78°C).

Following the properties, the main use of borohydrides is described in the next paragraphs followed by a more detailed analysis of their use for hydrogen storage applications.

### **General applications of borohydrides**

The hydroborate group  $[\text{BH}_4^-]$  is one of the most useful and extensively used reagents both in organic synthesis and in inorganic or organometallic chemistry. Borohydride compounds possess many valuable properties such as selective reducing agents, starting compounds in the syntheses of complex and organometallic derivatives, precursors for the production of borides, hydrides and other inorganic

materials and as catalysts of hydrogenation, isomerisation, oligomerisation, polymerisation etc.

- Catalysis: Borohydride complexes have been found to be effective catalysts for polymerisation, oligomerisation and hydrogenation of olifeins. Indeed, as described by Barone *et al.* [128] in homogeneous catalysis,  $BH_4^-$  could play many roles:

- ✓ Reduce the central metal to a lower oxidation state allowing the metal to undergo oxidative addition reactions, the first step in homogeneous hydrogenation catalysis;
- ✓ Provide a source of hydrogen in the form of a metal hydride;
- ✓ Provide a coordination sphere for the metal atom using fluctuations of the bonding mode since the presence of a vacant coordination site is of primary importance in homogenous catalysis;
- ✓ Activation ligand for other ligands bound to the same metal.

- Reducing reagent: Dr. Seyden Penne [129] wrote a practical guide on the selection of borohydrides as reducing reagents and she indicates how to obtain the main functional groups by using borohydride reagents. Among the main reducing borohydrides,  $NaBH_4$  and  $KBH_4$  are above all used for reducing aldehydes and ketones.  $LiBH_4$  rapidly reduces esters and also reduces tertiary amides and nitriles.  $Ca(BH_4)_2$  mainly reduces esters to alcohol. Complexes of  $Zn(BH_4)_2$  have a very good selectivity.

- CVD precursor: Transition metal borohydrides are volatile and thermolyse under mild conditions, this makes them excellent precursors for Chemical Vapour

Deposition production of borides and other inorganic materials as thin films. For instance, Jensen *et al.* [130] obtained  $\text{TiB}_2$ ,  $\text{ZrB}_2$  and  $\text{HfB}_2$  thin films by using gaseous CVD at about  $200^\circ\text{C}$  of the respective borohydride precursors.

The latest application of borohydrides is their use as hydrogen storage media and as it is the main subject of the thesis, the following section describes to which extent it might be possible.

#### 2.2.3.4 Borohydrides for hydrogen storage

Salts of  $[\text{BH}_4^-]$  have recently received considerable attention as potential hydrogen storage materials because of their large gravimetric and volumetric hydrogen density.

### **Background information**

The first report of the possible use of borohydrides for hydrogen storage has been reported in a patent from a French research group lead by A. Muller in 1980. Muller and co-workers [131] patented a method for using  $\text{LiBH}_4$  and Al-doped  $\text{LiBH}_4$  for both the storage and the generation of hydrogen. This first report in the line of the use of borohydrides for hydrogen storage was focused on the claim that an addition of aluminium to either  $\text{LiBH}_4$  or the decomposition products of  $\text{LiBH}_4$  could decrease the hydrogen release temperature and help to achieve reversibility more easily. Before this, Russian scientists in 1960s such as Fedneva [132] with lithium and Stasinevich [133] with alkali metals M (M=Li, Na and K) and magnesium investigated the thermal stability of some borohydrides and the conditions of liberation of the hydrogen

evolved. These first studies, though of great interest, were not hydrogen storage oriented and as we mention in the first part of this review were intended to find suitable materials to be used as fuels for rocket propellants. Borohydrides such that of lithium are particularly interesting for this special purpose as it has a very high heat capacity. Then, some tetrahydroborates such as  $\text{NaBH}_4$  and  $\text{LiBH}_4$  have in fact been utilised in hydrogen storage systems in which hydrogen is evolved from the hydride upon contact with water. However, the hydrolysis reactions are highly irreversible and could not serve as the basis for rechargeable hydrogen storage systems.

### **Challenges for the possible use of borohydrides as hydrogen stores**

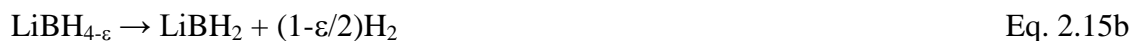
Some major challenges must be resolved before a possible commercial use of borohydrides as hydrogen storage materials: high temperature of dehydrogenation, lack of reversibility of the dehydrogenation reaction, slow kinetics of dehydrogenation and hydrogenation, evolution of diborane during dehydrogenation, and finally high cost of borohydrides.

In general, the thermal decomposition and/or recombination of hydrogen are difficult to achieve because of the strong B-H interactions. Also, the charge transfer from the cation to the borohydride group  $[\text{BH}_4^-]$  is a key feature for the stability of metal borohydrides. Recently, a systematic investigation [134] has been made on a series of metal borohydrides ( $\text{M} = \text{Li}, \text{Na}, \text{K}, \text{Cu}, \text{Mg}, \text{Zn}, \text{Sc}, \text{Zr}$  and  $\text{Hf}$ ;  $n = 1-4$ ) and it has been shown by first-principles calculations and also by some experimental investigations that the bond between  $\text{M}^{n+}$  cations and  $[\text{BH}_4^-]$  anions is ionic and the charge transfer from  $[\text{BH}_4^-]$  anions to  $\text{M}^{n+}$  cations is responsible for the stability of  $\text{M}(\text{BH}_4)_n$  so there would be a linear relationship between enthalpy change of formation of  $\text{M}(\text{BH}_4)_n$  and electronegativity of metal. For instance, the Pauling

electronegativity of magnesium and calcium are 1.31 and 1.00 respectively, which are greater than that of lithium (0.98), and hence,  $\text{Mg}(\text{BH}_4)_2$  and  $\text{Ca}(\text{BH}_4)_2$  are expected to be less stable than  $\text{LiBH}_4$ . Taking into consideration those challenges and the hydrogen capacity, the most promising systems seem to be:  $\text{LiBH}_4$ ,  $\text{Ca}(\text{BH}_4)_2$  and  $\text{Mg}(\text{BH}_4)_2$ .

• *Lithium borohydride, a viable hydrogen store?*

In recent years, there has been some progress on  $\text{LiBH}_4$  particularly on destabilisation and reversibility. The thermal hydrogen desorption [135] from  $\text{LiBH}_4$  has been elucidated and the compound liberates three out of four hydrogen in the compound upon melting around  $280^\circ\text{C}$  and decomposes into  $\text{LiH}$  and boron according to the following equations [112]:



The thermal desorption spectrum of pure  $\text{LiBH}_4$  exhibits four endothermic effects associated with:

- ✓ a reversible effect at **108-112°C** suggested to be due to a polymorphic transformation ;
- ✓ a second effect at **268-286°C** due to the solid melting ;
- ✓ the third effect at **483-492°C** due to the desorption of 50% of the hydrogen ;
- ✓ The fourth one around **600°C** when three of the four hydrogens are desorbed.

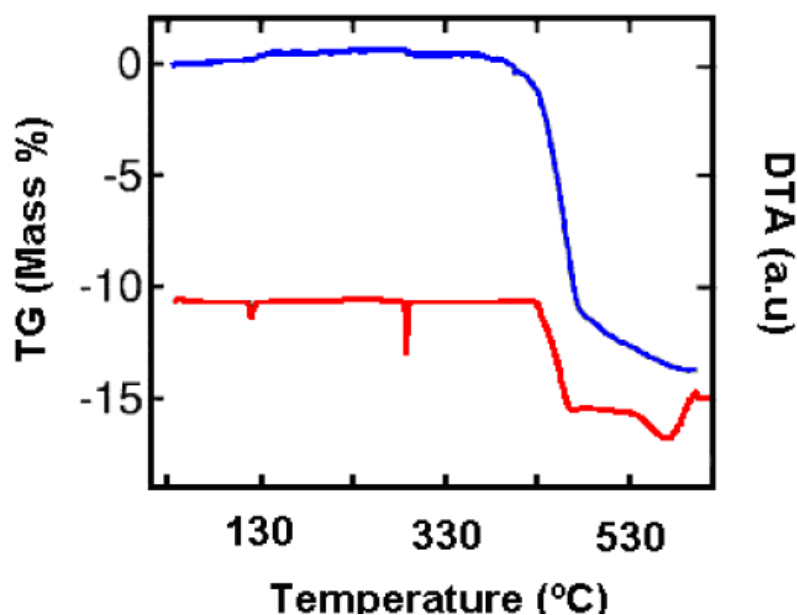


**Figure 2.14:** Thermal desorption spectra of pure LiBH<sub>4</sub> (Brampton *et al.* [Web 24])

Many efforts have been devoted for a significant lowering of the decomposition temperature up to 200°C using additives such as : oxides (TiO<sub>2</sub>, V<sub>2</sub>O<sub>5</sub>) and halides (TiCl<sub>3</sub>, TiF<sub>3</sub> and ZnF<sub>2</sub>) [136], MgH<sub>2</sub> [137], Al [138], carbon materials [139].

Among the strategies for a reduction in the dehydrogenation temperature, the following can be quoted:

- ✓ Adding chlorides (with higher valence cations and larger electronegativities) during the milling process: the expected reaction could be expressed as follows:



This reaction has been mostly used to describe chemical reactions involved in the synthesis of borohydrides. In fact, Nakamori *et al.* [134] reported that the Pauling electronegativity of the cation  $\text{M}^{n+}$  is strongly correlated to the internal stability of the

anion  $[BH_4^-]$ . It has been demonstrated that  $LiBH_4$  was highly destabilised through the addition of  $ZnCl_2$  as the onset desorption was observed around  $120^\circ C$ .

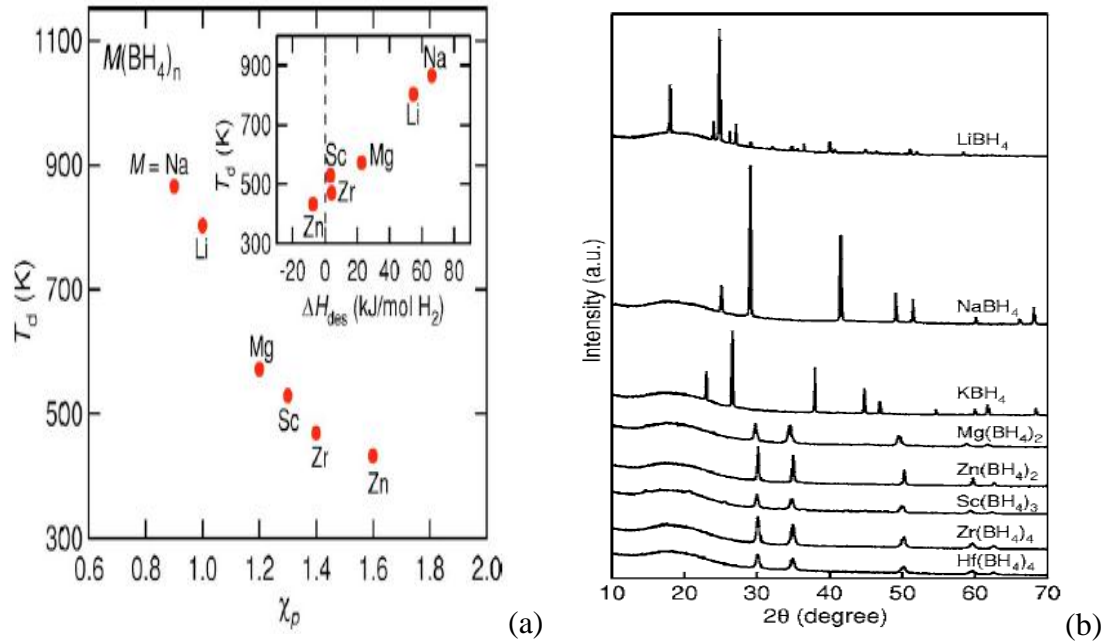


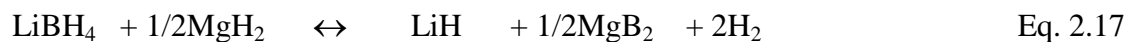
**Fig 2.15:** (a): The desorption temperature  $T_d$  as a function of the Pauling electronegativity  $P$ . Inset shows the correlation between  $T_d$  and estimated  $\Delta H_{des}$  from eq. 2.19 (b): Powder x-ray diffraction profiles of purchased  $MBH_4$  where  $M=Li, Na$ , and  $K$ , and prepared  $M(BH_4)_n$  where  $M=Mg, Zn, Sc, Zr$ , and  $Hf$  by mechanical milling (Nakamori *et al.* [134])

✓ Adding additives such as metal oxides in order to form an intermediate compound: Au *et al.* [136][140] identified several effective additives. In this case and in most of the studies, it has been observed that the hydrogen storage capacity of the oxide-modified lithium borohydrides decrease after cycling.

✓ Performing a partial cation substitution of  $Li$  by smaller-size elements: this strategy was experimentally investigated by Nakamori *et al.* [141]. It has been observed that after a partial substitution of  $Li$  by  $Mg$ , the starting and ending temperatures for  $LiNH_2$ :  $LiH$ , 1:2 is substantially lowered. Therefore, the same thing



has already been envisaged for  $\text{LiBH}_4$ . Recently, Vajo *et al.* [137] demonstrated that it is possible to destabilize  $\text{LiBH}_4$  by mixing with  $\text{MgH}_2$  as follows:



They reported that 11.4 wt % can be reversibly stored.

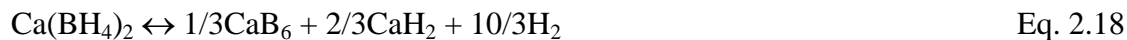
In contrast to the progresses achieved on tuning the thermodynamics, very few have been reported on the kinetic improvement strategies. In the cases when the rehydrogenation process is favourable, no effective catalyst [135]-[136] has been identified to allow the restoration of the borohydride under moderate conditions. Among the methods, Fang reported [138] that milling  $\text{LiBH}_4$  with SWNTs may catalyse the reversible dehydrogenation of  $\text{LiBH}_4$  by forming a net-like structure and by a combined effect of the carbon nanostructure scaffold and the metallic particles used to form nanotubes.

In conclusion, limited success has been achieved with the reduction of the decomposition temperature of  $\text{LiBH}_4$ , the kinetics and the reversibility. Hence, other borohydrides have been explored like the promising,  $\text{Ca}(\text{BH}_4)_2$  and  $\text{Mg}(\text{BH}_4)_2$ .

- ***Calcium borohydride, a possible hydrogen store?***

In the last 2 years, there has been a real interest reported on  $\text{Ca}(\text{BH}_4)_2$  especially on tuning thermodynamics and reversibility. The thermal hydrogen desorption from  $\text{Ca}(\text{BH}_4)_2$  has been predicted from DFT calculations by Ronnebro *et al.* [142] to occur

according to the following reaction with an anticipated reversible hydrogen capacity of around 9.6 wt% and a change of enthalpy of  $-40.6 \text{ kJ} \cdot \text{mol}^{-1} \cdot \text{H}_2$ :



However, according to recent results, the dehydrogenation pathway is more likely to involve a new intermediate identified by means of calculation to be  $\text{CaB}_2\text{H}_x$  (Riktor *et al.* [143] and Frankcombe *et al.* [144]) and experimentally by Wang *et al.* [145] to be:  $\text{CaB}_{12}\text{H}_{12}$ . This intermediate could no longer be found at temperatures around  $500^\circ\text{C}$  suggesting a two-step reaction for the dehydrogenation of  $\text{Ca}(\text{BH}_4)_2$ .

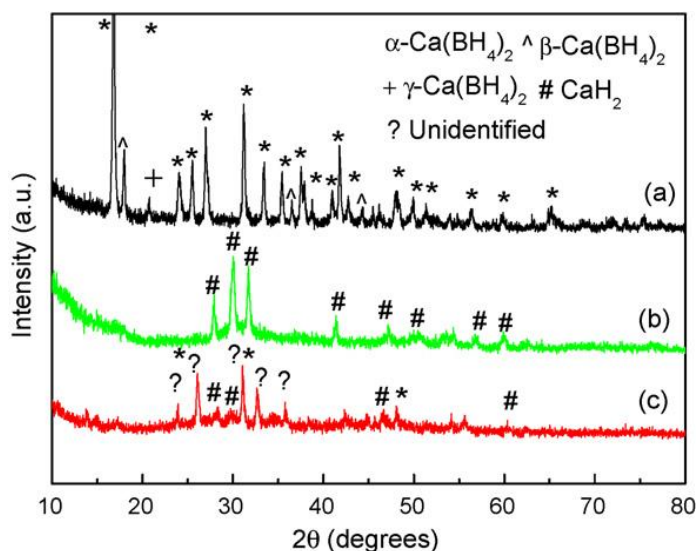


**Figure 2.16:** XRD patterns of  $\text{Ca}(\text{BH}_4)_2$  before dehydrogenation (a), after dehydrogenation at  $320^\circ\text{C}$  (b) and after dehydrogenation at  $500^\circ\text{C}$ , taken from Mao *et al.* [145]

Moreover, partial reversibility was indicated by Kim *et al.* [147] at a pressure of 90 bar and a temperature of 623K ( $350^\circ\text{C}$ ) for an uptake of around 3.8 wt % by adding  $\text{TiCl}_3$ . This value was later improved up to 5 wt % by the addition of  $\text{NbF}_5$  by the same researchers [148] showing the high potential in terms of improving the reversible capacity. Nonetheless, the dehydrogenation temperature is too still too high. In the

same view, magnesium borohydride ( $\text{Mg}(\text{BH}_4)_2$ ) has been the focus of research as presented in the following paragraph.

- ***Magnesium borohydride, a possible hydrogen store?***

Magnesium borohydride was thought by Chlopek *et al.* [105] to be decomposing in a two-step process involving only  $\text{MgH}_2$  as an intermediate compound but recently, a more complicated multistep decomposition pathway has been exhibited with the formation of a new intermediate phase similar in structure to  $\text{MgB}_{12}\text{H}_{12}$ .

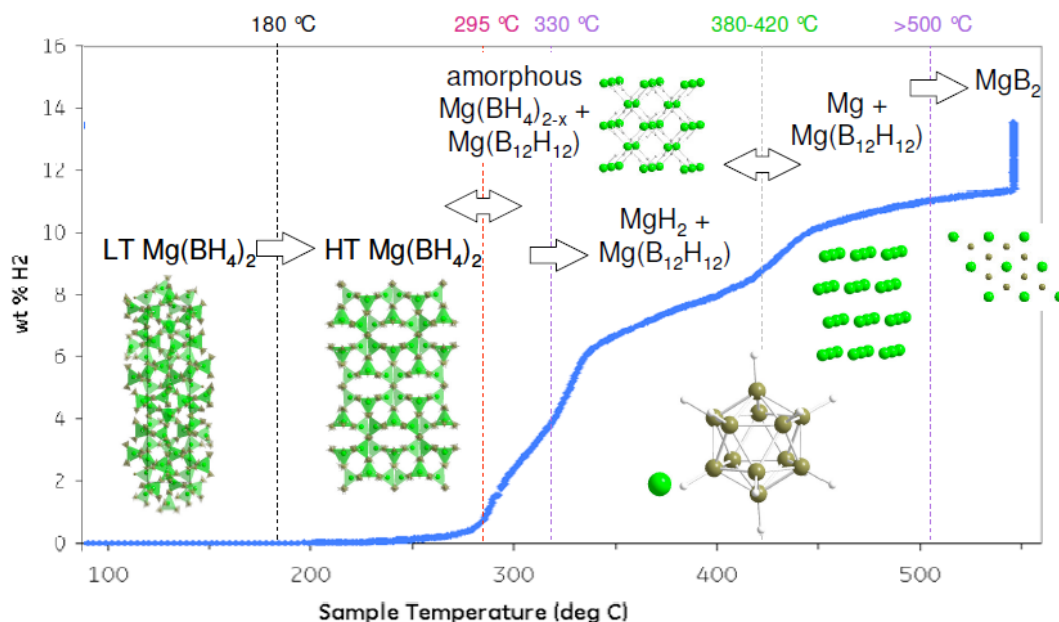
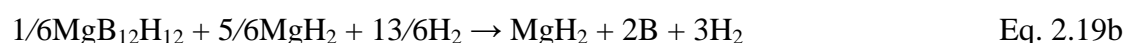
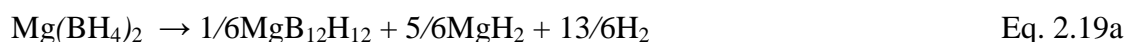


**Figure 2.17:** Graphic synopsis of the decomposition pathway of  $\text{Mg}(\text{BH}_4)_2$ , taken from Soloveichik *et al.* [150]

The decomposition of pristine  $\text{Mg}(\text{BH}_4)_2$  appears to occur around  $270^\circ\text{C}$  [150], which is better than the one of  $\text{LiBH}_4$  but as it is still too high for practical use of it as hydrogen storage medium, some attempts have been made to lower the decomposition temperature (down to around  $100^\circ\text{C}$ ) by using additives such as  $\text{TiCl}_3$  as shown in Figure 2.18 below.

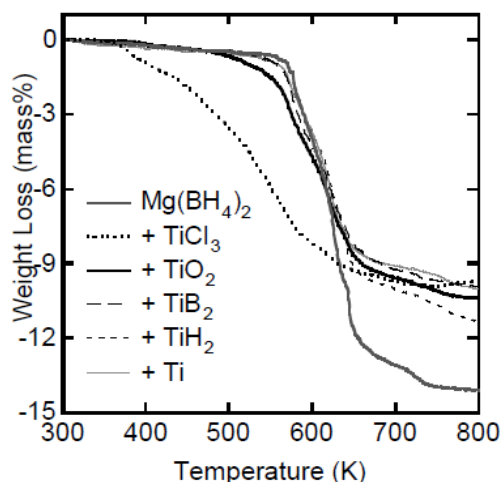


**Figure 2.18:** Thermogravimetric curves of  $\text{Mg}(\text{BH}_4)_2$  with or without additives such as:  $\text{TiCl}_3$ ,  $\text{TiO}_2$ ,  $\text{TiB}_2$ ,  $\text{TiH}_2$  and  $\text{Ti}$  with a mass ratio of 2 to 1, Taken from Li *et al.* [Web 25]

Reversibility of pure  $\text{Mg}(\text{BH}_4)_2$  has been demonstrated by Severa *et al.* [151] by rehydrogenating  $\text{MgB}_2$  under 95 MPa and  $400^\circ\text{C}$  to generate  $\text{Mg}(\text{BH}_4)_2$  but the cyclability has not been yet investigated knowing that it is a key feature along with improved desorption in establishing a material as a practical solution for on-board hydrogen storage.

In conclusion, the stabilities of the borohydrides are high and they even usually melt before they decompose. Also, the decomposition produces some undesirable volatile compounds such as  $\text{BH}_3$  and  $\text{B}_2\text{H}_6$ , which causes an unrecoverable boron loss. Finally, among all the borohydrides presented here, they all decompose to their corresponding binary hydrides, sequestering some hydrogen up to a very high temperature. The decomposition of such hydrides generally leads to a two-phase

elemental system, not favouring a recombination, hence reversibility. Despite their attractiveness, researchers have been focusing on alternative complex hydrides these recent years, the amine-boranes.

#### 2.2.4 Amine-boranes systems

Besides lithium borohydride ( $\text{LiBH}_4$ ), another very promising material, ammonia borane ( $\text{NH}_3\text{BH}_3$ ) and its related compounds (B-N-H compounds) have drawn the attention of several groups [157][159]. As nitrogen compounds are electron-rich and boron compounds are electron-deficient, amine-boranes are unique in their ability to store and release hydrogen because of their protonic ( $\text{H}^{\delta+}$  in N-H) and hydridic ( $\text{H}^{\delta-}$  in B-H) hydrogens.

The structure and physical properties of amine-boranes are influenced by dihydrogen bonding (arising from the electrostatic interactions between protonic ( $\text{H}^{\delta+}$ ) and hydridic ( $\text{H}^{\delta-}$ ) H atoms) and dative bonding (due to donation of non-bonding lone pair on nitrogen to the empty p-orbital on boron). A dihydrogen bond can be considered as having two components. These are generally described as ‘donor’ and ‘acceptor’ units. In the hydrogen-donor units, hydrogen is bonded to a more electronegative element, so that the hydrogen atom is positively polarized. Also, the hydrogen-acceptor unit has its hydrogen atom bonded to a more electropositive element. This negatively polarised hydrogen atom is regarded as accepting the positively charged hydrogen atom of the donor unit to form the dihydrogen bond.

Whereas for the dative bond, the bond strength is affected by the nature of the groups attached to both the boron and the nitrogen atom and consequently, the stability of an amine-borane (which is directly dependent upon the nature of the bond) can vary tremendously. Some of these compounds may be stable only at low temperatures

whereas others of comparable size can be isolated without decomposition even at atmospheric pressures. Also, B-N is isoelectronic with C-C.

A thorough literature search on the amine-boranes (B-N-H compounds) has been conducted and has exhibited compounds with interesting features such as ammonia borane, also known as borazane ( $\text{NH}_3\text{BH}_3$ , AB), aminoborane ( $\text{NH}_2\text{BH}_2$ ), iminoborane ( $\text{NHBH}$ ) precursor to borazole, also known as borazine ( $(\text{NHBH})_3$ ,  $\text{B}_3\text{N}_3\text{H}_6$ ), Polyaminoborane  $((\text{NH}_2\text{BH}_2)_n$ , PAB) and polyiminoborane  $(\text{NHBH})_n$ , PIB) products and, diammoniate of diborane  $((\text{NH}_3)_2\text{BH}_2\text{BH}_4$ , DADB).

#### 2.2.4.1 Ammonia borane (AB)

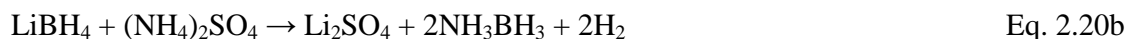
Among them, in late 1950s, Shore and Parry [152]-[155] extensively studied the chemistry of diborane and ammonia and unveiled a survey of the synthetic procedures for ammonia borane (AB) and related products and the difficulties involved in its preparation and especially in its purification.

45% yield



Diethyl ether

45% yield



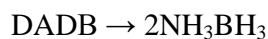
Diethyl ether

45% yield



Diethyl ether/NH<sub>3</sub>

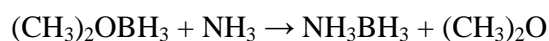
~80-91% yield



Eq. 2.20d

Polyether/B  $\frac{\text{H}}{2 \quad 6}$ 

70% yield



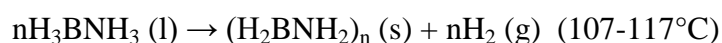
Eq. 2.20e

Dimethyl ether

**Figure 2.19:** Synthetic procedures by Shore, Parry and co-workers [152]-[155]

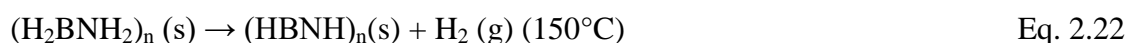
In summary, the two most important methods for laboratory scale preparation are the salt metathesis (with ammonium salts like chloride, sulphate, carbonate and formate) and the direct reaction (of B<sub>2</sub>H<sub>6</sub> with ammonia gas). Over the years, several other synthetic procedures have been developed to prepare AB. Among them, AB has been prepared from NH<sub>4</sub>Cl and NaBH<sub>4</sub> [156] via the intermediate ammonium borohydride NH<sub>4</sub>BH<sub>4</sub> in a solvent containing liquid ammonia with yields of 99%.

Also, AB is at ambient temperature and atmospheric pressure a colourless crystalline solid with relatively high hydrogen content of 19.6 wt%. The decomposition of AB is a multi-step process [157]. AB liberates one equivalent of hydrogen around 110°C upon melting of AB.

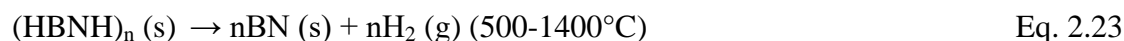


Eq. 2. 21

Upon further heating, the second equivalent of hydrogen is lost over a much broader temperature range, with a maximum around 150°C, up to 500°C.



The rest is released at much higher temperatures.



Since all steps are exothermic, the high temperature requirement reflects the significant kinetic barriers. Many attempts [158] have been made in order to increase the dehydrogenation rates by the inclusion of additives such as metal catalysts or chlorides or by intercalation of AB in a solid scaffold such as mesoporous silica or carbon cryogels. However all these approaches either contribute excess weight and volume to the storage system or require expensive precious metal catalysts. Recently, the first step has been described [159] by an induction, nucleation and growth mechanistic pathway in which DADB plays a major role after it is formed and reacts with a mobile form of AB. Hydrogen is subsequently formed through a condensation reaction between  $[(\text{NH}_3)_2\text{BH}_2]^+$  cation and  $\text{NH}_3\text{BH}_3$  eventually leading to the formation of PAB.

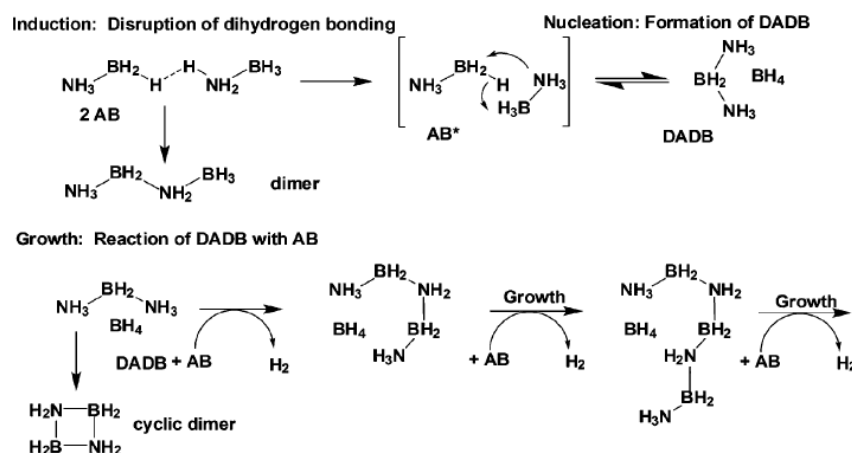


**Figure 2.20:** The proposed thermal dehydrogenation mechanism of AB, Taken from Wang *et al.* [159]



## 2.2.4.2 Diammoniate of diborane (DADB)

Diammoniate of diborane (DADB) is a compound with the same empirical composition  $\text{BNH}_6$  as AB as shown in Figure 2.22. Its molecular structure has been in discussion for several years and has been suggested by Parry and co-workers in late 1950s [164].

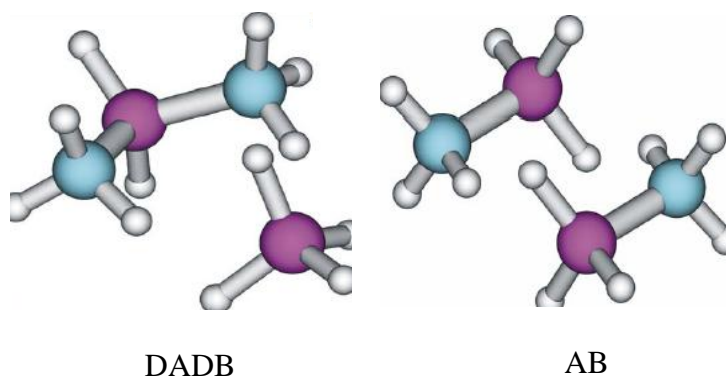


**Figure 2.21:** Structural similarities between diammoniate of diborane (left) and ammonia borane (right)

DADB has been successfully prepared in large scale by Shore and Boddeker [165] in 1963 with yields of up to 97 % by passing a stream of diborane (obtained in-situ by the reaction of  $\text{BF}_3(\text{C}_2\text{H}_5)_2\text{O}$  with  $\text{LiAlH}_4$  in ether) diluted in  $\text{N}_2$  into liquid ammonia at  $-78^\circ\text{C}$ . The conventional synthetic procedure involves the slow and low temperature (below  $-100^\circ\text{C}$ ) addition of diborane to ammonia. DADB is less stable than AB as it converts to either AB or  $\text{NH}_4\text{BH}_4$  over the time releasing hydrogen only up to  $130^\circ\text{C}$  but also borazine (also known as borazole) as shown in Figure 2.22 below.

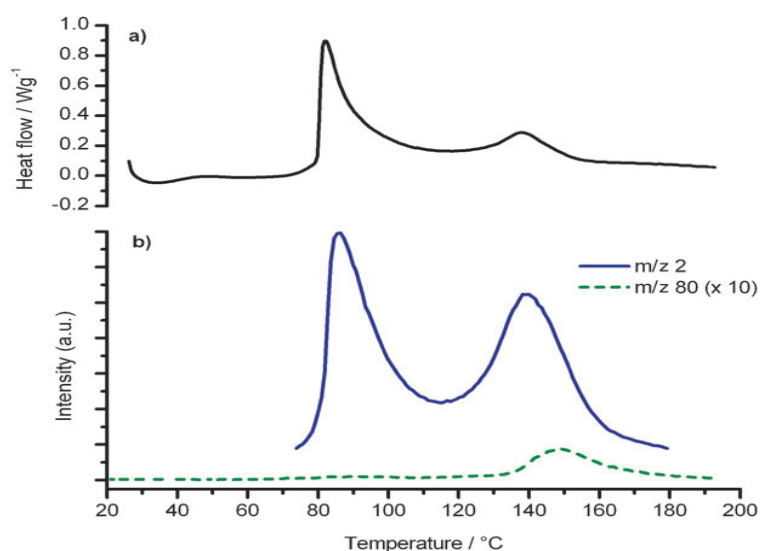


**Figure 2.22:** DSC curves (a) and MS curves (b) for hydrogen ( $m/z$  2) and borazine ( $m/z$  borazine) at a heating rate of  $1^{\circ}\text{C}.\text{min}^{-1}$

Also, the dehydrogenation of ammonia borane (AB) yields a variety of volatile compounds such as molecular aminoborane and borazole but also polymeric intermediates PAB and PIB.

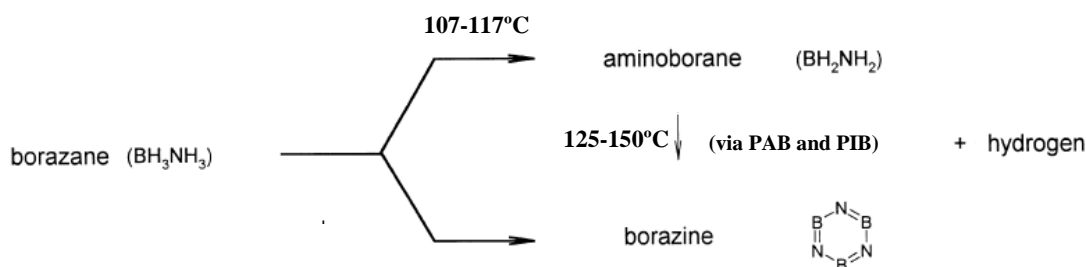


**Figure 2.23:** The thermal decomposition of AB under hydrogen release and formation of volatile compounds: aminoborane and borazole and polymeric intermediates, PAB and PIB, Wolf *et al.* [167]

#### 2.2.4.3 Borazole (also known as borazine)

In the 1960s, work by Schlesinger [160] Mikheeva [161] and Volkov [162], were carried out on the synthesis of borazoles. Borazole (also known as borazine) [163] is a heterocyclic boron-nitrogen compound  $\text{H}_3\text{B}_3\text{N}_3\text{H}_3$  (see Figure 2.21) with a melting

point of  $-58^{\circ}\text{C}$  and a boiling point of  $53^{\circ}\text{C}$ . It is of interest for some branches of technology as it is an ideal initial material to obtain boron nitride as powders, layers or coatings deposited from gas phase.

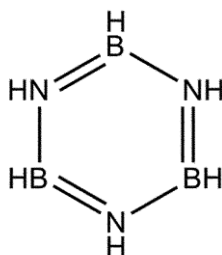
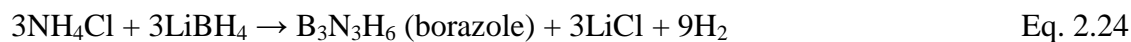


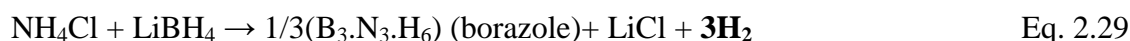
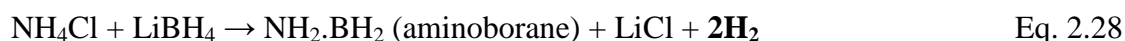
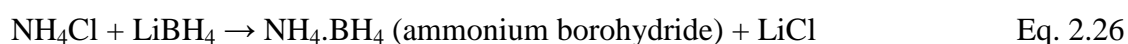
**Figure 2.24:** Heterocyclic structure of borazole  $\text{B}_3\text{N}_3\text{H}_6$

Up to now, the best method for the synthesis of borazoles involved lithium borohydride ( $\text{LiBH}_4$ ) and ammonium chloride ( $\text{NH}_4\text{Cl}$ ) as starting materials, but the release of hydrogen is considered as a side effect as summarised as follows:



The first of the two reactions (Eq. 2.24) was the focus of the separate work by Schlesinger [160], Mikheeva [161] and Volkov [162] and was intended to form borazole from lithium borohydride and ammonium chloride in the absence of solvents. Meanwhile, the second reaction was reported and described as a possible side reaction occurring at room temperature and had only been investigated in recent years [163] for the purpose of the synthesis of ammonia borane (AB).

No previous work on these systems has been reported with respect to hydrogen storage applications although all the possible reactions between  $\text{LiBH}_4$  and  $\text{NH}_4\text{Cl}$  were well documented as follows in the review by James and Wallbridge [96] in 1970 and clearly showed hydrogen evolution and therefore, a promising outcome for hydrogen storage purposes.



#### 2.2.4.4 Other volatile B-N-H compounds

Monomeric aminoborane ( $\text{NH}_2\text{BH}_2$ ) [168] oligomerizes spontaneously between  $-196^\circ\text{C}$  and  $-155^\circ\text{C}$  to form products of the type  $(\text{NH}_2\text{BH}_2)_n$ , known as polymeric aminoboranes: PAB. PAB is more nebulous as there are a variety of routes by which polymerization may occur, and as a result, the structures could be cyclic, linear or branched. The cyclic forms are thermally much more stable than linear species.

Monomeric iminoborane ( $\text{NHBH}$ ) [168] is only isolable at low temperatures like aminoborane. It readily oligomerizes as temperature and concentration increase. Borazole or borazine  $((\text{NHBH})_3)$  is a well-defined iminoborane oligomer.

Polymeric iminoboranes (PIB) have non-defined amounts of cross-linking and branching that are likely dependent on the synthetic conditions employed. In PAB and PIB, intramolecular and intermolecular interactions may play an important role.

To conclude, amine-boranes are unique in their ability to store and release hydrogen, nevertheless, the presence of other by-products along with hydrogen is a

potential drawback for their use in PEM fuel cells. Indeed, without a hydrogen purification unit, the hydrogen stream may be contaminated and poison the cell. This issue will form the primary focus of this study (see the experimental section in Chapters 4 and 5).

The above review clearly shows that:

- ✓ The most promising method to store hydrogen for its use for onboard applications is by using complex hydrides;
- ✓ Despite their increased hydrogen capacity, the temperature and reversibility are the main challenges encountered and yet to be solved;
- ✓ The main issues still to be addressed are: lowering the temperature of desorption and increasing the purity of the hydrogen delivery prior to addressing reversibility issues in the future.

Here, the objectives of the study are:

- ✓ Investigate suitable additives to pure  $\text{LiBH}_4$  such as transition metal chlorides, in order to lower the desorption temperature;
- ✓ Explore a new system based on B-N-H compounds involving  $\text{LiBH}_4$  but also  $\text{NH}_3\text{BH}_3$  as an intermediate, and the method in order to achieve a pure hydrogen delivery at low temperature and high capacity.

## **Chapter 3. Experimental Methods**

The literature review clearly points to some critical issues for hydrogen storage. Hence, the focus will be on preparing samples, that will then, be characterised to extract some vital information about their capability to be practical hydrogen storage media for onboard applications. All samples discussed in this study were routinely prepared, handled and analysed under inert atmosphere of argon.

### 3.1 Sample preparation

The materials were prepared using standard techniques detailed in previous publications e.g. mechanical milling. The samples were labelled as followed: for the addition of transition metal chlorides, ( $\text{LiBH}_4 + x\text{MCl}_n$ , X minutes) where x represents the molar ratio of  $\text{MCl}_n$  to  $\text{LiBH}_4$  and X represents the milling time in minutes; for the addition of ammonium chloride, ( $\text{LiBH}_4 (\text{NH}_3\text{BH}_3) + y\text{NH}_4\text{Cl}$ , Y minutes) where y represents the molar ratio of  $\text{NH}_4\text{Cl}$  to  $\text{LiBH}_4$  or  $\text{NH}_3\text{BH}_3$  and Y represents the milling time in minutes.

#### 3.1.1 Materials

Lithium borohydride ( $\text{LiBH}_4$ ), ammonia borane ( $\text{NH}_3\text{BH}_3$ ) and additives such as chlorides, e.g.  $\text{NH}_4\text{Cl}$  and  $\text{ZnCl}_2$ , and Carbon graphite, were selected as the primary materials. All these materials are very sensitive to air and moisture, so care should be taken when handling them, e.g. special facial mask and gloves. Some properties of chemicals may vary from one company to the other, so the chemicals have been

mainly ordered from Sigma Aldrich group ([Web 26]) except for  $\text{ZnCl}_2$  and  $\text{CrCl}_3$  and the sources of chemicals used in this project are listed in Table 3.1.

**Table 3.1:** Main characteristics of selected chemicals

Material	Materials supplier	Purity (%)
$\text{LiBH}_4$	Sigma-Aldrich	$\geq 95$
$\text{ZnCl}_2$	BDH	$\geq 97$
$\text{TiCl}_3$	Sigma-Aldrich	$\geq 99.99$
$\text{NiCl}_2$	Sigma-Aldrich	98
$\text{CrCl}_3$	Fisher Scientific	99
$\text{NH}_3\text{BH}_3$	Sigma-Aldrich	90
$\text{NH}_4\text{Cl}$	Sigma-Aldrich	$> 99.5$
Graphite	Sigma-Aldrich	$\geq 99.99$

### 3.1.2 Pre-treatment of powder mixtures

The glove box was permanently filled with pure Argon. The levels of oxygen and moisture are monitored and once exposed to air; cartridges are used to regenerate the atmosphere inside the glove box. The level of oxygen is maintained under 30 ppm and the level of moisture under 5 ppm. All the air- and moisture-sensitive chemicals are kept in the glove box under Argon at all times. Powder weighting and loading (in milling pot or in holders for TG, XRD or titration measurements) are all carried out inside the glove box.



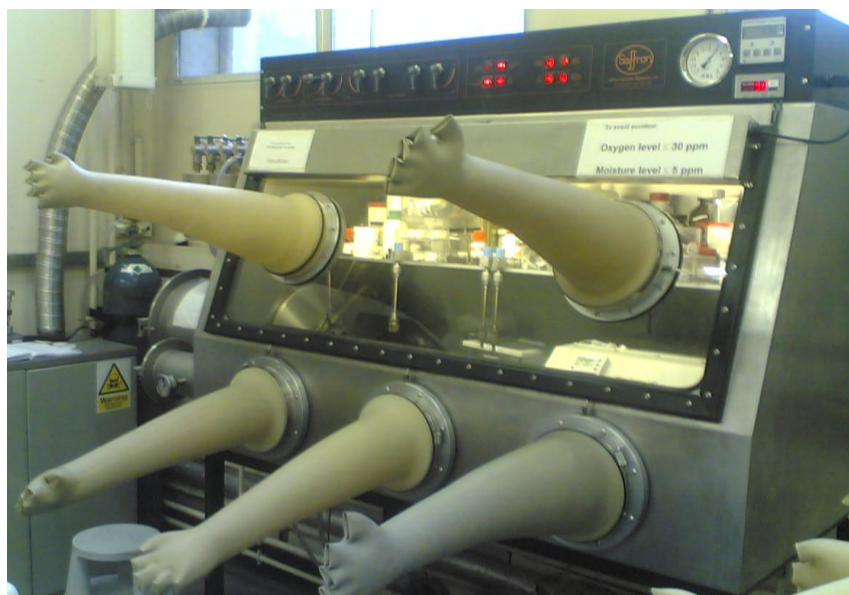


**Figure 3.1:** *Saffron Scientific Equipment Ltd Glove box*

### 3.1.3 Mechanical milling

Mechanical milling or alloying was originally invented as a method to manufacture oxide dispersion in strengthened nickel alloys. It is a high energy ball milling process, where alloying is the result of the repeated fracture and cold welding of the constitutive particles. In addition to attrition and agglomeration, high energy milling can induce chemical reactions, which can be used to influence the milling process and the sample composition.

A *Glen Creston Ltd SPEX 8000M* has been used throughout the project. The sample along with the steel grinding balls was loaded into one vial. The vial was secured in the clamp and swung back and forth approximately 1080 cycles per minute. Because of the amplitude and speed of the clamp, ball velocities are high ( $5\text{m.s}^{-1}$ ) and therefore, the energy from the balls are high, being the reason why it is known as high energy milling.

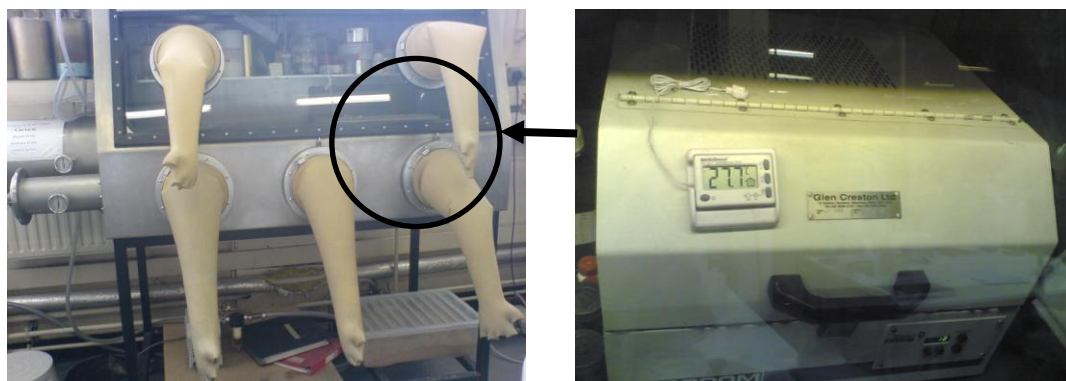


**Figure 3.2:** *Glen Creston Ltd SPEX 8000M* milling machine inside the argon filled glove box

Before the milling, the vial and milling balls are cleaned with ethanol and/or acetone and dried in an oven at 100°C for at least 1 hour. To optimize the effect of milling on the reaction mixture and obtain the desirable product and properties, milling parameters need to be set up during experiments. Among them, parameters such as: ball-to-powder ratio and milling time can be cited.

**Ball-to-powder-weight ratio:** Generally, a ratio of 10:1 is most commonly used for mixing. A large ratio results in high collision energy, which may introduce some unwanted reactions between powder mixtures. Hence, a ratio of 10:1 is used here for most powder mixings.

**Milling time:** This is the most important parameter. Normally, the time is chosen in the view of achieving a given mixing state. For different powder mixtures, e.g. different chemicals or same chemicals with different ratios, the optimised milling may vary. The milling time is closely associated with the factors mentioned above.

## 3.2 Sample characterisation

Based on the previous literature on hydrogen storage systems and the equipment available in the laboratories, the best experiments susceptible to provide information on the materials tested are: TG/DTA/MS, XRD, SEM/EDS and FT-IR.

### 3.2.1 TG-DTA-MS

The samples (between 5 and 15mg) were handled solely in the argon glove box in  $\text{Al}_2\text{O}_3$  sample holders (capacity: 70 $\mu\text{L}$ , annealed at 1100°C, *Mettler Toledo*) and then transferred as quickest as possible via a hermetic box to the thermobalance inside the machine without any contact with air. The apparatus allows us to use Thermogravimetry (TG), Differential Thermal Analysis (DTA) and Mass Spectrometry (MS) simultaneously.



**Figure 3.3:** *Setaram Setsys 16/18* TG/DTA facility (a) combined with MS (b)

The basic principle is that the sample is heated at a constant heating rate from the initial temperature up to the desired temperature. The samples properties measured are: the weight and the temperature by the TG/DTA facility and the composition of the gas stream by the MS facility.

Thermogravimetry (TG) is one of the oldest thermal analytical procedures which have been used extensively. The technique involves monitoring the weight loss or gain of a sample (and/or its reaction products) in a controlled atmosphere as a function of temperature.

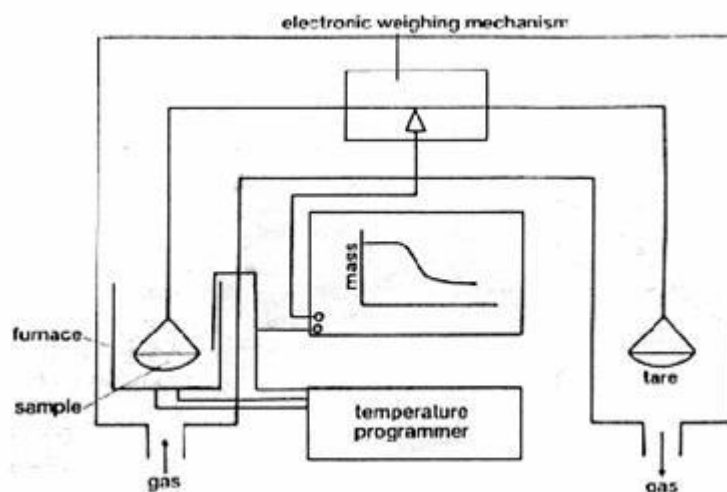


**Figure 3.4:** Schematic of a thermogravimetric apparatus, taken from [Web 27]

The gas chosen for the experiments is Argon with an adjustable flow rate of  $8\text{mL}\cdot\text{min}^{-1}$ . The experiments are carried out using a *Setaram Setsys 16/18* TG/DTA system with a precise of  $0.1\mu\text{g}$  during heating under a controlled atmosphere Argon flow or vacuum). The apparatus was operated by using the software “*Setsoft*” and can simultaneously collect the TG and DTA signals. The operational temperature range is from room temperature to  $1000^{\circ}\text{C}$ . A small turbo pump is also used in the system to induce a high vacuum environment.

Most TGA curves display weight losses. They are typically caused by:

- Chemical reactions such as combustions or reductions of oxides;
- Physical transitions such as evaporation or sublimation.

The shape of the curves is usually characteristic of the effect measured and can be used for identification purposes.

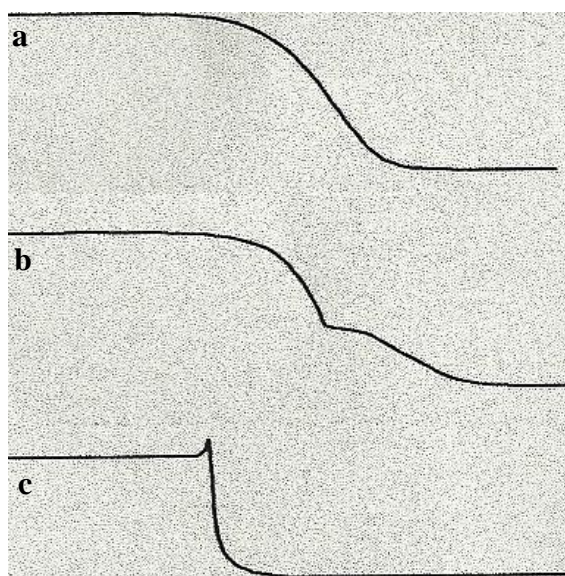


**Figure 3.5:** Typical TGA curves with characteristic effects: a) thermal decomposition with the formation of gaseous reaction products, b) multi-step decomposition, c) explosive decomposition with recoil effect, taken from Widmann [169]

Differential Thermal Analysis (DTA) involves heating the test sample and an inert reference under identical conditions, while recording any temperature difference between the sample and the reference. The two holders are individually equipped with a resistance sensor. On a heating cycle, the differential-temperature controller automatically adjusts the power to heat up either the reference or the sample identically. Therefore, phase changes and other thermal processes cause a difference in temperature between the sample and reference.

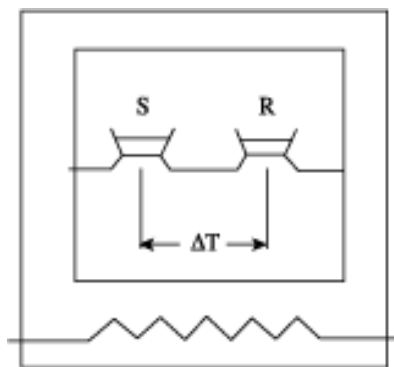


**Figure 3.6:** Schematic illustration of a DTA single cell, taken from web

The differential temperature is then plotted against time, or against temperature. The area under a DTA peak can be related to the enthalpy change and is not affected by the heat capacity of the sample.

Peaks may be characterised by:

1. Position (i.e., start, end, extrapolated onset and peak temperatures)
2. Size (related to the amount of material and energy of the reaction)
3. Shape (which can be related to the kinetics of the process).

The shape of a DTA peak does depend on sample weight and the heating rate used. Lowering the heating rate is roughly equivalent to reducing the sample weight; both lead to sharper peaks with improved resolution, although this is only useful if the signal to noise ratio is not compromised. The influence of heating rate on the peak shape and peak disposition can be used to advantage in the study of decomposition reactions, but for kinetic analysis, it is important to minimise thermal gradients by reducing specimen size or heating rate.

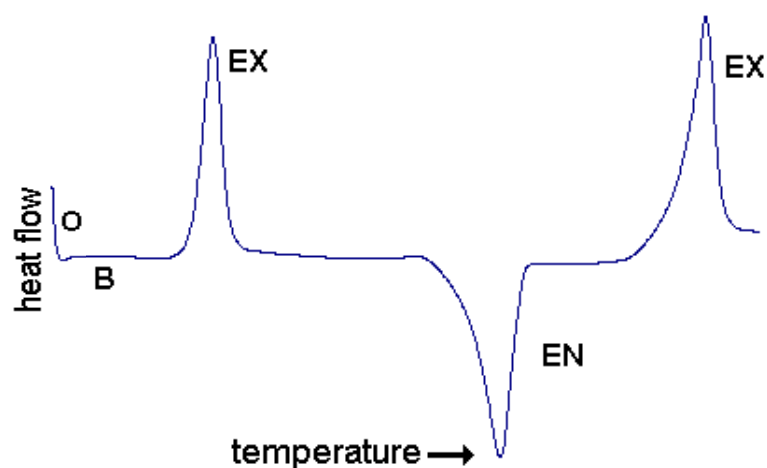


**Figure 3.7:** Typical DTA curve with characteristic effects, O: offset, B: baseline, EX: exothermic event, EN: endothermic event, taken from [Web 28]

Some possible processes giving enthalpy peaks are listed below:

**Table 3.2:** Nature of DTA peaks involved in typical processes

Process	EN*	EX**
Crystallisation	X	
Melting	X	
Vaporisation	X	
Sublimation	X	
Desorption	X	X
Decomposition	X	X
Solid-solid transition	X	X
Solid-solid reaction	X	X
Solid-liquid reaction	X	X
Solid-gas reaction	X	X

\*EN: endothermic event, \*\*EX: exothermic event

An alternative technique, which shares much in common with DTA, is Differential Scanning calorimetry (DSC). In this technique, it is the temperature of the sample and reference that remains the same rather than the heat flow. Both DSC and DTA provide similar information.

A mass spectrometer (MS) can be coupled to the TG-DTA instrument for continuous analysis and identification of the evolved gases during heating of the sample. The gases are routed to the MS via a capillary, which can be heated up to 200°C to keep the evolved gases from condensing.

Mass Spectrometry is an analytical technique that is used to identify unknown compounds, quantify known materials and elucidate the structural and physical properties of ions. It is a technique associated with very high levels of specificity and sensitivity.

A beam of energetic electrons is created inside a heated chamber by passing current through a filament. The negatively charged electrons are attracted away from the filament towards a plate called the trap by maintaining the trap at a relative positive potential. Sample molecules in the gas phase are directed into this high energy beam. The resulting direct interaction causes loss of an electron from the molecule, thus generating a positively charged molecular ion. Depending on the compound and the ionisation energy, the molecular ion may then fragment. Once ionised, the molecular ion may fragment, producing ions of lower mass than the original precursor molecule.

These fragment ions are dependent on the structure of the original molecule. The ions produced are repelled out of the ion source and accelerated towards the analyser region. Although both positive and negative ions may be generated at the same time, one polarity is chosen and either positive or negative ions are analysed and recorded.



Molecules that do not ionise, i.e. remain neutral, are pumped away and will not be detected. Ions entering a field experience a deflecting force, depending on the strength of the field and the mass-to-charge ratio of the ion. By scanning the field strength all the ions produced in the ion source are sequentially focused at the detector (which is usually a photomultiplier or an electron multiplier). The resulting pattern obtained is called a mass spectrum.

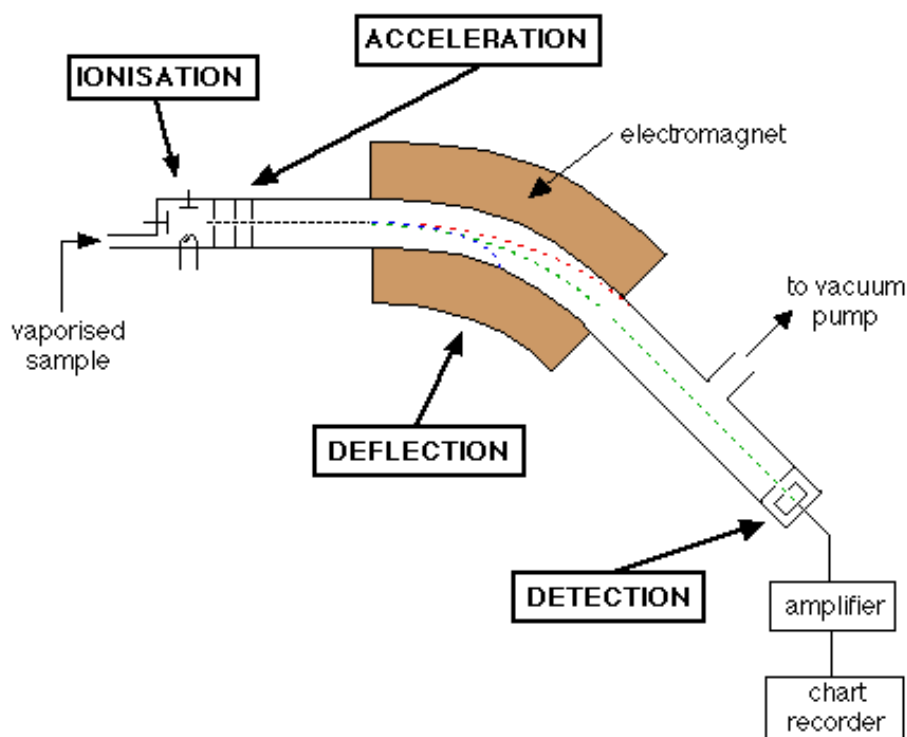


**Figure 3.8:** Schematic illustration of a mass spectrometer, taken from [Web 29]

The gas desorbed from the sample and generated inside the TG/DTA, is introduced into the mass spectrometer via the vial connected between TG and MS (Please refer to Figure 3.3). The mass spectrometer is generally kept under high vacuum ( $<10^{-5}$  mbar provided by a turbo pump).

The MS analysis software allows us to perform two kinds of scans:

1) MCD scan to detect the unknown compounds during the scanning, then these mass values need to be matched to the library database to decide the product.

2) MID scan to detect the already known compounds by setting up the mass of possible products before the scan, and the results can tell the product mass evolution during the experiment as a function of time. In this study, MID method was used for most experiments. MCD scan was first performed to allow the detection of all evolved gases then MID method was used for identification.

TG-DTA-MS data are generally presented in the form of a spectrum with temperatures as the x-axis and heat flow, mass loss or ion masses values as the y-axis as shown in the following figure.

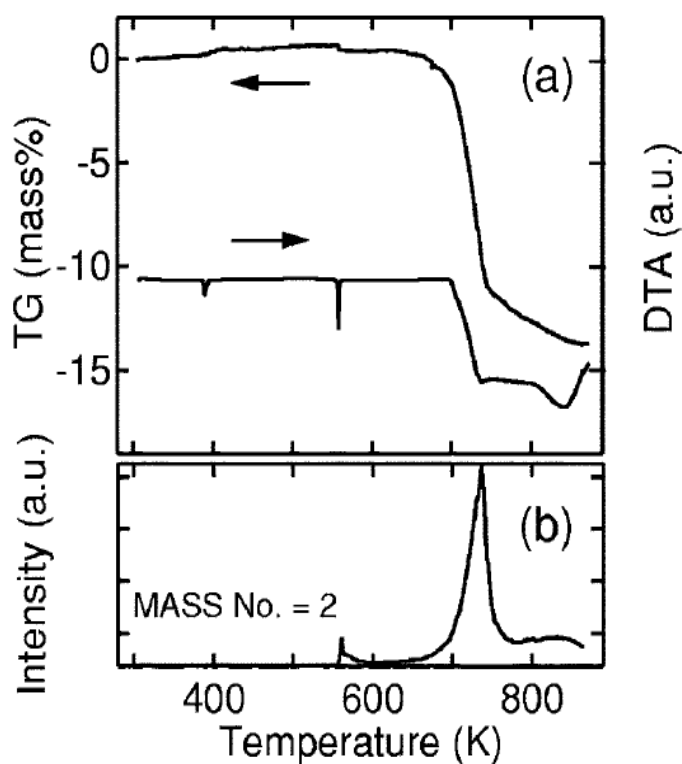


**Figure 3.9:** Example of TG-DTA-MS figures for pure  $\text{LiBH}_4$  taken from Orimo *et al.* [170]

### 3.2.2 X-Ray Diffraction (XRD)

X-ray Powder Diffraction (XRD) is an analytical technique used to identify and characterize unknown crystalline materials. X-rays are used to determine the interplanar spacings (d-spacing) of the unknown materials.

$$\lambda = 2d_{hkl} \sin \theta_{hkl} \quad \text{Eq. 3.1}$$

Where h, k and l are the Millar indices of a set of planes.

The samples were sealed in quartz glass capillaries and are analyzed as powders with millions of crystals randomly oriented to ensure that all the lattice planes diffract simultaneously. When the Bragg conditions for constructive interference are obtained, a "reflection" is produced, and the relative peak height is generally proportional to the number of grains in a preferred orientation.

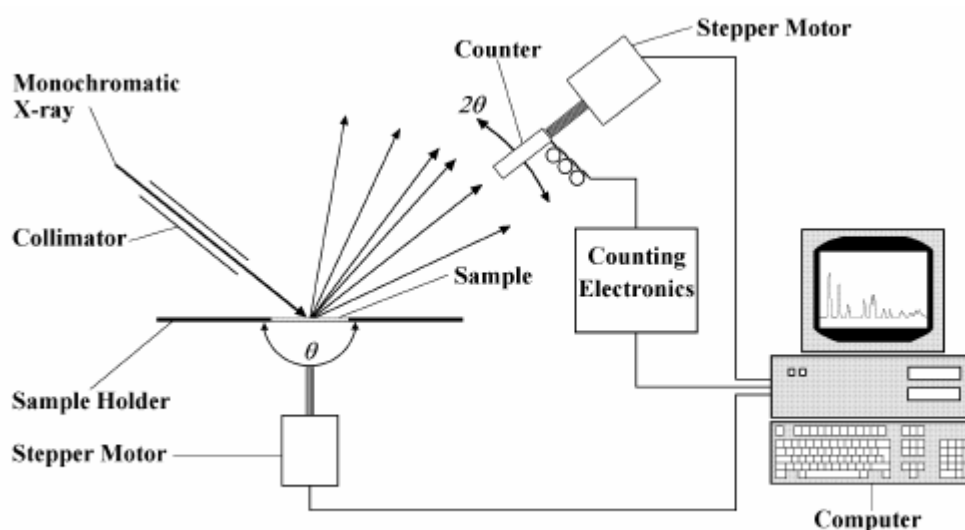


**Figure 3.10:** Schematic illustration of a X-RAY diffractometer, taken from web

Standard scans were carried out using a *STOE STADI-P* diffractometer. The source is Cu K $\alpha$  radiation ( $\lambda = 1.5406$  in Bragg-Brentano geometry) from a conventional water-cooled X-ray tube. The powder was protected from air and humidity by encapsulation in a capillary tube (bore diameter: 0.5 mm) made of quartz. The diffraction patterns were collected over the angular range  $10^\circ \leq 2\theta \leq 70^\circ$  in steps of  $0.05^\circ$  over 60 minutes with the attached software, *Diffraclus Basic 4.0*, which allows rapid scans and longer data collection. Diffraction data were initially analysed using *Eva* Software, a programme for phase identification.



**Figure 3.11:** *STOE STADI-P* diffractometer

A diffraction pattern can help to solve many problems:

1. Identification of known phases using databases: **Peak Position**
2. Quantitative analysis: amorphous or crystalline phases: **Peak Heights**
3. Powder properties: microstrain, size, texture, defects **Peak Width**

XRD has been used in the study for the detection of phase changes during the milling or after dehydrogenation.

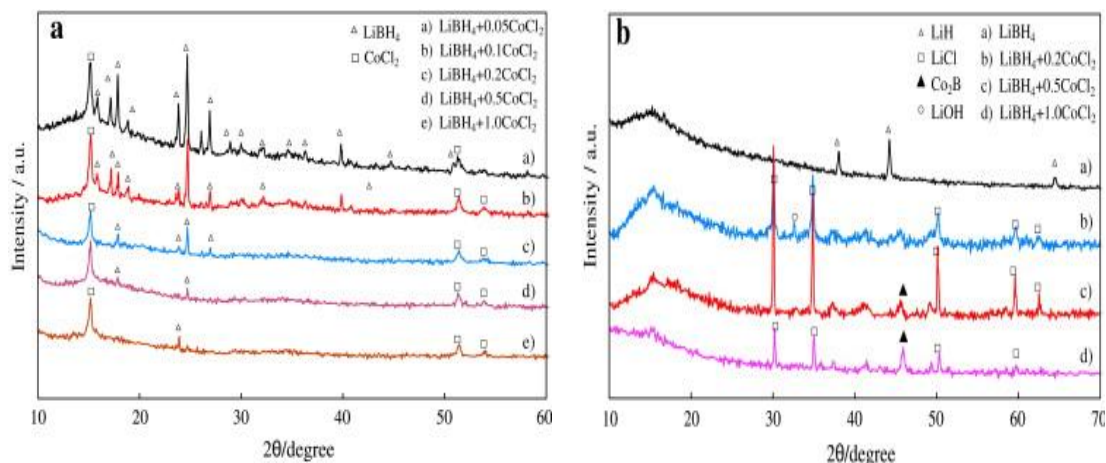


**Figure 3.12:** Example of XRD patterns for chlorides-added  $\text{LiBH}_4$  systems (a) before dehydrogenation and (b) after dehydrogenation taken from Zhang *et al.* [171]

### 3.2.3 Scanning Electron Microscopy / Energy Dispersive X-Ray Spectroscopy (SEM/EDS)

SEM was performed using a *JEOL JSM 6301F* apparatus which consists of a cold cathode field emission that requires a vacuum better than  $10^{-8}$  Torr to obtain high-resolution image. For the sample preparation, a small amount of sample powder was taken out from the sample vial and carefully blown to the SEM specimen holder. All these operations are carried out in the glove box and the specimen are transferred by a sealed holder to the SEM test. Usually, the samples do not need any coating before being tested as the elements are very light and Carbon could absorb all the emission and prevents a good analysis.

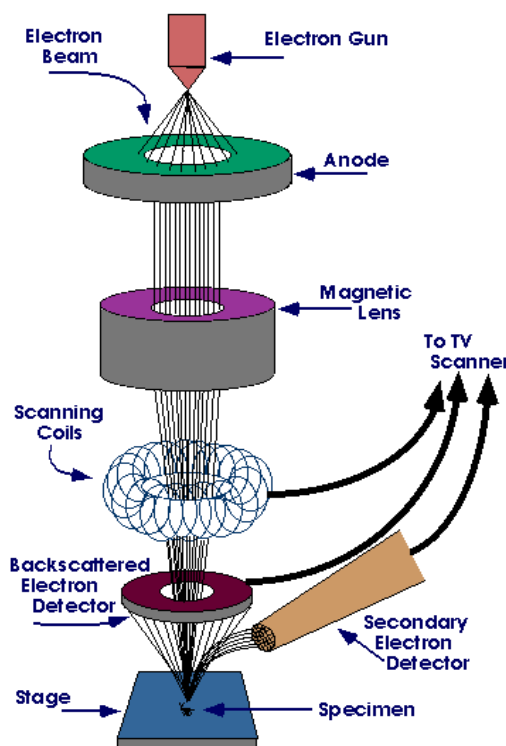


**Figure 3.13:** Schematic illustration of a Scanning Electron microscope, taken from [Web 30]

The scanning electron microscope (SEM) uses a focused beam of high-energy accelerated electrons to generate a variety of signals produced by electron-sample interactions.

The signals that derive from these interactions include secondary electrons, backscattered electrons, photons, visible light and heat. Secondary electrons and backscattered electrons are commonly used for imaging samples: secondary electrons are most valuable for showing morphology and topography on samples and backscattered electrons are most valuable for illustrating contrasts in composition in multiphase samples (i.e. for rapid phase discrimination).

X-ray generation is produced by inelastic collisions of the incident electrons with electrons in discrete orbitals (shells) of atoms in the sample. As the excited electrons return to lower energy states, they yield X-rays that are of a fixed wavelength (that is

related to the difference in energy levels of electrons in different shells for a given element).

Thus, characteristic X-rays are produced for each element in a mineral that is "excited" by the electron beam. SEM analysis is considered to be "non-destructive"; that is, x-rays generated by electron interactions do not lead to volume loss of the sample, so it is possible to analyze the same materials repeatedly.

Information about the sample such as external morphology (texture), chemical composition, and crystalline structure and orientation of materials making up the sample can be obtained. In most applications, data are collected over a selected area of the surface of the sample, and a 2-dimensional image is generated that displays spatial variations in these properties. In this particular case, the SEM is also capable of performing analyses of selected point locations on the sample; this approach is especially useful in qualitatively or semi-quantitatively determining chemical compositions using Energy Dispersive X-Ray Spectroscopy (EDS).

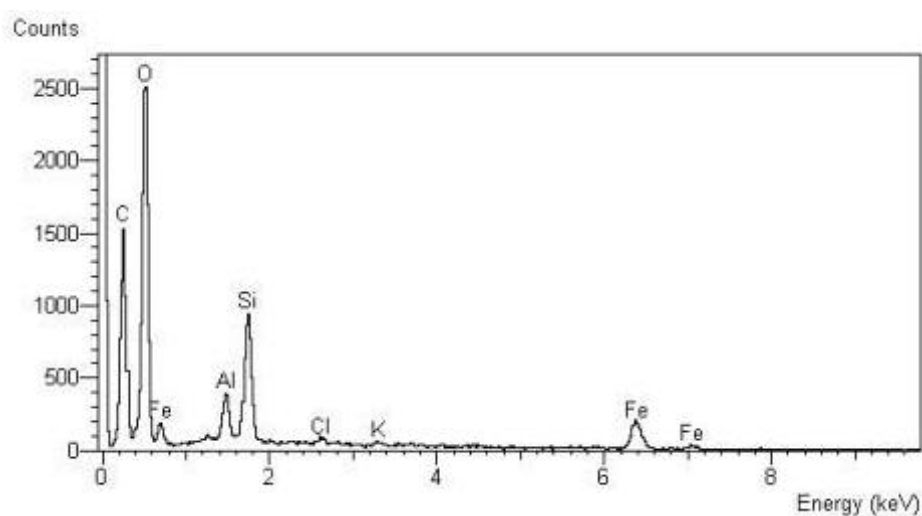


**Figure 3.14:** Typical EDS spectrum, taken from web

For these particular materials systems, Scanning Electron Microscopy (SEM) was conducted to characterize the particle size, phase distribution and particle morphology of milled powders before and after hydrogen release.

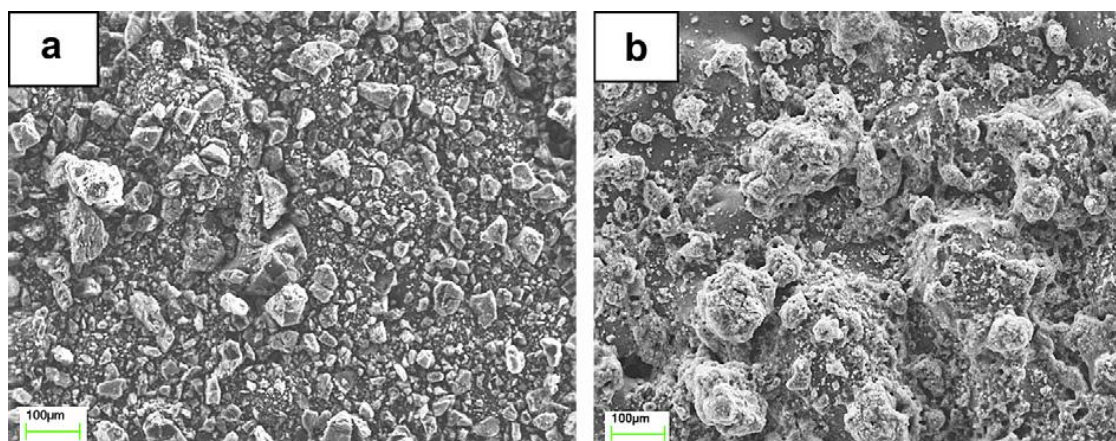


**Figure 3.15:** Example of SEM morphologies for  $\text{LiBH}_4$ -based systems (a): after dehydrogenation and (b): after rehydrogenation on taken from Fang *et al.* [172]

### 3.2.4 Fourier Transformation Infrared (FT-IR) Spectroscopy

At temperature above absolute zero, all the atoms in molecules are in continuous vibration with respect to each other, and the major types of molecular vibrations are stretching ( $\nu$ ) and bending ( $\sigma$ ). When the frequency of a specific vibration is equal to the frequency of the IR radiation directed on the molecule, the molecule absorbs the radiation.

Each type of bond, between the different atoms, will absorb the IR radiation and begin to vibrate at slightly different frequencies from one to another. This phenomenon can be used and assessed to examine various molecules by observing the different vibrational signals.



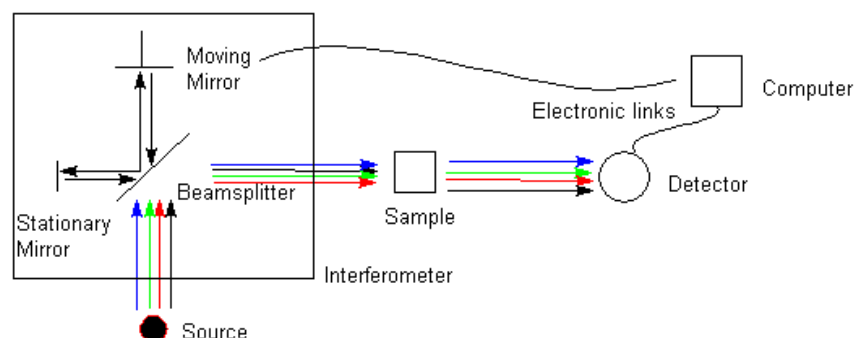


**Figure 3.16:** Schematic illustration of a Fourier Transformation Infrared Spectroscopy, taken from [Web 31]

Different functional groups absorb characteristic frequencies of IR radiation. Using various sampling accessories, IR spectrometers can accept a wide range of sample types. Thus, IR spectroscopy is an important and popular tool for the identification of compounds and structures.



**Figure 3.17:** Digilab Excalibur IR spectrophotometer connected to the MS via a T connection

Infrared radiation spans a section of the electromagnetic spectrum having wavenumbers from 13,000 to 10  $\text{cm}^{-1}$ , or wavelengths from 0.78 to 1000  $\mu\text{m}$ .

**Table 3.3: the 3 smaller areas of the IR region**

	Near IR	Mid IR	Far IR
<b>Wavenumber (cm<sup>-1</sup>)</b>	13,000 – 4,000	4,000 - 200	200 - 10
<b>Wavelength (μm)</b>	0.78 – 2.5	2.5 - 50	50 – 1,000

In this project, IR absorption positions are generally presented in terms of wavenumbers, which defines the number of waves per unit length.

IR absorption data are generally presented in the form of a spectrum with wavenumbers as the x-axis and absorption intensity or percent transmittance as the y-axis. Transmittance,  $T$ , is the ratio of radiant power transmitted by the sample ( $I$ ) to the radiant power incident on the sample ( $I_0$ ). Absorbance ( $A$ ) is the logarithm to the base 10 of the reciprocal of the transmittance ( $T$ ).

$$A = \log_{10}(1/T) = -\log_{10} T = -\log I / I_0 \quad \text{Eq. 3.2}$$

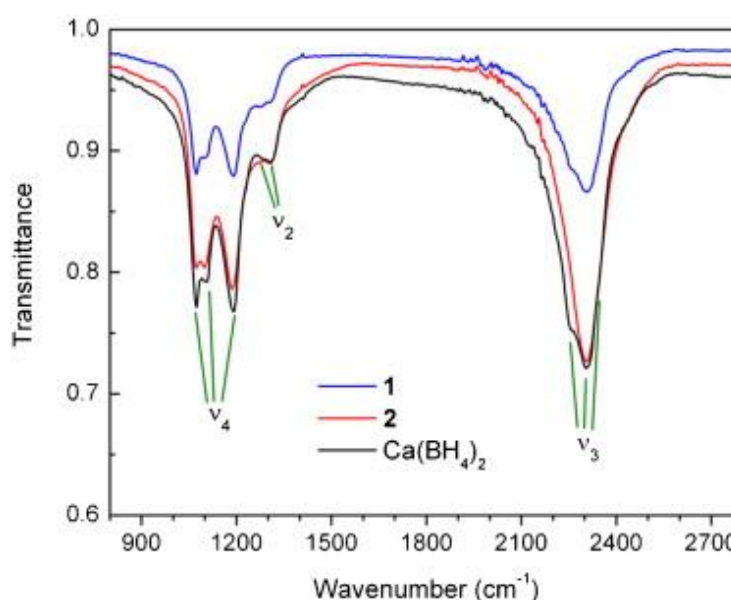


**Figure 3.18:** Examples of FT-IR spectra – Asymmetric bending, symmetric bending, and asymmetric stretching modes of  $[\text{BH}_4]^-$  are labelled as  $\nu_4$ ,  $\nu_2$  and  $\nu_3$  respectively taken from Youn Lee *et al.* [173]

The transmittance spectra provide better contrast between intensities of strong and weak bands because Transmittance  $T$  ranges from 0 to 100 % whereas Absorbance  $A$  ranges from infinity to Zero.

For the experiments in this study, the IR spectrum of the sample was collected with a *Digilab Excalibur IR* spectrophotometer. The samples (powder) were directly placed in the sample holder. The sample holder is suited in a specially designed cell made of KBr walls, connected with heating, cooling and purging system.

Fourier Transformation Infrared (IR) Spectroscopy is also used to identify the compounds, by matching spectrum of unknown compound with reference spectrum.

**Table 3.4:** Example of vibrational frequencies of relevant borohydrides from various sources

Compound	Source	Spectral information	Frequency ( $\text{cm}^{-1}$ )	
			Stretching vibrations	Bending vibrations
$\text{LiBH}_4$	[96]	IR	2290	1094
$\text{Zn}(\text{BH}_4)_2$	[108]	IR	2084-2307-2454	1108-1396

Once the different experimental methods have been presented, the most pertinent results obtained are described and discussed thoroughly in the following experimental section.

## **Chapter 4. Experimental Results**

### 4.1 Pure $\text{LiBH}_4$

## 4.1 Decomposition of pristine lithium borohydride, $\text{LiBH}_4$

Clear understanding of the thermal decomposition of  $\text{LiBH}_4$  is primarily essential for the following study of binary compositions of  $\text{LiBH}_4$  associated with chlorides or,  $\text{NH}_4\text{Cl}$ . It is also vital to compare the obtained results with the ones reported in the literature.

### 4.1.1 Dehydrogenation properties using TG-DTS-MS

Thermogravimetry (TG) coupled with Mass Spectrometry (MS) are used to determine the nature of the evolved gases during the thermal decomposition of pure  $\text{LiBH}_4$ . Also, MCD scan was performed over the entire mass spectral region from 0 to 200. Hydrogen appeared to be the main gas evolved along with other gases identified as  $\text{N}_2$ ,  $\text{O}_2$ ,  $\text{H}_2\text{O}$  and Argon as consigned in Table 4.1 below.

**Table 4.1:** Ion masses and tentative identification for  $\text{LiBH}_4$  mass spectra

Mass charge ratio (m/z)	Ion identification
2	$^1\text{H}_2^+$
17	$^{16}\text{O}^1\text{H}^+$
18	$^1\text{H}_2^{16}\text{O}^+$ , $^{17}\text{O}^1\text{H}^+$ , $^{18}\text{O}^+$
20	$^1\text{H}_2^{18}\text{O}^+$ ,
28	$^{14}\text{N}_2^+$ , $^{11}\text{B}_2^1\text{H}_6^+$
36	$^{18}\text{O}_2^+$ , $^{36}\text{Ar}^+$
38	$^{38}\text{Ar}^+$
40	$^{40}\text{Ar}^+$

The evolution of gas such as  $\text{H}_2\text{O}$ ,  $\text{N}_2$ ,  $\text{O}_2$  and Ar is negative and indicates that they were initially present in the chamber and can be classified as residual gases not directly linked to the thermal desorption of  $\text{LiBH}_4$ .

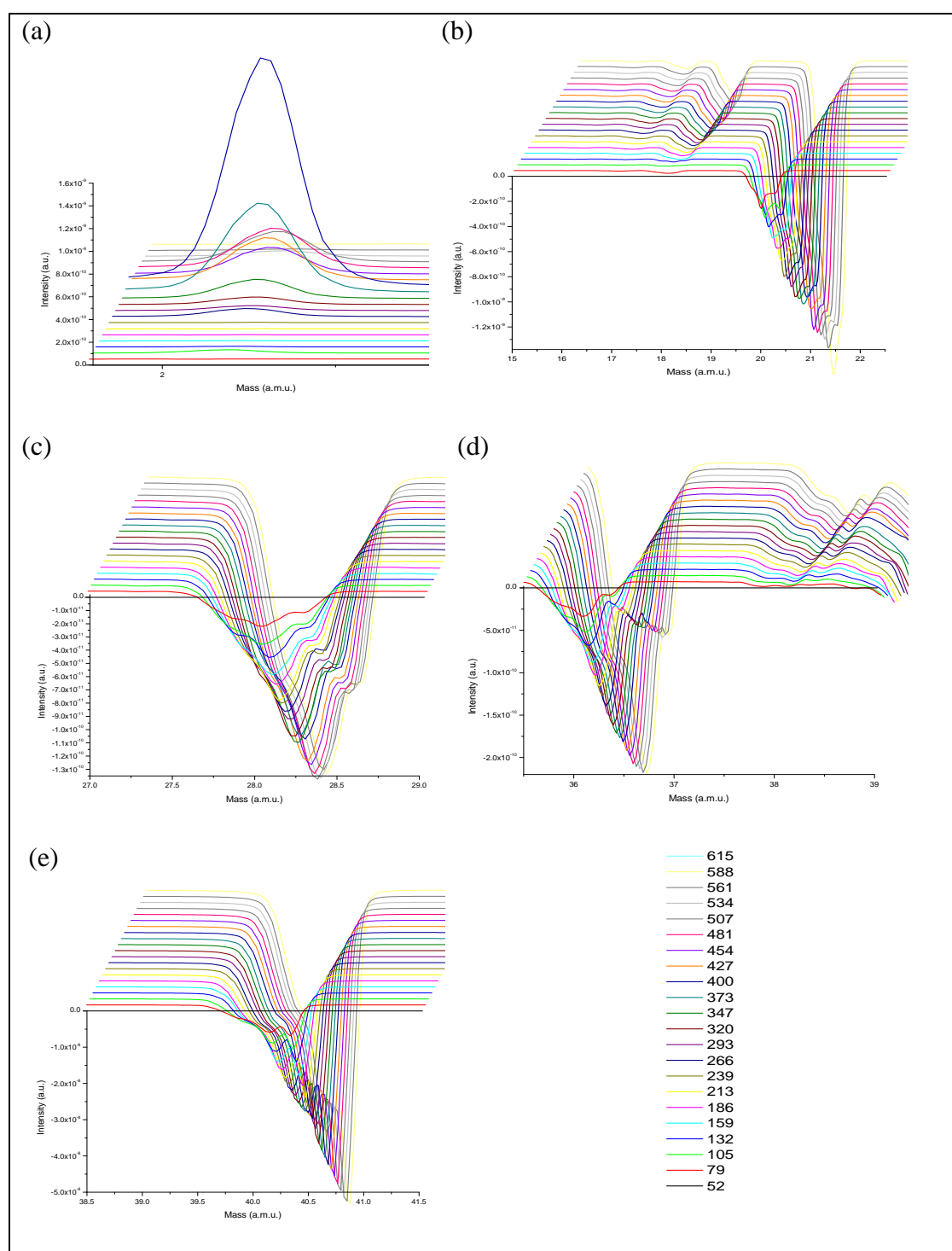


**Figure 4.1:** MCD scans (a): mass 2, (b): masses 17, 18, 20, (c): mass 28, (d): masses 36, 38, (e): mass 40 as a function of cycle temperature

Only  $H_2$  has a positive evolution when the temperature is increased from room temperature up to around  $600^\circ C$ . The 3D representation allows us to identify a huge surge of hydrogen around  $400^\circ C$ .

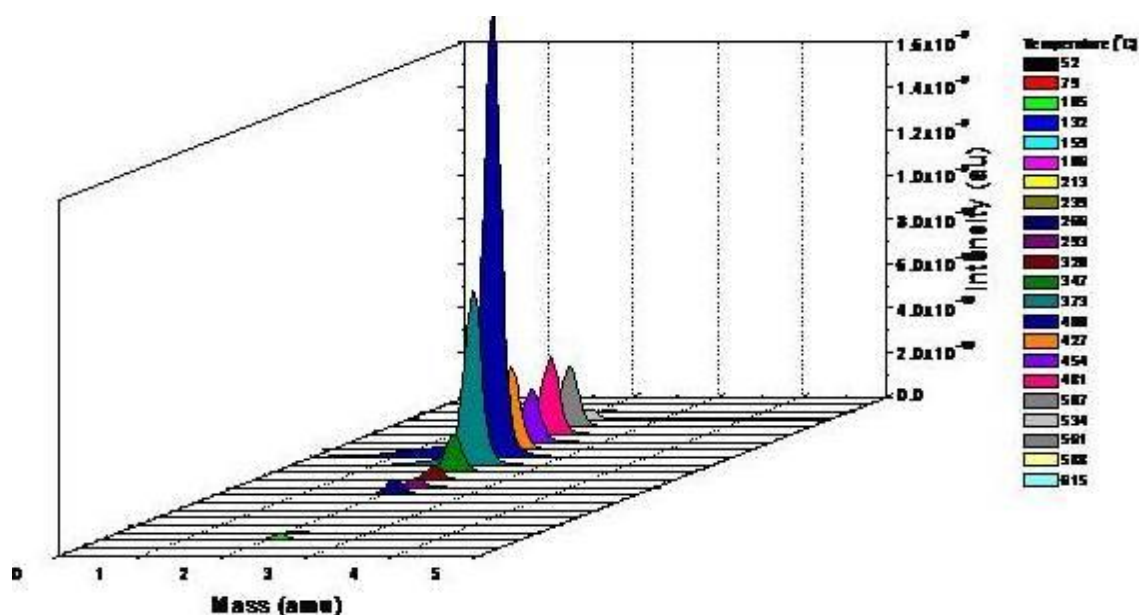


Figure 4.2: 3D representation of  $H_2$  ( $m/z=2$ ) measurements as a function of cycle temperatures

The simultaneous TG, DTA and MS measurements of pure  $LiBH_4$  are consigned on the next figure.

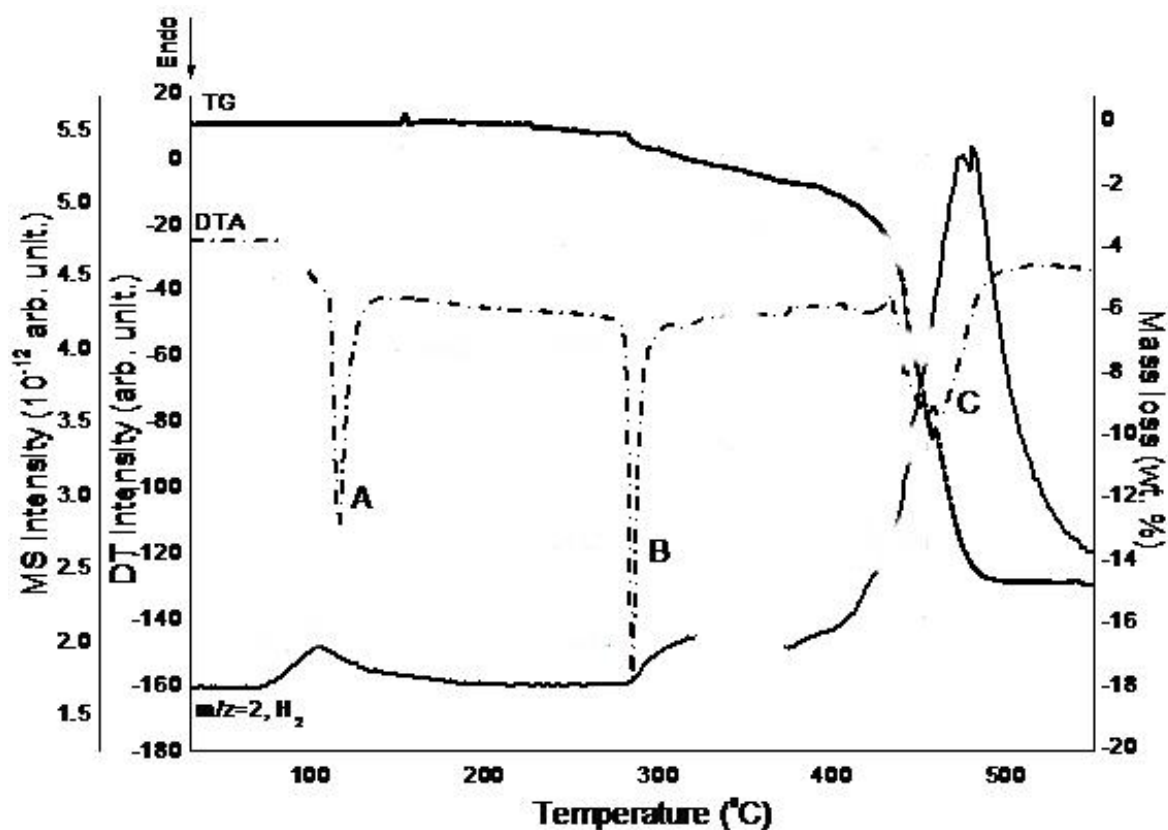


Figure 4.3: Simultaneous DTA, TG and MS of pure  $LiBH_4$  – Heating rate:  $5^{\circ}C.min^{-1}$  to a maximum temperature of  $550^{\circ}C$

For the as-received  $\text{LiBH}_4$ , the first stage started from 80°C until 135°C and is characterised by a sharp endothermic DTA peak (A) with small shoulders peaked at 110°C. The latter was not accompanied by a detectable simultaneous mass loss; however, on the MS results, some hydrogen is detected suggesting that it is a minor loss of hydrogen which accompanied this effect.

In fact, the second stage was observed to start around 280°C with a sharp and acute endothermic DTA peak (B). It could be seen that the onset for desorption occurred after this event. About approximately 4 wt % of mass loss is observed simultaneously on the TG after 280°C until 380°C. It is accompanied on the MS results with a release of hydrogen.

The third stage began around 380°C and up to 480°C with a broad endothermic DTA peak (C), 10.6 wt % of mass loss was recorded. Correspondingly, a sharp release of hydrogen was observed on the MS results.

#### 4.1.2 Structural and morphological properties using XRD and SEM/EDS

X-Ray Diffraction has been performed on the as-received  $\text{LiBH}_4$ . The experimental pattern has been confronted with reference data and all the peaks have been attributed to the presence of crystalline  $\text{LiBH}_4$ .



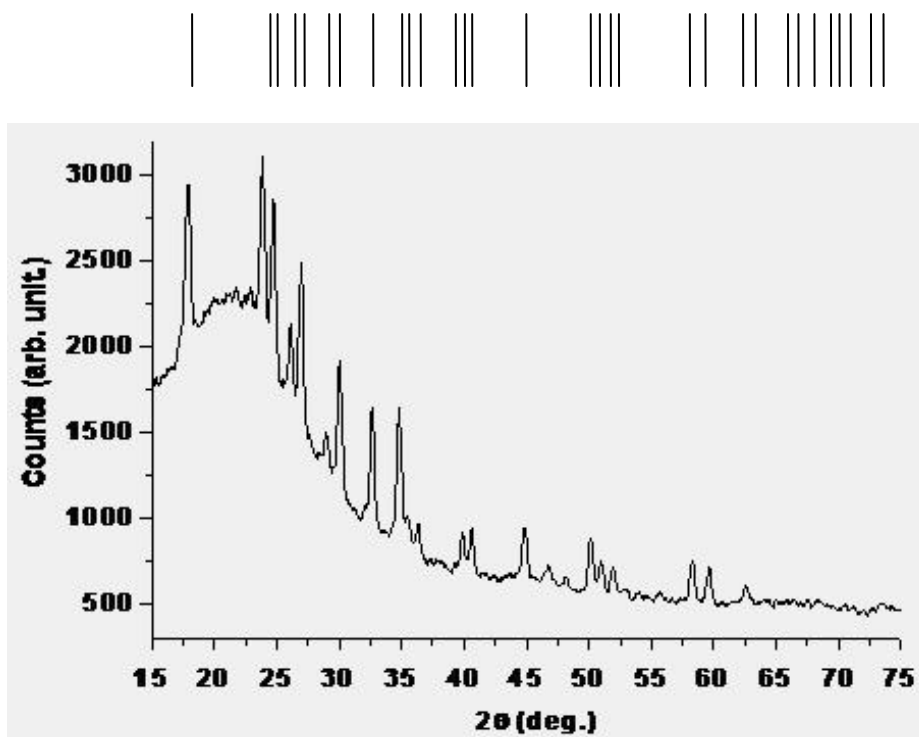


**Figure 4.4:** XRD diffraction pattern of as-received pure  $\text{LiBH}_4$ : experimental curve and fitted peaks on top

Alongside XRD, SEM has been used to observe the morphology of pure  $\text{LiBH}_4$  and they will be used as a reference to determine if after applying milling to  $\text{LiBH}_4$ -based mixtures, the particle size and morphology are different. In Figure 4.5, the low magnification on the left image showed a uniform distribution of big particles, confirmed to be agglomerates of smaller particles as seen on the right image.

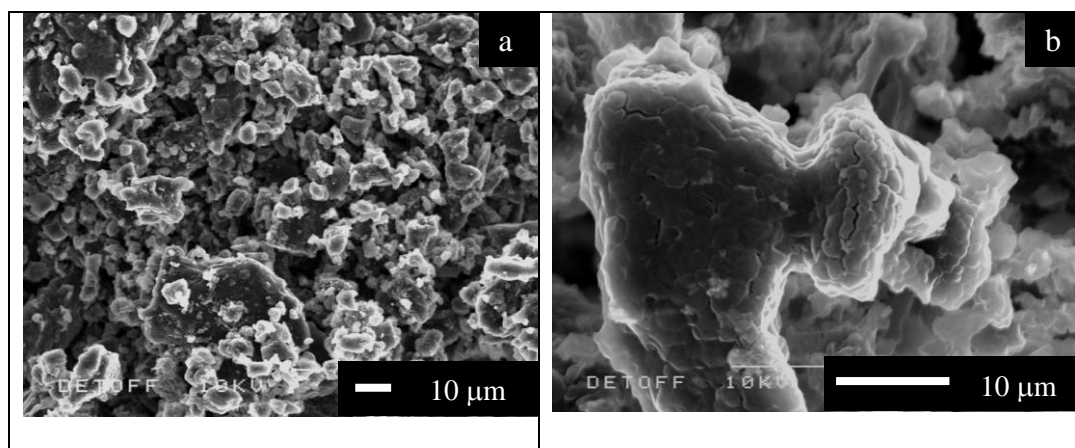


**Figure 4.5:** SEM images of pure  $\text{LiBH}_4$  after 5 minutes milling at low (a) and high (b) magnifications

In summary, the figures show that the evolution of phase transitions of  $\text{LiBH}_4$  occurred in 3 stages between room temperature and  $550^\circ\text{C}$  with 3 endothermic peaks at these temperatures:  $110^\circ\text{C}$ ,  $280^\circ\text{C}$  and  $460^\circ\text{C}$  with a total mass loss of 13.9 wt %. The main desorption started around  $380^\circ\text{C}$ , which is very high and needs to be reduced. Also, only hydrogen has been detected in the gas stream liberated upon heating of  $\text{LiBH}_4$ .

This very first analysis set our work around 2 key features:

- 1- Decrease the main onset desorption temperature i.e. improve the hydrogen release temperatures;**
- 2- Keep the hydrogen delivery the purest possible i.e. monitor the composition of the emitted gases.**

## **Chapter 4. Experimental Results**



## 4.2 Decomposition of ( $n\text{LiBH}_4 + \text{MCl}_n$ )

After the dehydrogenation characteristics of pure  $\text{LiBH}_4$  have been confirmed in the first experimental section, the decomposition of mixtures of  $\text{LiBH}_4$  with additives has been investigated.

### 4.2.1 Experimental design

In this work, the effect of metal chlorides of Ti, Cr, Ni and Zn additions on the dehydrogenation characteristics of  $\text{LiBH}_4$  has been investigated. The addition of chlorides to  $\text{LiBH}_4$  has already been investigated showing promising results [136]-[141].

The idea is to modify desorption patterns by mixing  $\text{LiBH}_4$  with different metal chloride additives,  $\text{MCl}_n$ . The selection of 4 metal chlorides (see Figure 4.6) for this specific study is guided by a study of Nakamori *et al.* [142] suggesting that the cation  $\text{M}^{n+}$  in  $\text{M}(\text{BH}_4)_n$  plays an important role in deciding the stability of the supposedly formed borohydride.

The thermal desorption temperature of  $\text{M}(\text{BH}_4)_n$  has been found to be inversely proportional to the Pauling electronegativity of the metal cation M. According to this relation, Li *et al.* [174] showed that the stability of  $\text{LiBH}_4$  could be adjusted by the formation of  $\text{MLi}_{m-n}(\text{BH}_4)_m$ , where M is a metal with large Pauling electronegativity such as Zn. Pauling [175] described the electronegativity as the tendency of an atom to attract electron towards itself, and thus the tendency to form negative ions. Nevertheless, the electronegativity is not typically an atomic property but the property

of an atom in a molecule. In this view, Zn (1.65) and other transition metals such as Ti (1.54) and Cr (1.66), with similar Pauling electronegativities and Ni (1.91) with a very large electronegativity have been selected.

As a matter of fact, the work was carried out in different steps but the main objective was to understand the interaction between  $\text{LiBH}_4$  and  $\text{MCl}_n$  by gaining information such as desorption capacity, desorption temperature and the link with cation electronegativities. As the mixing is performed by means of SPEX ball milling, it is necessary to identify the milling effect, e.g. the possible change of structure, and the presence of precursor species affecting the thermal desorption properties of mixtures of  $\text{LiBH}_4$  and  $\text{MCl}_n$ .

**PERIODIC TABLE OF THE ELEMENTS**

<http://www.kjf-split.hr/periodni/en/>

**Legend:**

- Metal
- Semimetal
- Nonmetal
- Alkali metal
- Alkaline earth metal
- Transition metals
- Lanthanide
- Actinide
- Chalcogens element
- Halogens element
- Noble gas

**Standard State (25 °C; 101 kPa):**

- Ne - gas
- Fe - solid
- Ga - liquid
- Synthetic

**Period 4 Elements (Highlighted):**

Element	Symbol	Atomic Number	Relative Atomic Mass
Potassium	K	19	39.098
Calcium	Ca	20	40.078
Scandium	Sc	21	44.956
<b>Ti</b>	<b>Ti</b>	<b>22</b>	<b>47.867</b>
<b>V</b>	<b>V</b>	<b>23</b>	<b>50.942</b>
<b>Cr</b>	<b>Cr</b>	<b>24</b>	<b>51.996</b>
Manganese	Mn	25	54.938
Iron	Fe	26	55.845
Cobalt	Co	27	58.933
<b>Ni</b>	<b>Ni</b>	<b>28</b>	<b>58.693</b>
Copper	Cu	29	63.546
<b>Zn</b>	<b>Zn</b>	<b>30</b>	<b>65.38</b>
Gallium	Ga	31	69.723
Germanium	Ge	32	72.64
Arsenic	As	33	74.922
Selenium	Se	34	78.96
Bromine	Br	35	79.904
Krypton	Kr	36	83.80

**Lanthanide Series:**

Element	Symbol	Atomic Number	Relative Atomic Mass
Lanthanum	La	57	138.91
Cerium	Ce	58	140.12
Praseodymium	Pr	59	140.91
Neodymium	Nd	60	144.24
Promethium	Pm	61	(145)
Samarium	Sm	62	150.36
Europium	Eu	63	151.96
Gadolinium	Gd	64	157.25
Terbium	Tb	65	158.93
Dysprosium	Dy	66	162.50
Holmium	Ho	67	164.93
Erbium	Er	68	167.26
Thulium	Tm	69	168.93
Ytterbium	Yb	70	173.04
Lutetium	Lu	71	174.97

**Actinide Series:**

Element	Symbol	Atomic Number	Relative Atomic Mass
Actinium	Ac	89	(227)
Thorium	Th	90	232.04
Protactinium	Pa	91	231.04
Uranium	U	92	238.03
Neptunium	Np	93	(237)
Plutonium	Pu	94	(244)
Americium	Am	95	(243)
Curium	Cm	96	(247)
Berkelium	Bk	97	(247)
Californium	Cf	98	(251)
Einsteinium	Es	99	(252)
Fermium	Fm	100	(257)
Mendelevium	Md	101	(258)
Nobelium	No	102	(259)
Lawrencium	Lr	103	(262)

Editor: Aditya Vardhan (adivur@netlinx.com)

**Figure 4.6:** Periodic table highlighting selected metals at fourth period in the periodic table forming chlorides added to  $\text{LiBH}_4$  taken from [Web 32]

The properties of the starting materials are consigned in Table 4.2 in order to identify the events occurring during the dehydrogenation of the different mixtures. Attention is drawn to the nature of the cation metal present in chlorides as transition metals are heavy materials, therefore the hydrogen capacity of the overall system mixture is lowered considerably as indicated in the table. Indeed, the overall hydrogen capacity of the different systems is limited to around 5 wt %, which is still acceptable at the condition that hydrogen desorption occurs at very mild conditions.

**Table 4.2:** Properties of starting materials and possibly formed metal borohydrides

$n\text{LiBH}_4 + \text{MCl}_n$	Pauling electronegativity of the metal cation [Web 33]	Overall hydrogen capacity (wt % $\text{H}_2$ )	Chloride melting point ( $^{\circ}\text{C}$ )
$3\text{LiBH}_4 + \text{TiCl}_3$	1.54	5.5	425
$2\text{LiBH}_4 + \text{ZnCl}_2$	1.65	4.5	293
$3\text{LiBH}_4 + \text{CrCl}_3$	1.66	5.4	1150
$2\text{LiBH}_4 + \text{NiCl}_2$	1.91	4.6	1001

Results of the structural and thermal analyses are presented in the next 2 subsections followed by a summary.

#### 4.2.2 Effect of milling from structural and morphological analyses using XRD, FT-IR and SEM/EDS

In our quest to understand the hydrogen desorption mechanisms of the  $\text{LiBH}_4\text{-MCl}_n$  mixtures, some FT-IR, SEM-EDS and XRD analyses were carried out. The combination of all the results gives a complete overview over the possible mechanisms

induced by the milling treatment. Thus, complex mixtures of ( $2\text{LiBH}_4 + \text{ZnCl}_2$ ) were analysed by FT-IR whereas the others were investigated by SEM-EDS and/or XRD.

FT-IR spectroscopic was useful in identifying characteristic ionic bands in  $\text{LiBH}_4$ ,  $\text{ZnCl}_2$  and a possible new compound formed during the milling treatment.

The B-H bonding environment of the complex mixtures of ( $2\text{LiBH}_4 + \text{ZnCl}_2$ ) milled for 1 (a) and 5 (b) minutes was determined as shown in Figure 4.7.

The presence of  $\text{BH}_4^-$  ion from  $\text{LiBH}_4$  could be detected from the observation of characteristic transmission bonds around  $2300\text{ cm}^{-1}$ , whereas in  $\text{LiBH}_4$ -based mixtures, the stretching mode  $\nu(\text{B-H})$  occurs between  $2000\text{ cm}^{-1}$  and  $2500\text{ cm}^{-1}$  with a complex pattern involving multiple stretches suggesting the formation of new intermediates, in addition to the parent B-H stretch ( $2000\sim 2500\text{ cm}^{-1}$ ).

The 3  $\text{BH}_2$  bending modes  $\delta(\text{B-H})$  are also present for both samples around  $1100\text{ cm}^{-1}$ . Also, The FT-IR spectra show the characteristic peaks of pure  $\text{ZnCl}_2$  at around  $950\text{ cm}^{-1}$ ,  $1600\text{ cm}^{-1}$  and a broad band between  $3000$  and  $3500\text{ cm}^{-1}$  but also a Zn-H stretch around  $1400\text{ cm}^{-1}$  more emphasized in the sample milled for 5 minutes than in the one milled for 1 minute. The presence of this stretch indicates a change in the ionic bonding inside the mixtures, thus the formation of a new intermediate involving Zn-H bond.

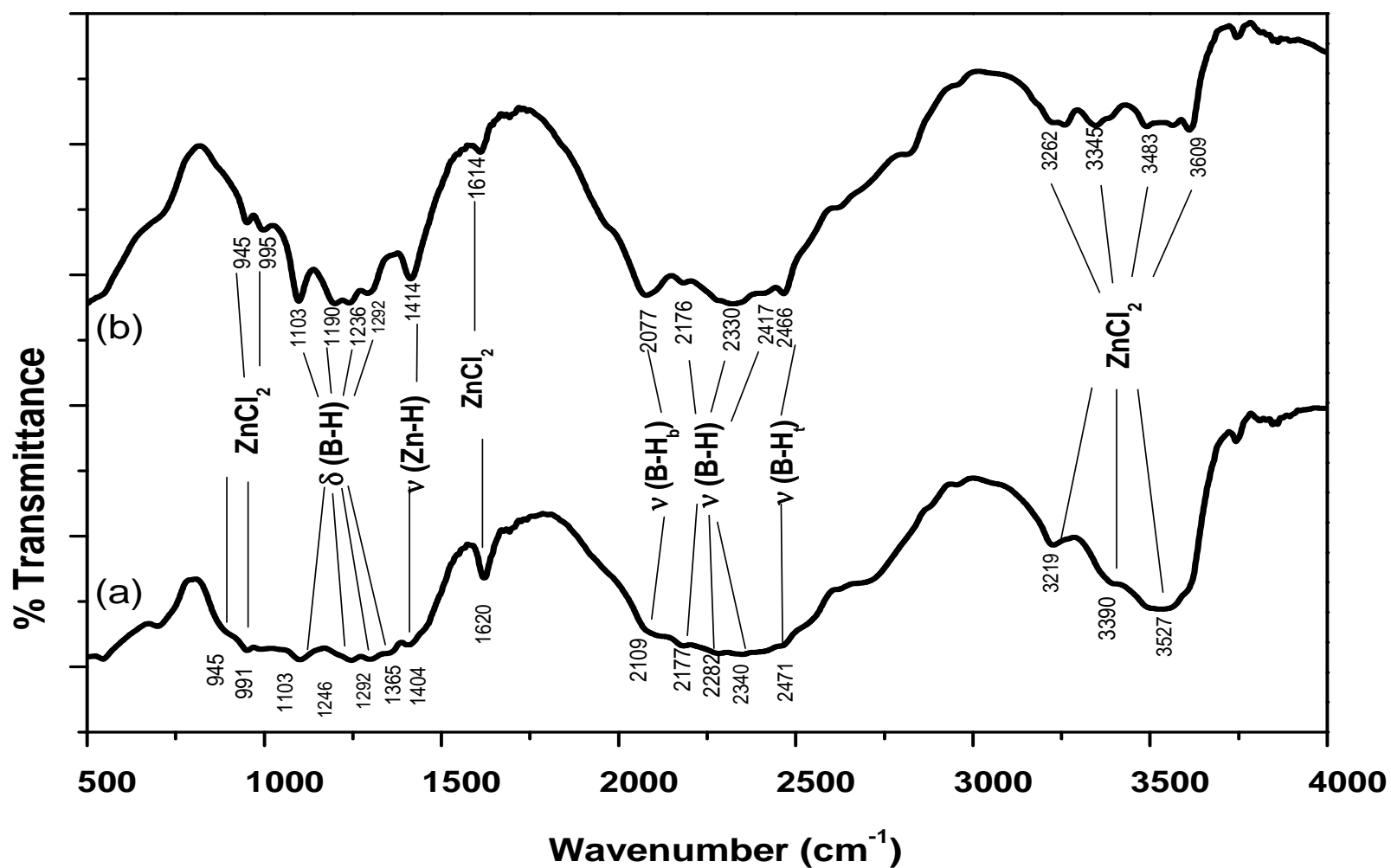


**Figure 4.7:** FT-IR profiles of  $2\text{LiBH}_4 + \text{ZnCl}_2$  ball milled for 1 (a) and 5 (b) minutes after milling representing different bond environments



The second technique that can be utilised to determine the milling effect is Scanning Electron Microscopy (SEM) associated with Energy Dispersive Spectrometry (EDS). In Figure 4.8, SEM micrographs of pure  $\text{LiBH}_4$  and mixtures of  $(3\text{LiBH}_4 + \text{TiCl}_3)$ ,  $(2\text{LiBH}_4 + \text{NiCl}_2)$  and  $(3\text{LiBH}_4 + \text{CrCl}_3)$  mechanically milled for only 5 minutes suggested a high reactivity associated with the mixtures. Indeed, the pure sample does not show the sponge-like structure observed on the  $\text{TiCl}_3$ -added sample image. The  $\text{CrCl}_3$ -added sample shows some similarities with pure  $\text{LiBH}_4$  whereas the  $\text{NiCl}_2$ -added sample shows some particle size reduction and a more homogenous structure.

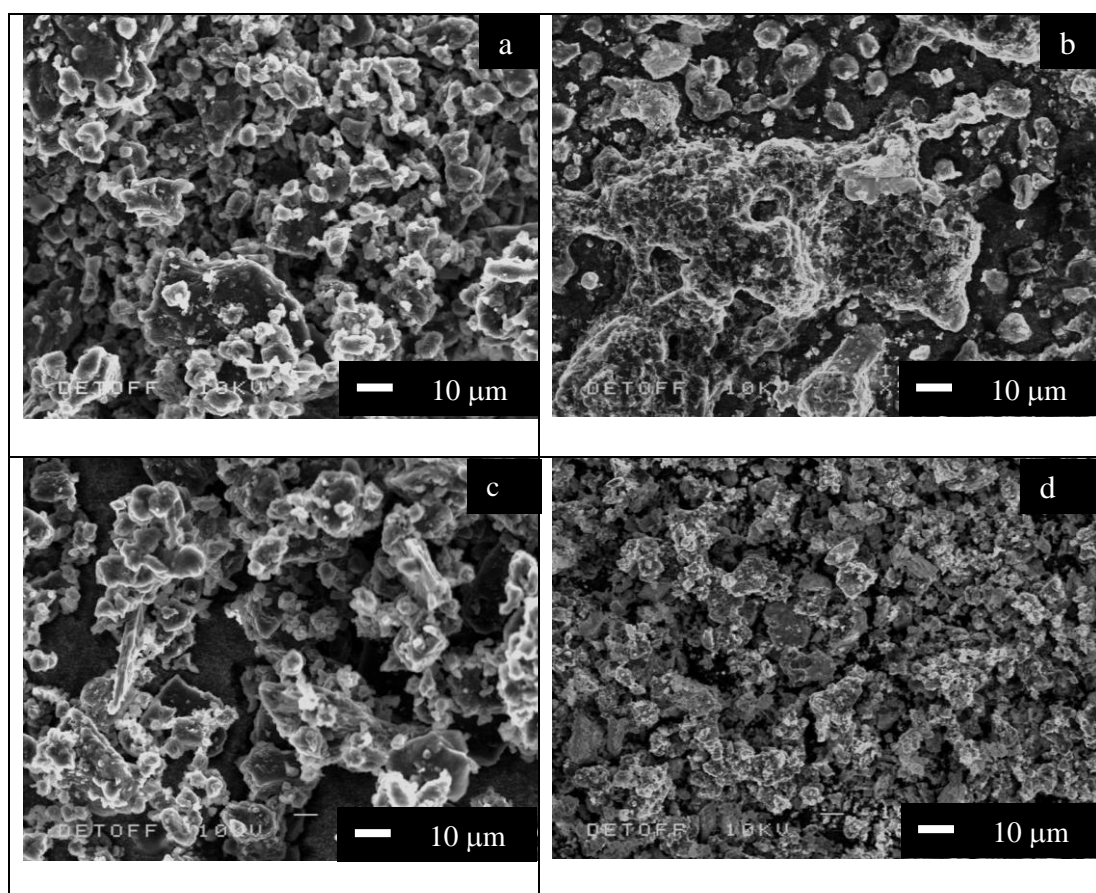


**Figure 4.8:** SEM images a: pure  $\text{LiBH}_4$  after 5 minutes milling b:  $(\text{LiBH}_4:\text{TiCl}_3=3:1)$  after 5 minutes milling c:  $(\text{LiBH}_4:\text{CrCl}_3=3:1)$  after 5 minutes milling d:  $(\text{LiBH}_4:\text{NiCl}_2=2:1)$  after 5 minutes milling

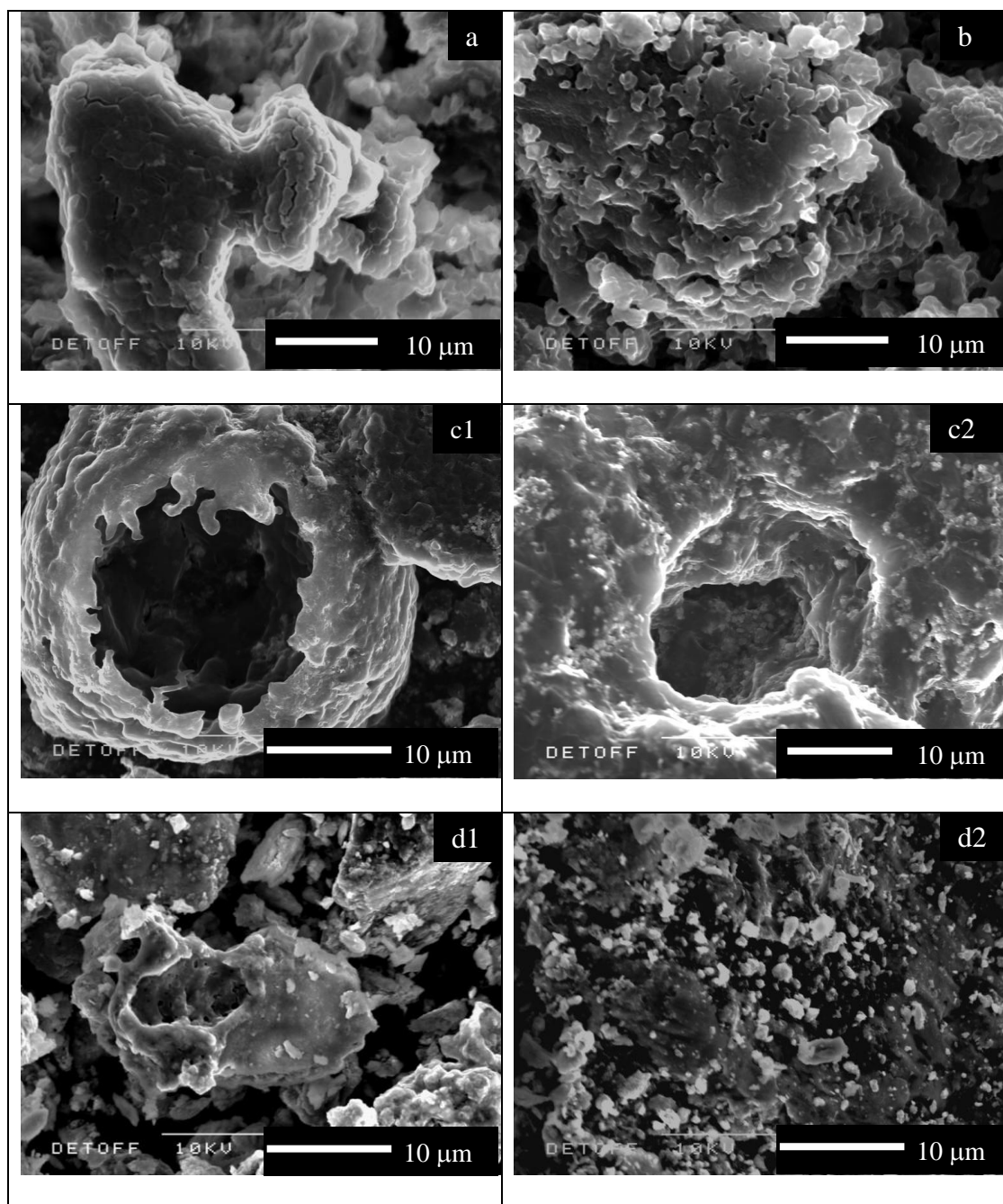


**Figure 4.9:** SEM images a: pure  $\text{LiBH}_4$  after 5 minutes milling b: ( $\text{LiBH}_4\text{:CrCl}_3=3\text{:}1$ ) after 5 minutes milling c1 and c2: ( $\text{LiBH}_4\text{:TiCl}_3=3\text{:}1$ ) after 5 minutes milling d1 and d2: ( $\text{LiBH}_4\text{:NiCl}_2=2\text{:}1$ ) after 5 minutes milling

EDS combined with SEM provided further qualitative information about the composition of different phases with the different morphologies identified. It should be noted that with EDS, all elements can be detected except from lithium, hydrogen and helium.

With higher magnifications in Figure 4.9, three different morphologies were exposed: Relatively large flaky particles in which small grains are embedded e.g. for the complex mixture ( $2\text{LiBH}_4 + \text{NiCl}_2$ ); Coalescence effect of grains, e.g., for pure  $\text{LiBH}_4$  and the complex mixture ( $2\text{LiBH}_4 + \text{CrCl}_3$ ); Porous-like morphology which suggests a vigorous liberation of a gas phase during the milling process e.g. for the complex mixture ( $3\text{LiBH}_4 + \text{TiCl}_3$ );

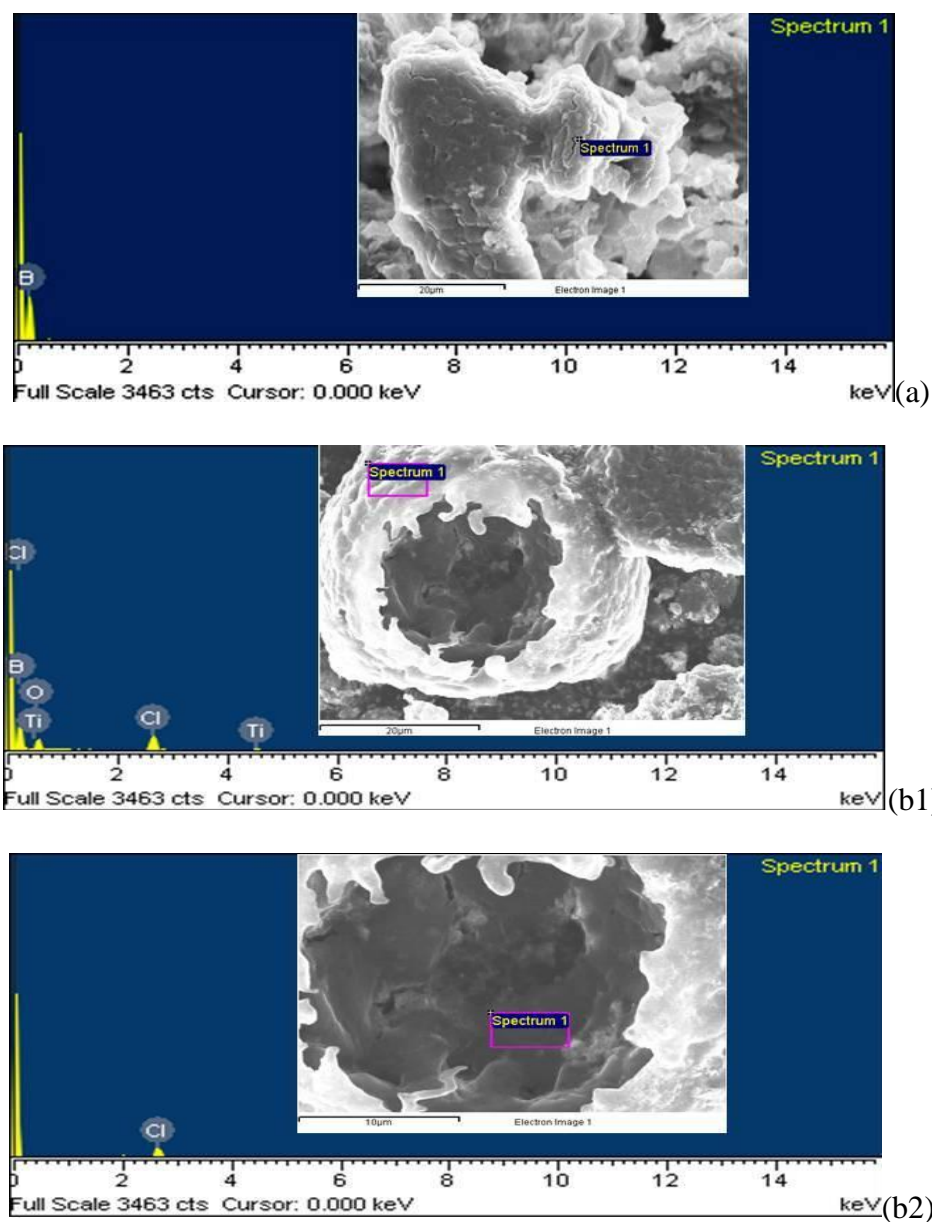


**Figure 4.10:** SEM-EDS profiles of (a): pure  $\text{LiBH}_4$ , (b1) and (b2): ( $\text{LiBH}_4:\text{TiCl}_3=3:1$ ) after 5 minutes milling

In Figure 4.10 a, the elemental analysis of pure  $\text{LiBH}_4$  sample showed the presence of boron only, which is consistent with the composition of  $\text{LiBH}_4$ . Also, the elemental analysis of a remarkable spot (Figure 4.10 b2) in a porous zone indicated the presence of elemental chlorine only which can be linked to  $\text{LiCl}$ . This suggests that the porous-like morphology observed in  $\text{TiCl}_3$ -added mixtures can be associated with the formation of a new phase,  $\text{LiCl}$ , detected after only 5 minutes of milling.

The flaky morphology observed in complex mixture ( $2\text{LiBH}_4 + \text{NiCl}_2$ ) was also analysed by elemental analysis. Two representative spots in Figure 4.11 were scanned and it shows that  $\text{NiCl}_2$  has been uniformly distributed.

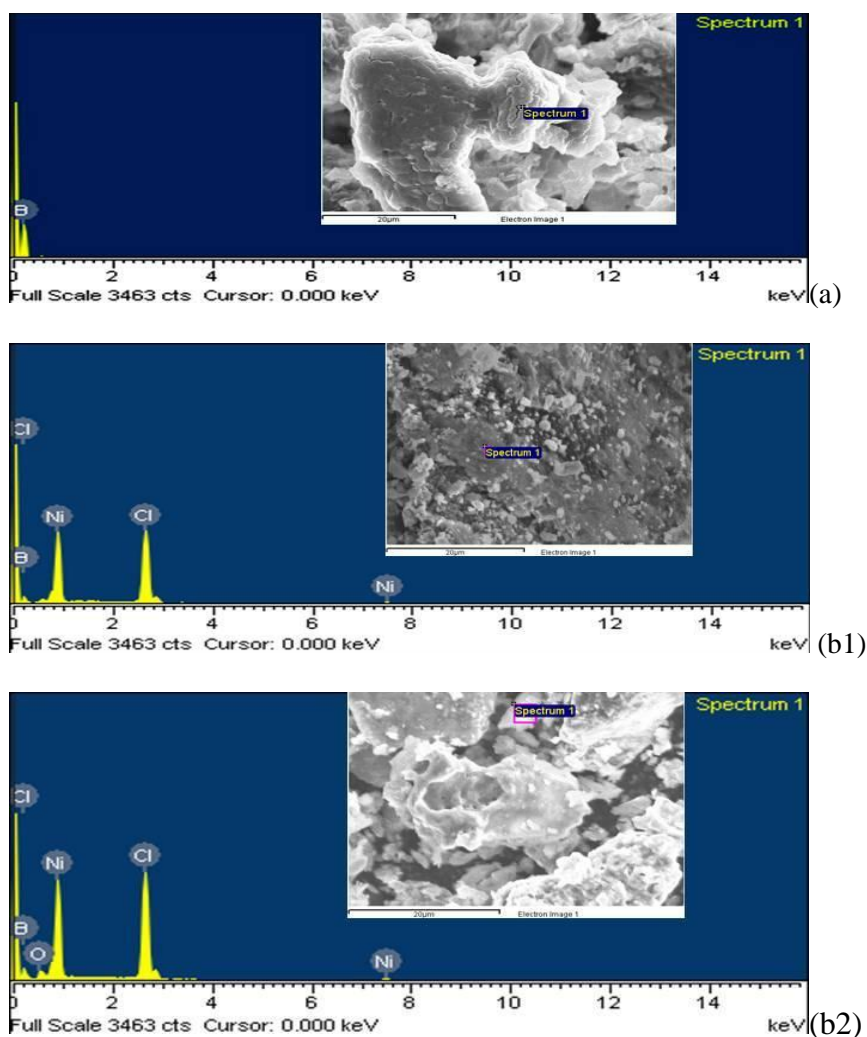


**Figure 4.11:** SEM-EDS profiles of (a): pure  $\text{LiBH}_4$ , (b1) and (b2): ( $\text{LiBH}_4:\text{NiCl}_2=2:1$ ) after 5 minutes milling

Another technique may be used to identify the effect of the milling on the  $\text{LiBH}_4\text{-MCl}_n$  mixtures especially for complex mixture ( $3\text{LiBH}_4 + \text{CrCl}_3$ ) which had a very similar morphology to pure  $\text{LiBH}_4$ : X-Ray Diffraction (XRD).

For instance, Figure 4.12 below represents the powder x-ray diffraction patterns of the complex mixture ( $3\text{LiBH}_4 + \text{CrCl}_3$ ) mechanically milled for different time durations of 5 minutes and 15 minutes.

The major peaks observed correspond to  $\text{LiBH}_4$ ,  $\text{LiCl}$  and  $\text{Li}_5\text{CrCl}_8$ . It is interesting to note that no parent  $\text{CrCl}_3$  compound is present in both mixtures.

Meanwhile, although  $\text{LiBH}_4$  is present in the mixture after 5 minutes of milling, very little or none is present after 15 minutes of milling whereas the intermediate  $\text{Li}_5\text{CrCl}_8$  clearly present after 5 minutes of milling seems to be replaced gradually by  $\text{LiCl}$  as clearly shown at  $2\theta \sim 15^\circ$  and  $2\theta \sim 53^\circ$ .

However, no peaks of  $\text{Cr}(\text{BH}_4)_3$  has been found suggesting either an amorphous phase or a partial desorption of the newly formed borohydride.

This further corroborates the idea that the milling applied to these samples activates the reactivity and initiates the reaction between the two starting materials.

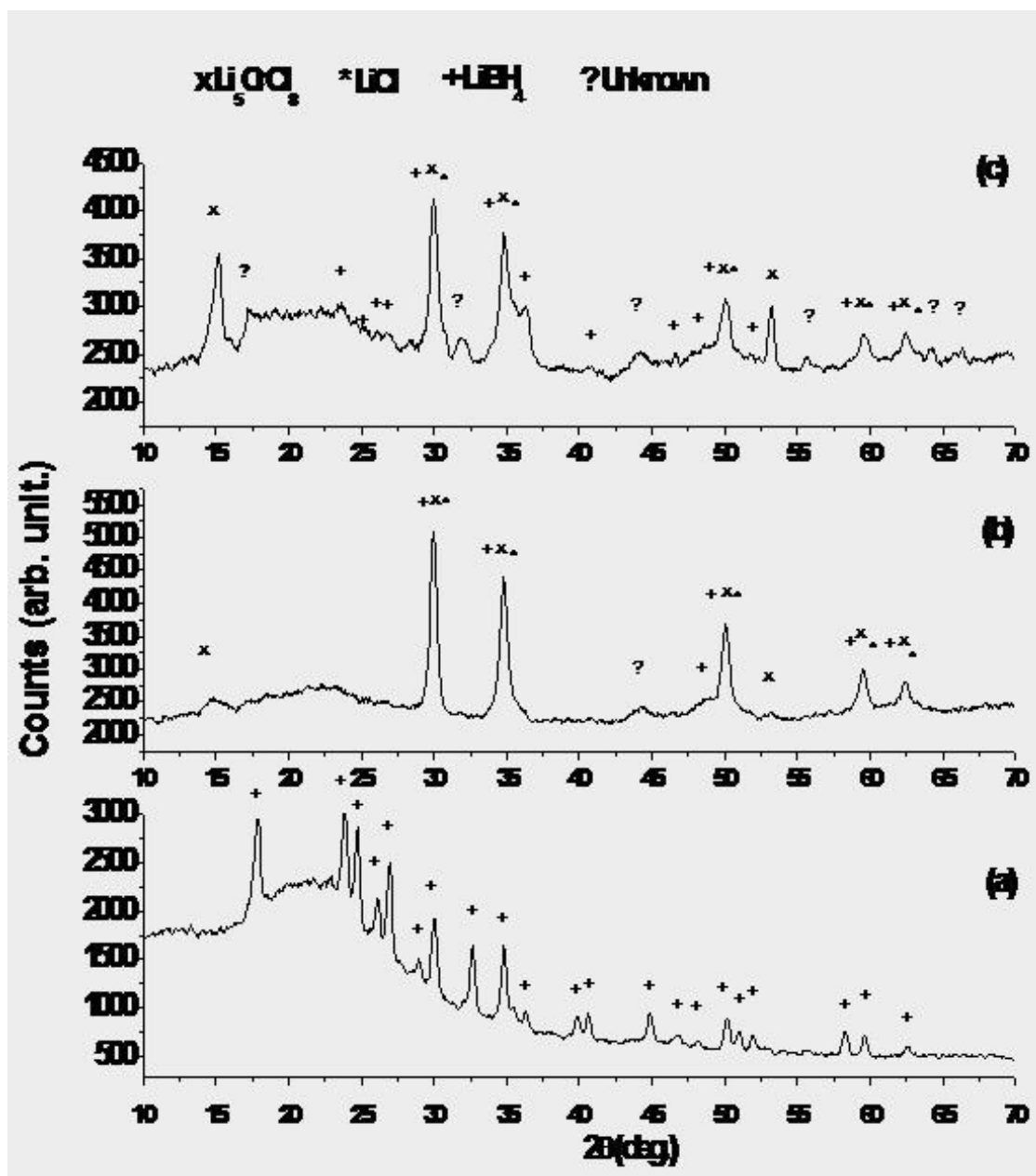


**Figure 4.12:** XRD data of  $\text{CrCl}_3$ -added  $\text{LiBH}_4$  as-milled for 5 minutes (a) and 15 minutes (b) compared to pure as-received  $\text{LiBH}_4$  (a)

After demonstrating the presence of newly formed intermediate species during the milling treatment for time durations as little as 5 minutes, the samples were subjected to heating from room temperature up to  $300^\circ\text{C}$  and the thermal desorption profiles are analysed comparatively to pure  $\text{LiBH}_4$ .

### 4.2.3 Dehydrogenation properties using TG-DTS-MS

The thermal analysis of the different mixtures is described thoroughly in the following paragraphs. Milling has been found to have a detrimental effect when milling time is superior to 5 minutes except for  $\text{ZnCl}_2$ -added mixtures as indicated in Figure 4.13 below.

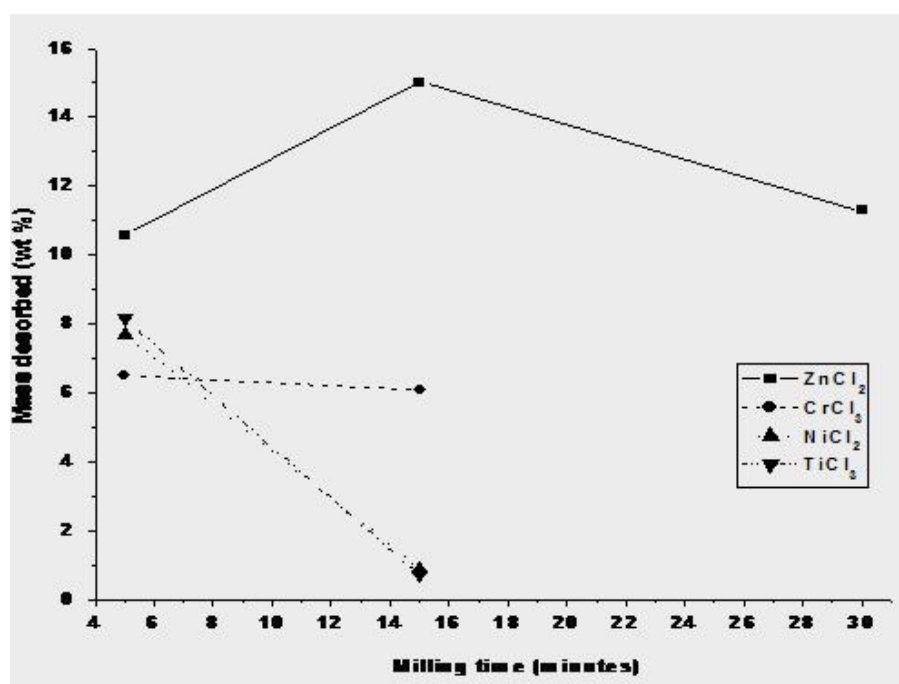


**Figure 4.13:** Total mass desorbed when heated up to  $300^\circ\text{C}$  as a function of milling time

Therefore, the figures show only results for 5 minutes of milling as they are the best achievable when samples are submitted to a milling treatment. Figure 4.14 shows that comparatively to pure  $\text{LiBH}_4$ ,  $\text{MCl}_n$ -added mixtures all showed a bigger mass loss in the temperatures ranging from room temperature to  $300^\circ\text{C}$  accompanied with hydrogen evolution.

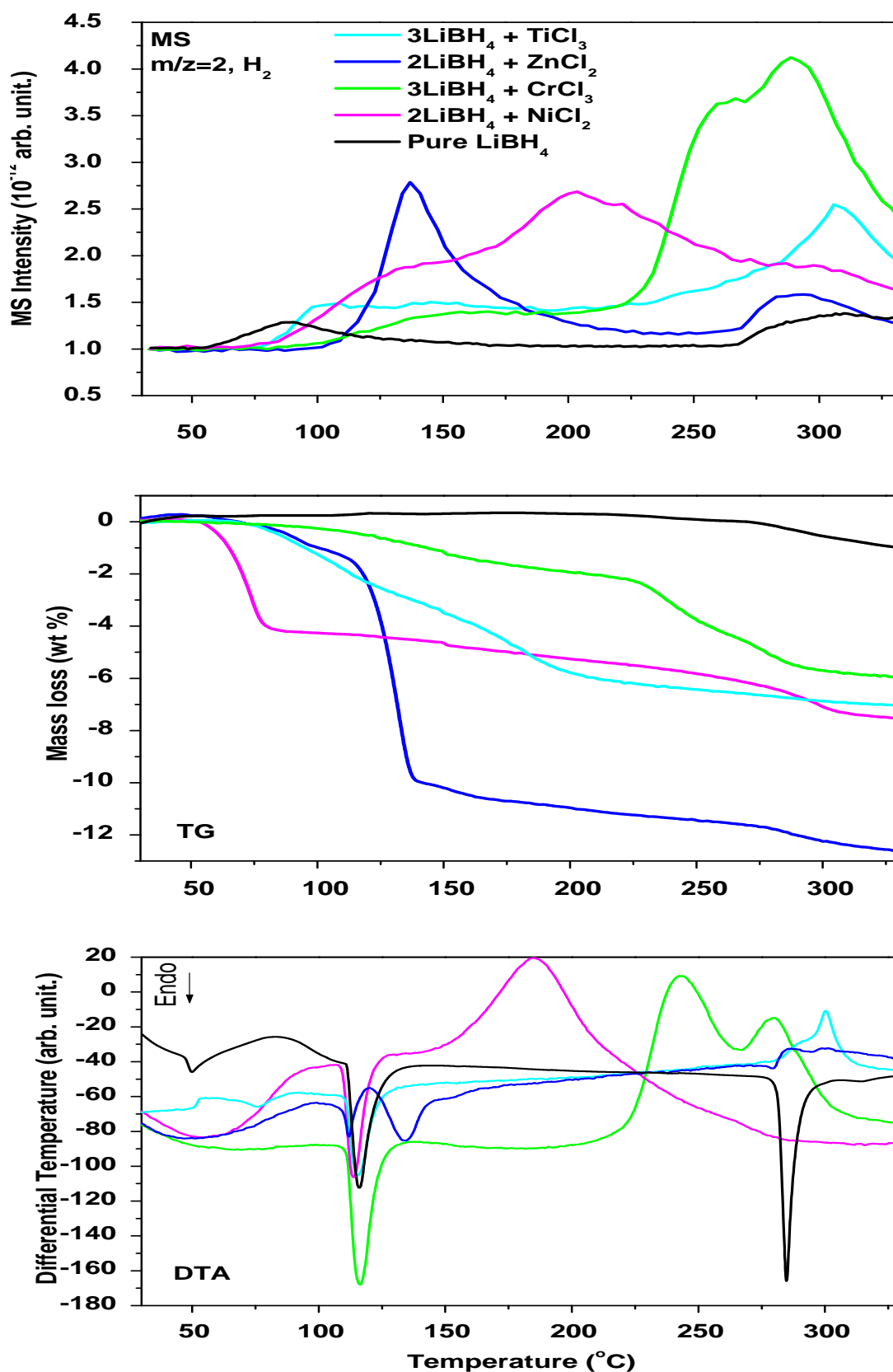


**Figure 4.14:** DTA-TG-MS analyses of  $\text{LiBH}_4$  and  $n\text{LiBH}_4 + \text{MCl}_n$  ( $M=\text{Zn, Ti, Ni, Cr}$ ) at a heating rate of  $5^{\circ}\text{C}.\text{min}^{-1}$



On the DTA curve, there is a common feature around 110°C: a sharp endothermic suggesting a phase change. Although, this thermal event is not followed by significant mass loss and hydrogen evolution in the case of pure  $\text{LiBH}_4$ , it is a slightly different story for the chlorides-added mixtures. Indeed, an endothermic DTA peak with large shoulders is observed from as low as 50°C preceding the phase change peak and accompanied by a mass loss of between 1 and 4 wt % on the TG and variable hydrogen desorption peaks on the MS. Also, in the case of chloride additions, the phase change peak is followed by an intermediary step well before the melting point of  $\text{LiBH}_4$ . This step has either an exothermic ( $\text{TiCl}_3$ ,  $\text{CrCl}_3$ ,  $\text{NiCl}_2$ ) or endothermic ( $\text{ZnCl}_2$ ) character and induces further mass loss and hydrogen desorption.

#### 4.2.3.1 2:1 molar ratio of $\text{LiBH}_4$ to $\text{ZnCl}_2$

When  $\text{ZnCl}_2$  was added to  $\text{LiBH}_4$  with a molar ratio  $\frac{\text{LiBH}_4}{\text{ZnCl}_2} = 2$ , the thermal decomposition of the mixture was investigated. Different milling times ranging from 5 minutes to 30 minutes were also tested. The results being very similar to each other, the sample which has the best results in terms of desorbed mass is presented in Figure 4.15.

Also, the MS results showed 1 gas species with a major ( $10^{-9}$  order) hydrogen peak ( $m/z=2$ ).

The decomposition was initiated for temperatures as low as 80°C. The process could be divided into three stages: the first desorption wave began around 80°C, followed by a second desorption wave starting from around 180°C. In the temperature

range from room temperature up to 300°C, none of the desorption waves were similar to those of pure  $\text{LiBH}_4$ , suggesting a completely different decomposition pattern.

However, in terms of thermal events, the first stage was characterised by a sharp endothermic DTA peak (A) from 80°C until 130°C accompanied by a huge mass loss of around 14 wt %. The following stages were characterised by a double small thermal event (B) and (C) at around 220°C and 275°C associated with a total and continued mass loss of 0.5 wt % only. Double Peaks B could be associated with further decomposition steps but double peaks C were clearly linked to either the melting points of  $\text{LiBH}_4$  (lit. 268°C) or  $\text{ZnCl}_2$  (lit. 293°C).

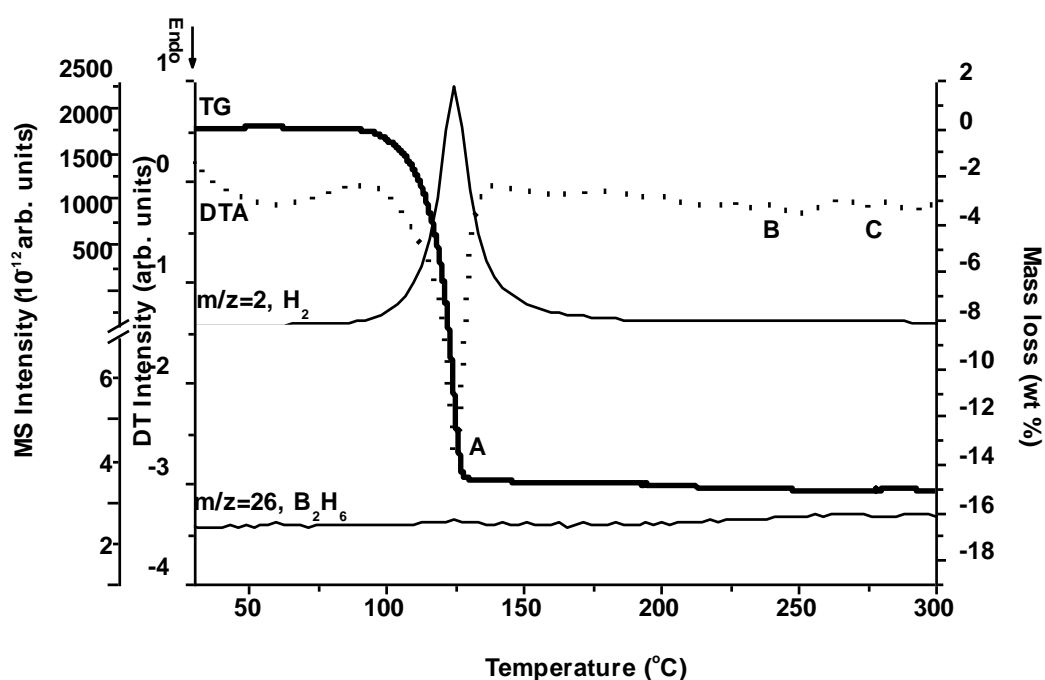


**Figure 4.15:** TG-DTA-MS profiles with a 2:1 molar ratio of  $\text{LiBH}_4$  to  $\text{ZnCl}_2$  after 15 minutes of mechanical milling

::

As the expected amount from the whole system with a 2:1 molar ratio of  $\text{LiBH}_4$  to  $\text{ZnCl}_2$  is 4.5 wt % and higher mass losses have been observed, it suggests that a boron loss from the release of  $\text{B}_n\text{H}_m$  compounds might occur during the desorption process.

#### 4.2.3.2 3:1 molar ratio of $\text{LiBH}_4$ to $\text{TiCl}_3$

When  $\text{TiCl}_3$  was added to  $\text{LiBH}_4$  with a molar ratio  $\frac{\text{LiBH}_4}{\text{TiCl}_3} = 3$ , the thermal decomposition of the mixture was under scrutiny. As opposed to  $\text{ZnCl}_2$ -added mixtures, milling times ranging from 5 to 30 minutes were tested but showed different outcomes and a detrimental effect when longer milling times were applied. For a milling time of as little as 5 minutes, an obvious reactivity was observed physically right after the milling process as a pressure rise applied in the milling pot. It inevitably led to the loss of a gaseous phase. The thermal desorption profiles of mixtures milled for more than 5 minutes showed a dramatic decrease in the desorbed mass forcing to concentrate the study on the sample milled for 5 minutes only (see Figure 4.16). Under this condition, the decomposition is initiated for temperatures as low as  $60^\circ\text{C}$ . Also, the MS results showed sole release of hydrogen (mass 2) in the spectrometer detection range.

The process could be divided into three stages: the first desorption wave began around  $60^\circ\text{C}$ , followed by a second desorption wave starting from around  $100^\circ\text{C}$  and a third one from around  $200^\circ\text{C}$ . In the temperature range from room temperature up to  $300^\circ\text{C}$ , none of the desorption waves except the one around  $100^\circ\text{C}$  were similar to those of pure  $\text{LiBH}_4$ , suggesting a slightly different decomposition pattern. However, in terms of thermal events, the first stage was characterised by a broad and weak peak (A) from  $60^\circ\text{C}$  until  $100^\circ\text{C}$  accompanied by a mass loss of 6 wt %, then followed the second stage with a strong DTA peak (B) from  $100^\circ\text{C}$  until  $130^\circ\text{C}$  accompanied by a mass loss of around 0.5 wt % only making it a common feature with the phase change observed in pure  $\text{LiBH}_4$ . The following stage was characterised by an exothermic peak

(C) starting from 220°C and peaked at around 300°C associated with a total and continued mass loss of 2 wt %.

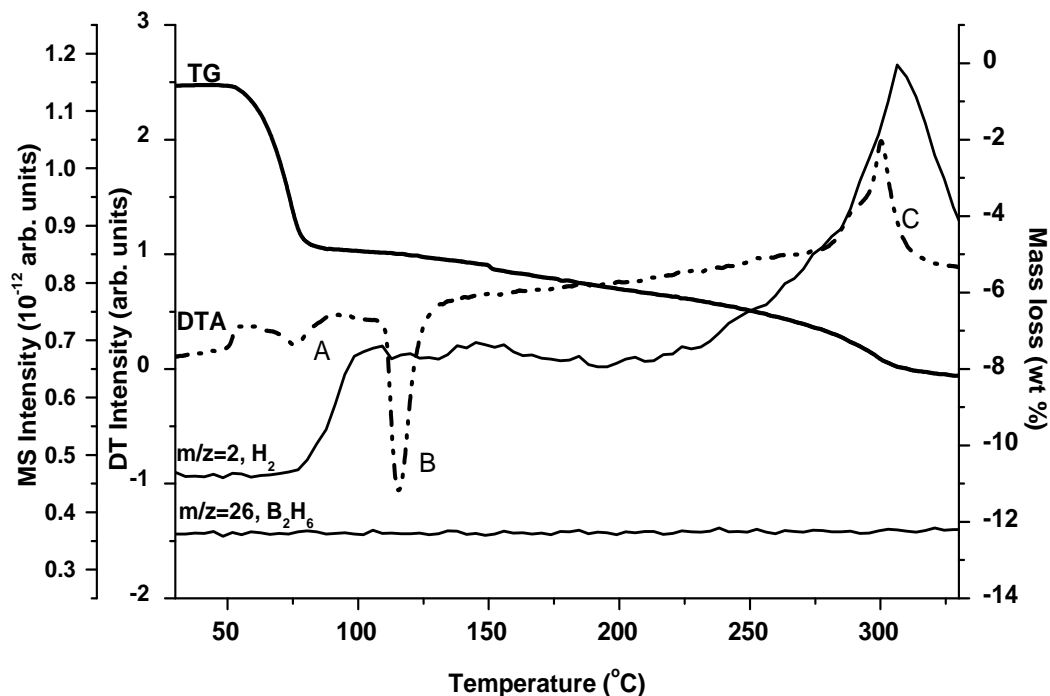


**Figure 4.16:** TG-DTA-MS profiles with a 3:1 molar ratio of LiBH<sub>4</sub> to TiCl<sub>3</sub> after 5 minutes of mechanical milling

#### 4.2.3.3 2:1 molar ratio of LiBH<sub>4</sub> to NiCl<sub>2</sub>

When NiCl<sub>2</sub> was added to LiBH<sub>4</sub> with a molar ratio  $\frac{\text{LiBH}_4}{\text{NiCl}_2} = 2$ , the thermal decomposition of the mixture was investigated. The decomposition was initiated for temperatures as low as 50°C. Also, the MS did not detect any other gas species apart from hydrogen (m/z=2). The first endothermic peak before 110°C is accompanied by a mass loss of 2 wt %. On further heating, an exothermic peak was observed at 180°C with a mass loss of 4 wt %. Finally, the fact that no endothermic effect was observed on DTA curves at the melting point of pure LiBH<sub>4</sub> which is 280-300°C could indicate

that almost all the  $\text{LiBH}_4$  was involved in the decomposition reactions prior to  $280^\circ\text{C}$ . Concerning the hydrogen desorption record, the onset starts at  $70^\circ\text{C}$  and the 3 observed  $\text{H}_2$  peaks nearly merged together as they were very close to each other.

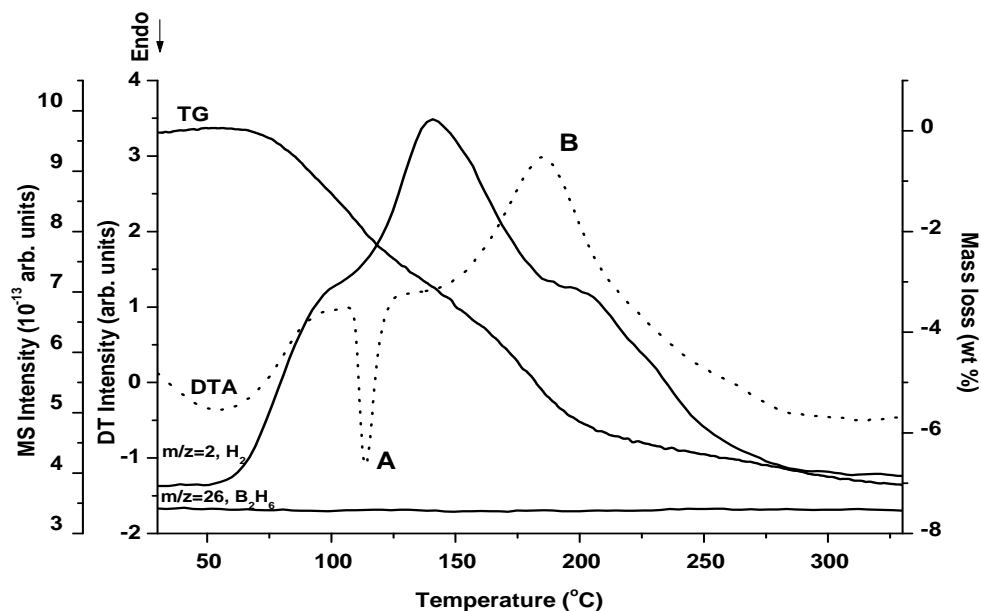


**Figure 4.17:** TG-DTA-MS profiles with a 2:1 molar ratio of  $\text{LiBH}_4$  to  $\text{NiCl}_2$  after 5 minutes of mechanical milling

#### 4.2.3.4 3:1 molar ratio of $\text{LiBH}_4$ to $\text{CrCl}_3$

Mixtures of  $\text{LiBH}_4$  and  $\text{CrCl}_3$  with a 3:1 molar ratio were investigated. Besides  $\text{ZnCl}_2$ -added mixtures, different milling times ranging from 5 minutes to 15 minutes were also tested. The results being very similar to each other, the sample which had the best results in terms of desorbed mass is presented in Figure 4.18.

The results indicated that the 2 samples had similar behaviour upon heating them. They showed that the reaction between  $\text{LiBH}_4$  and  $\text{CrCl}_3$  occurred with an exothermic effect in the temperature area of  $220\text{--}300^\circ\text{C}$ . For the sample milled for 5 minutes, we observed two distinct areas on the DTA curve:

- An endothermic effect at 110°C associated with a TG mass loss of 2 wt % strictly corresponding to the “LiBH<sub>4</sub>-as-received” peak at 110°C
- A double exothermic effect at 240°C and 280°C with a total mass loss of 4 wt % possibly related to a double decomposition reaction occurring in this range of temperature and thus, to a 2-step mechanism.

On the TG curve, the mass loss started almost immediately on heating at 40-50°C and up to 300°C, 6 wt % of the total mass of the product was lost. The gas evolution exhibited only 3 H<sub>2</sub> peaks at 110°C, 240°C and 280°C. It should also be noted that the maximum mass loss recorded by the TG analyser was around 6 wt % whereas the calculated hydrogen content of the mixture is 5.4 wt %. The obtained results are very similar to the ones expected and calculated and that is the indication that there are possibly no other gas species than molecular hydrogen involved in this decomposition.

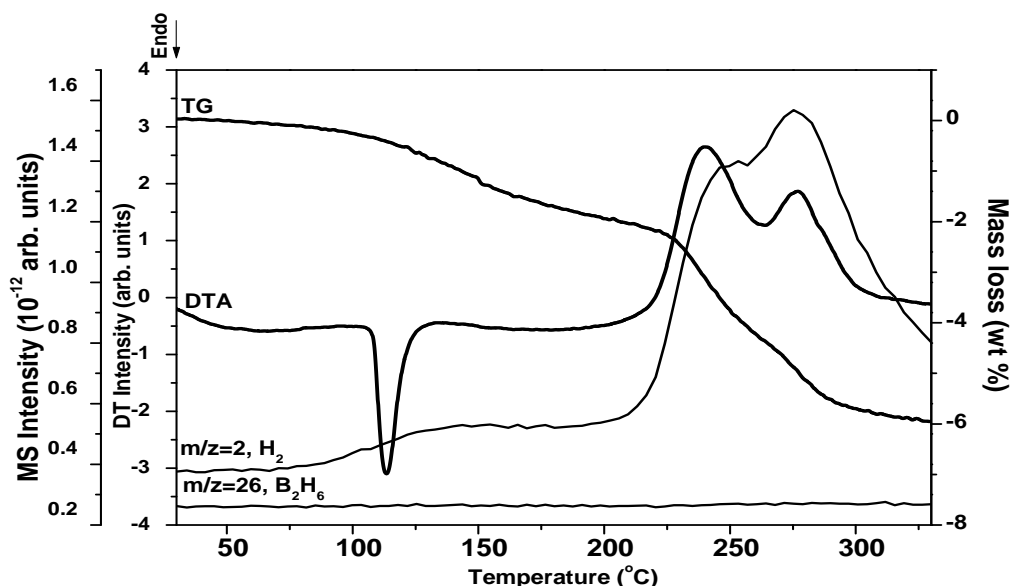


**Figure 4.18:** TG-DTA-MS profiles with a 3:1 molar ratio of LiBH<sub>4</sub> to CrCl<sub>3</sub> after 5 minutes of mechanical milling

After presenting the most significant results, the discussion will highlight the decomposition process and corroborate the results obtained on the present study with the ones from the literature.

Overall, the 2 key requirements identified during the study of pure  $\text{LiBH}_4$  have been fulfilled:

- 1- Decrease the main onset desorption temperature from  $380^\circ\text{C}$  (above  $\text{LiBH}_4$  melting temperature) to  $120\text{-}250^\circ\text{C}$  (below  $\text{LiBH}_4$  melting temperature);**
- 2- Keep the hydrogen delivery the purest possible: it has potentially been achieved with the  $\text{CrCl}_3$ -added mixture, however, the release of  $\text{B}_2\text{H}_6$  cannot be ruled out.**

## **Chapter 4. Experimental Results**

4.3  $\text{LiBH}_4 + x\text{NH}_4\text{Cl}$  ( $x=1, 2, 3$ )

$\text{NH}_3\text{BH}_3 + y\text{NH}_4\text{Cl}$  ( $y=1, 2$ )



### 4.3 Hydrogen desorption from complex mixtures ( $\text{LiBH}_4 + x\text{NH}_4\text{Cl}$ , $x=1,2,3$ ) and ( $\text{NH}_3\text{BH}_3 + y\text{NH}_4\text{Cl}$ , $y=1,2$ )

#### 4.3.1 Experimental design

Following investigations on the thermal desorption from pure  $\text{LiBH}_4$  and from mixtures of  $\text{LiBH}_4$  with chlorides of the fourth period metals: Ti, Zn, Cr and Ni, the study was focussed on lowering the hydrogen desorption temperature of  $\text{LiBH}_4$  and ensuring the delivery of high purity hydrogen. The essential idea was to add a hydrogen-containing compound which would react with  $\text{LiBH}_4$  and form hydrogen-rich intermediates capable of liberating a large amount of hydrogen, at a relatively low temperature.. The dehydrogenation properties of  $\text{LiBH}_4$  ball-milled with various molar equivalents of  $\text{NH}_4\text{Cl}$  (1:1, 1:2 and 1:3) have been investigated.

Indeed, it has been reported some time ago in the 1950s and 1970s [160][161] that mixtures of  $\text{LiBH}_4$  and  $\text{NH}_4\text{Cl}$  could lead to the formation of  $\text{NH}_n\text{BH}_n$  ( $n=1\dots4$ ) and more importantly to the release of different amounts of hydrogen depending on thermodynamic conditions, mainly temperature. Ammonia borane,  $\text{NH}_3\text{BH}_3$ , often forms the intermediates in the reaction between  $\text{LiBH}_4$  and  $\text{NH}_4\text{Cl}$ . Together with  $\text{LiBH}_4$ , it is one of the most promising materials studied in recent years. An investigation on the mixtures of  $\text{NH}_3\text{BH}_3$  and  $\text{NH}_4\text{Cl}$  was performed here in order to evaluate the interaction between the intermediate compound and an excess of 1 mole and 2 moles of  $\text{NH}_4\text{Cl}$  in the compositions with (1:2) and (1:3) molar ratios of ( $\text{LiBH}_4\text{:NH}_4\text{Cl}$ ) respectively.

Indeed, the overall hydrogen capacities of the different doped and undoped binary compositions are consigned in Table 4.3 below and are limited to no more than 12 wt %, which is much better than the 5 wt % for chlorides-added  $\text{LiBH}_4$  investigated in Part 2 of Chapter 4.

**Table 4.3: Properties of starting materials and details of mechanical milling treatment**

Starting Materials	Molar ratio	Overall hydrogen capacity / wt% $\text{H}_2$	Milling time / min
$\text{LiBH}_4/\text{NH}_4\text{Cl}$	1:1	10.7	1, 5, 10
	1:2	9.4	1, 5, 10
	1:3	8.9	1, 5, 10
$\text{LiBH}_4/\text{NH}_4\text{Cl}$ + graphite	1:2:0.05	9.3	1, 5
	1:3:0.05	8.7	1, 5
$\text{NH}_3\text{BH}_3/\text{NH}_4\text{Cl}$	1:1	12.0	1, 5
	1:2	10.3	1
$\text{NH}_3\text{BH}_3/\text{NH}_4\text{Cl}$ + graphite	1:1:0.05	11.8	1, 5
	1:2:0.05	10.1	1

The work was carried out in different steps but the main objective was to understand the interaction between  $\text{LiBH}_4$  and  $\text{NH}_4\text{Cl}$  by gaining information such as desorption capacity, desorption temperature and intermediate compounds identification and effect in order to get the optimum conditions in which the desorption of pure hydrogen is maximal.

As the mixing is still performed by means of SPEX ball milling/mixing, it is important to look at different milling times (consigned in Table 4.3) and it is necessary to identify the milling effect, e.g. the possible change of structure, and the presence of precursor species mainly detected by XRD and SEM/EDS affecting the thermal desorption properties of mixtures of  $\text{LiBH}_4$  and  $\text{NH}_4\text{Cl}$ .

### 4.3.2 Effect of milling and heat treatment: structural and morphological analyses using XRD and SEM/EDS

In our quest to understand the hydrogen desorption mechanisms of the  $\text{LiBH}_4$ -  $\text{NH}_4\text{Cl}$  mixtures, SEM-EDS and XRD analysis were carried out. The combination of all the results gives a complete overview over the possible mechanisms induced by the milling treatment. The XRD patterns presented on the next pages showed the high reactivity of different mixtures of  $\text{LiBH}_4$  and  $\text{NH}_4\text{Cl}$ , after either 1 or 5 minutes of milling and before the heat treatment.

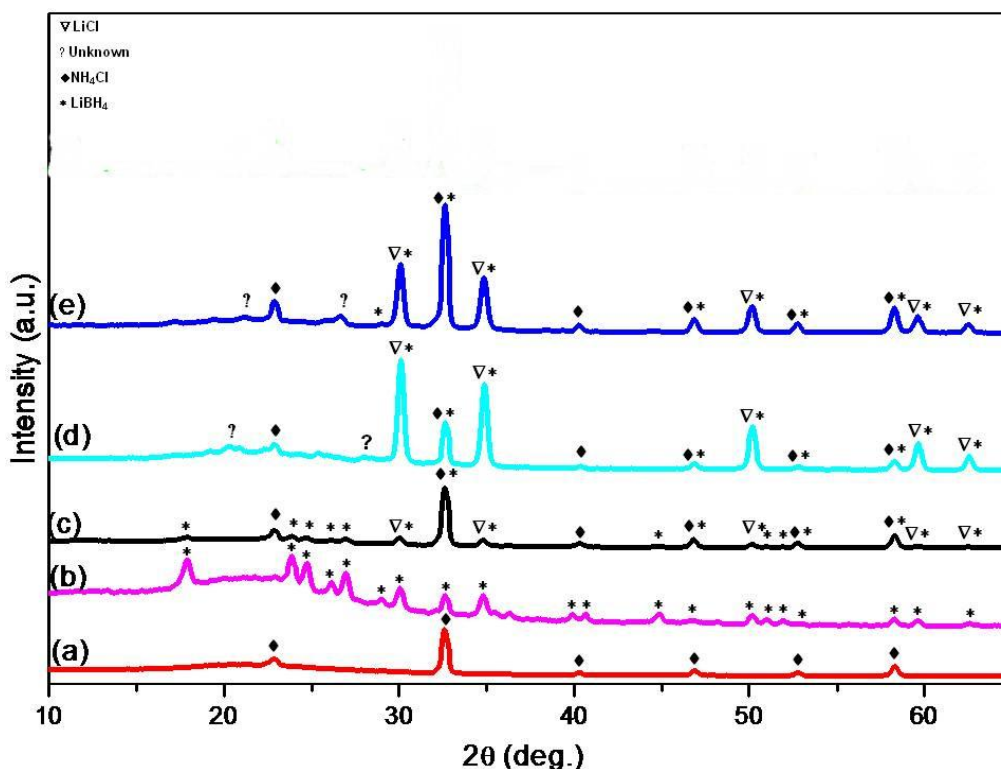


**Figure 4.20:** Powder X-ray diffraction patterns of: (a): pure  $\text{NH}_4\text{Cl}$ , (b): pure  $\text{LiBH}_4$ , (c):  $(\text{LiBH}_4:\text{NH}_4\text{Cl})=(1:1)$ , 5 minutes, (d):  $(\text{LiBH}_4:\text{NH}_4\text{Cl})=(1:2)$ , 5 minutes, (e):  $(\text{LiBH}_4:\text{NH}_4\text{Cl})=(1:3)$ , 1 minute

The figures show clearly the starting materials,  $\text{LiBH}_4$  and  $\text{NH}_4\text{Cl}$  and, newly formed crystalline phases such as  $\text{LiCl}$  and an unknown phase which may be due to other borohydride structures. The unknown phase appears to be different depending on the molar ratio of the starting materials.

This shows that there is a strong possibility that  $\text{LiBH}_4$  and  $\text{NH}_4\text{Cl}$  react at room temperature to form an intermediate compound, ( $\text{NH}_4\text{BH}_4$ ?  $\text{LiNH}_2\text{BH}_3$ ?  $\text{H}_y\text{LiBNH}_x$ ?)

We also noticed that the new phases are more emphasized in samples milled for 5 minutes as opposed to samples milled for only 1 minute. This also suggests that the milling treatment may activate through the reduction of the average particle size.

This is well demonstrated in Figure 4.20: the mixture with a 1:1 molar ratio of  $\text{LiBH}_4$  to  $\text{NH}_4\text{Cl}$  not submitted to any milling treatment (c) shows the sole contribution of  $\text{NH}_4\text{Cl}$  and  $\text{LiBH}_4$  in contrast to the same mixture milled for only 1 minute (d) which sees the contribution of a new, unknown phase. Especially, for (d), there is more contribution from  $\text{LiBH}_4/\text{LiCl}$  than  $\text{NH}_4\text{Cl}$  as observed in (c). With increasing amounts of  $\text{NH}_4\text{Cl}$ , from (d) to (f), the presence of  $\text{NH}_4\text{Cl}$  is detected more clearly especially at specific  $\text{NH}_4\text{Cl}$   $2\theta$ :  $2\theta=23^\circ$  and  $2\theta=41^\circ$ .

The second technique that can be utilised to determine the milling and heating effect is Scanning Electron Microscopy (SEM) associated with Energy Dispersive Spectrometry (EDS). It provides further qualitative information about the composition of different phases with the different morphologies identified. It should be noted that with EDS, all elements can be detected except for lithium, hydrogen and helium, meaning for instance, the presence of  $\text{LiBH}_4$  is only detected by elemental boron. Also, the elemental analysis of a porous zone like in the figure below indicated the presence of elemental chlorine Cl only which could be linked to  $\text{LiCl}$ . Whereas another elemental analysis pointed at a different zone indicated the presence of elements linked to a mixture of  $\text{LiBH}_4$  and  $\text{NH}_4\text{Cl}$ .

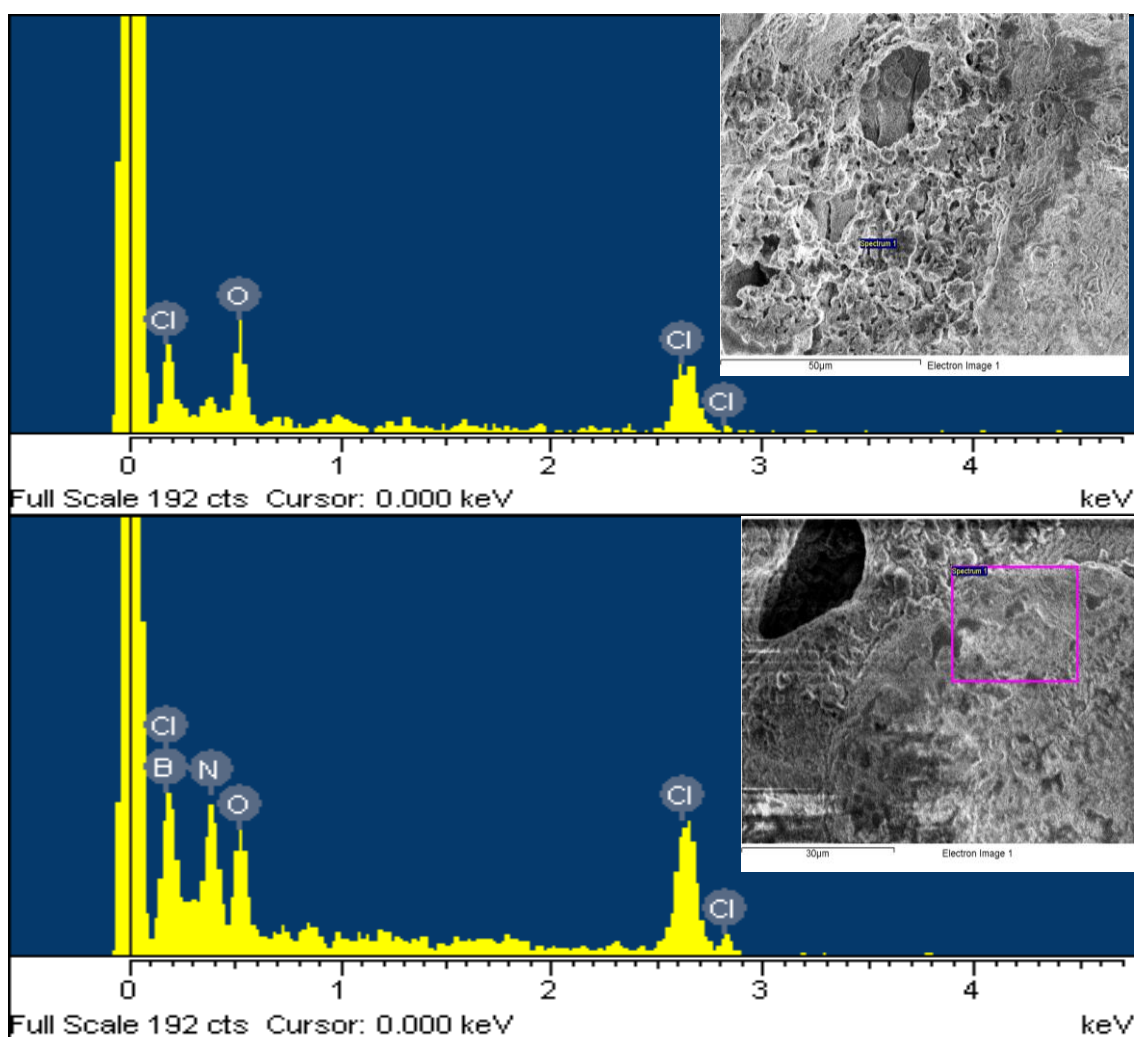


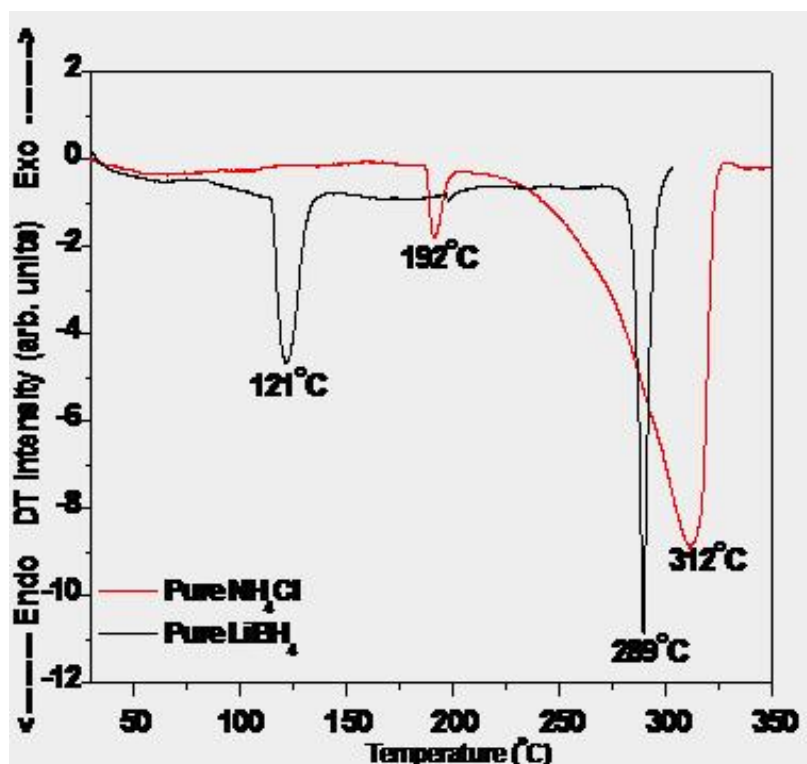
**Figure 4.21:** SEM-EDS profiles of mixtures of  $\text{LiBH}_4$  and  $\text{NH}_4\text{Cl}$  mechanically milled for 1 minute

After demonstrating the high reactivity of mixtures of  $\text{LiBH}_4$  and  $\text{NH}_4\text{Cl}$  during mechanical milling for times as short as 1 minute, the samples were subjected to a ramp temperature from room temperature to  $225^\circ\text{C}$  and the thermal desorption profiles were analysed comparatively to pure  $\text{LiBH}_4$ .

### 4.3.3 Dehydrogenation properties using TG-DTA-MS

For comparison purposes, DTA measurements have been carried out on the as-received materials up to  $350^\circ\text{C}$ . They exhibit four distinct characteristics that would be used to indicate the presence of pure materials in the mixtures i.e. which have not reacted:

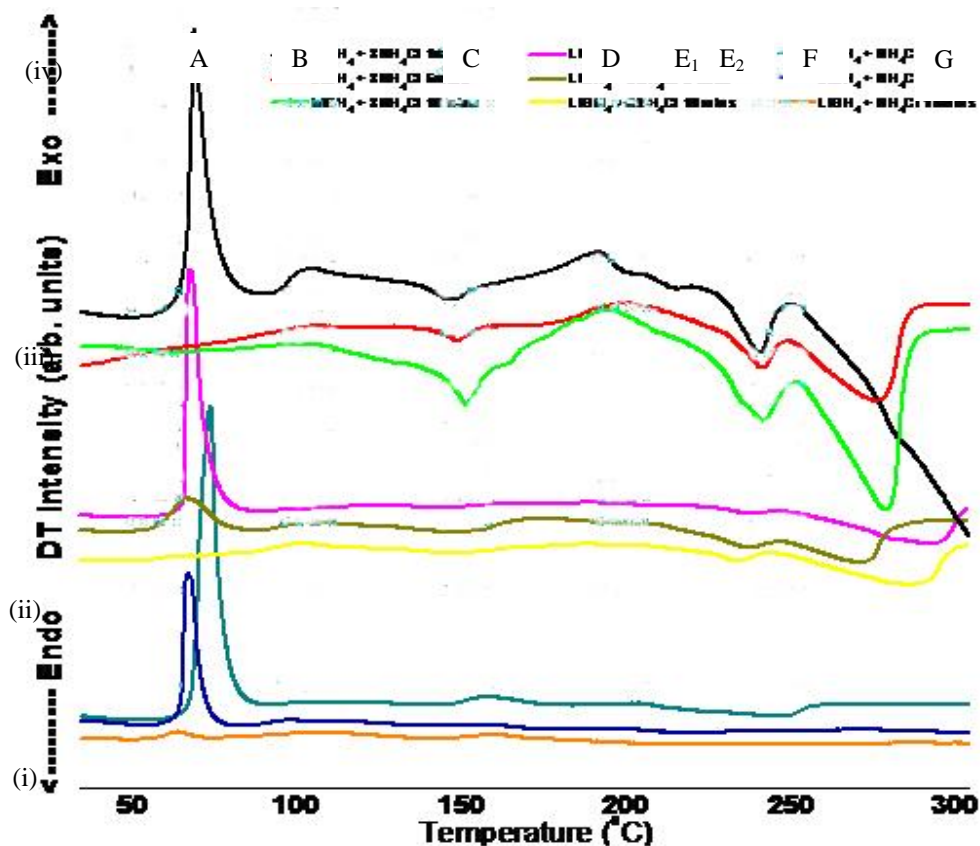
- Endothermic structural changes at 121°C and 192°C for  $\text{LiBH}_4$  and  $\text{NH}_4\text{Cl}$  respectively;
- Melting points of pure  $\text{LiBH}_4$  around 289°C and of pure  $\text{NH}_4\text{Cl}$  around 312°C and starting right after the structural change.



**Figure 4.22:** DTA profiles of pure  $\text{LiBH}_4$  and pure  $\text{NH}_4\text{Cl}$

DTA profiles of samples with molar ratios of 1:1, 1:2 and 1:3 of  $\text{LiBH}_4$  to  $\text{NH}_4\text{Cl}$  and milling times of 1, 5 and 10 minutes in Figure 4.23 below exhibit a series of thermal events. They all show a common feature around 65-70°C: a sharp exothermic peak (A) with small shoulders. As the milling time increases, the peak weakens suggesting that the thermal event is undermined by the milling process; therefore, the milling treatment may have impacted negatively. The second peak (B) around 100-105°C is also exothermic and much weaker. It is well emphasized in samples at molar ratios of 1:3 of  $\text{LiBH}_4$  to  $\text{NH}_4\text{Cl}$ . The subsequent peaks are all endothermic except peak (D), which is exothermic:

- Peak (C) is around 145-155°C. It is stronger with increasing milling times especially for samples at 1:2 and 1:3 molar ratios of  $\text{LiBH}_4$  to  $\text{NH}_4\text{Cl}$ . It is very weak with samples at a 1:1 molar ratio of  $\text{LiBH}_4$  to  $\text{NH}_4\text{Cl}$  suggesting that the excess of  $\text{NH}_4\text{Cl}$  found in samples at 1:2 and 1:3 molar ratios of  $\text{LiBH}_4$  to  $\text{NH}_4\text{Cl}$  s has a significant effect on this thermal effect.
- Peak (D) is around 180-185°C and exothermic.
- Peaks ( $E_1$ ) and ( $E_2$ ) are around 190-195°C and 205-210°C and are not present in samples at 1:1 molar ratio of  $\text{LiBH}_4$  to  $\text{NH}_4\text{Cl}$ .
- Peak (F) is around 235-240°C and is stronger with an increasing amount of  $\text{NH}_4\text{Cl}$ .
- Peak (G) is around 275-285°C and is stronger with an increasing amount of  $\text{NH}_4\text{Cl}$ .

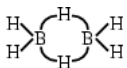
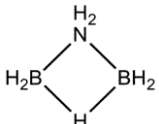
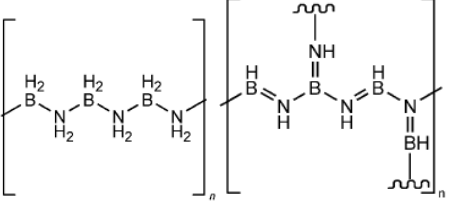
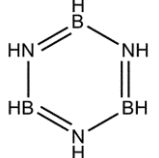


**Figure 4.23:** DTA profiles of mixtures of  $\text{LiBH}_4$  and  $\text{NH}_4\text{Cl}$  with different molar ratio 1:1 (i), 1:2 (ii), 1:2.5 (iii) and 1:3 (iv) and several thermal events around 65°C (A), 100°C (B), 145°C (C), 185°C (D), 195°C ( $E_1$ ), 210°C ( $E_2$ ), 235°C (F), 280°C (G)

TGA coupled with MS was used in order to determine the nature of the evolved gases during the degradation of the different binary compositions. Hydrogen has been found to be the main gas evolved during heating along with some other gas species identified as: ammonia (A), iminoborane (IB), aminoborane ( $A_2B_2$ ), aminodiborane (ADB), polyaminoborane (PAB) or polyiminoborane (PIB) products, polymeric versions of aminoborane or iminoborane for small chain lengths and borazine (BZ).

A full mass scan (refer to Table 4.4 below) from 1 to 100 (as for pure  $LiBH_4$  in Part 1 of Chapter 4) has been preliminarily performed in order to identify the whole range of gas desorbed and the detected mass numbers are given in the table below together with a possible assignment of the gas species.

**Table 4.4: Detected masses during the dehydrogenation of binary compositions**

Gas species	Mass charge ratio / m/z	Name	Formula
$H_2$	2	dihydrogen	<b>H-H</b>
$NH_3$	15, 16, 17, 18	ammonia	<b><math>H_2N-H</math></b>
$B_2H_6$	27, 28	diborane	
$NHBH$	26, 27, 28	iminoborane	$HN \equiv BH$
$NH_2BH_2$	29, 30	aminoborane	$H_2N \equiv BH_2$
$NH_2BH_2BH_3$	41	aminodiborane	
$(NHBH)_n$ $(NH_2BH_2)_n$ $n < 3$	50, 51, 52, 53, 58, 59, 60, 61, 62, 63 74, 75, 76, 77, 78, 79	polyiminoborane or polyaminoborane products	
$(NHBH)_{n=3}$	80	Borazine	



Correspondingly, at least three to four overlapped peaks were confirmed on the MS profile associated with mass losses observed on the TG profile, which shows that a 3 to 4 step-decomposition pattern can be outlined in all cases. All the mixtures exhibit an “immediate” release of gas upon heating for temperatures as low as 40°C (onset desorption) followed by 2 to 3 subsequent gas releases.

The next figures show the thermal desorption profiles of mixtures with 1:1, 1:2 and 1:3 molar ratios of  $\text{LiBH}_4$  to  $\text{NH}_4\text{Cl}$  and different milling times e.g. 1, 5 and 10 minutes; the figures also have two ranges of MS as the first half figure show the high range ( $10^{-9}$  to  $10^{-10}$  order) and the second half the low range ( $10^{-12}$  order).

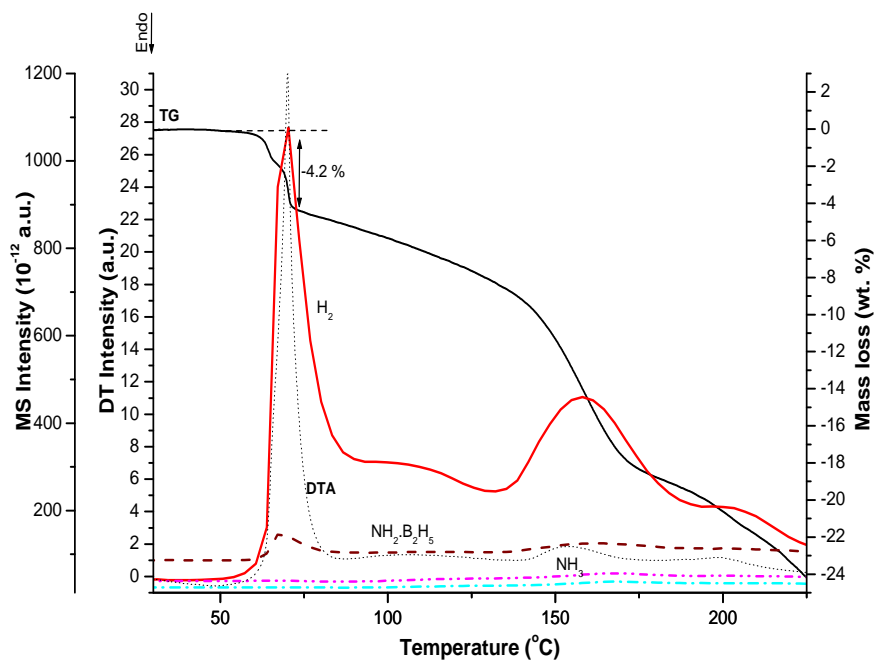
#### 4.3.3.1 *1:1 molar ratio of $\text{LiBH}_4$ to $\text{NH}_4\text{Cl}$*

For compositions with a 1:1 molar ratio of  $\text{LiBH}_4$  to  $\text{NH}_4\text{Cl}$  (as shown in Figures 4.26, 4.27, and 4.28), there is a huge surge of hydrogen accompanied by a systematic release of ADB in much smaller proportions occurring with an especially vigorous exothermic event registered on the DTA in the first stage of decomposition starting at around 60°C and peaking at 70°C. There is also a release of  $\text{A}_2\text{B}_2$  and other amine-borane species (e.g., BZ and PAB-PIB), which makes, during this first step, the mass loss (4.2 wt %) registered on TG less relevant as it is not due to the release of pure hydrogen.

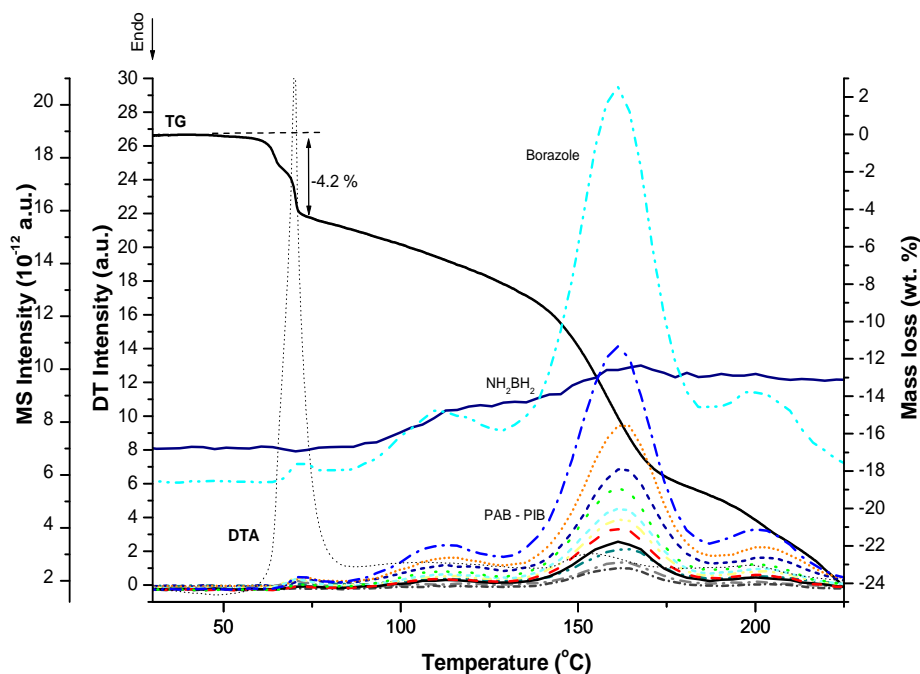
The other thermal events are much lower in terms of intensity and see the release of concomitant hydrogen and other amine-borane species.

Also, the release of the amine-borane species seem to be diminished as the milling time increases from 1 to 5 minutes, and then from 5 to 10 minutes. More, there

is no more release of  $A_2B_2$ , BZ or PAB-PIB in the first stage of decomposition, with a dramatic drop in the mass loss to 0.8 wt %.



(a)



(b)

**Figure 4.26:** Thermal desorption profiles of a sample with a 1:1 molar ratio of  $LiBH_4$  to  $NH_4Cl$  after 1 minute of milling (a): high range of MS  $10^{-9}$  order (b): low range of MS  $10^{-12}$  order

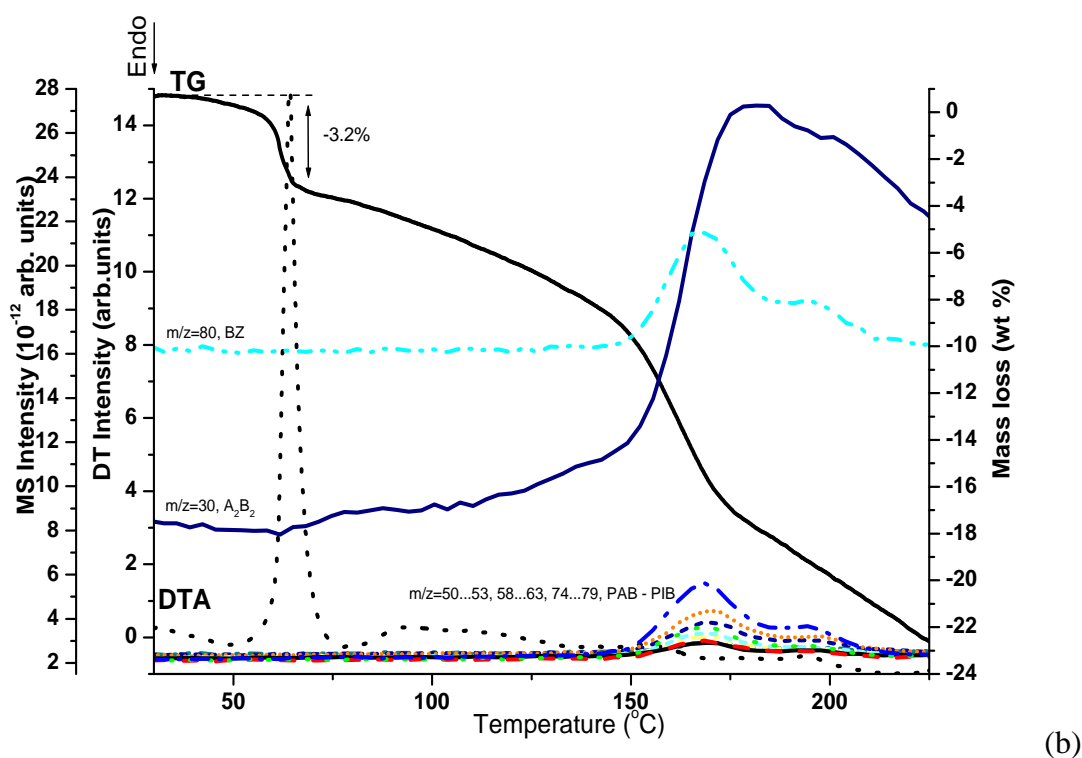
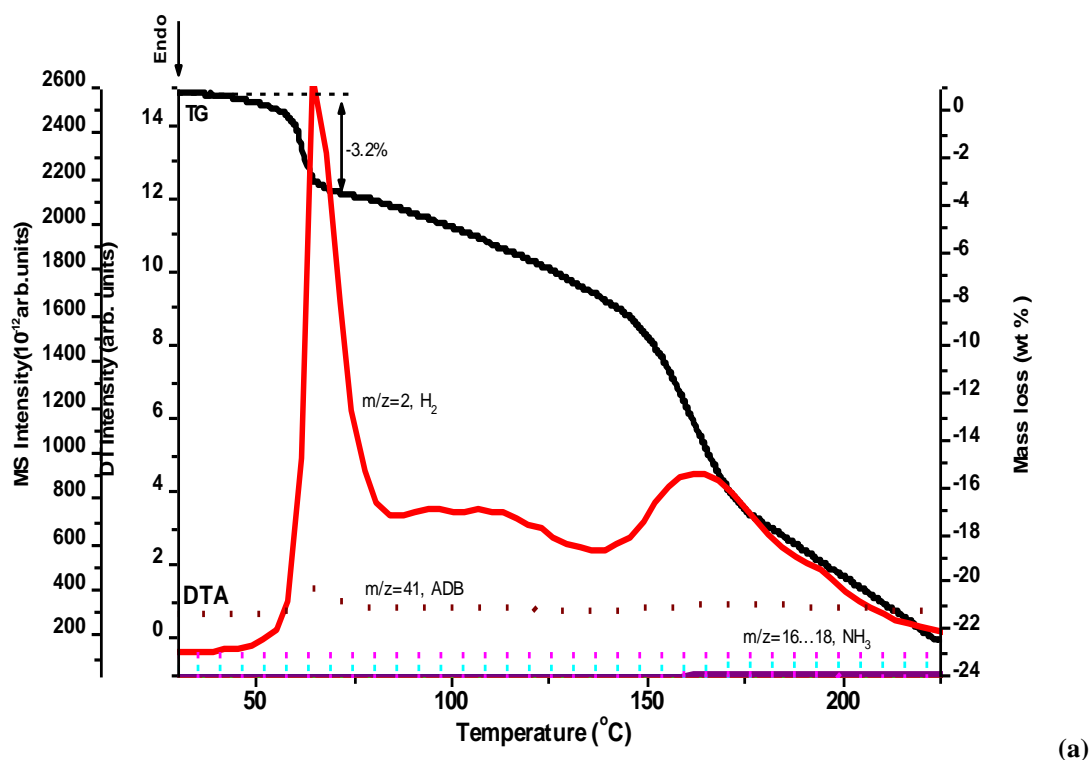
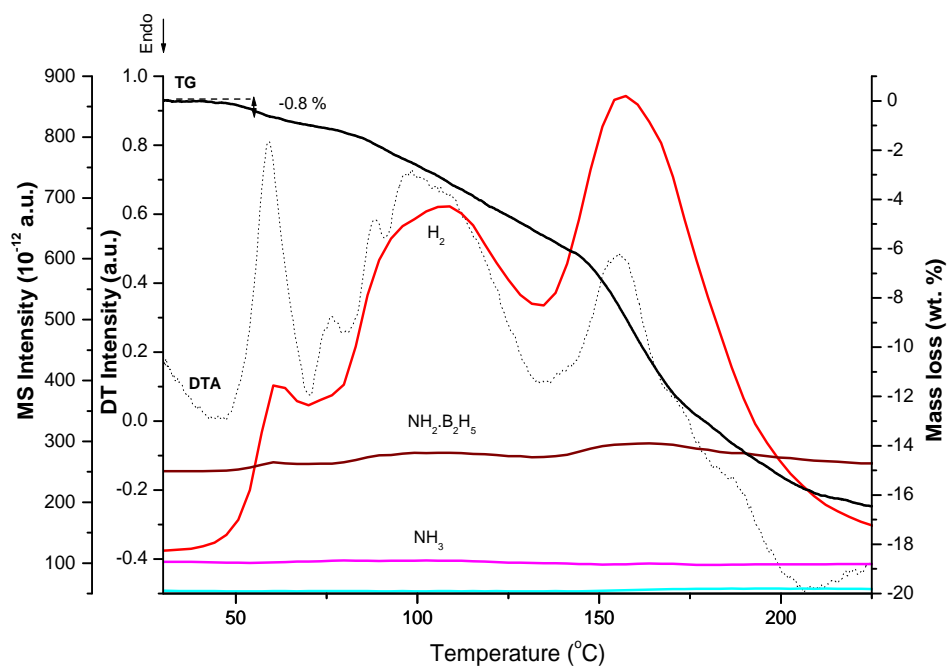
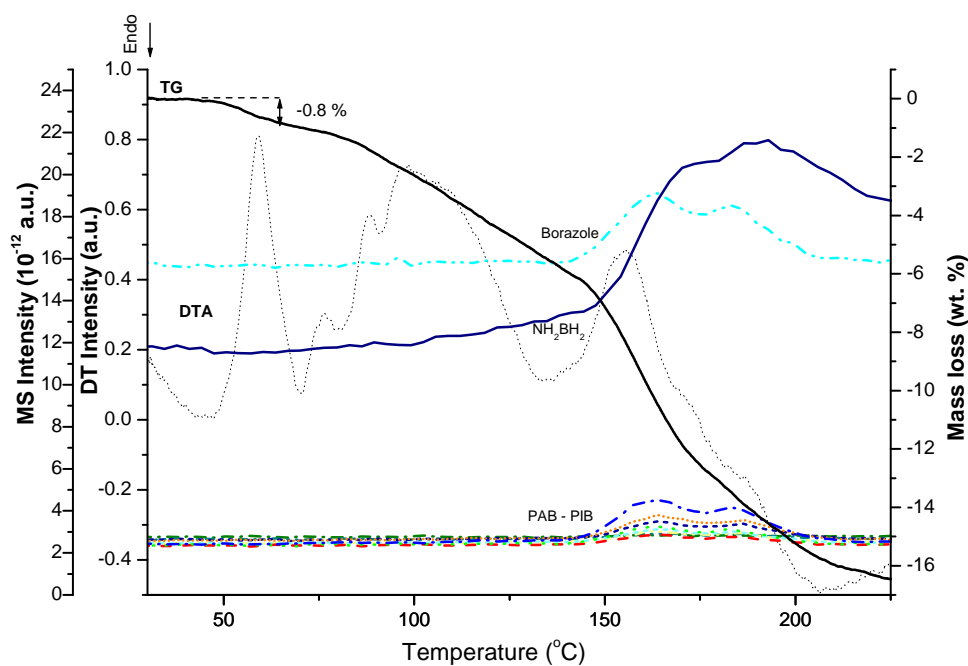


**Figure 4.27:** Thermal desorption profiles of a sample with a 1:1 molar ratio of  $\text{LiBH}_4$  to  $\text{NH}_4\text{Cl}$  after 5 minutes of milling (a): high range of MS  $10^{-9}$  order (b): low range of MS  $10^{-12}$  order



(a)



(b)

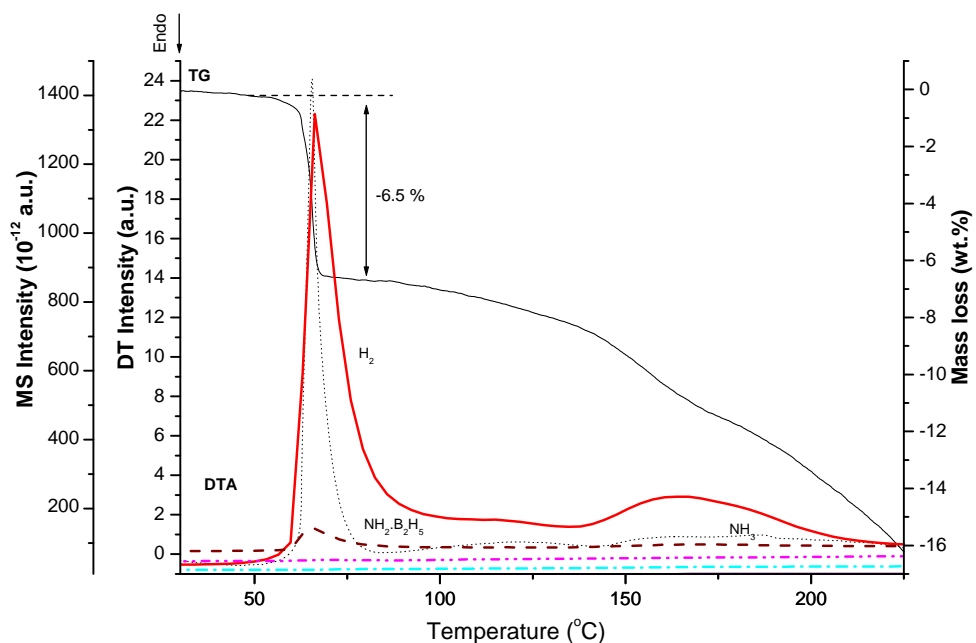
**Figure 4.28:** Thermal desorption profiles of a sample with a 1:1 molar ratio of  $\text{LiBH}_4$  to  $\text{NH}_4\text{Cl}$  after 10 minutes of milling (a): high range of MS  $10^{-9}$  order (b): low range of MS  $10^{-12}$  order

#### 4.3.3.2 1:2 molar ratio of $\text{LiBH}_4$ to $\text{NH}_4\text{Cl}$

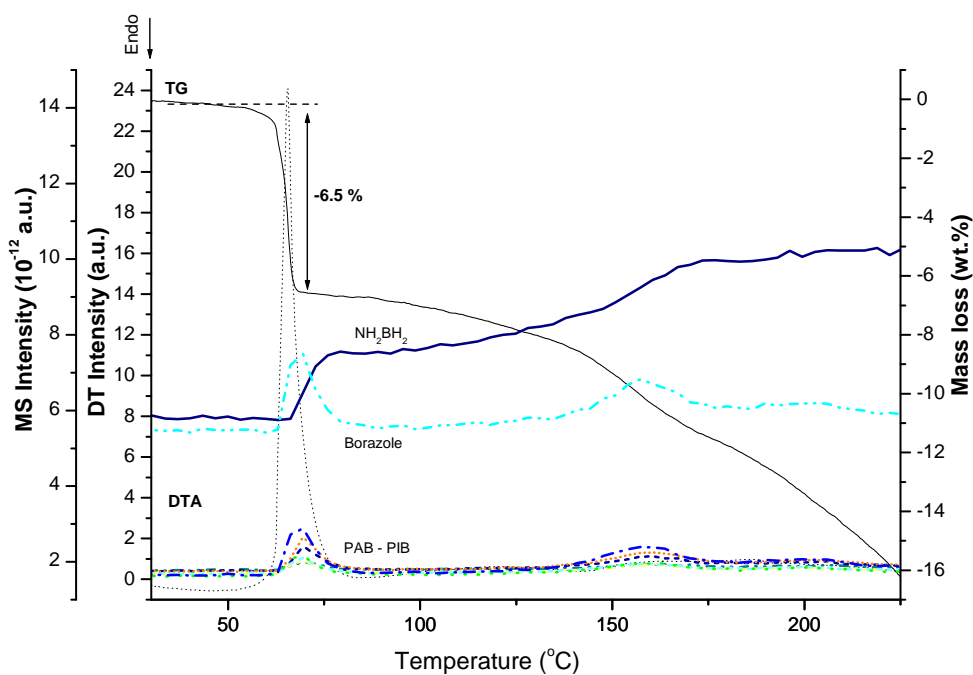
For compositions with a 1:2 molar ratio of  $\text{LiBH}_4$  to  $\text{NH}_4\text{Cl}$  (as shown in Figures 4.29, 4.30, and 4.31), there is still a huge surge of hydrogen accompanied by a systematic release of ADB in much smaller proportions occurring with a significantly vigorous exothermic event registered on the DTA in the first stage of decomposition starting at around  $55^\circ\text{C}$  and peaking at  $70^\circ\text{C}$ . As for the stoichiometric ratio (1:1), there is also a release of  $\text{A}_2\text{B}_2$  and other amine-borane species (e.g., BZ and PAB-PIB) but in smaller proportions, which makes, during this first step, the mass loss (6.5 wt %) registered on TG less significant as it is not due to the only contribution of hydrogen.

The other thermal events (steps 2 and 3) are much lower in terms of intensity and see the release of hydrogen only for step 2 with a differential mass loss of 2.5~3 wt % up to  $150^\circ\text{C}$  and concomitant hydrogen and other amine-borane species for step 3.

Also, there is no more release of amine-borane species ( $\text{A}_2\text{B}_2$ , BZ or PAB-PIB) as the milling time increases from 1 to 5 minutes, and then from 5 to 10 minutes during steps 1 and 2. Especially, for the first step, there is a dramatic drop in the mass loss to 0.9 wt % (5 minutes milling) and to 2.1 wt % (10 minutes milling).

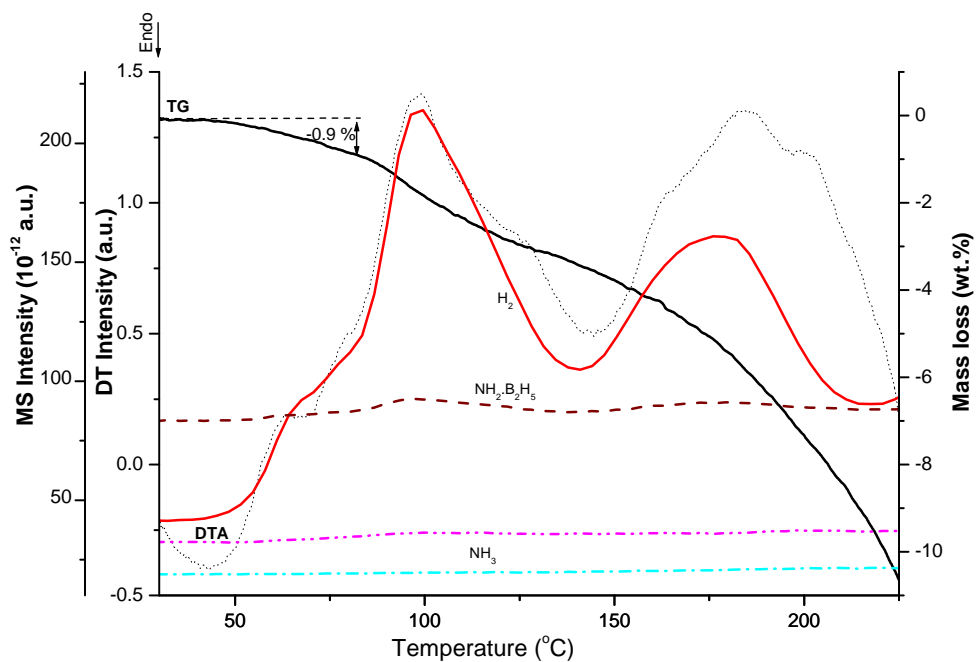


(a)

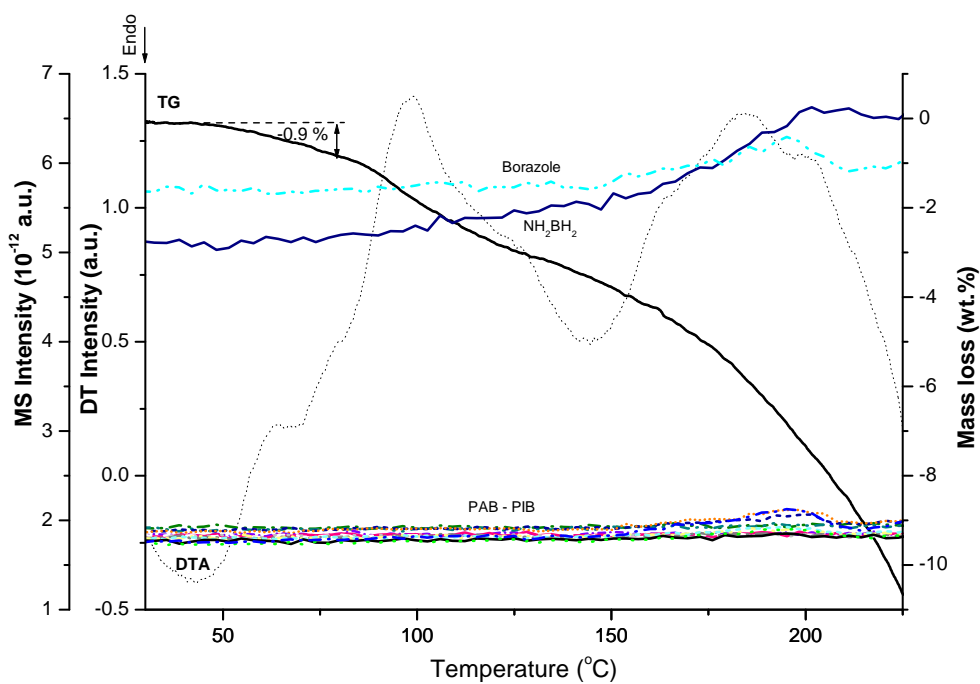


(b)

**Figure 4.29:** Thermal desorption profiles of a sample with a 1:2 molar ratio of  $\text{LiBH}_4$  to  $\text{NH}_4\text{Cl}$  after 1 minute of milling (a): high range of MS  $10^{-9}$  order (b): low range of MS  $10^{-12}$  order

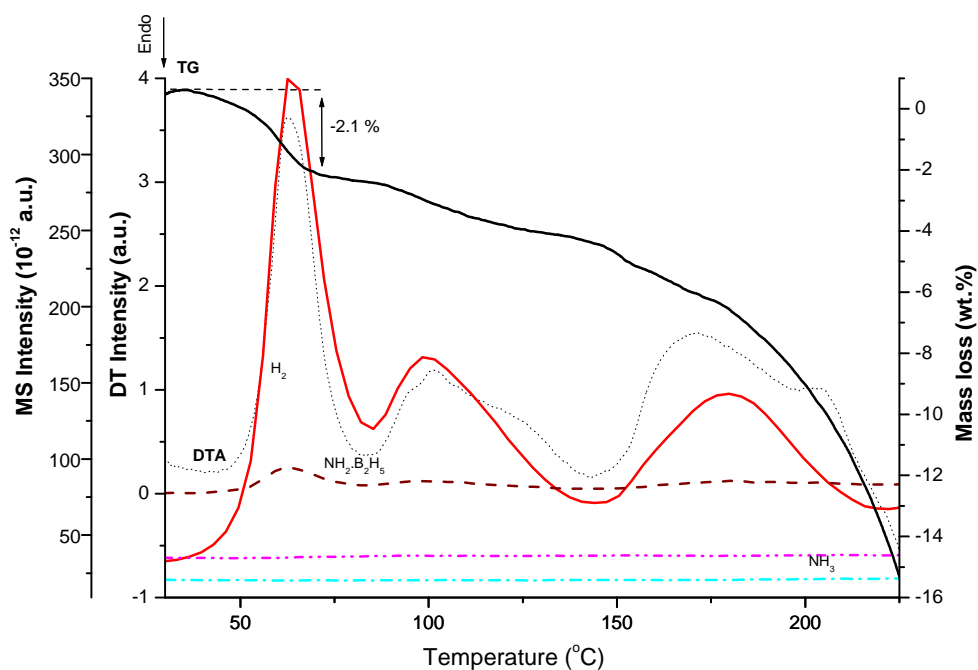


(a)

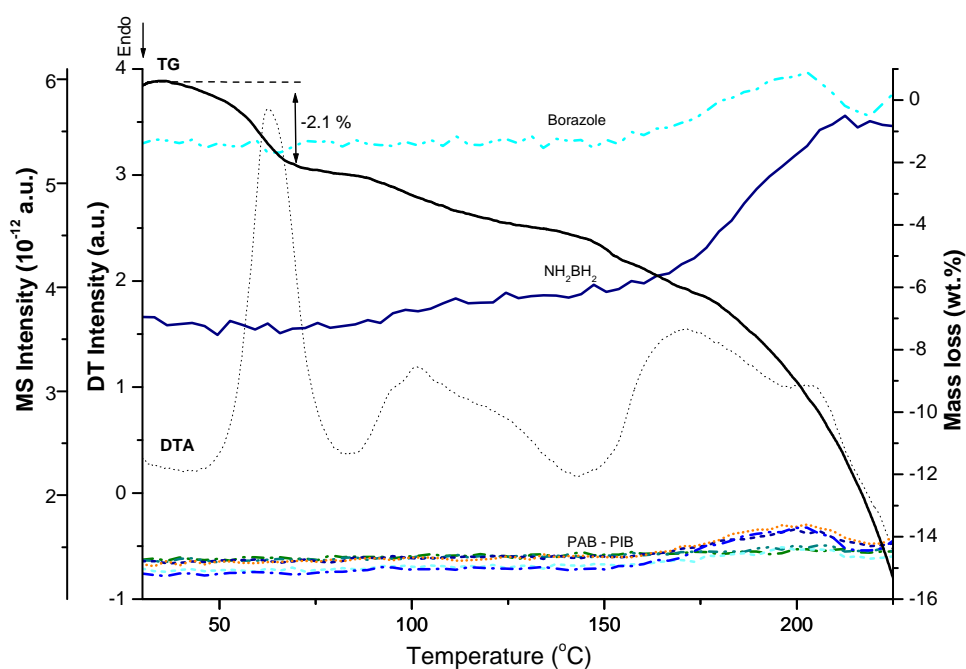


(b)

**Figure 4.30:** Thermal desorption profiles of a sample with a 1:2 molar ratio of  $\text{LiBH}_4$  to  $\text{NH}_4\text{Cl}$  after 5 minutes of milling (a): high range of MS  $10^{-9}$  order (b): low range of MS  $10^{-12}$  order



(a)



(b)

**Figure 4.31:** Thermal desorption profiles of a sample with a 1:2 molar ratio of  $\text{LiBH}_4$  to  $\text{NH}_4\text{Cl}$  after 10 minutes of milling (a): high range of MS  $10^{-9}$  order (b): low range of MS  $10^{-12}$  order

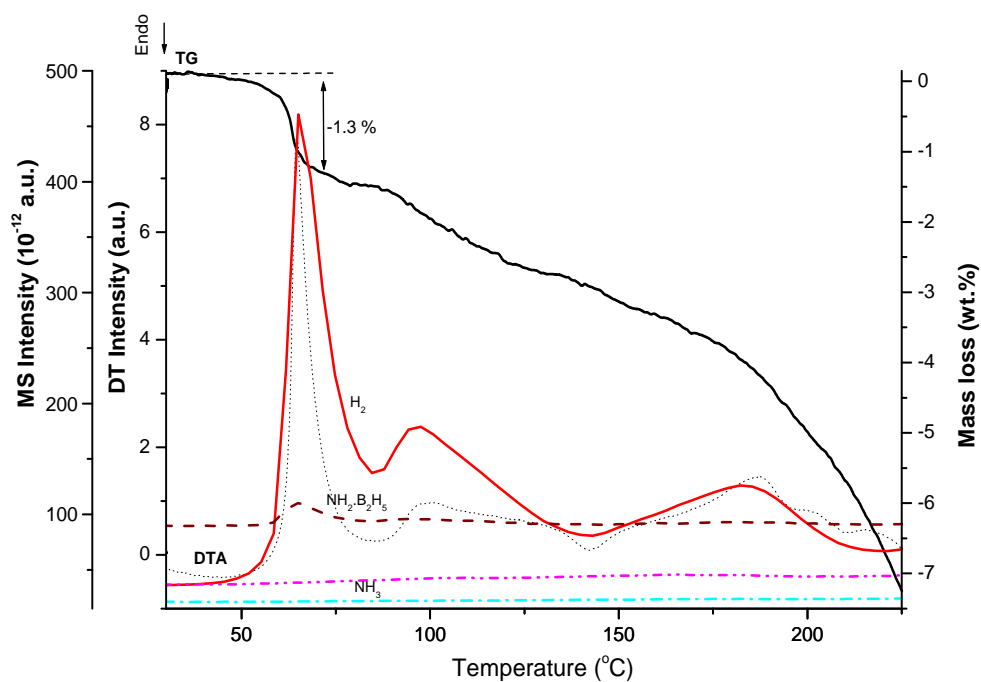


#### 4.3.3.3 1:3 molar ratio of $\text{LiBH}_4$ to $\text{NH}_4\text{Cl}$

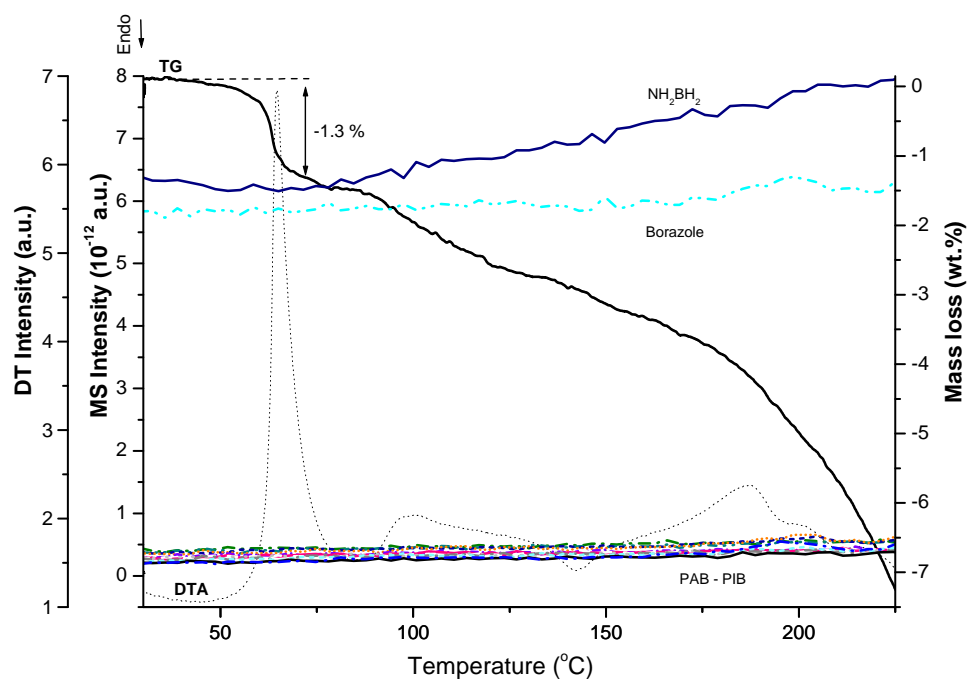
For compositions with a 1:3 molar ratio of  $\text{LiBH}_4$  to  $\text{NH}_4\text{Cl}$  (as shown in Figures 4.32, 4.33, and 4.34), there is still a huge surge of hydrogen accompanied by a systematic release of ADB in much smaller proportions occurring with a significantly vigorous exothermic event registered on the DTA in the first stage of decomposition starting at around  $55^\circ\text{C}$  and peaking at  $70^\circ\text{C}$ . Contrary to the 2 precedent molar ratios, there is no release of AB and other amine-borane species (e.g., BZ and PAB-PIB), which makes, during the first step, the mass loss (1.3 wt %) registered on TG relevant this time.

The other thermal events (steps 2 and 3) are much lower in terms of intensity with a new endothermic event registered around  $145^\circ\text{C}$  and see the release of hydrogen and continuous  $\text{A}_2\text{B}_2$  with a differential mass loss of 1.5~2 wt % up to  $150^\circ\text{C}$  and 4.5~5 wt % up to  $225^\circ\text{C}$ .

As the milling time increases from 1 to 5 minutes, and then from 5 to 10 minutes, the first thermal event is displaced at higher temperatures: starting at  $70^\circ\text{C}$  and peaking at  $100^\circ\text{C}$ , which is in fact, compared to the other ratios, the second step. Also, AB is not released anymore, which confirms the TG registered as the only contribution of hydrogen: ~3 wt % up to  $150^\circ\text{C}$  and ~4 wt % from  $150^\circ\text{C}$  up to  $225^\circ\text{C}$ .

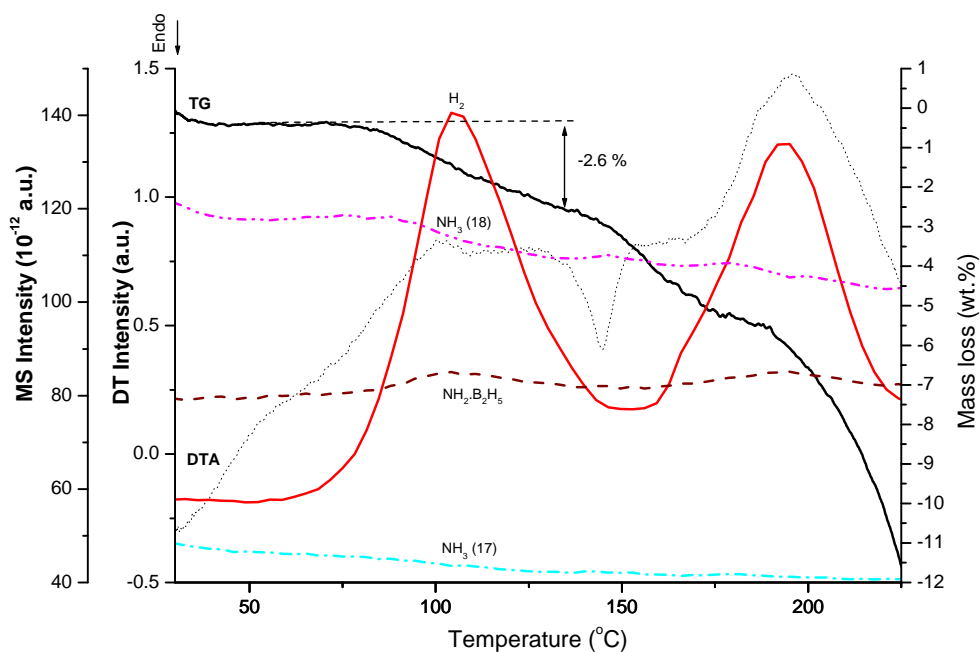


(a)

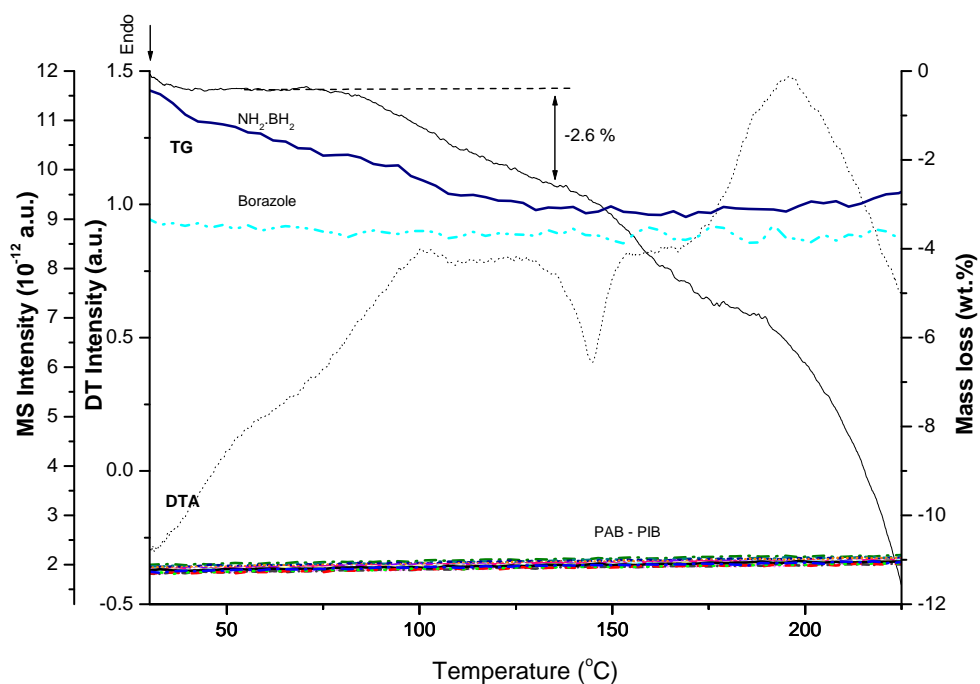


(b)

**Figure 4.32:** Thermal desorption profiles of a sample with a 1:3 molar ratio of  $\text{LiBH}_4$  to  $\text{NH}_4\text{Cl}$  after 1 minute of milling (a): high range of MS  $10^{-9}$  order (b): low range of MS  $10^{-12}$  order

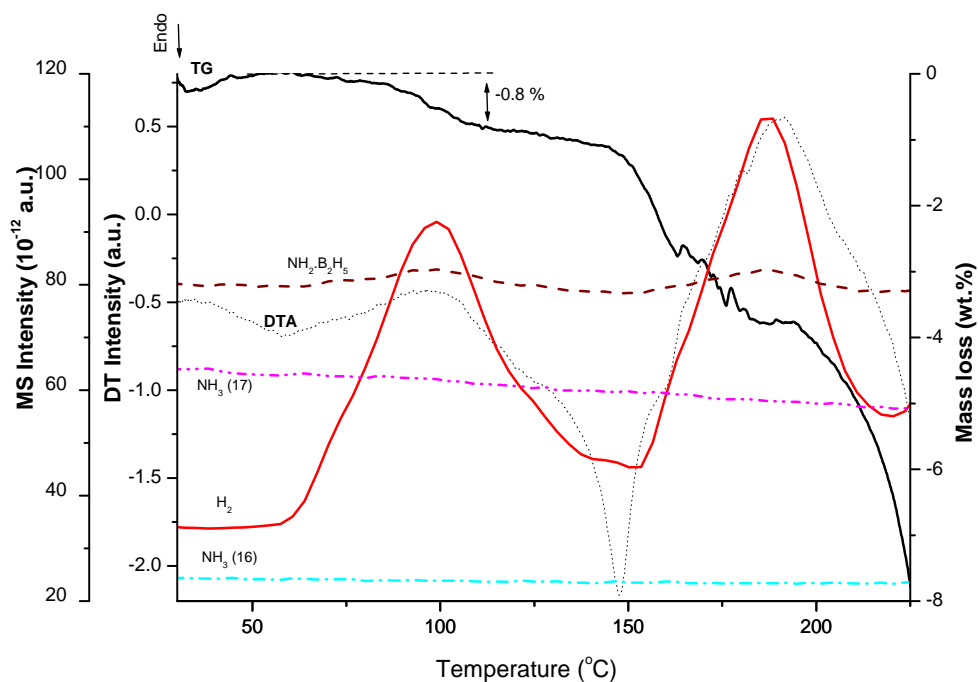


(a)

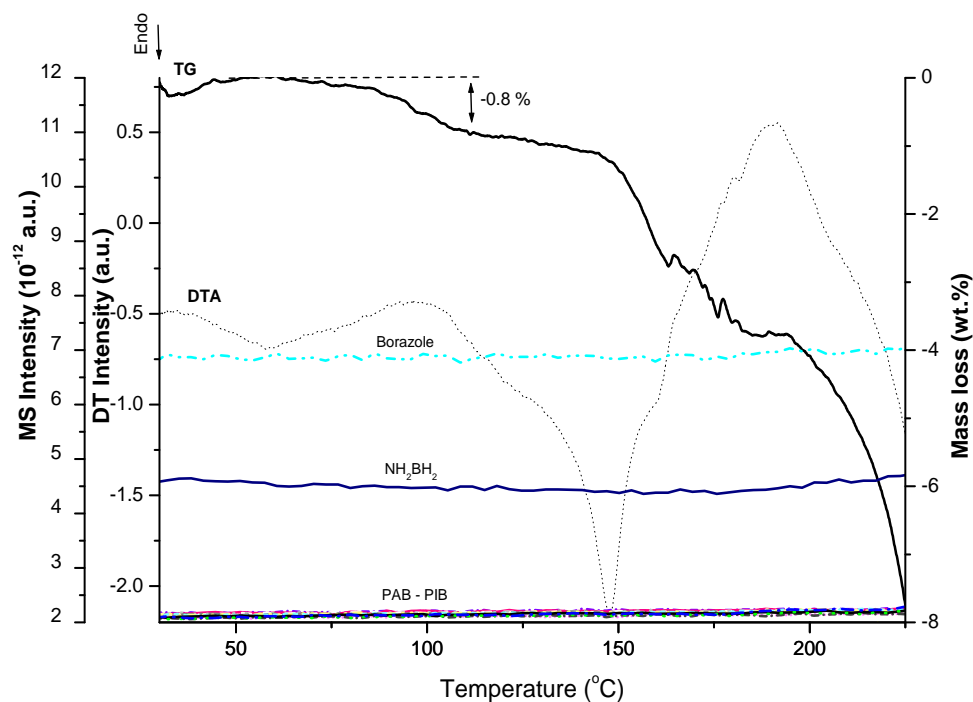


(b)

**Figure 4.33:** Thermal desorption profiles of a sample with a 1:3 molar ratio of  $\text{LiBH}_4$  to  $\text{NH}_4\text{Cl}$  after 5 minutes of milling (a): high range of MS  $10^{-9}$  order (b): low range of MS  $10^{-12}$  order



(a)



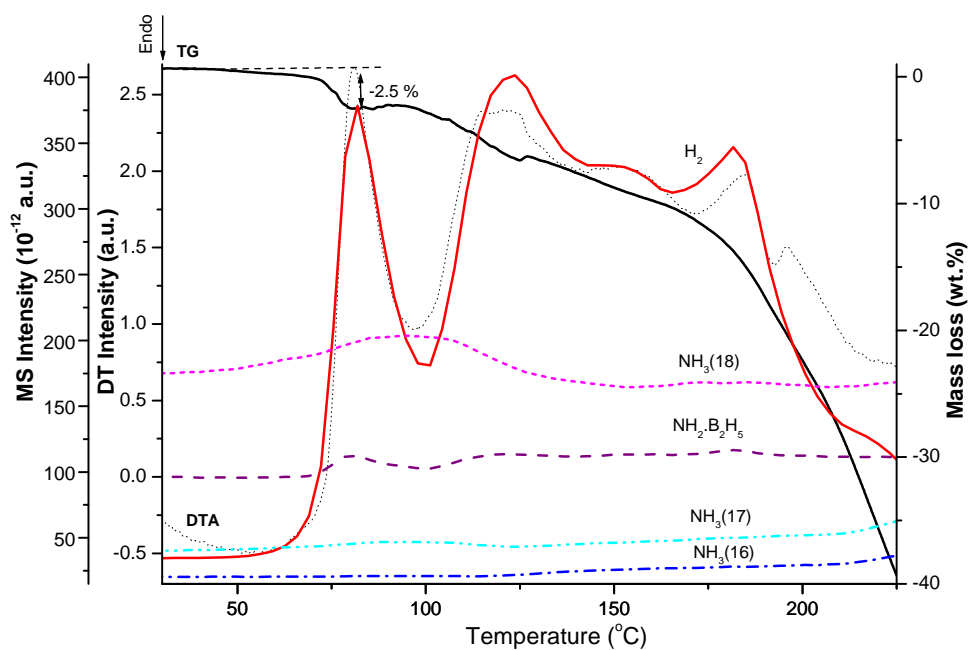
(b)

**Figure 4.34:** Thermal desorption profiles of a sample with a 1:3 molar ratio of  $\text{LiBH}_4$  to  $\text{NH}_4\text{Cl}$  after 10 minutes of milling (a): high range of MS  $10^{-9}$  order (b): low range of MS  $10^{-12}$  order

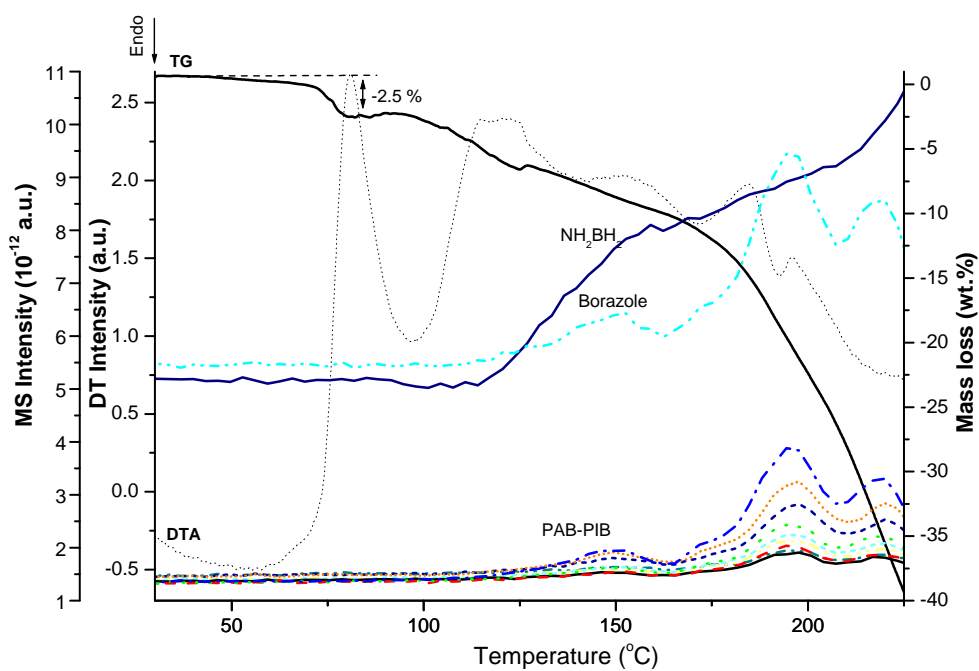
With the combined results from XRD, SEM-EDS and TG-DTA-MS after the first step (above 60°C), it proves that the first reaction involves the formation of LiCl. Also, the absence of NH<sub>4</sub>Cl presumes that a possible step 1 reaction product could be NH<sub>3</sub>BH<sub>3</sub>. Thus, there is still room for improvement for the second step in particular. As a result, TG-DTA-MS measurements on mixtures of NH<sub>3</sub>BH<sub>3</sub>, the commercial version of the assumed product of step 1, and NH<sub>4</sub>Cl (1 and 2 moles) submitted to a milling of 1 and 5 minutes have been performed. The different graphs are presented in the following figures.

#### 4.3.3.4 1:1 and 1:2 molar ratios of NH<sub>3</sub>BH<sub>3</sub> to NH<sub>4</sub>Cl

For compositions with a 1:1 molar ratio of NH<sub>3</sub>BH<sub>3</sub> to NH<sub>4</sub>Cl (as shown in Figures 4.35 and 4.36), there is still a huge surge of hydrogen accompanied by a systematic release of ADB in much smaller proportions occurring with a significantly vigorous exothermic event registered on the DTA in the first stage of decomposition starting at around 70°C and peaking at 80°C. Contrary to the 3 precedent ratios involving LiBH<sub>4</sub> and NH<sub>4</sub>Cl, NH<sub>3</sub> is released whereas no other amine-borane species (e.g., A<sub>2</sub>B<sub>2</sub>, BZ and PAB-PIB) are registered on the MS, which makes, during the first step, the mass loss (2.5 wt %) registered on TG less significant. The next thermal event (step 2) is of same intensity as the first one and it is also exothermic with an onset at 100°C and a peak at 125°C. The release of hydrogen starts right from the beginning of the event whereas the other releases (A<sub>2</sub>B<sub>2</sub>, PAB-PIB and BZ) start from the peak temperature around 125°C. The following thermal events are of much lower intensity and see the concomitant release of amine-borane species. As the milling time increases from 1 to 5 minutes, there is no real change as the profiles are very similar.

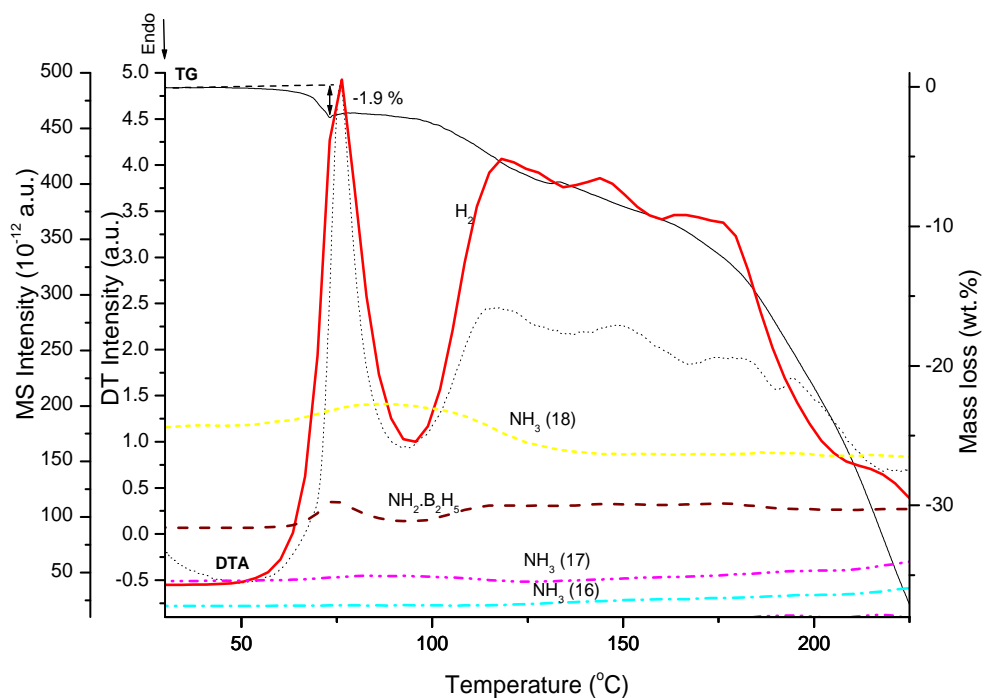


(a)

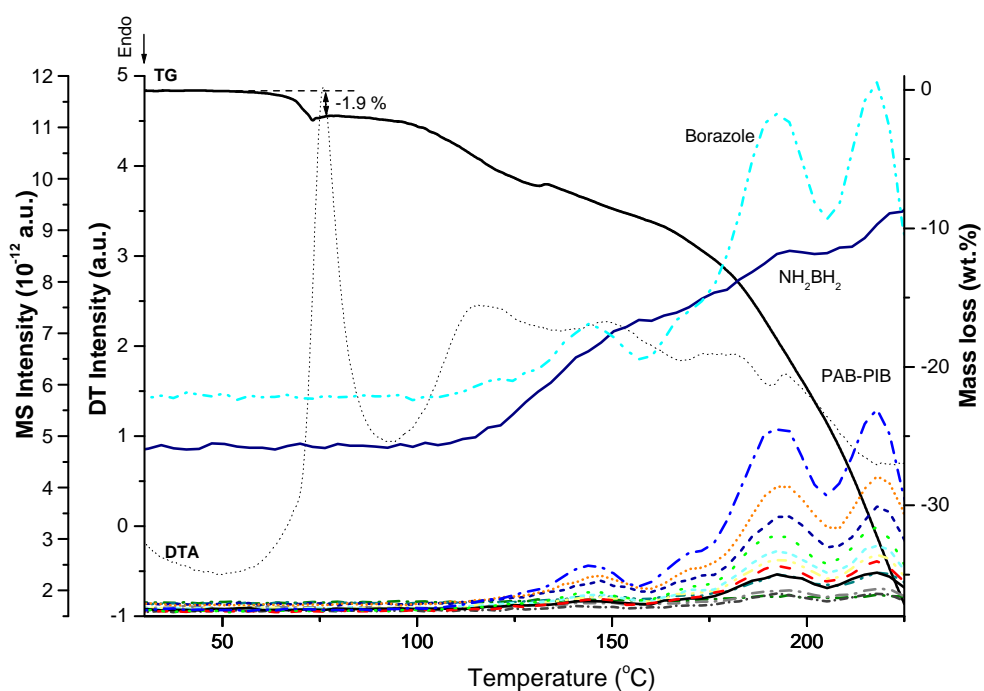


(b)

**Figure 4.35:** Thermal desorption profiles of a sample with a 1:1 molar ratio of  $\text{NH}_3\text{BH}_3$  to  $\text{NH}_4\text{Cl}$  after 1 minute of milling (a): high range of MS  $10^{-10}$  order (b): low range of MS  $10^{-12}$  order



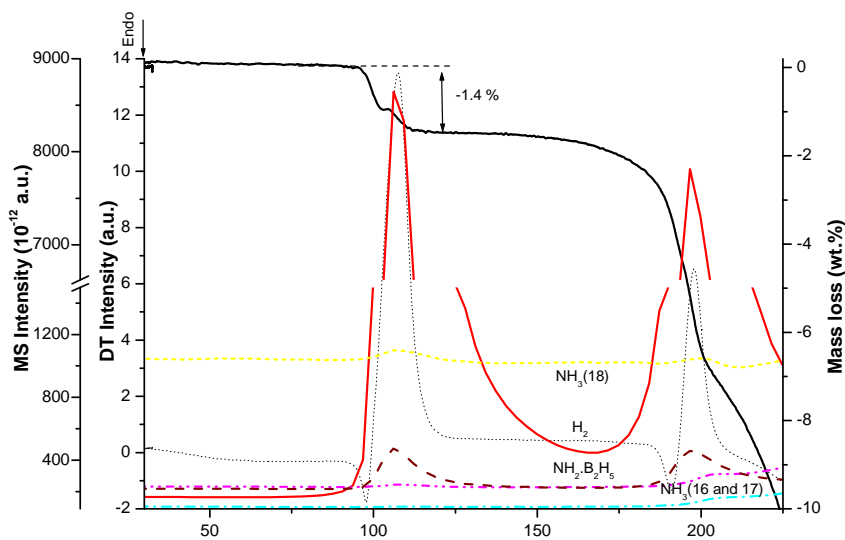
(a)



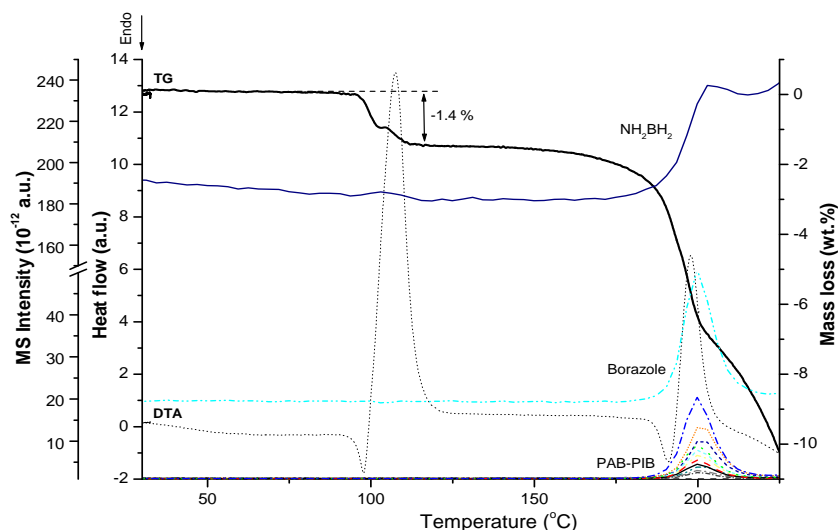
(b)

**Figure 4.36:** Thermal desorption profiles of a sample with a 1:1 molar ratio of  $\text{NH}_3\text{BH}_3$  to  $\text{NH}_4\text{Cl}$  after 5 minutes of milling (a): high range of MS  $10^{-10}$  order (b): low range of MS  $10^{-12}$  order

For compositions with a 1:2 molar ratio of  $\text{NH}_3\text{BH}_3$  to  $\text{NH}_4\text{Cl}$  (as shown in Figure 4.37), the desorption profile is very different with 2 distinct steps characterised by 2 double thermal events: only the second one peaked at  $200^\circ\text{C}$  sees the release of heavy amine-borane species (PAB-PIB and BZ) whereas the first one peaked at  $110^\circ\text{C}$  sees the release of ADB and  $\text{NH}_3$  along with hydrogen.



(a)



(b)

**Figure 4.37:** Thermal desorption profiles of a sample with a 1:2 molar ratio of  $\text{NH}_3\text{BH}_3$  to  $\text{NH}_4\text{Cl}$  after 1 minute of milling (a): high range of MS  $10^{-9}$  order (b): low range of MS  $10^{-10}$  order



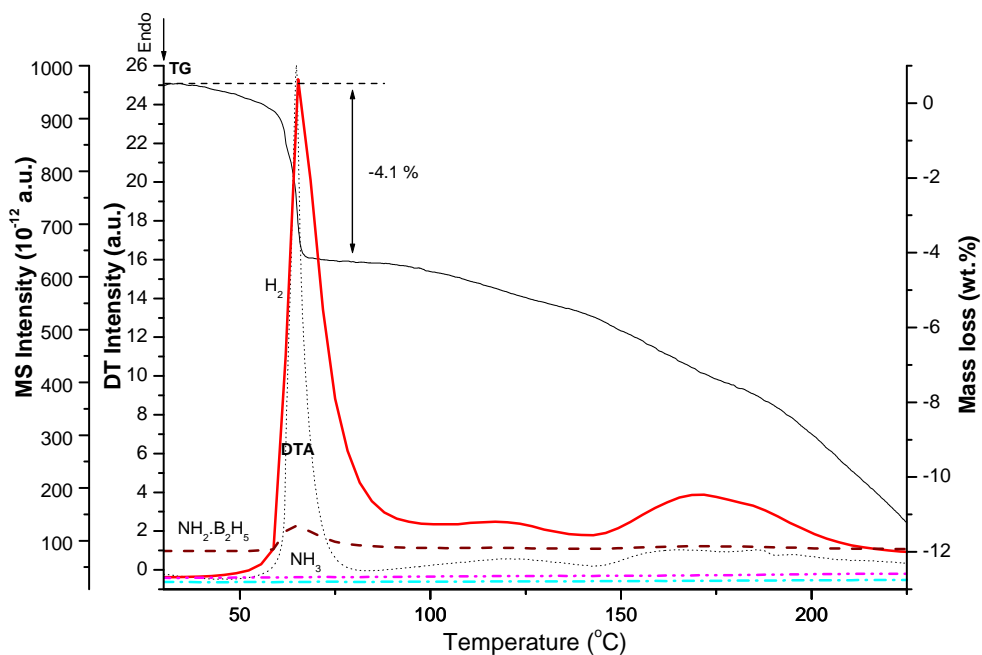
Finally, small quantities (5 mol %) of graphite powder were added to the binary compositions in order to facilitate the mixing between  $\text{LiBH}_4$  or  $\text{NH}_3\text{BH}_3$  and  $\text{NH}_4\text{Cl}$  and thus, increase the contact surface between the two materials.

The following figures show the thermal desorption profiles of the C-added ( $\text{LiBH}_4\text{-NH}_4\text{Cl}$ ) and ( $\text{NH}_3\text{BH}_3\text{-NH}_4\text{Cl}$ ) mixtures with different molar ratios and different milling times ranging from 1 to 5 minutes.

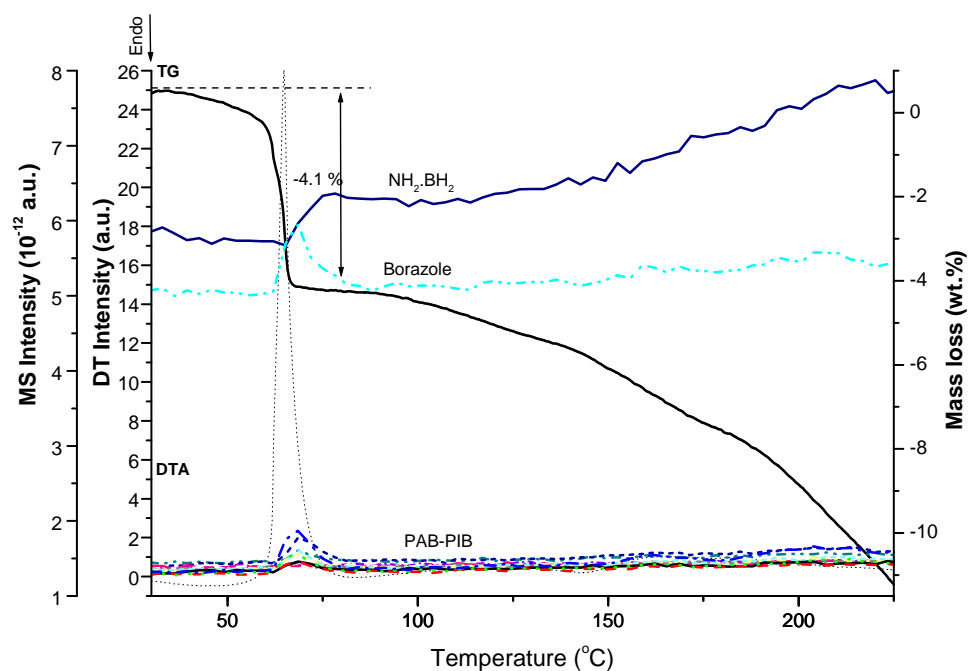
The figures also show two ranges of MS as the first half figure shows the high range ( $10^{-10}$  order) and the second half the low range ( $10^{-12}$  order).

#### *4.3.3.5 Carbon additions to $\text{LiBH}_4\text{-NH}_4\text{Cl}$ and $\text{NH}_3\text{BH}_3\text{-NH}_4\text{Cl}$ compositions*

For compositions with 5 mol % doping of carbon graphite and a 1:2 molar ratio of  $\text{LiBH}_4$  to  $\text{NH}_4\text{Cl}$  (as shown in Figure 4.38 and 4.39), there is still a release of hydrogen accompanied by a systematic release of ADB in much smaller proportions occurring with a significantly vigorous exothermic event registered on the DTA in the first stage of decomposition starting at around  $50^\circ\text{C}$  and peaking at  $65^\circ\text{C}$ . As the milling time increases from 1 to 5 minutes, comparatively to the same mixture without any carbon addition, Step 1 is very similar whereas Step 2 is considerably enhanced as the differential mass loss associated with a release of hydrogen and ADB to a much lower extent is topping at 4 wt % up to  $150^\circ\text{C}$  compared to 2-3 wt % obtained previously.

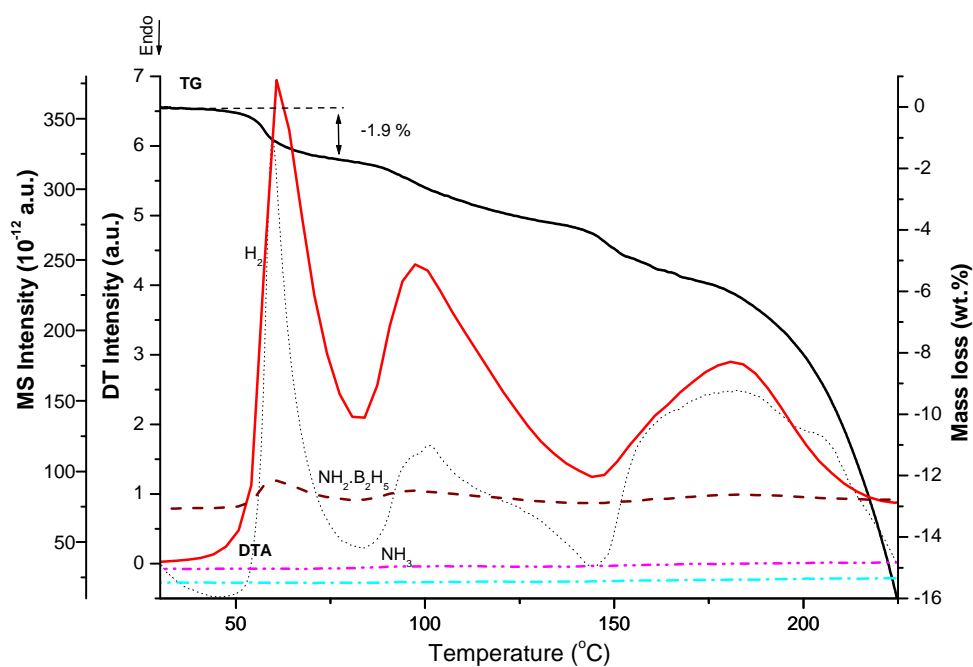


(a)

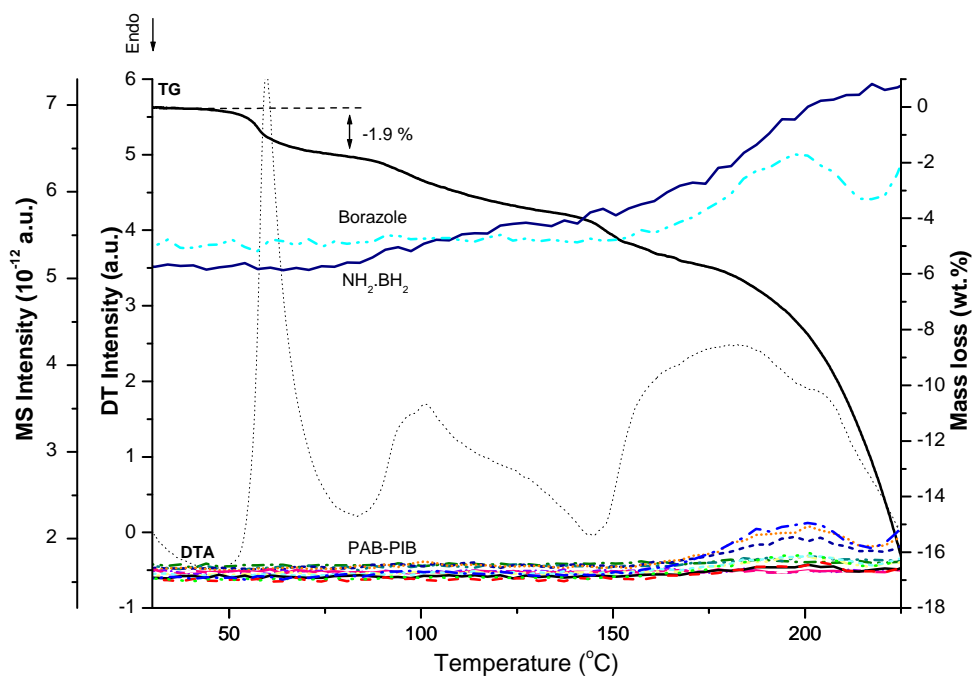


(b)

**Figure 4.38:** Thermal desorption profiles of a sample with a 1:2:5 mol % molar ratio of  $\text{LiBH}_4$  to  $\text{NH}_4\text{Cl}$  and C after 1 minute of milling (a): high range of MS  $10^{-10}$  order (b): low range of MS  $10^{-12}$  order



(a)



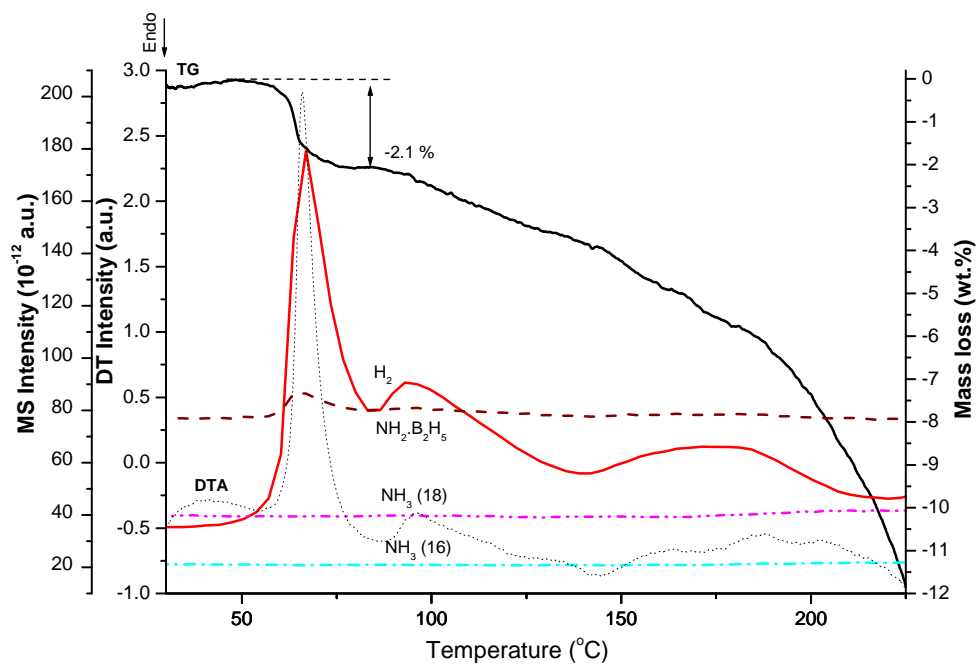
(b)

**Figure 4.39:** Thermal desorption profiles of a sample with a 1:2:5 mol % molar ratio of  $\text{LiBH}_4$  to  $\text{NH}_4\text{Cl}$  and C after 5 minutes of milling (a): high range of MS  $10^{-10}$  order (b): low range of MS  $10^{-12}$  order

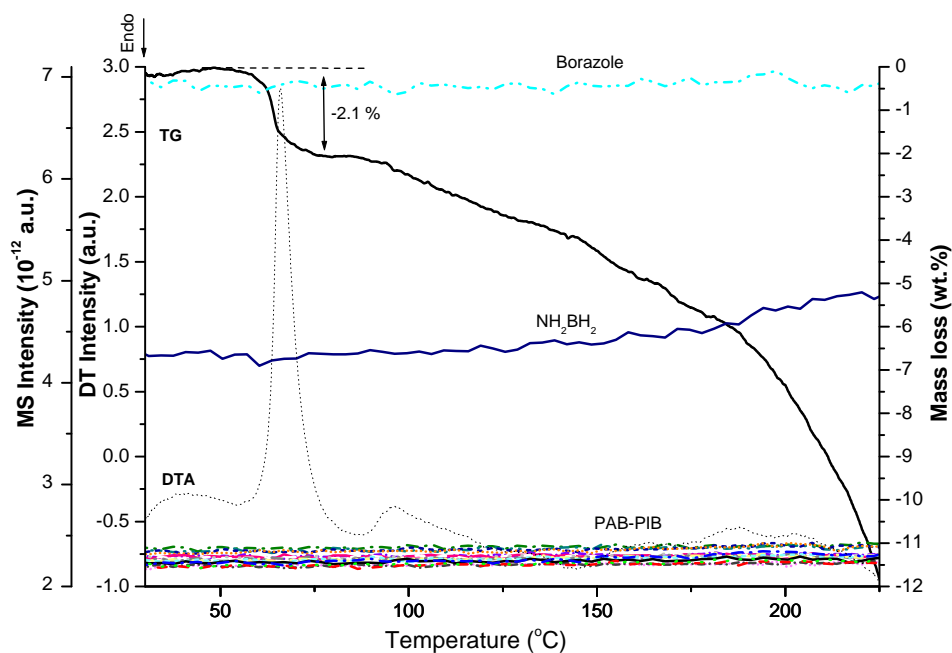
For compositions with 5 mol % doping of carbon graphite and a 1:3 molar ratio of  $\text{LiBH}_4$  to  $\text{NH}_4\text{Cl}$  (as shown in Figures 4.40 and 4.41), there is still a release of hydrogen accompanied by a systematic release of ADB in much smaller proportions occurring with a significantly vigorous exothermic event registered on the DTA in the first stage of decomposition starting at around  $60^\circ\text{C}$  and peaking at  $75^\circ\text{C}$ .

As the milling time increases from 1 to 5 minutes, comparatively to the same mixture without any carbon addition, Step 1 is very similar with a bigger mass loss of 2.1 wt % (compared to 1.3 wt %) whereas Step 2 sees an improvement as the differential mass loss associated with a release of hydrogen and ADB to a much lower extent is topping at 3.5 wt % up to  $150^\circ\text{C}$  compared to 1.5~2 wt % obtained previously.

Step 3 is also enhanced with a differential mass loss of 6 wt % up to  $225^\circ\text{C}$  compared to 4.5~5 wt % attained previously. Also, the displacement observed when the milling time was increased is no longer present. Instead, there still is a first step with a very small mass loss of 0.7 wt %.



(a)



(b)

**Figure 4.40:** Thermal desorption profiles of a sample with a 1:3:5 mol % molar ratio of  $\text{LiBH}_4$  to  $\text{NH}_4\text{Cl}$  and C after 1 minute of milling (a): high range of MS  $10^{-10}$  order (b): low range of MS  $10^{-12}$  order

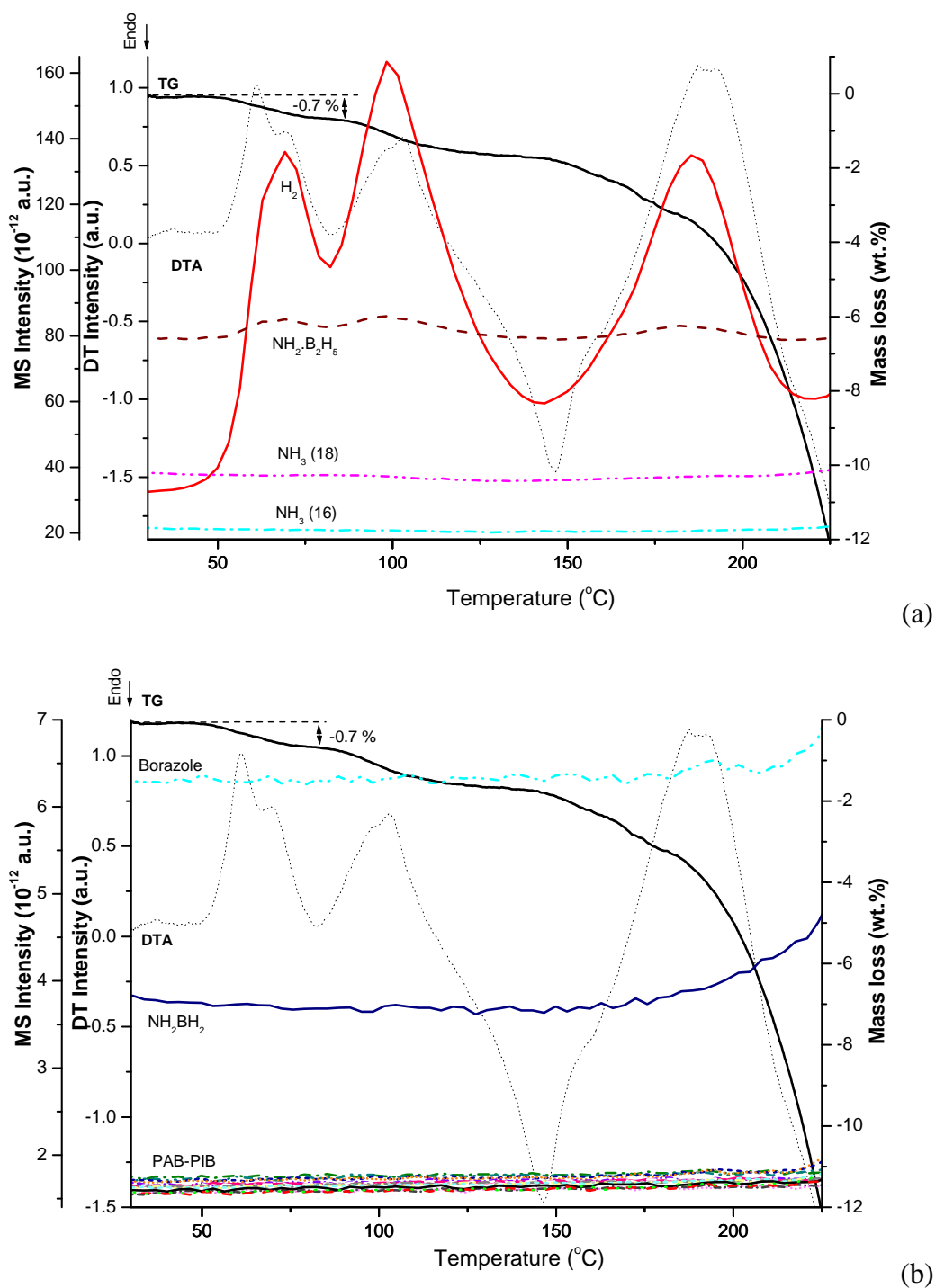
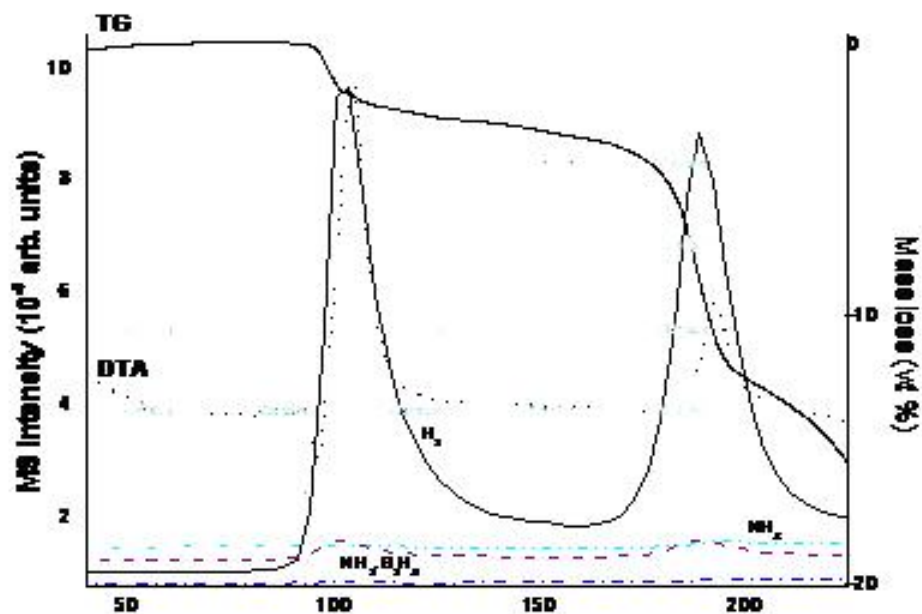
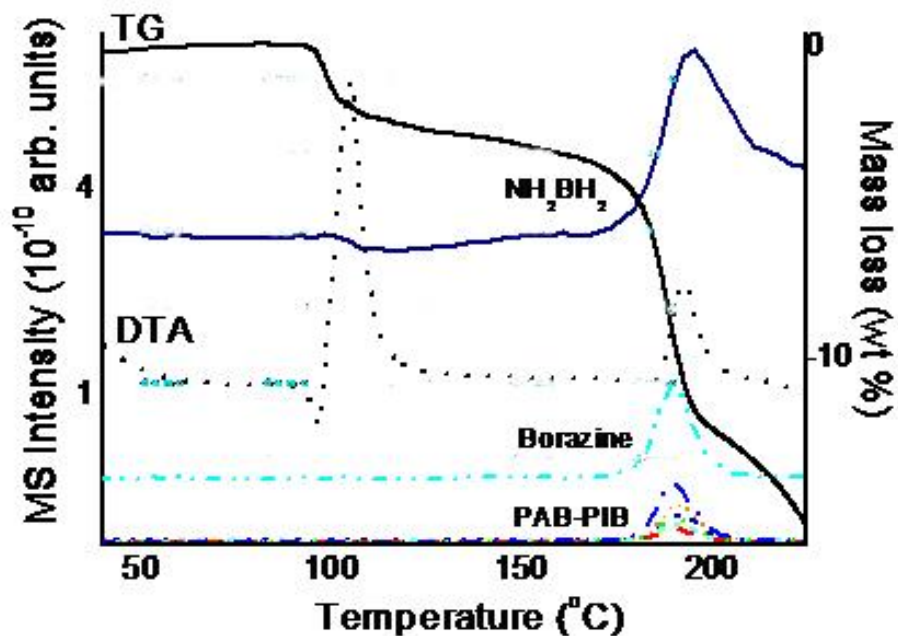


**Figure 4.41:** Thermal desorption profiles of a sample with a 1:3:5 mol % molar ratio of  $\text{LiBH}_4$  to  $\text{NH}_4\text{Cl}$  and C after 5 minutes of milling (a): high range of MS  $10^{-10}$  order (b): low range of MS  $10^{-12}$  order

For compositions with 5 mol % doping of carbon graphite and a 1:1 molar ratio of  $\text{NH}_3\text{BH}_3$  to  $\text{NH}_4\text{Cl}$  (as shown in Figures 4.42 and 4.43),

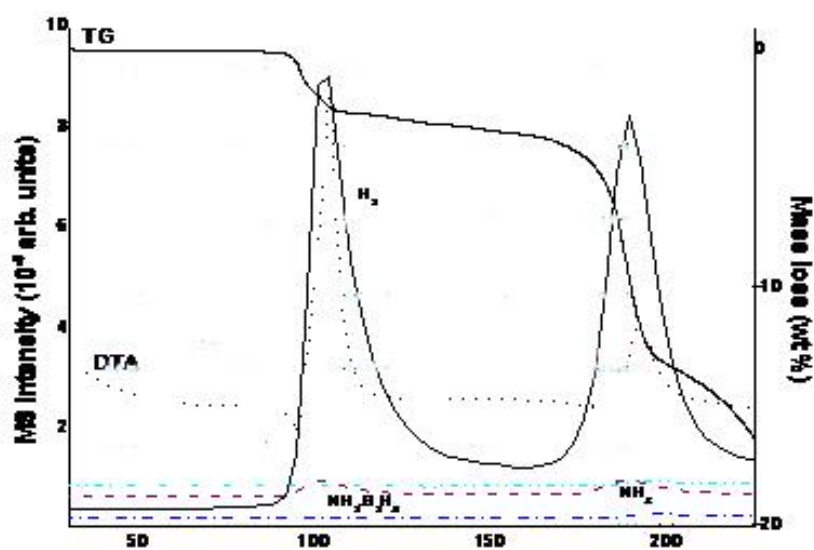


(a)

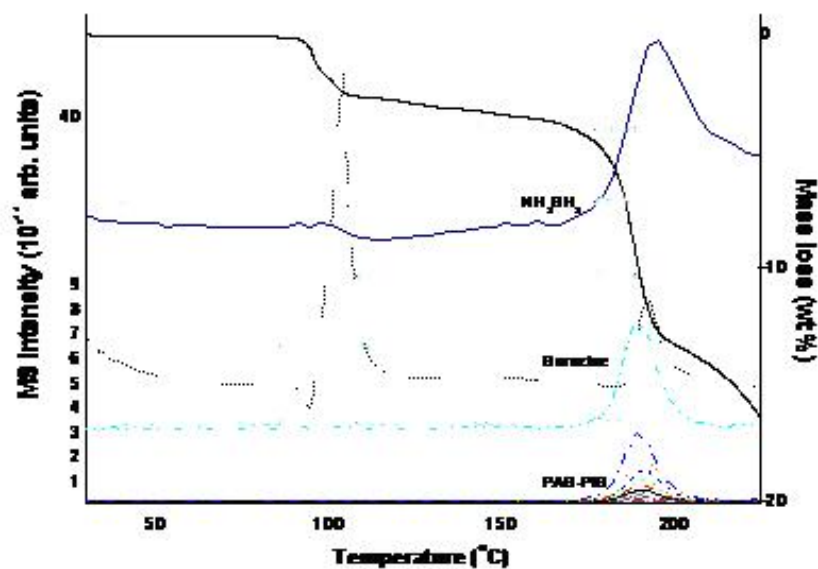


(b)

**Figure 4.42:** Thermal desorption profiles of a sample with a 1:1:5 mol % molar ratio of  $\text{NH}_3\text{BH}_3$  to  $\text{NH}_4\text{Cl}$  and C after 1 minute of milling (a): high range of MS  $10^{-9}$  order (b): low range of MS  $10^{-10}$  order



(a)

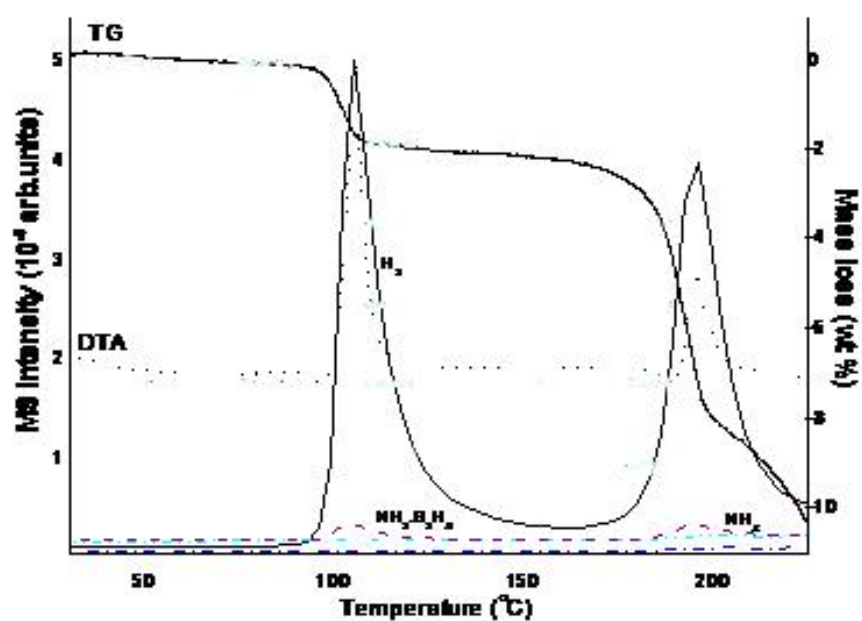


(b)

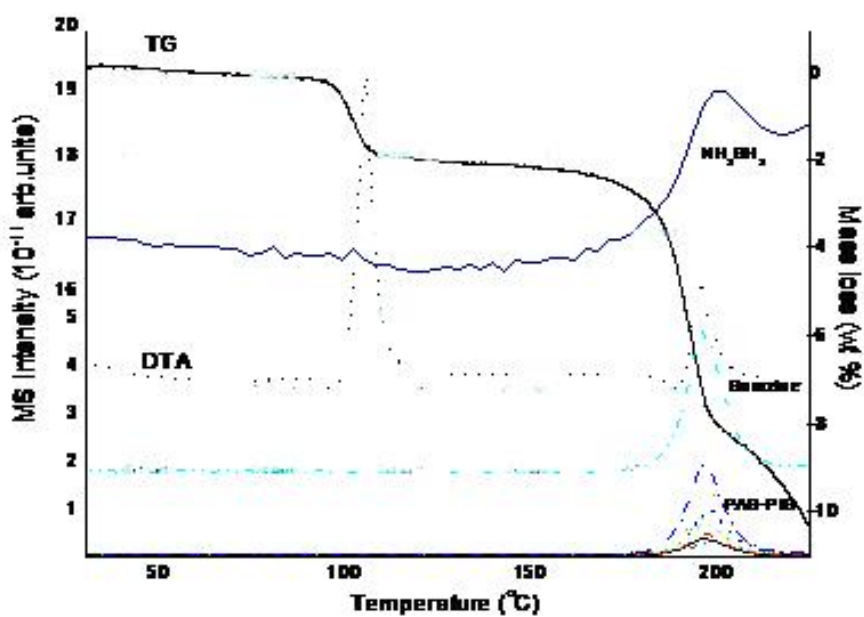
**Figure 4.43:** Thermal desorption profiles of a sample with a 1:1:5 mol % molar ratio of  $\text{NH}_3\text{BH}_3$  to  $\text{NH}_4\text{Cl}$  and C after 5 minutes of milling (a): high range of MS  $10^{-9}$  order  
(b): low range of MS  $10^{-11}$  order

For the composition with 5 mol % doping of carbon graphite and a 1:2 molar ratio of  $\text{NH}_3\text{BH}_3$  to  $\text{NH}_4\text{Cl}$  (as shown in Figure 4.44),





(a)



(b)

**Figure 4.44:** Thermal desorption profiles of a sample with a 1:2:5 mol % molar ratio of  $\text{NH}_3\text{BH}_3$  to  $\text{NH}_4\text{Cl}$  and C after 1 minute of milling (a): high range of MS  $10^{-9}$  order (b): low range of MS  $10^{-11}$  order

Overall, the 2 key requirements identified during the study of pure  $\text{LiBH}_4$  have been fulfilled:

- 1- Decrease the main onset desorption temperature from  $380^\circ\text{C}$  (above  $\text{LiBH}_4$  melting temperature) to  $60\text{-}250^\circ\text{C}$  (below  $\text{LiBH}_4$  melting temperature);**
- 2- Keep the hydrogen delivery the purest possible: it has potentially been achieved with the C-added ( $\text{LiBH}_4\text{:NH}_4\text{Cl}=1\text{:}3$ ) mixture.**

In the discussion chapter (Chapter 5), we will compare our findings to the ones reported in the literature, knowing that for  $\text{NH}_4\text{Cl}$ -added mixtures, nothing has been reported before with respect to hydrogen storage.

## **Chapter 5.    General Discussion**

The safe and convenient storage of hydrogen is one of the critical issues that limit hydrogen energy systems, especially for transportation applications. Storing hydrogen in solids seems to be one of the most promising solutions. In the case of hydrides, they must face thermodynamic and kinetic barriers: metal hydrides have fast kinetics and appropriate thermodynamics [41] but are low in hydrogen capacity whereas complex hydrides have high hydrogen capacity but are challenged on thermodynamics and kinetics [46].

Different types of materials have been investigated, but so far very few materials can meet the number 1 requirements for on-board hydrogen storage in vehicles, which is a **hydrogen** capacity above **4.5 wt %** at a manageable temperature (~100-150°C). In terms of high hydrogen capacity, complex hydrides have been mainly regarded as good candidates for hydrogen storage, but in most cases, the purity of the hydrogen delivery is the main drawback along with an irreversibility of the process.

LiBH<sub>4</sub> has received particular attention in recent years, since the report of pure hydrogen desorption of up to 13.5 wt % at 500°C [135]. However, this is a multistep process and most of desorption occurs at a temperature, too high for on-board vehicular applications. Hence, unmodified LiBH<sub>4</sub> seems ideal for the targeted application.

Therefore, current efforts have been devoted to reduce the main desorption temperature, and to understand the possible destabilisation mechanisms of modified

$\text{LiBH}_4$ , i.e. the reactivity of  $\text{LiBH}_4$  with new additives such as fourth-period metal chlorides or N-H based compounds i.e. ammonium chloride.

Hence,  $\text{LiBH}_4$ ,  $(n\text{LiBH}_4 + \text{MCl}_n)$  and  $(\text{LiBH}_4 + x\text{NH}_4\text{Cl})$  were comparatively investigated to clarify further the destabilisation mechanism of  $\text{LiBH}_4$  and thus improve the hydrogen desorption properties of this promising compound. Thermal analysis coupled with Mass Spectrometry (MS) was used to fully characterise the products formed during decomposition. Whenever possible, XRD and FTIR were also used to examine more closely the desorption products at different temperatures.

## 5.1 Dehydrogenation from as-received lithium borohydride, $\text{LiBH}_4$

In order to establish the baseline for objective comparison, the dehydrogenation properties of as-received  $\text{LiBH}_4$  were investigated first. The hydrogen desorption mechanisms of  $\text{LiBH}_4$  have been studied previously [135][170], but have not always been clearly elucidated. From the TG-DTA-MS results, similar DTA endothermic peaks to those reported in the literature by Züttel *et al.* [135], and Orimo *et al.* [170] were found:

- 1- The first endothermic effect accompanying a sharp peak at  $110^\circ\text{C}$  is consistent with the work by Züttel *et al.* [177] who determined this was due to polymorphic transformation of  $\text{LiBH}_4$ . This temperature-induced

structural transition has been known for years and is well documented in LiBH<sub>4</sub>-related hydrogen storage studies.

Indeed, Gomes *et al.* [178], Soulie *et al.* [179], Hagemann *et al.* [180] and some others reported a transition from a low-temperature orthorhombic structure to a high-temperature hexagonal structure of LiBH<sub>4</sub>. The nature of this order to disorder transition is still a subject for further study. To this effect, Callear *et al.* [181] suggested that it was not a simple order to disorder transition as the hexagonal phase shows some short range disorder identified well below the transition temperature. Instead, they have identified rotational motions of BH<sub>4</sub><sup>-</sup> units.

From the TG result, no mass loss has been registered, which indicates a relative good stability of not only the low temperature phase but also the disordered high temperature phase from which the disordering only involves some minor gas release. Indeed, the MS result shows a small level of hydrogen release, which is consistent with similar observations by Züttel *et al.* [135] of a small desorption of 0.3 wt % occurring around 110°C.

Our own understanding of what's happening during the phase transition could be as follows: the movement of the lattices involves the relaxation of the bonding on the surfaces liberating some hydrogen.

- 2- The second endothermic peak at approximately 280°C corresponds to the melting of LiBH<sub>4</sub>. It is consistent with all the data reported in the literature.

The melting of  $\text{LiBH}_4$  seems to trigger a destabilisation reaction inside the molten  $\text{LiBH}_4$  as up to 2 wt % was reported to be desorbed from 280°C until 380°C.

Martelli *et al.* [182] attempted to investigate the self-diffusion of  $\text{BH}_4^-$  in molten  $\text{LiBH}_4$ , which could give a clue onto why the main destabilisation occurs only after melting. They documented that the melting of  $\text{LiBH}_4$  around 280°C is characterised by translations of  $\text{BH}_4^-$  units as opposed to rotational motions observed during the structural transition around 100°C.

Züttel *et al.* [135] did report a mass loss starting around 320°C accompanied with a mass loss of up to 1 wt % to 400°C and the other studies all referred to Züttel's work for this particular step.

The MS result shows some hydrogen release, therefore, this step could be described as an intermediate stage involving liberation of hydrogen.

- 3- The third endothermic effect is linked to the main desorption event in  $\text{LiBH}_4$  upon heating to 600°C, with a major double DTA peak at around 450°C accompanied with a huge mass loss of up to 12 wt %. The onset starts at 380°C and by 450°C, total desorption has occurred.

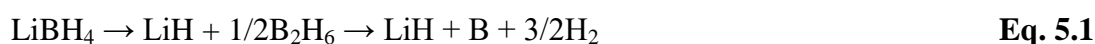
On the MS results, a huge surge of hydrogen has been observed between 380 and 450°C. These results match well with those by Züttel *et al.* [135] and Orimo *et al.* [170].

As the main desorption is concentrated at high temperatures, all the efforts have been devoted to lower the main desorption temperature.

Before clarifying the reaction path in comparison with the one proposed in the literature, a small observation about the purity of the gas stream liberated from as-received  $\text{LiBH}_4$  upon heating is essential.

From the experimental study undertaken, no other gas species have been detected. Is it the case with other studies reported? The possible other gas species could be diborane ( $\text{B}_2\text{H}_6$ ) and its derivatives. This gas is not only poisonous but detrimental to the system capacity as its liberation implies a loss of boron from the system. The presence of  $\text{B}_2\text{H}_6$  has not been mentioned in early studies except in a publication by Au *et al.* [136] in which trace amounts of  $\text{BH}_3$  released from the decomposition of commercial  $\text{LiBH}_4$  have been detected.

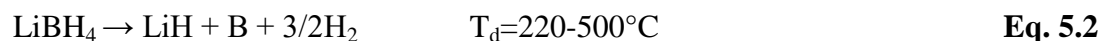
Nevertheless, Kostka *et al.* [183] investigated the composition of emitted gases during desorption of as-received  $\text{LiBH}_4$ . Some diborane has been detected under high vacuum conditions and the total liberation of diborane has been estimated to be 3 mol %, i.e. 2.3 wt % (according to reaction:  $\text{LiBH}_4 \rightarrow \text{LiH} + 1/2\text{B}_2\text{H}_6$ ) leading to this possible reaction path:



However, diborane emissions seem to be considerably suppressed at normal pressure conditions. Otherwise, the total mass loss would have been around 16.1 wt % taking into consideration 3 mol % (~2.3 wt %) of  $\text{B}_2\text{H}_6$ . As the TG results found

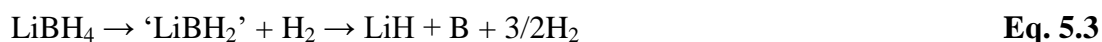


in the present study show a total mass loss of around 14.5 wt% at most, they are consistent with the decomposition of  $\text{LiBH}_4$  into  $\text{LiH} + \text{B} + 3/2\text{H}_2$ . All the reports agree on the overall decomposition of  $\text{LiBH}_4$  as described below:

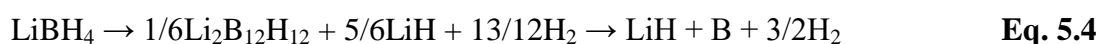


Could it be single step decomposition or are intermediate reactions involved? Indeed, there have been some divergences onto the intermediate reactions involved.

Early reports [135] suggest that  $\text{LiBH}_4$  may decompose via intermediate species “ $\text{LiBH}_2$ ”, without indicating the temperature range, according to the following overall path:



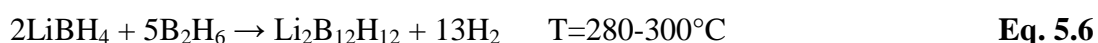
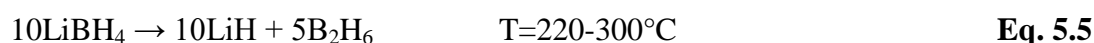
Kang *et al.* [184] reported the possibility of the intermediate to be ‘ $\text{LiBH}$ ’. Some computational work has been carried out by Ohba *et al.* [185] and both  $\text{LiBH}_2$  and  $\text{LiBH}$  have been ruled out in preference of  $\text{Li}_2\text{B}_{12}\text{H}_{12}$  according to the following overall path:



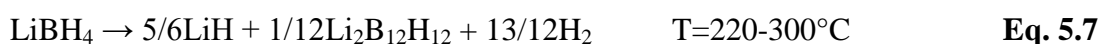
Experimental studies by Orimo *et al.* [170] confirm the intermediate as  $\text{Li}_2\text{B}_{12}\text{H}_{12}$ . This compound is stable and its structure has been elucidated recently by

XRD and by Her *et al.* [186].  $\text{Li}_2\text{B}_{12}\text{H}_{12}$  has a cubic crystal structure with Pa3 symmetry.

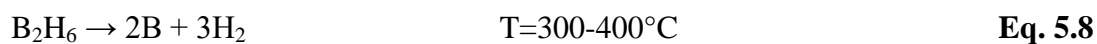
Recently, Friedrichs *et al.* [187] demonstrated that  $\text{Li}_2\text{B}_{12}\text{H}_{12}$  could be formed by the reaction of  $\text{LiBH}_4$  with liberated diborane,  $\text{B}_2\text{H}_6$ , in the temperature range below  $300^\circ\text{C}$  (as diborane is very unstable and starts to decompose to boron and hydrogen above  $300^\circ\text{C}$  [187]), according to the following reactions:



As these reactions (from Eqs. 5.5 and 5.6) are likely to be simultaneous,  $\text{B}_2\text{H}_6$  is probably a reaction intermediate. Thus, the overall process can be summed up into the following global reaction:



From our TG/MS results, some mass loss has been detected from  $220^\circ\text{C}$  confirming the possibility of this pathway (from Eq. 5.7) occurring. Also, as no gas is evolved at this temperature, it could mean that the gas might be a reactant in another reaction right after being liberated, and it correlates our previous hypothesis. Hydrogen is liberated from  $280^\circ\text{C}$  in small amounts, probably from the successive reaction of molten  $\text{LiBH}_4$  with  $\text{B}_2\text{H}_6$  (before it decomposes) and from the decomposition of residual  $\text{B}_2\text{H}_6$ .



However, if the conditions don't allow  $\text{B}_2\text{H}_6$  to react with  $\text{LiBH}_4$  to form  $\text{Li}_2\text{B}_{12}\text{H}_{12}$ ,  $\text{B}_2\text{H}_6$  would be liberated as it is formed in the low range temperature (below  $300^\circ\text{C}$ ) and this needs to be avoided as boron is lost for good.

Also, the intermediate  $\text{Li}_2\text{B}_{12}\text{H}_{12}$  is likely to be a very stable component and from our own observations, it does not decompose until  $400^\circ\text{C}$  when large quantities of hydrogen are evolved. In fact, Kim *et al.* [189] predicted that  $\text{Li}_2\text{B}_{12}\text{H}_{12}$  would decompose around  $680^\circ\text{C}$ , which appears to be too high and not in agreement with experimental results. The following reaction is likely to occur:



The aim of this very first study was to corroborate our results with the ones from the literature (computational and experimental results) as the study of pristine  $\text{LiBH}_4$  is a start point to all the other studies and it was important to successfully match the results for the thermal desorption from pure  $\text{LiBH}_4$  and propose a viable pathway for decomposition of as-received  $\text{LiBH}_4$  as summed up in the following figure.

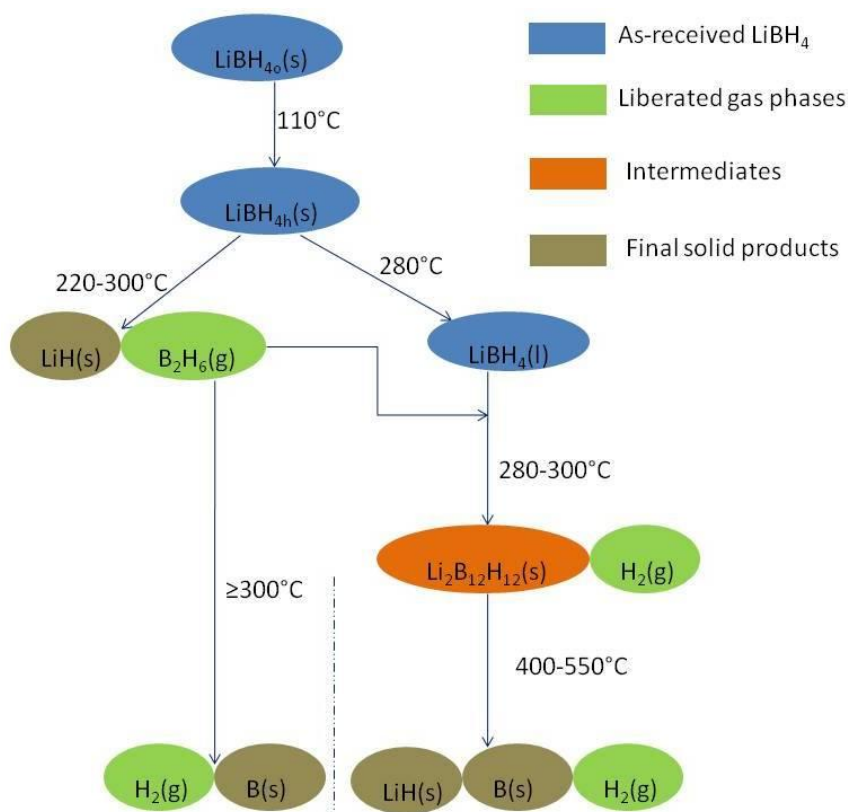


**Figure 5.1:** Possible decomposition paths of as-received  $\text{LiBH}_4$

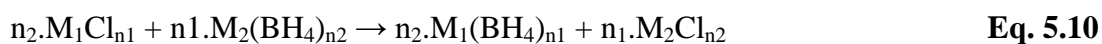
The study primordially shows the limitations of unmodified  $\text{LiBH}_4$  and the necessity to investigate modified  $\text{LiBH}_4$ . It also shows that as boron is a component of  $\text{LiBH}_4$ , it is likely to liberate borane compounds and this must be avoided by the formation of less stable intermediates capable of decomposing at moderate temperatures.

The research was then focused on strategies to lower the high hydrogen desorption temperature and bring it before melting (around  $280^\circ\text{C}$ ) in order to destabilise the ordered structure.

## 5.2 Dehydrogenation from ( $n\text{LiBH}_4 + \text{MCl}_n$ )

From the preliminary study on pure  $\text{LiBH}_4$ , it has been shown that  $\text{LiBH}_4$  is a very stable compound undergoing structural transition around  $110^\circ\text{C}$  and desorbing hydrogen in small amounts once in a molten state (above  $280^\circ\text{C}$ ) and in large amounts only **above  $420^\circ\text{C}$** . Also,  $\text{Li}_2\text{B}_{12}\text{H}_{12}$  and  $\text{B}_2\text{H}_6$  have been identified by previous studies as possible reaction intermediates but this carries the risks of unwanted diborane release and good stability of the intermediate  $\text{Li}_2\text{B}_{12}\text{H}_{12}$ .

So, the challenge would be to lower the decomposition temperature, i.e. to increase the reactivity of solid  $\text{LiBH}_4$ . One of the strategies would be to add additives which react instantaneously upon heating to liberate essentially hydrogen at moderate temperatures. The halides have been demonstrated [134][173] to be suitable additives for the destabilisation of  $\text{LiBH}_4$ . It has been widely shown in the literature [96], that an addition of chloride to an alkali metal borohydride, can lead to an ionic transfer between the metal ion  $M_1^{n1+}$  from the chloride  $M_1\text{Cl}_{n1}$  and the metal ion  $M_2^{n2+}$  from the borohydride  $M_2(\text{BH}_4)_{n2}$ , the so-called metathesis or exchange reaction.



Nakamori *et al.* [134] documented that  $M_1(\text{BH}_4)_{n1}$  with Pauling electronegativities ( $X_p(M_1)$ ) superior to 1.5 are thermodynamically unstable. Inspired by this finding, an approach of producing to form unstable borohydrides  $M_1(\text{BH}_4)_{n1}$

with M1=Zn, Ti, Cr or Ni. Nakamori *et al.* [134] gave the example of the effective destabilisation of  $\text{LiBH}_4$  through the addition of  $\text{ZnCl}_2$ .

Therefore, we selected chlorides of metals at fourth period (cf. Figure 4.6 p. x) in periodic table with electronegativities superiors to 1.5: Ti→ 1.54, Zn→1.65, Cr→1.66, and Ni→1.91. They are all part of the transition metals group except for Zn, which is classified as a post-transition metal [190].  $\text{ZnCl}_2$  and  $\text{TiCl}_3$  have been selected because they have been used previously to destabilise  $\text{LiBH}_4$ .  $\text{CrCl}_3$  and  $\text{NiCl}_2$  have been rarely mentioned as additives to  $\text{LiBH}_4$ . Therefore, our results are bringing a supplementary clue as to why Zn, which has a similar electronegativity value to that of Cr and Ti; and Ni which has an electronegativity value much higher than the other ones may contribute to the destabilisation of  $\text{LiBH}_4$ .

However, ‘transition metal’ cations are heavy and this is a main drawback as the overall hydrogen capacity do not exceed 5.5 wt %  $\text{H}_2$  (cf. Table 4.2 p. x).

### 5.2.1 Summary of results:

In this section, systematic investigation on  $\text{LiBH}_4$  milled with chlorides of fourth period metals:  $\text{ZnCl}_2$ ,  $\text{NiCl}_2$ ,  $\text{CrCl}_3$  and  $\text{TiCl}_3$  was reported, in order to identify the effect of milling and additives on the thermal desorption of  $\text{LiBH}_4$ . The FT-IR, SEM-EDS and XRD results reveal the possibility of the formation of new intermediate phase during mechanical milling of  $\text{LiBH}_4$  with the selected additives.

However, thermal analysis showed that milling time durations of more than 5 minutes possibly had a detrimental effect on the thermal desorption of the different complex mixtures including for  $\text{ZnCl}_2$ -added mixtures, with an increasing mass loss probably linked to the liberation of diborane.

Thus, all the results presented in the thesis were for mixtures submitted to a milling of 5 minutes only. The thermal analysis combined with gas analysis suggested that only hydrogen was released from all the mixtures, thus unexpected high registered mass losses of up to 15 wt % compared to the theoretical hydrogen contents of up to about 6 wt %. The mass spectrometer has a sensitivity which may not allow detecting very small amounts of diborane ( $\text{B}_2\text{H}_6$ ). In this instance, the best sample is  $\text{CrCl}_3$ -added  $\text{LiBH}_4$  even though it is far from being the sample with the minimum onset desorption temperature.

In terms of thermal events, they all presented the  $\text{LiBH}_4$  phase transformation peak around  $110^\circ\text{C}$  preceded or followed by a series of endothermic and/or exothermic desorption peaks but for the mixtures, the main desorption occurred below  $280^\circ\text{C}$  ( $\text{LiBH}_4$  melting point) as opposed to pure  $\text{LiBH}_4$  which starts decomposing substantially well after its melting point around  $380^\circ\text{C}$ . The onset desorption temperature may be linked to the difference in electronegativities. Indeed, when atoms with different electronegativities react to form molecules, the electrons are not shared equally. This difference could be expressed in the percent ionic character, a notion introduced by Pauling in 1960 [176]. The percent ionic character can be described as: the capability for 2 atoms to attract bonding electrons and form either ionic or covalent bonds. It has an empirical formula as follows:

$$\% \text{ ionic character} = 100 * (1 - e^{-0.25 * (X_a - X_b)^2}) \quad \text{Eq. 5.11}$$

where  $X_a$  and  $X_b$  are the higher and lower electronegativities respectively.

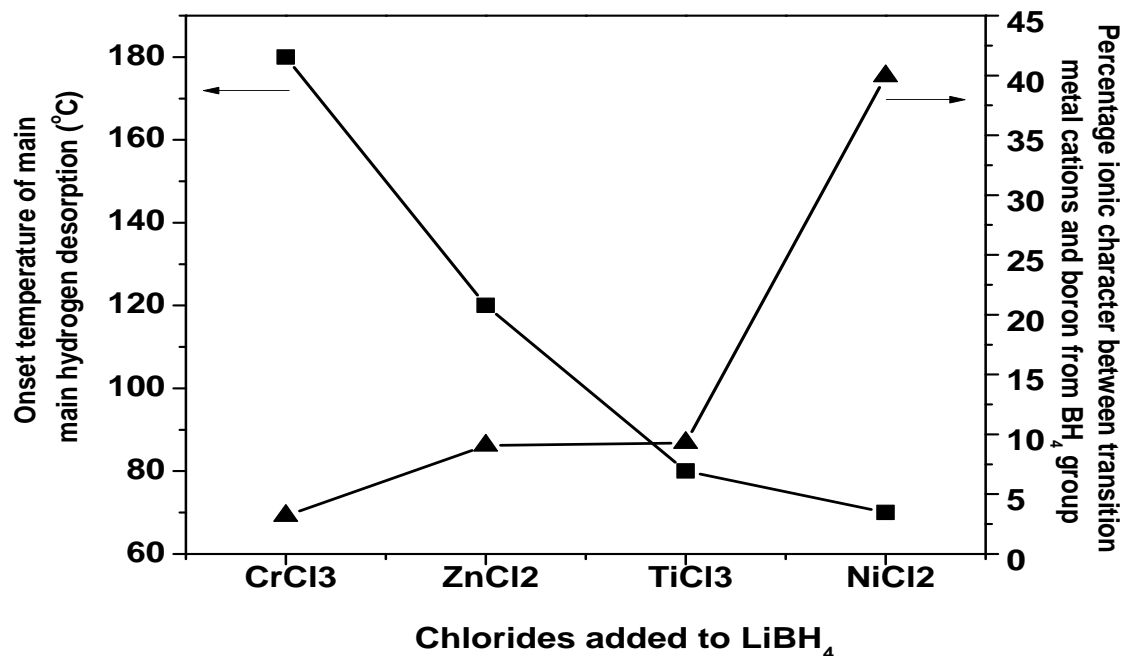


**Figure 5.2:** Percent ionic character between metal cation and boron from BH<sub>4</sub> group as a function of the onset desorption temperature

Thus, a plot of the temperature of the onset hydrogen desorption peak as a function of the percentage ionic character between the metal in chlorides (M) and the boron present in the tetrahydroborate group B has been drawn. It was found that the highest the ionic character is, the lower is the onset desorption temperature. To be more specific, the better the attraction between the electrons of the metal cation and the boron from the tetrahydroborate group in LiBH<sub>4</sub>, the lower will the onset desorption temperature.

In summary, the figures show that the thermal evolution of mixtures of LiBH<sub>4</sub> and chlorides of fourth period metals occurred in 3 stages between room temperature and 280°C with a total mass loss of up to 15 wt %. The range of mass losses should



have been between 4.5 and 5.5 wt % for a sole hydrogen release, however, no other gas species has been detected in the gas stream, pointing the MS equipment's sensitivity. The right range of mass loss is only achieved with the  $\text{CrCl}_3$ -added mixture, which has also the highest onset desorption temperature.

However, for all the mixtures, the main desorption (endothermic for  $\text{ZnCl}_2$ -added mixture and exothermic for the other transition metal added mixtures) is observed between 120°C and 250°C, which is a huge improvement compared to pure  $\text{LiBH}_4$ .

The DTA-MS results of all the chlorides-added mixtures show several decomposition steps except for  $\text{ZnCl}_2$ , which is a single step process. Also, there still is the phase change DTA peak at 110°C (as described in the previous sub-section 5.1) demonstrating the presence of pure  $\text{LiBH}_4$  partially or totally in the mixtures upon heating to 110°C. However, the characteristic melting point of  $\text{LiBH}_4$  (as described in the previous sub-section 5.1) is not detected for any of the mixtures, which indicates that  $\text{LiBH}_4$  is not present around 280°C. Therefore, the destabilisation is effective and happens mainly between 110°C and 280°C as follows.

Our own observations strongly suggest that  $\text{LiBH}_4$  is successfully destabilised by the addition of chlorides of Zn, Ti, Ni and Cr. The main issue which is not sufficiently stressed in earlier reports is the purity of the liberated gas stream taking into account the hydrogen capacity not exceeding 6 wt %.

### 5.2.2 Comparative discussion:

Indeed, for all the chloride additions, thermal analysis coupled with Mass Spectrometry (MS) (See Figure 4.14 p. x) was used to characterise the products formed during decomposition. Various chloride additives have been considered to modify  $\text{LiBH}_4$  and reduce the desorption temperature such as  $\text{TiCl}_3$  and  $\text{ZnCl}_2$ . It has been shown by Au *et al.* [191] that  $\text{TiCl}_3$  can effectively lower the  $\text{H}_2$  desorption temperature to the range of 80~120°C.

Also, Nakamori *et al.* [134] successfully demonstrated that  $\text{ZnCl}_2$  addition to  $\text{LiBH}_4$  enhances the hydrogen desorption. The role of these additives on the dehydrogenation mechanism of  $\text{LiBH}_4$  remains unclear, though they are believed to be involved in the formation of less stable borohydrides as described previously in the section.

#### 5.2.2.1 For $\text{ZnCl}_2$ addition:

The IR spectroscopy of  $\text{ZnCl}_2$ -added mixtures after milling (see Figure 4.7) allows us to follow the reaction involved since the B-H wavenumbers are characteristic for covalent and ionic borohydrides as described in an article by Mal'tseva *et al.* [205]:

- $\nu_{\text{B-H}} = 1100 \text{ cm}^{-1}$  for the  $\text{BH}_4^-$  anion
- $\nu_{\text{B-Hb}} = 2050\text{-}2150 \text{ cm}^{-1}$  for  $\text{Zn}(\text{BH}_4)_2$ ?
- $\nu_{\text{B-Ht}} = 2400\text{-}2460 \text{ cm}^{-1}$  for  $\text{Zn}(\text{BH}_4)_2$ ?

Also, the addition of  $\text{ZnCl}_2$  seems to affect the bonding in only a small proportion of  $\text{ZnCl}_2$  and  $\text{LiBH}_4$  since a new wavelength identified to be an absorption band of  $\text{ZnH}_2$ , is detected around  $1400\text{ cm}^{-1}$  and yet, the characteristic bands of  $\text{LiBH}_4$  ( $1100\text{ cm}^{-1}$  and  $2300\text{ cm}^{-1}$ ) and  $\text{ZnCl}_2$  ( $900\text{ cm}^{-1}$  and  $3600\text{ cm}^{-1}$ ) are at similar positions to those from the literature (see Jeon *et al.* [192]).

In summary, the presence of bands characteristic of bridging ( $2050\text{-}2150\text{ cm}^{-1}$ ) and terminal ( $2400\text{-}2460\text{ cm}^{-1}$ ) B-H stretching bonds in the range  $2000\text{-}2500\text{ cm}^{-1}$  in the IR spectrum of the product indicates the formation of a covalent hydroborate as described by Mikheeva *et al.* [204] along with an intermediate compound “ $\text{ZnH}_2$ ”.

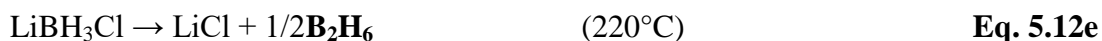
In other words,  $\text{LiBH}_4$  and  $\text{ZnCl}_2$  do interact chemically during mechanical milling but to a small extent, maybe due to the short period of milling: 1 and 5 minutes. Indeed, studies by Mal'tseva *et al.* [205] have shown that after mechanical activation only (without any heating being applied) of much longer times (1.5 and 5 hours),  $\text{ZnCl}_2$  reacts with  $\text{LiBH}_4$  to form zinc tetrahydroborate or its complexes with  $\text{LiBH}_4$ . They also demonstrated that when the milling time is increased, the reaction is more complete.

In addition, from the TG-DTA-MS data, the mass loss of up to 15 wt % between  $100^\circ\text{C}$  and  $120^\circ\text{C}$  could only be due to the release of hydrogen alongside other gas species as the maximum hydrogen content is not supposed to exceed 4.5 wt %. However, the release of diborane alongside hydrogen from  $100^\circ\text{C}$  is not observed on the MS curve. This contradicts observations by Srinivasan *et al.* [109], Jeon *et al.* [192] and D.A. Lesh *et al.* [193] in which, at the temperature range  $85\text{-}$

140°C, B<sub>2</sub>H<sub>6</sub> evolves from a mixture of Zn(BH<sub>4</sub>)<sub>2</sub> (+ NaCl) obtained after milling ZnCl<sub>2</sub> and NaBH<sub>4</sub>. It is to be noted that, for all these accounts, ZnCl<sub>2</sub> has been milled with NaBH<sub>4</sub> and not LiBH<sub>4</sub>, which may explain the discrepancies between the previous results reported in the literature and our own results.

In terms of desorption temperature, our report is consistent with earlier reports on desorption of (2LiBH<sub>4</sub> + ZnCl<sub>2</sub>), namely by Nakamori *et al.* [134]. But, the amount of hydrogen released has never been documented but only indication of the peak desorption temperature which is reported to be around 145°C is given. The peak desorption temperature recorded on our own results show a maximum peak temperature of 120°C, which is 20°C lower than the one reported by Nakamori *et al.* [134].

The following pathway could be anticipated:



#### 5.2.2.2 For TiCl<sub>3</sub> addition:

EDS elemental analysis and SEM images (see Figure 4.8 and Figure 4.9 p. x-x) show that there is high probability of a new phase ‘LiCl’ and an intermediate

' $\text{Ti}_x\text{B}_y\text{Cl}_z$ ' generated during the milling of  $\text{LiBH}_4$  with  $\text{TiCl}_3$  for time duration as small as 5 minutes. This confirms the high reactivity of the mixture ( $\text{TiCl}_3 + 3\text{LiBH}_4$ ). Indeed, Volkov *et al.* [206] confirms this assumption with experiments carried out on mixtures of  $\text{TiCl}_3$  and  $\text{LiBH}_4$  in the absence of solvents and submitted to mechanical activation at room temperature. The best yield has been found to be up to around 75 % for a milling of up to 2h.

Also, the porous morphology suggests that there is a possible liberation of a gas phase during mechanical milling.

TG-DTA-MS results in Fig. 4.16 p. x show an endothermic event occurring around  $60^\circ\text{C}$  well before the structural change and liberating 4.5 wt %. Moosegard *et al.* [194] reported that upon addition of  $\text{TiCl}_3$  of up to 15 mol %:

- between room temperature and  $50^\circ\text{C}$ ,  $\text{LiCl}$  is formed ;
- between  $50^\circ\text{C}$  and  $110^\circ\text{C}$ , the signal of  $\text{LiCl}$  has increased ;
- and above  $110^\circ\text{C}$ , the signal of  $\text{LiCl}$  is declining indicating that solid  $\text{LiCl}$  formed below  $110^\circ\text{C}$  may be dissolved in the structure of HT  $\text{LiBH}_4$  [195].

HT  $\text{LiBH}_4$  is known to be highly unstable which may explain why HT  $\text{LiBH}_4$  might have increased structural flexibility and reactivity. The low temperature release of hydrogen may also be due to the decomposition of  $\text{Ti}(\text{BH}_4)_3$  possibly formed along with  $\text{LiCl}$  [196]. The decomposition temperature of a possible intermediate  $\text{Ti}(\text{BH}_4)_3$  has been reported by Hoekstra *et al.* [197] to be at around  $25^\circ\text{C}$ .

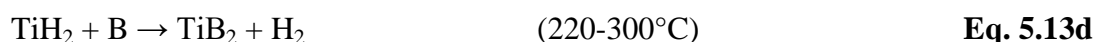
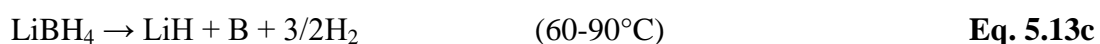
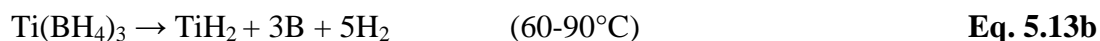
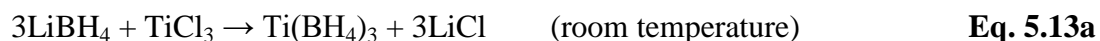
The results also showed that the component of the desorbed gas is confirmed to be only hydrogen within the accuracy of the MS apparatus. This is consistent with

the mass losses recorded on the TG spectrum until after LiBH<sub>4</sub> phase change around 130°C. Above this characteristic temperature of 130°C up until 300°C, there is a further mass loss of 2.5 wt %, making up the total mass loss to 8 wt %, well above the overall hydrogen capacity of the mixture. This suggests the presence of other gas species. In fact, no diborane has been detected but this does not rule out the formation of trace amounts of B<sub>2</sub>H<sub>6</sub> due to the limit of instrument sensitivity.

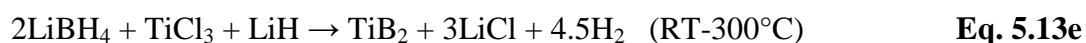
Indeed, Au *et al.* [191] demonstrated that an increasing proportion of TiCl<sub>3</sub> make LiBH<sub>4</sub> less stable even near room temperature but there is an unrecoverable loss of boron due to diborane emission. They also showed that TiCl<sub>3</sub>-added LiBH<sub>4</sub> desorbed between 6 and 9 wt % from 100°C.

More, there is an exothermic release of hydrogen above 220°C which could be linked to the exothermic formation of borides reported in the literature [198]-[199] .

From all our own observations and literature reports, the following reaction path could be anticipated:



From Eq. 5.12b, 5.12c and 5.12d,



This global reaction (in **Eq. 5.13e**) has been recently detailed in a publication by Kim *et al.* [199] as a room temperature process activated by mechanical milling in order to form nanoboride of Ti.

#### 5.2.2.3 For $\text{NiCl}_2$ addition:

According to the SEM image in Figure 4.11 p. x, the mixture ( $\text{NiCl}_2 + 2\text{LiBH}_4$ ) milled for 5 minutes showed a flaky morphology with embedded grains, very distinct from the physical agglomerates observed in pure  $\text{LiBH}_4$  suggesting a possible high reactivity between the starting materials and the presence of 2 distinct phases. The complementary EDS elemental analysis demonstrated the formation of an intermediate with elements Ni, B and Cl detected on the same measurement.

The TG-DTA-MS profile is very similar to that of complex mixtures ( $\text{TiCl}_3 + 3\text{LiBH}_4$ ) and ( $\text{CrCl}_3 + 3\text{LiBH}_4$ ) as seen in Figure 4.14 p. x, but the main difference is the occurrence of the exothermic event at  $150^\circ\text{C}$  (lower than  $220^\circ\text{C}$  for  $\text{TiCl}_3$  and  $180^\circ\text{C}$  for  $\text{CrCl}_3$ , see Figure 5.1 below). The exothermic character of the thermal events has been widely associated [198]-[199], [202] with the formation of borides accompanied by hydrogen liberation. Kuznetsov *et al.* [202] even indicated the presence of another gas, hydrogen chloride but since no MS measurements have been presented to clarify this observation, doubt can be raised.

Only,  $\text{ZnCl}_2$ -added  $\text{LiBH}_4$  did not present exothermic thermal events in the temperature range from RT to  $300^\circ\text{C}$ . This is consistent with the formation of Zn as an overall reaction product. Au *et al.* [136] even mentioned that lithium

borohydrides modified by halides containing metals that cannot form metal borides with boron are likely to evolve diborane during dehydriding, which is the case for the  $\text{ZnCl}_2$ -added  $\text{LiBH}_4$  sample.

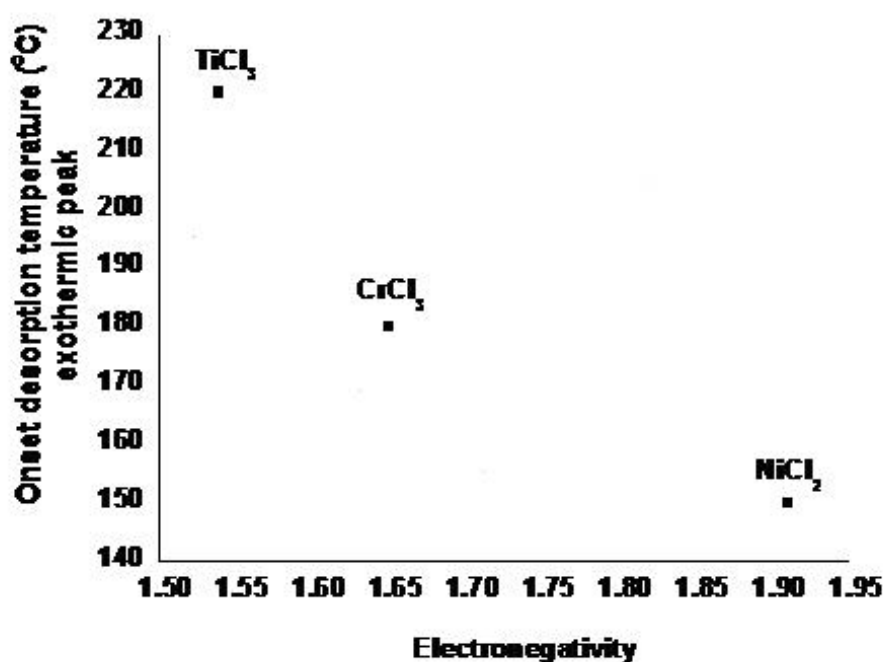


**Figure 5.3:** Influence of the electronegativity on the hydrogen liberation temperature during the formation of borides of transition metals

The higher is the electronegativity of the transition metal cation, the lower is the hydrogen liberation temperature. The exothermic character of the liberation of hydrogen in  $\text{NiCl}_2$ -added  $\text{LiBH}_4$  has also been discussed by Zhang *et al.* [200] and they found 3 exothermic peaks at  $210^\circ\text{C}$ ,  $238^\circ\text{C}$  and  $285^\circ\text{C}$  as opposed to only one exothermic peak found at  $150^\circ\text{C}$ , at a much lower temperature. They also identified the main product as  $\text{Ni}_4\text{B}_3$  with hydrogen being the only gas phase detected.

The evolution of hydrogen has been well demonstrated long ago in a publication by Brown *et al.* [201] where a sufficient amount of hydrogen has been reported to be released from the addition of nickel chloride to sodium borohydride.



Similarly, our results show hydrogen to be the only gas desorbed. However, it is not consistent with the mass loss of around 7 wt % up to 300°C. There probably is the liberation of diborane at some stage as indicated in a publication by Kotska *et al.* [183] in which they measured the relative concentration of diborane compared to hydrogen. In the temperature ranging from RT to 300°C, they demonstrated that the relative diborane concentration amounted to up to 7 mol % at temperatures around 170°C, at a much lower temperature than the hydrogen peak temperature, 260°C. The temperature of 170°C found in this publication coincides with the one found with our own results and would back up the possible simultaneous release of hydrogen and diborane, however, with dominant hydrogen signals.

Kuznetsov *et al.* [202] identified the intermediate boride to be Ni<sub>3</sub>B. In fact, the stable phases of binary compounds (Ni-B) are: NiB, Ni<sub>2</sub>B, Ni<sub>3</sub>B and Ni<sub>4</sub>B<sub>3</sub>. The product could be a mixture of all these compounds.

The main highlight of the TG-DTA-MS profile is the endothermic event around **70°C** accompanied with a mass loss of **2 wt %** and liberation of **hydrogen**.

Accordingly, the following path could be anticipated:



Here, reaction in Eq. 5.13c seems to be the main desorption event.

#### 5.2.2.4 For $\text{CrCl}_3$ addition:

According to the SEM image in Figure 4.8 and Figure 4.9 pp. x-x, the reactivity of mixture ( $\text{CrCl}_3 + 3\text{LiBH}_4$ ) milled for 5 minutes, is not evident as the morphology is quite similar to that of pure  $\text{LiBH}_4$  with physical agglomerates.

Data from XRD (as shown in Figure 4.12 p. xxx) seem to indicate the presence of an intermediate compound identified to be:  $\text{Li}_5\text{CrCl}_8$  gradually replacing  $\text{LiBH}_4$  in the mixture when the milling time is increased from 5 minutes to 15 minutes.

Indeed, Volkov *et al.* [203] indicated that when an extensive mechanical milling is applied at room temperature, it favours reactions which give thermodynamically unstable product such as  $\text{B}_2\text{H}_6$ . Also, they identified an intermediate compound to be  $\text{Na}_3\text{CrCl}_6$  when heating is applied.

As for the TG-DTA-MS profile, it is very similar to that of the mixture ( $\text{TiCl}_3 + 3\text{LiBH}_4$ ). The main difference resides in the first event observed around  $60^\circ\text{C}$  which is nearly inexistent with a small release of hydrogen. Also, hydrogen seems to be the only gas desorbed and it is consistent with the mass loss of around 5.5 wt % up to  $300^\circ\text{C}$ . This constitutes the only mass loss registered by TG which is consistent with a sole release of hydrogen. In the same view, Volkov *et al.* [203] also determined that after little or no mechanical activation, the only gas desorbed after heating a mixture of  $\text{LiBH}_4$  and  $\text{CrCl}_3$  is hydrogen in contrast with extensive

milling time of up to 280 minutes which can lead to a yield of diborane of up to 60 %.

We can argue that this could be due to the fact that the borohydride of Cr supposed to be formed is stable and only liberates hydrogen at higher temperatures than room temperature (RT).

The main highlight of the TG-DTA-MS profile is the double exothermic event more emphasized than for  $(\text{TiCl}_3 + 3\text{LiBH}_4)$  and occurring at a lower temperature i.e. from 180°C probably due to the formation of borides.

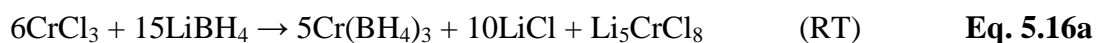
Reports on the addition of  $\text{CrCl}_3$  to any alkaline borohydride have been scarce in the literature except for the publication by Volkov *et al.* [203]. Actually, they also presented some thermodynamic estimation of the probability of competing reactions, by supplying thermodynamic functions based on published data. Here is a summary of the results:

**Table 5.1:** Calculated thermodynamic functions for the different probable reactions between  $\text{LiBH}_4$  and  $\text{CrCl}_3$ , taken from Volkov *et al.* [203]

Reaction	$-\Delta H^\circ_{298}$ (kJ.mol <sup>-1</sup> )	$-\Delta G^\circ_{298}$ (kJ.mol <sup>-1</sup> )
$6\text{LiBH}_4 + 2\text{CrCl}_3 = 6\text{LiCl} + 3\text{B}_2\text{H}_6 + 3\text{H}_2 + 2\text{Cr}$ <b>Eq. 5.15a</b>	84.9	321.3
$3\text{LiBH}_4 + \text{CrCl}_3 = 3\text{LiCl} + \text{CrB}_2 + \text{B} + 6\text{H}_2$ <b>Eq. 5.15b</b>	215.0	410.5
$3\text{LiBH}_4 + \text{CrCl}_3 = 3\text{LiCl} + 6\text{H}_2 + 3\text{B} + \text{Cr}$ <b>Eq. 5.15c</b>	89.5	283.8

The calculated values of  $\Delta G^\circ_{298}$  show that the reaction (in Eq. 5.15a) taking place on mechanical activation with the formation of  $B_2H_6$  are thermodynamically less probable than the reaction (in Eq. 5.15b) accompanied by the formation of  $CrB_2$ , and slightly more probable than the reaction (in Eq. 5.15c) accompanied by the formation of hydrogen, elemental chromium and boron.

From our own results and the thermodynamic calculations extracted from the literature, the following path could be anticipated as follows:



#### 5.2.2.5 *Summary of comparative discussions for chloride additions to $LiBH_4$ :*

In the previous sections 5.2.2.1 to 5.2.2.4, the decomposition of  $LiBH_4$  milled with chloride additives  $TiCl_3$ ,  $ZnCl_2$ ,  $NiCl_2$  and  $CrCl_3$  were comparatively discussed, in order to identify the effect of milling and additives on the thermal desorption of  $LiBH_4$ .

XRD and IR results firmly confirmed that mechanical milling may induce the exchange reaction between Li and the other metal cations. It has been confirmed by exclusive studies on the effect of milling at extended times realised by russian studies [202]-[206].

The investigations on the desorptions of  $(n\text{LiBH}_4 + \text{MCl}_n)$  showed that the decomposition of  $\text{LiBH}_4$  mainly generated  $\text{H}_2$  which was released at different temperatures, depending on the nature of the chloride added: from as little as  $60^\circ\text{C}$  for  $\text{TiCl}_3$  addition up to  $170^\circ\text{C}$  for  $\text{CrCl}_3$  addition. Overall, the main  $\text{H}_2$  desorption temperature of all the mixtures were all below the melting point of  $\text{LiBH}_4$ , ie. below  $280^\circ\text{C}$  but the above-described thermal analyses of the mixtures of  $\text{LiBH}_4$  and fourth-period metal chlorides ( $\text{M}=\text{Zn}, \text{Ti}, \text{Ni}, \text{Cr}$ ) strongly indicates a multi-step and rather complex dehydriding process.

Nevertheless, it generated  $\text{B}_2\text{H}_6$  which can further decompose into  $\text{B}$  and  $\text{H}_2$  at elevated temperature.  $\text{B}_2\text{H}_6$  release is even thought [203] to be favoured by the application of an extended milling. Also, the difference between the expected hydrogen release and the amount of gas desorbed strongly indicates that other gas species are released alongside hydrogen except for  $\text{CrCl}_3$ -added  $\text{LiBH}_4$  which has similar figures for both parameters. Non-uniform mixing can lead to the escape of  $\text{B}_2\text{H}_6$  from the mixtures but our evidence further support the notion that most of  $\text{B}_2\text{H}_6$  supposedly released is acting as a transient gas in the thermal desorption of  $(n\text{LiBH}_4 + \text{MCl}_n)$ . This transient gas is likely to decompose further into  $\text{B}$  and  $\text{H}_2$ .

The discrepancies between the amount of gas desorbed and the expected amount of hydrogen content observed in all but  $\text{CrCl}_3$ -added mixtures make sense in that view.

For all these reactions, adding  $\text{LiCl}$  could be interested to avoid an increase of temperature during mechanical milling and subsequent reactions involving hydrogen liberation inside the milling pot.

Although  $\text{NiCl}_2$ ,  $\text{TiCl}_3$ ,  $\text{CrCl}_3$  and  $\text{ZnCl}_2$  showed resemblance in destabilising  $\text{LiBH}_4$ , they also revealed differences in some aspects, especially on the issue of diborane formation. The results demonstrate further that in the search for the perfect  $\text{LiBH}_4$ -based system that could deliver hydrogen at low temperature, there has to be some sort of compromise between desorption temperature and the purity of hydrogen delivery. So much so, when the 4 additives are compared,  $\text{CrCl}_3$  seems to be the ideal one even though it starts delivering hydrogen at the highest temperature, which is  $170^\circ\text{C}$ .

It is a new approach in the assessment of ideal systems, as up to now, only the main desorption temperature was evaluated without taking into account the delivery of other by-products such as  $\text{B}_2\text{H}_6$ . It is wrong to do so because even minimal, the release of diborane should be completely avoided. In this view, the relationship between the desorption temperature and the electronegativity of the cation additive stressed out by Nakamori *et al.* [134] may not be so accurate as it should integrate a third parameter which is the presence of  $\text{B}_2\text{H}_6$ .

Finally, from our results alone, it is not easy to judge if all the reactions involved are complete as post-heated measurements are almost impossible to achieve but it gives a good indication of the tendency to form borides or hydrides in the process of liberating the hydrogen. Indeed, the formation of borides is often accompanied with an exothermic effect whereas the formation of hydrides is accompanied with an endothermic effect.

### 5.3 Dehydrogenation from ( $\text{LiBH}_4 + x\text{NH}_4\text{Cl}$ ) and from ( $\text{NH}_3\text{BH}_3 + y\text{NH}_4\text{Cl}$ )

In the search for more interesting materials, amine-boranes (boron-nitrogen-hydrogen compounds) have been investigated.

Indeed, thermal decomposition characteristics of  $\text{LiBH}_4$  ball-milled with various ratios of  $\text{NH}_4\text{Cl}$  have been compared.  $\text{LiBH}_4/\text{NH}_4\text{Cl}$  mixtures showed an improved dehydrogenation process with the onset of hydrogen desorption starting at temperatures as low as  $65^\circ\text{C}$  when compared to that of pure  $\text{LiBH}_4$  and even to  $\text{MCl}_n$ -added  $\text{LiBH}_4$ .

#### 5.3.1 Summary of results:

In the previous sections, the decomposition of  $\text{LiBH}_4$  and  $\text{LiBH}_4$  milled with additives  $\text{TiCl}_3$ ,  $\text{ZnCl}_2$ ,  $\text{NiCl}_2$  and  $\text{CrCl}_3$  was reported in order to identify the effect of milling and additives on the thermal desorption and structure of  $\text{LiBH}_4$ . We successfully showed that a destabilisation through the addition of halides is possible but again, attention must be driven to the purity of the gas being released.

With the combined results from XRD and SEM-EDS after the first step (above  $60^\circ\text{C}$ ), it proves that the first reaction involves the formation of  $\text{LiCl}$  and the absence of  $\text{NH}_4\text{Cl}$  which assumes that the assumed product could be  $\text{NH}_3\text{BH}_3$ . Thus, there is

still room for improvement for the first and second steps and it is crucial to understand the different events occurring during these stages.

The TG results all show a bigger mass loss comparatively to pure  $\text{LiBH}_4$  in the temperature range from room temperature to  $225^\circ\text{C}$ . In terms of mass losses, on the range going from room temperature to  $225^\circ\text{C}$ , the total mass losses range from 7.5 up to 24 wt %, which is quite far from the range expected to be if only hydrogen was liberated, i.e., between 8 and 11 wt %. The first observation shows that only ( $\text{LiBH}_4\text{:NH}_4\text{Cl}=1\text{:}3$ ) mixtures achieve this range of mass losses, i.e., between 7.5 and 11.5 wt %. The MS results show that  $\text{H}_2$  is the main desorbed gas along with ammonia diborane ( $\text{NH}_2\text{B}_2\text{H}_5$ ) as the other gas species are observed in the low to very low range (ratio 1:1000). It may be worth noting that ammonia diborane is a compound with a low boiling point ( $76.7^\circ\text{C}$ ) which may explain why it is consistently released at the same time as hydrogen.

All the figures presented in the results chapter have been conveniently summarised into the following 3 tables as to identifying the major events. In fact, the three tables correspond to the 3-step decomposition pathway believed to be associated. Finally, mass losses have also been reported in the tables.

The figures highlighted in bold black represents the most interesting and promising results in terms of the purity of the gas stream. This feature is expected to be the main drawback in the study of the ( $\text{LiBH}_4\text{:NH}_4\text{Cl}$ ) systems. PAB-PIB and borazine are heavy molecular species and their presence must be avoided. The data



corresponding to the pure materials  $\text{LiBH}_4$  and  $\text{NH}_4\text{Cl}$  have been reported for comparison purposes.

#### 5.3.1.1 $\text{LiBH}_4$ -based systems

**Step 1:** All the mixtures show an “immediate” release of gas upon heating for temperatures as low as  $40^\circ\text{C}$  (onset desorption).

Table 5.2 summarises the results and highlights the samples with “sole release” of hydrogen.

For all the mixtures, it was found that there was one major thermal event between  $30$  and  $80^\circ\text{C}$  with a peak temperature at  $65$ - $70^\circ\text{C}$  corresponding to a mass loss of up to  $6.3$  wt % during the desorption but these results also show that the big mass losses are not directly related to the sole release of hydrogen but also to the release of undesirable gas species except for the ( $\text{LiBH}_4\text{:NH}_4\text{Cl}=1\text{:}1$ ) sample milled for 1 minute with a maximum mass loss of  $2.2$  wt % around  $50^\circ\text{C}$  and the ( $\text{LiBH}_4\text{:NH}_4\text{Cl}=1\text{:}1$ ) sample milled for 10 minutes and the ( $\text{LiBH}_4\text{:NH}_4\text{Cl}=1\text{:}3$ ) sample milled for 5 minutes with a maximum mass loss of  $1.4$  wt % and  $0.9$  wt % respectively around  $65^\circ\text{C}$ .

**Table 5.2:** Summary of TG and MS results – Step 1 – 30-80°C (peaks at 50 and/or 70°C)

<b>NH<sub>4</sub>Cl/LiBH<sub>4</sub> molar ratio</b>	<b>Milling time (minutes)</b>	<b>Mass loss (wt %)</b>	<b>Gaseous products MS Low range (10<sup>-12</sup> order)</b>	<b>Gaseous products MS High range (10<sup>-9</sup> order)</b>
Pure LiBH <sub>4</sub>	0	-0	-	-
Pure NH <sub>4</sub> Cl	0	-0	-	-
<hr/>				
1	1	<b>-2.2 (*)</b>	-	<b>H<sub>2</sub></b>
		-2	PAB-PIB, BZ	H <sub>2</sub> , ADB
1	5	-3.2	A <sub>2</sub> B <sub>2</sub>	H <sub>2</sub> , ADB
1	10	<b>-1.4</b>	-	<b>H<sub>2</sub></b>
<hr/>				
2	1	-6.3	A <sub>2</sub> B <sub>2</sub> , PAB-PIB, BZ	H <sub>2</sub> , ADB
2	5	-0.9	-	H <sub>2</sub> , ADB
2	10	-2.1	-	H <sub>2</sub> , ADB
<hr/>				
3	1	-1.5	-	H <sub>2</sub> , ADB
3	5	<b>-0.9</b>	-	<b>H<sub>2</sub></b>
3	10	-0.2	-	H <sub>2</sub> , ADB

(\*) : first of 2 subsequent mass losses occurring at 50°C

**Step 2:** All the mixtures show a second step spreading from 80°C to 140°C characterised by one exothermic effect peaked around 95°C.

Also, the second step is characterised by a second peak of hydrogen which is broader than the one observed during step 1 and which is taking over the first peak as the milling time is increased.

**Table 5.3:** Summary of TG and MS results – Step 2 – 80-140°C (peak at 95°C)

<b>NH<sub>4</sub>Cl/LiBH<sub>4</sub> molar ratio</b>	<b>Milling time (minutes)</b>	<b>Mass loss (wt %)</b>	<b>Gaseous products MS Low range (10<sup>-12</sup> order)</b>	<b>Gaseous products MS High range (10<sup>-9</sup> order)</b>
Pure LiBH <sub>4</sub>	0	-0.5	-	H <sub>2</sub>
Pure NH <sub>4</sub> Cl	0	-	-	-
-----	-----	-----	-----	-----
1	<b>1</b>	-4.6	A <sub>2</sub> B <sub>2</sub> , PAB-PIB, BZ	H <sub>2</sub>
1	5	<b>-5</b>	<b>A<sub>2</sub>B<sub>2</sub></b>	<b>H<sub>2</sub></b>
1	<b>10</b>	-4.3	A <sub>2</sub> B <sub>2</sub>	H <sub>2</sub> , ADB
-----	-----	-----	-----	-----
2	1	<b>-1.7</b>	<b>A<sub>2</sub>B<sub>2</sub></b>	<b>H<sub>2</sub></b>
2	5	-2.8	A <sub>2</sub> B <sub>2</sub>	H <sub>2</sub> , ADB
2	10	-2.2	A <sub>2</sub> B <sub>2</sub>	H <sub>2</sub> , ADB
-----	-----	-----	-----	-----
3	1	<b>-1.4</b>	<b>A<sub>2</sub>B<sub>2</sub></b>	<b>H<sub>2</sub></b>
3	5	-2.3	-	H <sub>2</sub> , ADB
3	10	-0.9	-	H <sub>2</sub> , ADB

During the second step, the mass loss is inversely related to the amount of added NH<sub>4</sub>Cl (please refer to Figure 4.42) and accompanied with a drop in the release of amine-borane species clearly indicating that the huge mass loss observed for 1:1 mole ratio sample milled for 1 minute is mainly due to the simultaneous release of by-species, especially the heavy species PAB-PIB and borazine.

As the milling time increased, NH<sub>2</sub>B<sub>2</sub>H<sub>5</sub> is detected in the gas stream whereas PAB-PIB is not any more. Thus, the almost sole release of hydrogen in the temperature ranging from 80°C to 140°C is observed for 1:1 mole ratio samples

milled for 5 minutes, 1:2 mole ratio milled for 1 minute and 1:3 mole ratio milled for 1 minute.

This shows that when  $\text{NH}_4\text{Cl}$  is added in excess into the mixture, it may mop up or react with the amine-boranes released during the dehydrogenation of mixtures of  $\text{LiBH}_4$  and  $\text{NH}_4\text{Cl}$  to release more hydrogen.

In this case, the mass loss is lowered considerably as hydrogen is much lighter than amine-borane species.

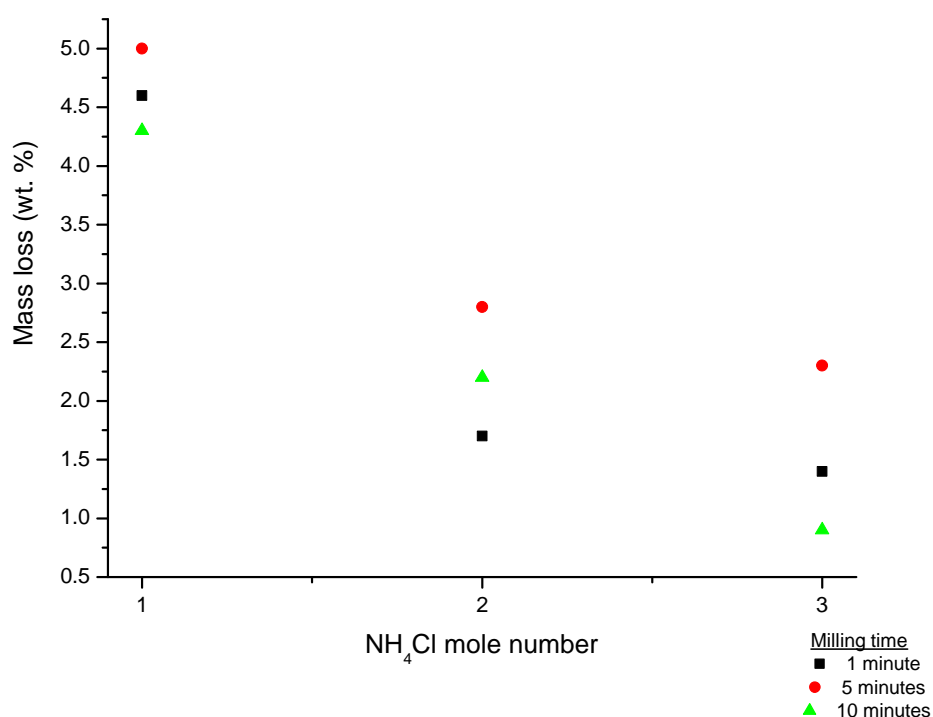


**Figure 5.4:** TG mass loss of different mixtures of  $\text{LiBH}_4$  as a function of the amount of  $\text{NH}_4\text{Cl}$ , Step 2: 80-140°C

**Step 3:** All the mixtures show a third step spreading from 130°C to 225°C. Also, the third step is characterised by a single peak attributed to  $\text{H}_2$  and  $\text{NH}_2\text{B}_2\text{H}_5$  but 2 distinct peaks (135-180°C and 180-225°C) attributed to PAB-PIB and  $\text{NH}_2\text{BH}_2$ . The only samples that solely released hydrogen were those which were in a 1:3 molar ratio of  $\text{LiBH}_4$  to  $\text{NH}_4\text{Cl}$ .

Upon heating, amine-borane species are released in much greater quantities hence the huge mass loss but once again, the “sole” release of hydrogen is observed for 1:3 mole ratio samples milled for 5 and 10 minutes with very high amounts of mass desorbed from the sample at 8.5 wt % and 4 wt % respectively.

**Table 5.4:** Summary of TG and MS results – Step 3 – 140-185°C and 185-225°C (peaks at 165°C and 195°C)

NH <sub>4</sub> Cl/LiBH <sub>4</sub> molar ratio	Milling time (minutes)	Mass Loss (wt %)	Gaseous products MS Low range (10 <sup>-12</sup> order)	Gaseous products MS High range (10 <sup>-9</sup> order)
Pure LiBH <sub>4</sub>	0	-	-	-
Pure NH <sub>4</sub> Cl	0	-3.1	-	NH <sub>3</sub> , HCl
-----	-----	-----	-----	-----
1	1	-11	A <sub>2</sub> B <sub>2</sub> , PAB-PIB, BZ	H <sub>2</sub> , ADB
		-2.7	A <sub>2</sub> B <sub>2</sub> , PAB-PIB, BZ	H <sub>2</sub>
1	5	-9.9	A <sub>2</sub> B <sub>2</sub> , PAB-PIB, BZ	H <sub>2</sub> , ADB
		-3.7	A <sub>2</sub> B <sub>2</sub> , PAB-PIB, BZ	H <sub>2</sub>
1	10	-7.1	A <sub>2</sub> B <sub>2</sub> , PAB-PIB, BZ	H <sub>2</sub> , ADB
		-3.6	A <sub>2</sub> B <sub>2</sub> , PAB-PIB, BZ	-
-----	-----	-----	-----	-----
2	1	-3.6	A <sub>2</sub> B <sub>2</sub> , PAB-PIB, BZ	H <sub>2</sub>
		-4.5	A <sub>2</sub> B <sub>2</sub> , PAB-PIB, BZ	-
2	5	-1.3	A <sub>2</sub> B <sub>2</sub> , PAB-PIB, BZ	H <sub>2</sub> , ADB
		-6.6	A <sub>2</sub> B <sub>2</sub> , PAB-PIB, BZ	-
2	10	-4.2	A <sub>2</sub> B <sub>2</sub> , PAB-PIB, BZ	H <sub>2</sub> , ADB
		-6.5	A <sub>2</sub> B <sub>2</sub> , PAB-PIB, BZ	-
-----	-----	-----	-----	-----
3	1	<b>-1.4</b>	A <sub>2</sub> B <sub>2</sub> , PAB-PIB, BZ	<b>H<sub>2</sub></b>
		-2.9	-	-
3	5	-8.5	-	H <sub>2</sub> , ADB
		-	-	-
3	10	<b>-4</b>	-	<b>H<sub>2</sub>, ADB</b>
		-	-	-

5.3.1.2  $\text{NH}_3\text{BH}_3$ -based systems

The results of the addition of  $\text{NH}_4\text{Cl}$  to  $\text{NH}_3\text{BH}_3$  may offer hope in terms of improvement of step 1 and step 2 of  $\text{LiBH}_4$ -based systems previously presented.

Table 5.5 summarises the results obtained for mixtures of  $\text{NH}_3\text{BH}_3$  and  $\text{NH}_4\text{Cl}$ .

**Table 5.5:** Summary of TG and MS results for mixtures of  $\text{NH}_3\text{BH}_3$  and  $\text{NH}_4\text{Cl}$  – Steps 1, 2 and 3

$\text{NH}_4\text{Cl}/\text{NH}_3\text{BH}_3$ molar ratio	Milling time (minutes)	Mass loss (wt %)	Gaseous products MS Low range ( $10^{-12}$ order)	Gaseous products MS High range ( $10^{-10}$ order)
<b><u>Step 1</u></b>	<b><u>Step 1</u></b>	<b><u>Step 1</u></b>	<b><u>Step 1</u></b>	<b><u>Step 1</u></b>
1	1	-2.5	-	$\text{H}_2$ , ADB, $\text{NH}_3$
-----	-----	-----	-----	-----
1	5	-1.9	-	$\text{H}_2$ , ADB, $\text{NH}_3$
-----	-----	-----	-----	-----
2	1	-	-	-
<b><u>Step 2</u></b>	<b><u>Step 2</u></b>	<b><u>Step 2</u></b>	<b><u>Step 2</u></b>	<b><u>Step 2</u></b>
1	1	-5	AB	$\text{H}_2$ , ADB, $\text{NH}_3$
-----	-----	-----	-----	-----
1	5	-4	AB	$\text{H}_2$
-----	-----	-----	-----	-----
2	1	-1.8	-	$\text{H}_2$ , ADB, $\text{NH}_3$
<b><u>Step 3</u></b>	<b><u>Step 3</u></b>	<b><u>Step 3</u></b>	<b><u>Step 3</u></b>	<b><u>Step 3</u></b>
1	1	-2.5	AB, PAB-PIB, BZ	$\text{H}_2$
-----	-----	-----	-----	-----
		-30	AB, PAB-PIB, BZ	$\text{H}_2$
-----	-----	-----	-----	-----
1	5	2	AB, PAB-PIB, BZ	$\text{H}_2$
-----	-----	-----	-----	-----
		-27	AB, PAB-PIB, BZ	$\text{H}_2$
-----	-----	-----	-----	-----
2	1	-1	-	$\text{H}_2$
-----	-----	-----	-----	-----
		-7.4	AB, PAB-PIB, BZ	$\text{H}_2$ , ADB, $\text{NH}_3$

As opposed to the 3 different mixtures involving  $\text{LiBH}_4$  and  $\text{NH}_4\text{Cl}$ , mixtures of  $\text{NH}_3\text{BH}_3$  and  $\text{NH}_4\text{Cl}$  involve the release of noxious  $\text{NH}_3$ .

When  $\text{NH}_4\text{Cl}$  is added in excess in the ( $\text{NH}_3\text{BH}_3:\text{NH}_4\text{Cl}=1:2$ ) mixture milled for 1 minute, the first step observed in all the mixtures so far is not observed at all. There seems to be a delay in the release of gas products, maybe resulting from the reaction of the gas products with the excess  $\text{NH}_4\text{Cl}$ ?

#### *5.3.1.3 Carbon additions*

The results of the addition of carbon with an excess of  $\text{NH}_4\text{Cl}$  added to  $\text{LiBH}_4$  are summarised in the following table.

The total sum of the results for the mixtures with carbon addition indicates that when the mixtures are heated, reactions take place with a major exothermic event between 30 and 80°C at a peak temperature at 75°C. A considerable mass loss of up to 4.8 wt % corresponding to this peak has been registered. The best improvements are observed for the ( $\text{LiBH}_4:\text{NH}_4\text{Cl}$ , C=1:2, 5 mol %) sample milled for 5 minutes and the ( $\text{LiBH}_4:\text{NH}_4\text{Cl}$ , C=1:3, 5 mol %) sample milled for 1 minute as 1 wt % has been added to the total release without it to be linked to a release of undesirable gas products.

All the mixtures show a second step but the results for the carbon-added mixtures are very similar to the ones from the non-added mixtures proving that the possible improvement does not occur during this second step.

The most spectacular improvement occurs during the third step especially for the ( $\text{LiBH}_4\text{:NH}_4\text{Cl}$ , C=1:3, 5 mol %) sample milled for 1 minute as 7.9 wt % of mass loss is registered corresponding to a release of hydrogen and aminoborane ( $\text{A}_2\text{B}_2$ ) only.

**Table 5.6:** Summary of TG and MS results for Carbon-added  $\text{LiBH}_4$ -based mixtures – Steps 1, 2 and 3

$\text{NH}_4\text{Cl/LiBH}_4$ molar ratio	Milling time (minutes)	Mass loss (wt %)	Gaseous products MS ( $10^{-12}$ order)	Gaseous products MS ( $10^{-9}$ order)
<b><u>Step 1</u></b>	<b><u>Step 1</u></b>	<b><u>Step 1</u></b>	<b><u>Step 1</u></b>	<b><u>Step 1</u></b>
2	1	-4.8	$\text{A}_2\text{B}_2$ , PAB-PIB, BZ	$\text{H}_2$ , ADB
-----	-----	-----	-----	-----
2	5	-2	-	$\text{H}_2$ , ADB
-----	-----	-----	-----	-----
3	1	-2.5	-	$\text{H}_2$ , ADB
-----	-----	-----	-----	-----
3	5	-0.7	-	$\text{H}_2$ , ADB
<b><u>Step 2</u></b>	<b><u>Step 2</u></b>	<b><u>Step 2</u></b>	<b><u>Step 2</u></b>	<b><u>Step 2</u></b>
2	1	-1.1	$\text{A}_2\text{B}_2$	$\text{H}_2$
-----	-----	-----	-----	-----
2	5	-2	-	$\text{H}_2$ , ADB
-----	-----	-----	-----	-----
3	1	-1.5	$\text{A}_2\text{B}_2$	$\text{H}_2$
-----	-----	-----	-----	-----
3	5	-0.9	-	$\text{H}_2$ , ADB
<b><u>Step 3</u></b>	<b><u>Step 3</u></b>	<b><u>Step 3</u></b>	<b><u>Step 3</u></b>	<b><u>Step 3</u></b>
2	1	-1.1	$\text{A}_2\text{B}_2$	$\text{H}_2$
-----	-----	-----	-----	-----
2	5	-2	$\text{A}_2\text{B}_2$ , PAB-PIB, BZ	$\text{H}_2$ , ADB
-----	-----	-----	-----	-----
3	1	-7.9	$\text{A}_2\text{B}_2$	$\text{H}_2$
-----	-----	-----	-----	-----
3	5	-6.1	$\text{A}_2\text{B}_2$	$\text{H}_2$ , ADB



The results of the addition of carbon with an excess of  $\text{NH}_4\text{Cl}$  added to  $\text{NH}_3\text{BH}_3$  are summarised in the following table.

**Table 5.7:** Summary of TG and MS results for Carbon-added  $\text{NH}_3\text{BH}_3$ -based mixtures – Steps 1, 2 & 3

$\text{NH}_4\text{Cl}/\text{NH}_3\text{BH}_3$ molar ratio	Milling time (minutes)	Mass loss (wt %)	Gaseous products MS ( $10^{-12}$ order)	Gaseous products MS ( $10^{-9}$ order)
<u>Step 1</u> 1 -----	<u>Step 1</u> 1 -----	<u>Step 1</u>  -----	<u>Step 1</u>  -----	<u>Step 1</u>  -----
1 -----	5 -----	 -----	 -----	 -----
2 <u>Step 2</u> 1 -----	1 <u>Step 2</u> 1 -----	<u>Step 2</u>  -----	<u>Step 2</u>  -----	<u>Step 2</u>  -----
1 -----	5 -----	 -----	 -----	 -----
2 <u>Step 3</u> 1 -----	1 <u>Step 3</u> 1 -----	<u>Step 3</u>  -----	<u>Step 3</u>  -----	<u>Step 3</u>  -----
1 -----	5 -----	 -----	 -----	 -----
2	1			

The main focal point here is that with the addition of carbon to mixtures of  $\text{NH}_3\text{BH}_3$  and  $\text{NH}_4\text{Cl}$ ,  $\text{NH}_3$  is not released any more. It shows that carbon may help assumed product of step 1, ie.  $\text{NH}_3\text{BH}_3$  to be in intimate contact with excess  $\text{NH}_4\text{Cl}$  to during step 2 and therefore prevent the release of other amine-borane species,

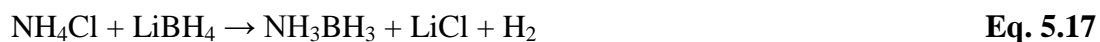
In summary, the figures show that the thermal evolution of mixtures of LiBH<sub>4</sub> and ammonium chloride (NH<sub>4</sub>Cl) occurred in 3 stages between room temperature and 250°C with a total mass loss of up to 24 wt %. Furthermore, the MS detected several other amine-borane species. The right range of mass losses (7.5 -11.5 wt %) is only achieved with the (LiBH<sub>4</sub>:NH<sub>4</sub>Cl=1:3) mixtures.

However, for all the mixtures of LiBH<sub>4</sub> and NH<sub>4</sub>Cl, the main desorption is enabled during the first and second steps (below 250°C), which is a remarkable improvement compared to pure LiBH<sub>4</sub> and MCl<sub>n</sub>-added mixtures. Meanwhile, this result opens the way for additional investigation to be performed on the suspected intermediate compound, NH<sub>3</sub>BH<sub>3</sub> and its possible interaction with NH<sub>4</sub>Cl.

### 5.3.2 Comparative discussion:

#### 5.3.2.1 For NH<sub>4</sub>Cl addition to LiBH<sub>4</sub>

The stoichiometry mostly reported in the literature is the one given by the equation of borazine formation and is presented as follows:



The stoichiometric conditions which we referred to are the one related to this particular reaction.

Compared to the as-received LiBH<sub>4</sub> (see section 5.1 of the thesis), the decomposition of LiBH<sub>4</sub> mixed with NH<sub>4</sub>Cl was reduced by more than 300°C, Figures 4.26, 4.27 and 4.28. The earlier H<sub>2</sub> desorption, although accompanied by the

concomitant release of other gas species (especially in stoichiometric conditions) is possibly due to many reasons such as the partial decomposition of  $\text{LiBH}_4$  from the milled sample, as XRD analysis showed (see Figure 4.20 p. xx). XRD results suggest that there is a significant chemical interaction between the additive  $\text{NH}_4\text{Cl}$  and host  $\text{LiBH}_4$ . Milling reduces particle size and increases the surface area to facilitate the gas diffusion.

### **In stoichiometric proportions**

Thermal decomposition characteristics are compared in Figures 4.26, 4.27 and 4.28 for the ( $\text{LiBH}_4\text{:NH}_4\text{Cl}=1\text{:}1$ ) compositions with different milling times ranging from 1 minute to 10 minutes. The SEM-EDS profiles of this mixture right after milling durations as short as 1 minute (in Figure 4.23) show its high reactivity. This was confirmed by comparative XRD analysis (in Figure 4.20) of mixtures of  $\text{LiBH}_4$  and  $\text{NH}_4\text{Cl}$  after no milling and a milling of 1 minute have been applied. Indeed, it was suggested in a publication by Volkov et al. [207] that mechanical milling of  $\text{NaBH}_4$  and  $\text{NH}_4\text{Cl}$  could lead to the formation of an unstable  $\text{NH}_4\text{BH}_4$  compound at room temperature by the reaction:



This could possibly be extrapolated to  $\text{LiBH}_4$ . RT stands for room temperature.

The TG results show several decomposition steps, which are mainly due to the release of  $\text{H}_2$  and amine-borane species as identified on the MS spectra. The major exothermic peak at around 65-70°C in the DTA curve corresponds to the release of

hydrogen but unfortunately other amine-borane species. To this extent, it has been reported by Parry *et al.* [152] and Schaeffer *et al.* [160] that  $\text{NH}_4\text{BH}_4$  could liberate hydrogen and form DADB which then forms  $\text{A}_3\text{B}_3$  ( $\text{NH}_3\text{BH}_3$ ).



RT stands for room temperature.

Karkamkar *et al.* [208] described the decomposition pattern for  $\text{NH}_4\text{BH}_4$  isolated and exhibited 3 steps below  $160^\circ\text{C}$  yielding 3 equivalents of  $\text{H}_2$ .

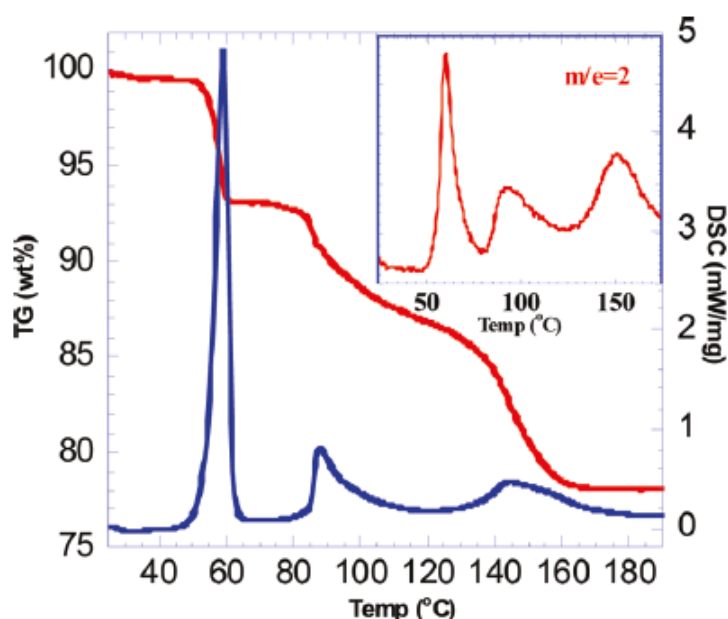


**Figure 5.5:** TG-DTA-MS data for the decomposition of ammonium borohydride,  $\text{NH}_4\text{BH}_4$ , taken from Karkamkar *et al.* [208]

Hydrogen release is shown to proceed through a multi-step pathway leading to the formation of  $\text{A}_3\text{B}_3$ , DADB, PAB and PIB consecutively.

**Table 5.8:** Different steps during decomposition of ammonium borohydride,  $\text{NH}_4\text{BH}_4$ , taken from Karkamkar *et al.* [208]

Reaction	$-\Delta H^\circ_{298} (\text{kJ.mol}^{-1})$	$T_d (^\circ\text{C})$
$\text{NH}_4\text{BH}_4 = \text{NH}_3\text{BH}_3 + \text{H}_2$ <b>Eq. 5.21a<sub>1</sub></b>	40	50
$\text{NH}_4\text{BH}_4 + \text{NH}_3\text{BH}_3 = \text{DADB} + \text{H}_2$ <b>Eq. 5.21a<sub>2</sub></b>		
$\text{DADB} = \text{PAB} + \text{H}_2$ <b>Eq. 5.21b</b>	15	85
$\text{PAB} + \text{H}_2 = \text{PIB} + \text{H}_2$ <b>Eq. 5.21c</b>	13	130

Right after the first step, around  $75^\circ\text{C}$ , the SEM micrograph (in Figure 4.22) shows the high reactivity of the mixture and the specific morphology confirms the vigorous liberation of gas phases. Also, XRD analysis (in Figure 4.21) of the heated product after this first step firmly confirmed it.

It is noted that the analyses of solid residues after each subsequent step have been made impossible as the texture of the products is polymer-like and the quality of the XRD spectra is poor. However, the thermal analyses give strong indications of reactions involved through the MS results essentially. Clearly, the subsequent steps see the strong release of other gas species along with hydrogen but the thermal events registered on the DTA curves are of much lower intensities than the first one.

As the milling time is increased from 1 minute to 5 minutes and then to 10 minutes, the first event is overpowered by the subsequent steps with less hydrogen released but also, noticeably with lower amine-borane species leaving the total mass desorbed falling from 24 wt % to 22 wt % and then to 16 wt %. It shows room for

improvement especially for the first step around 65-75°C, by adding  $\text{NH}_4\text{Cl}$  in excess to host  $\text{LiBH}_4$ ?

### With excess $\text{NH}_4\text{Cl}$

It was found in a publication by Mikheeva *et al.* [161] that an increasing amount of  $\text{NH}_4\text{Cl}$  added to host  $\text{LiBH}_4$  could lead to a decrease in the yield of borazine. The reported data have been extracted and are plotted in the following Figure 5.6.

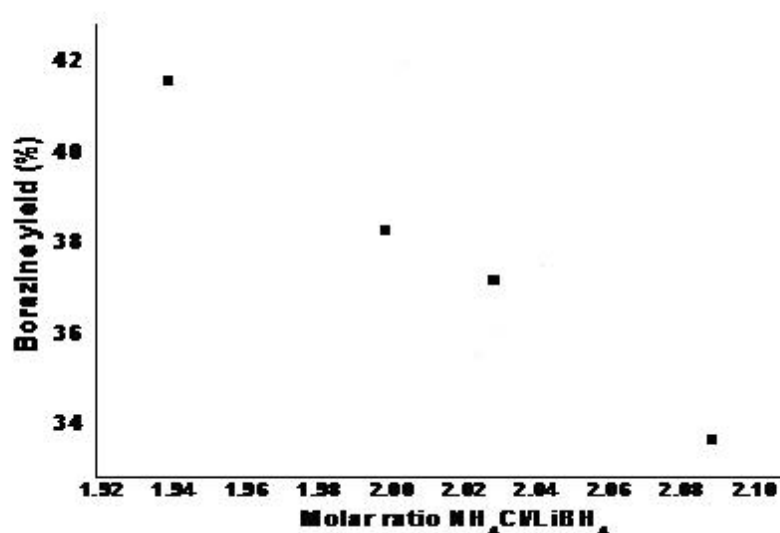


**Figure 5.6:** Yield of borazine as a function of  $\text{NH}_4\text{Cl}$  proportion (data extracted from Mikheeva *et al.* [161])

Thus, the trend in order to get less amine-borane species such as borazine would be to increase gradually the amount of  $\text{NH}_4\text{Cl}$ , bearing in mind the overall hydrogen content. Therefore,  $\text{NH}_4\text{Cl}/\text{LiBH}_4$  molar ratios of 2 and 3 have been investigated.

Thermal decomposition characteristics are compared in Figures 4.29, 4.30 and 4.31 for the ( $\text{LiBH}_4\text{:NH}_4\text{Cl}=1\text{:}2$ ) compositions with different milling times ranging from 1 minute to 10 minutes. Three decomposition steps were unveiled by the TG results as for stoichiometric proportions and similarly, MS results mainly showed the release of  $\text{H}_2$  and amine-borane species. The major exothermic peak at around 65-70°C in the DTA curve corresponds to the release of hydrogen but unfortunately also AB and other amine-borane species but as expected in a much lesser extent than for stoichiometric conditions previously presented.

Right after the first step, around 75°C, XRD analysis (in Figure 4.21) of the solid residue strongly showed LiCl presence mixed with very tiny amounts of starting materials ie  $\text{LiBH}_4$  and  $\text{NH}_4\text{Cl}$ .

As the milling time is increased up to 10 minutes, the first event is not accompanied with a concomitant release of amine-borane species, meaning a purer gas stream liberated from the sample.

Furthermore, the subsequent steps see the declining release of other gas species along with hydrogen especially when the milling time is increased.

Thermal decomposition characteristics are compared in Figures 4.32, 4.33 and 4.34 for the ( $\text{LiBH}_4\text{:NH}_4\text{Cl}=1\text{:}3$ ) compositions with different milling times ranging from 1 minute to 10 minutes.

Similarly to the ( $\text{LiBH}_4\text{:NH}_4\text{Cl}=1\text{:}2$ ) compositions, three decomposition steps were revealed by the TG results. However, MS results mainly showed the release of  $\text{H}_2$  along with very few ADB and  $\text{A}_2\text{B}_2$ . BZ is not released any more, which confirms the trend demonstrated by Mikheeva *et al.*[161]. As the gas stream is much purer, it is relevant only now to give figures of mass loss as they are likely to be very close to the real amount of hydrogen desorbed from the samples. Accordingly, the major exothermic peak at around 65-70°C in the DTA curve is still registered for the sample milled for 1 minute but a peak shift is encountered for samples milled for longer times. For the latter samples, the main peak is registered around 100°C. There is also a new sharp endothermic event registered around 145°C. Coincidentally, the mass losses are much increased up to this specific temperature and the maximum is reached at **6 wt % around 150°C** for the sample milled for 5 minutes.

Right after the first step, around 75°C, XRD analysis (in Figure 4.21) of the solid residue strongly showed LiCl presence but in a much lesser extent than for the other  $\text{NH}_4\text{Cl/LiBH}_4$  molar ratios. Could this be meaning that the reaction occurring at 65-70°C and forming LiCl is minimised and overpowered by another one?

### **With Carbon addition**

It has been reported by Xiong *et al.* [209] that graphite addition to mixtures of  $\text{A}_3\text{B}_3$  could improve ball milling efficiency and so, provide intimate contact in our case between  $\text{LiBH}_4$  and  $\text{NH}_4\text{Cl}$ .



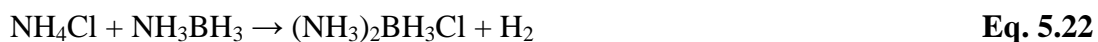
Thermal decomposition characteristics are compared in Figures 4.38 and 4.39 for the ( $\text{LiBH}_4\text{:NH}_4\text{Cl:C}=1\text{:}2\text{:}5\%$ ) compositions with two milling times at 1 minute and 5 minutes. The main three decomposition steps were also uncovered by the TG results as for the undoped samples. Similarly, MS results mainly showed the release of  $\text{H}_2$  as well as amine-borane species such as ADB and PAB-PIB. These latter species are no longer present for the sample milled for 5 minutes during step 1 and step 2 but still present during step 3. Step 2 is much enhanced with 1% more released before  $150^\circ\text{C}$ .

Thermal decomposition characteristics are compared in Figures 4.40 and 4.41 for the ( $\text{LiBH}_4\text{:NH}_4\text{Cl, C}=1\text{:}3, 5\%$ ) compositions with two milling times at 1 minute and 5 minutes. The main three decomposition steps were also uncovered by the TG results as for the undoped samples. Similarly, MS results mainly showed the release of  $\text{H}_2$  as well as amine-borane species such as ADB and PAB-PIB. These latter species are no longer present for the sample milled for 5 minutes during step 1, step 2 and step 3. Step 3 is much enhanced with 11.5 wt % released before  $225^\circ\text{C}$ .

#### 5.3.2.2 For $\text{NH}_4\text{Cl}$ addition to $\text{NH}_3\text{BH}_4$

$\text{A}_3\text{B}_3$  and  $\text{NH}_4\text{Cl}$  were investigated in order to engineer steps 2 and 3 as step 1 (see Eq. 5.17) seems difficult to improve but still good as 2.66 wt % are potentially released at  $60^\circ\text{C}$  during this step. But also, the mixture of  $\text{A}_3\text{B}_3$  and  $\text{NH}_4\text{Cl}$  may be a good hydrogen storage system itself as the potential hydrogen content is up to 2.5 wt % higher than  $\text{LiBH}_4$  and  $\text{NH}_4\text{Cl}$ .

Heldebrant *et al.*[210] demonstrated that the addition of  $\text{NH}_4\text{Cl}$  to  $\text{A}_3\text{B}_3$  could lead to the formation of DADB and the liberation of gaseous hydrogen as shown in the following reaction:



Thus, the stoichiometric conditions which we referred to are the one related to this particular reaction.

Compared to the mixtures of  $\text{LiBH}_4$  and  $\text{NH}_4\text{Cl}$ , the decomposition of  $\text{NH}_3\text{BH}_3$  mixed with  $\text{NH}_4\text{Cl}$  is also a multi-step decomposition pattern as seen in Figures 4.35, 4.36 and 4.37.

With the  $(\text{NH}_3\text{BH}_3:\text{NH}_4\text{Cl}=1:1)$  molar ratio, step 1 occurs at around  $80^\circ\text{C}$ , very close to the first step temperature in  $(\text{LiBH}_4:\text{NH}_4\text{Cl})$  mixtures. Heldebrant *et al.* [210] has found this temperature to be the reaction temperature between equimolecular ratios of  $\text{NH}_3\text{BH}_3$  and  $\text{NH}_4\text{Cl}$ . This temperature is also largely reported to be the main temperature involved in the thermal decomposition of  $\text{NH}_3\text{BH}_3$  as shown in Wolf *et al.* [167].

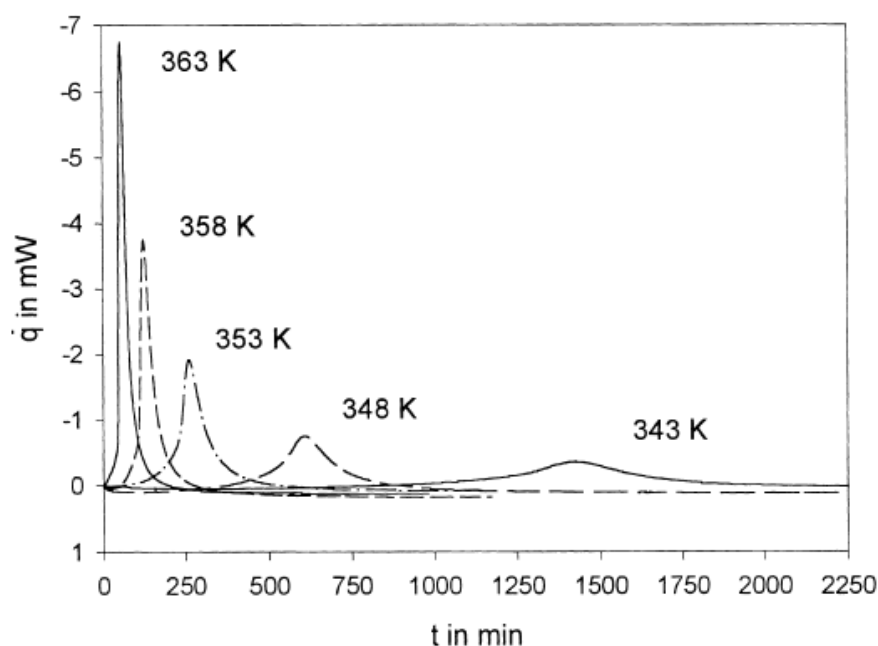


**Figure 5.7:** Isothermal measurements of main DSC peaks (data extracted from Wolf *et al.*[167])

During this step, there is a release of  $H_2$ , ADB but also ammonia. The latter has never been registered during the decomposition of  $(LiBH_4:NH_4Cl)$  mixtures and is a very noxious by-product. Ammonia generated at such low temperature region is probably caused by the local overheating since the reaction is exothermic.

In this particular case, the release of heavy by-products is avoided but the reverse effect is that a substantial of hydrogen resides in  $[(NH_3)_2.BH_2]^+Cl^-$  until it decomposes into  $NH_4Cl$  and  $A_2B_2$ .

4 subsequent and overlapping steps are registered on the thermal analysis thereafter with the liberation of increasing amounts of amine-borane species indicating that the main scope of this specific study would be to increase the amount of  $NH_4Cl$  in order to engineer these steps.

### 5.3.2.3 Summary of comparative discussions for $\text{NH}_4\text{Cl}$ addition to $\text{LiBH}_4$ and $\text{NH}_3\text{BH}_3$

The gas liberation starts nearly immediately on heating. There is a vigorous evolution of gas for mixtures with  $\text{LiBH}_4\text{:NH}_4\text{Cl}$  molar ratio of 1:1, 1:2 and 1:3 accompanying an exothermic reaction between 40 and 80°C, which gets weaker as the milling time is increased.

During the mechanical milling, some induced by-reactions may have occurred at room temperature leading to the formation of  $\text{LiCl}$  and an unknown phase .

When  $\text{NH}_4\text{Cl}$  is added in excess,  $\text{NH}_4\text{Cl}$  may react with AB and form  $[(\text{NH}_3)_2.\text{BH}_2]^+\text{Cl}^-$  which withholds a significant amount of hydrogen until it is released thereafter.

In summary, the figures show that the thermal evolution of mixtures of  $\text{LiBH}_4$  and ammonium chloride ( $\text{NH}_4\text{Cl}$ ) occurred in 3 stages between room temperature and 250°C with a total mass loss of up to 24 wt %. The right range of mass losses (7.5 -11.5 wt %) is only achieved with the ( $\text{LiBH}_4\text{:NH}_4\text{Cl}$ =1:3) mixtures.

However, for all the mixtures of  $\text{LiBH}_4$  and  $\text{NH}_4\text{Cl}$ , the main desorption is enabled during the first and second steps (below 250°C), which is a remarkable improvement compared to pure  $\text{LiBH}_4$  and  $\text{MCl}_n$ -added mixtures. Meanwhile, this result opened the way for additional investigation to be performed on the suspected intermediate compound,  $\text{NH}_3\text{BH}_3$  and  $\text{NH}_4\text{Cl}$ .

This investigation showed that it is better to start with  $\text{LiBH}_4$  and  $\text{NH}_4\text{Cl}$  than with  $\text{NH}_3\text{BH}_3$  and  $\text{NH}_4\text{Cl}$  although potentially the latter contains more hydrogen. It is due to the fact that  $\text{NH}_3$  is an unwanted by-product in this particular case. Indeed,  $\text{NH}_3$  release is not observed for  $\text{LiBH}_4/\text{NH}_4\text{Cl}$  mixtures, which is a huge advantage. This parallel investigation also demonstrated that in the case of  $\text{LiBH}_4/\text{NH}_4\text{Cl}$  mixtures, the formation of intermediate  $\text{NH}_3\text{BH}_3$  as a stable phase must be avoided by adding an excess of  $\text{NH}_4\text{Cl}$ .

The dehydrogenation of mixtures of  $\text{LiBH}_4$  and  $\text{NH}_4\text{Cl}$  has many advantages compared to the sole decompositions of  $\text{LiBH}_4$  and  $\text{NH}_3\text{BH}_3$  for hydrogen generation and among them, we can cite: 1) Up to 11.5 wt %  $\text{H}_2$  released below a relatively lower temperature  $225^\circ\text{C}$  and in a definitely purer gas stream; 2) Lower material cost as  $\text{NH}_4\text{Cl}$  is widely available and at a much lower cost than  $\text{LiBH}_4$  and  $\text{NH}_3\text{BH}_3$ ;

## **Chapter 6.    Conclusions**

A systematic investigation has been carried out on  $\text{LiBH}_4$  and its extended hydrogen desorption characteristics when mixed with “transition metal” chlorides ( $\text{NiCl}_2$ ,  $\text{ZnCl}_2$ ,  $\text{TiCl}_3$  and  $\text{CrCl}_3$ ) and ammonium chloride ( $\text{NH}_4\text{Cl}$ ). The effect of milling on phase composition and desorption of these binary compositions is characterised using SEM-DS, XRD, FTIR and TG-DTA-MS. From the results and discussion, following points may be concluded:

**$\text{LiBH}_4$  decomposition:**

1.  $\text{LiBH}_4$  decomposes into hydrogen upon heating after the phase change at  $120^\circ\text{C}$  and melting at  $280^\circ\text{C}$ .
2. The endothermic nature of the main desorption reaction and the amount of hydrogen desorbed suggest a reaction leading to the formation of  $\text{LiH}$ .

**For the  $(n\text{LiBH}_4 + \text{MCl}_n)$  System:**

3. By reducing the milling time duration to 5 minutes, the formation of intermediates is only initiated and they are not decomposing during the process as observed for samples  $(3\text{LiBH}_4 + \text{TiCl}_3)$  and  $(2\text{LiBH}_4 + \text{NiCl}_2)$ . For the other samples  $(2\text{LiBH}_4 + \text{ZnCl}_2)$  and  $(3\text{LiBH}_4 + \text{CrCl}_3)$ , even though the presence of intermediates has been demonstrated, the morphologies are not being changed right after milling and are very similar to that of pure  $\text{LiBH}_4$ .

4. Thermal desorption results suggest that complex mixtures ( $n\text{LiBH}_4 + \text{MCl}_n$ ) mainly evolves  $\text{H}_2$  however some diborane ( $\text{B}_2\text{H}_6$ ) was detected for ( $2\text{LiBH}_4 + \text{ZnCl}_2$ ) which explains the differences between the effective mass loss and the theoretical hydrogen content. However, this discrepancy is attenuated in the other chlorides – added mixtures and even null for ( $3\text{LiBH}_4 + \text{CrCl}_3$ ).
5. In terms of the purity of the hydrogen delivery, ( $3\text{LiBH}_4 + \text{CrCl}_3$ ) is the best composition even though it does not have the lowest onset desorption temperature. It reaches 2 wt % up to  $180^\circ\text{C}$  and 6 wt % at  $280^\circ\text{C}$ .
6. They all present the  $\text{LiBH}_4$  phase transformation suggesting the presence of residual  $\text{LiBH}_4$  in the mixture upon heating up to  $120^\circ\text{C}$ , however, the onset desorption either precedes or follows the phase transformation. The thermal nature of desorption may help in finding out the desorption products involved in the reaction. For instance, the exothermic character observed in ( $3\text{LiBH}_4 + \text{CrCl}_3$ ) and ( $2\text{LiBH}_4 + \text{NiCl}_2$ ) may be linked to the formation of borides of Ni and Cr reported in the literature whereas the endothermic character observed in ( $3\text{LiBH}_4 + \text{TiCl}_3$ ) and ( $2\text{LiBH}_4 + \text{ZnCl}_2$ ) may be attached to the formation of other reaction products such as the binary hydride,  $\text{ZnH}_2$ .
7. Finally, as opposed to pure  $\text{LiBH}_4$ , the main hydrogen delivery from complex mixtures ( $n\text{LiBH}_4 + \text{MCl}_n$ ) is started below  $280^\circ\text{C}$  ( $\text{LiBH}_4$  melting point) and even completed below  $410^\circ\text{C}$  ( $\text{LiBH}_4$  main onset desorption temperature), which is a



huge improvement even though the hydrogen storage capacity of the system is massively impacted by the large molecular weights of the chlorides and decreased to no more than 5.5 wt %.

**For the ( $\text{LiBH}_4 + x\text{NH}_4\text{Cl}$ ) system:**

8. In the  $\text{LiBH}_4/\text{NH}_4\text{Cl}$  case, the reaction temperature is lower than the melting points of the two reactants, indicating that the melting of solid reactants is not the prerequisite of solid-state reactions.
9. Thermal desorption results suggest that complex mixtures ( $\text{LiBH}_4 + x\text{NH}_4\text{Cl}$ ) mainly evolves  $\text{H}_2$  however some other amine-borane species are detected such as ammonia borane ( $\text{NH}_2\text{BH}_2$  or  $\text{A}_2\text{B}_2$ ), aminodiborane ( $\text{NH}_2\text{B}_2\text{H}_5$  as ADB), PIB, PAB and borazine ( $\text{B}_3\text{N}_3\text{H}_6$  as BZ).
10. The maximum yield of gaseous hydrogen is not observed at the equimolecular ratio of  $\text{LiBH}_4$  to  $\text{NH}_4\text{Cl}$  but with a molar ratio  $\text{NH}_4\text{Cl}/\text{LiBH}_4$  equal to 3. The presence of the intermediate  $\text{NH}_3\text{BH}_3$  is suspected after the first step (around 65-80°C) however it has not been proved by XRD results due to the possible amorphous nature of this compound.
11. The parallel study of mixtures of  $\text{NH}_3\text{BH}_3$  and  $\text{NH}_4\text{Cl}$  explicitly proved and confirmed that during the decomposition of mixtures of  $\text{LiBH}_4$  and  $\text{NH}_4\text{Cl}$ , the

decomposition of the intermediate  $\text{NH}_3\text{BH}_3$  and therefore, the liberation of heavy by-products must be avoided by adding an excess of  $\text{NH}_4\text{Cl}$ .

12. A significant decrease in the yield of other amine-borane species is observed as and when the excess of ammonium chloride is increased and it can be attributed to the occurrence of side reactions avoiding further decomposition and subsequent polymerization into  $\text{BNH}_x$  compounds.
13. Solid reactions between  $\text{LiBH}_4$  and  $\text{NH}_4\text{Cl}$  have several advantages over the decomposition of  $\text{LiBH}_4$  for the  $\text{H}_2$  production. These include:
  - Higher  $\text{H}_2$  wt % (up to 11.5 wt %) released at relatively low temperature (below  $225^\circ\text{C}$ ) ;
  - Lower overall cost since  $\text{H}_2$  is provided by cheaper  $\text{NH}_4\text{Cl}$ .

## **Chapter 7. Future work**

From the present findings, several issues need further investigation for the novel systems which have been uncovered, which include in-depth understanding of the current systems and the development of more desirable Li-B-N-H systems. These are described as follows:

- a) To modify  $H_2$  desorption properties of the Li-B-N-H system, including structural modification on  $LiBH_4$  to improve its reactivity with chlorides;
- b) To develop an alternative method of processing the powder mixtures so as to efficiently reduce the impurity gas desorption, e.g. pre-milling  $LiBH_4$ , addition of an optimal amount of carbon graphite;
- c) To explore other alternative systems, e.g.  $LiBH_4 + NH_3BH_3/NH_4Cl$ , research still needs to focus on the basic hydrogen sorption properties and mechanism of both absorption and desorption processes;
- d) To synthesis Li-B-N-H related materials, e.g.  $LiBNH_2$ , by gas-solid reaction or wet chemistry synthesis.

## Appendices



Appendix 1 Patent Application

Appendix 2 Poster

## **Appendix 1 Patent Application**

<b>Publication number</b>	WO2010136774 A1
<b>Publication type</b>	Application
<b>Application number</b>	PCT/GB2010/001066
<b>Publication date</b>	2 Dec 2010
<b>Filing date</b>	28 May 2010
<b>Priority date</b>	29 May 2009
<b>Inventors</b>	<a href="#">Zheng Xiao Guo</a> , <a href="#">Kondo François AGUEY-ZINSOU</a> , <a href="#">Kouassi Gaelle Anguie</a>
<b>Applicant</b>	<a href="#">Ucl Business Plc</a>

### **Hydrogen production and storage**

**WO 2010136774 A1**

#### **ABSTRACT**

The present invention relates to a material system comprising a solid ammonium halide and a further reactant, a device comprising the same and methods for producing and storing hydrogen.

#### **CLAIMS<sup>(22)</sup>**

Claims:

1. A material system comprising a solid ammonium halide and a further reactant selected from the group consisting of a metal, a hydride, an imide, an amide, a ceramic compound, and mixtures thereof.
2. The material system according to claim 1, wherein the solid ammonium halide is  $\text{NH}_4\text{Cl}$ .
3. The material system according to claim 1 or claim 2, wherein the hydride is a metal hydride and comprises one or more of the metals Li, B, Na, Mg, Al, Si, K or Ca.
4. The material system according to claim 3, wherein the hydride is  $\text{LiH}$ ,  $\text{LiBH}_4$ ,  $\text{NaBH}_4$ , or a mixture thereof.
5. The material system according to any one of the preceding claims, wherein the imide is a metal imide and comprises one or more of the metals Li, B, Na, Mg, Al, Si, K or Ca.

6. The material system according to any one of the preceding claims, wherein the amide is a metal amide and comprises one or more of the metals Li, B, Na, Mg, Al, Si, K or Ca.
7. The material system according to any of the preceding claims, wherein at least one of the solid ammonium halide and the further reactant is present as particles having a maximum diameter of about 5000 micrometers.
8. The material system according to any of the preceding claims, wherein at least one of the solid ammonium halide and the further reactant is present on a support.
9. The material system according to any one of the preceding claims, containing a catalyst.
10. The material system according to claim 9, wherein the catalyst is selected from the group consisting of a transition metal, an alloy of one or more transition metals, a metal oxide, a metal carbide, a metal nitride a metal halide and mixtures thereof.
11. The material system according to claim 9 or claim 10, wherein the catalyst is present on a support.
12. The material system according to any one of claims 1 to 11 for producing hydrogen.
13. A device comprising the material system as defined in any one of claims 1 to 12.
14. The device according to claim 13 for producing hydrogen.
15. The device according to claim 13 or claim 14, wherein the solid ammonium halide is present in a first compartment and the further reactant is present in at least a second compartment and wherein the device comprises a means for mixing the solid ammonium halide and the further reactant.
16. The device according to any of claims 13 to 15, which is a fuel cell or a hydrogen combustion engine.
17. A method for producing hydrogen by reacting solid ammonium halide and a further reactant selected from the group consisting of a metal, a hydride, an imide, an amide, a ceramic compound, and mixtures thereof.
18. A method for producing hydrogen using the material system or device according to any one of claims 1 to 16.
19. The method according to claim 17 or 18, wherein the reaction is carried out at a temperature of about 200°C or less.
20. A method for hydrogen absorption, said method comprising the steps of subjecting the dehydrogenated product of claim 17 or claim 18 to hydrogen at a pressure of from about 0.1 to about 70 MPa and a temperature of from about 20 to about 600°C to produce a solid ammonium halide and a further reactant selected from the group consisting of a metal, a hydride, an imide, an amide, a ceramic compound, and mixtures thereof.
21. The method according to any one of claims 17 to 20, which is carried out in a fuel cell or a hydrogen combustion engine.
22. Use of solid ammonium halide and a further reactant selected from the group consisting of a metal, a hydride, an imide, an amide, a ceramic compound, and mixtures thereof for the production of hydrogen.

## DESCRIPTION

### Hydrogen production and storage

The present invention relates to a material system, a device and methods for producing and storing hydrogen.

Hydrogen is a clean and enabling energy vector for future portable devices and transport vehicles, to mitigate green-house gas and pollutant emissions. Practical hydrogen storage (and then its supply or production) is one of the critical issues in the development of fuel-cell devices and vehicles. Conventional storage of hydrogen in either compressed gas or liquid form requires substantial energy input, either to compress or liquefy the hydrogen, and there are serious safety concerns in high-pressure hydrogen and in hydrogen boiling-off.

The authoritative standard with regard to desired levels of hydrogen storage capacity is that released by U.S. Department of Energy (DOE). For hydrogen-powered fuel cell vehicles, the main standard to quantify the storage of hydrogen is that the system volume density should reach  $40 \text{ kg/m}^3$ , mass fraction of 5.5% (<http://www1.eere.energy.gov/hydrogenandfuelcells/storage/currenttechnology.html>). Hydrogen release should be around the fuel cell operation temperature, 80-100 °C.

Various metal hydrides, compound hydrides and complex/chemical hydrides have been investigated as hydrogen storage candidates. However, the hydrogen desorption or supply temperature from the materials previously investigated are all too high ( $>200^\circ\text{C}$ ) for practical applications. Such high temperatures are also disadvantageous due to the risk of explosion.

An alternative option which has been investigated is physi-sorbents, such as MOFs (metal-organic frameworks) and carbon nanostructures, which require cryogenic conditions to store a reasonable amount of hydrogen, i.e. typically  $< 1\text{-}2 \text{ wt}\%$  under 1 bar, though a high value of  $10\text{wt}\%$  at 77 bar has been reported at 77 K ( $-196^\circ\text{C}$ ) (van den Berg et al, Chem. Commun. 2008, 6, 668). Another chemical compound, ammonia ( $\text{NH}_3$ ), is also of great interest as a hydrogen storage medium (with a theoretical density of hydrogen at  $17.6\text{wt}\%$ ), but it is hazardous for practical use as a hydrogen store and a separate stage is also required to extract high purity hydrogen from it in order to feed into targeted fuel cells. Several methods have been proposed to facilitate the use of ammonia:

1 Stabilise ammonia with metals by forming metal amides e.g.  $\text{Mg}(\text{NH}_2)_2$ , but a catalyst and high temperatures are still needed to convert ammonia into hydrogen (Lai- Peng Ma et al, Journal of Physical Chemistry C, 2008, 112 (46), 18280-18285);



2 React ammonia gas over a metal hydride to release hydrogen at a relatively low temperature, e.g. reaction of  $\text{NH}_3$  gas over  $\text{LiH}$  powder, but the temperature is still too high for practical applications (Yun Hang Hu et al, Journal of Physical Chemistry A, 2003, 107 (46), 9737-9739);

3 Use amide compounds, e.g.  $\text{LiNH}_2$ , to react with metal hydrides (e.g.  $\text{MgH}_2$  or  $\text{LiH}$ ) to produce hydrogen, but hydrogen is only released at high temperatures ( $>200^\circ\text{C}$ ) which is too high for practical applications (P. Chen, Z et al, Nature 420 (2002), pp. 302-304).

Therefore, there is a need for a safe, solid device which produces hydrogen at temperatures suitable for on-board fuel cell vehicles and for back-up power {i.e. temperatures of  $150^\circ\text{C}$  or less}.

The object of the present invention is to provide an improved material system and device for storing and producing hydrogen.

A further object of the present invention is to provide a material system and device which can store and produce increased amounts of hydrogen.

A further object of the present invention is to provide a material system and device which can produce hydrogen or increased amounts of hydrogen at temperatures suitable for on-board fuel cell vehicles. The present invention provides a material system comprising a solid ammonium halide and a further reactant selected from the group consisting of a metal, a hydride, an imide, an amide, a ceramic compound, and mixtures thereof.

Advantageously, it has been found that such a material system produces increased amounts of hydrogen at low temperatures, e.g. temperatures suitable for on-board fuel cell vehicles.

The present invention further provides a method for producing hydrogen by reacting solid ammonium halide and a further reactant selected from the group consisting of a metal, a hydride, an imide, an amide, a ceramic compound, and mixtures thereof.

The present invention further provides a method for producing hydrogen using the material system or device according to the present invention.

The methods of the present application are particularly advantageous because they can be used to produce hydrogen at low temperatures, e.g. temperatures suitable for on-board fuel cell vehicles and for back-up power. This is particularly useful for vehicles and back-up power devices.

The present invention further provides a method of hydrogen absorption, said method comprising the steps of subjecting the dehydrogenated product of the hydrogen production

methods of the present invention to hydrogen at a pressure of from about 0.1 to about 70 MPa and a temperature of from about 20°C to about 600°C to produce a solid ammonium halide and a further reactant selected from the group consisting of a metal, a hydride, an imide, an amide, a ceramic compound, and mixtures thereof.

This method reverses the hydrogen production process to hydrogenate the de- hydrogenated products back into the ammonium halide and the further reactant for re-use if required. This provides easy recycling of the devices of the present invention resulting in less waste being produced. The present invention further provides the use of solid ammonium halide and a further reactant selected from the group consisting of a metal, a hydride, an imide, an amide, a ceramic compound, and mixtures thereof for the production of hydrogen.

The material system of the present invention comprises the solid ammonium halide and the further reactant. These materials may be mixed or separate in the material system of the present invention.

The solid ammonium halide of the present invention may be selected from the group consisting of  $\text{NH}_4\text{F}$ ,  $\text{NH}_4\text{Cl}$ ,  $\text{NH}_4\text{Br}$  and  $\text{NH}_4\text{I}$ . The solid ammonium halide may include more than one solid ammonium halide, e.g. 2, 3 or 4 solid ammonium halides. For example, the solid ammonium halide may include  $\text{NH}_4\text{Cl}$  and  $\text{NH}_4\text{Br}$ .

In one embodiment of the present invention, the solid ammonium halide is  $\text{NH}_4\text{Cl}$ . This is preferred over other types of halide because of the ease with which hydrogen is released at relatively low temperatures.

It has been surprisingly found that solid ammonium halides are very good at storing hydrogen. The quantity of hydrogen capable of being reversibly absorbed by a solid ammonium halide, by weight percentage, may be within the range of from about 1% to about 12%, about 1% to about 11%, about 2% to about 10%, about 2% to about 9%, about 3% to about 8% or about 3% to about 8%.

The release of hydrogen occurs through the reaction of the solid ammonium halide with a further reactant selected from the group consisting of a metal, a hydride, an imide, an amide, a ceramic compound, and mixtures thereof.

As used herein, the term "metal" is taken to include metalloids, e.g. B and Si, and alloys, e.g. Ti containing Al or Ni in its lattice, and pure and metal-doped intermetallics of the type: AB (TiFe),  $\text{A}_2\text{B}$  ( $\text{Mg}_2\text{Ni}$ ),  $\text{AB}_2$  ( $\text{CeNi}_2$ ),  $\text{AB}_3$  ( $\text{CeNi}_3$ ),  $\text{A}_2\text{B}_7$  ( $\text{Gd}_2\text{Co}_7$ ),  $\text{AB}_5$  ( $\text{LaNi}_5$ ), and mixtures thereof. As used herein, the term "a further reactant" covers "one or more further reactants", e.g. one or more hydrides ( $\text{LiH}$ ,  $\text{LiNH}_4$ ,  $\text{BNH}_6$ ).

Where the further reactant is a metal, it may comprise one or more of the metals selected from the group consisting of alkali, alkaline earth, transition metals, and other metals, e.g. Li, B, Na, Mg, Al, Si, K and Ca.

The term "hydride" refers to a compound comprising hydrogen and one or more other elements or chemical groups that are more electropositive than hydrogen, including metal hydrides, e.g. LiH,  $\text{MgH}_2$ ,  $\text{NaAlH}_4$  and  $\text{BNH}_6$ , and non-metal hydrides, e.g.  $\text{H}_2\text{O}$ ,  $\text{NH}_3$ ,  $\text{H}_2\text{S}$ ,  $\text{CH}_4$ .

In one embodiment, the hydride is a metal hydride. The metal hydride may comprise one or more of the metals selected from the group consisting of alkali, alkaline earth, transition metals, other metals and metalloids, e.g. Li, B, Na, Mg, Al, Si, K and Ca. The metal hydride may comprise more than one of these metals, e.g. 2, 3, 4, 5 or 6 metals. In this respect, the metal hydride may be represented by the formula  $\text{MiM}_2\text{H}_x$ , wherein  $x = 1$  to 4 and  $\text{Mi}$  and  $\text{M}_2$  are selected from the group consisting of alkali, alkaline earth, transition metals, other metals and metalloids, e.g. Li, B, Na, Mg, Al, Si, K and Ca.  $\text{Mi}$  and  $\text{M}_2$  may be the same or different. One of  $\text{Mi}$  and  $\text{M}_2$  may be a non-metal, e.g. N, O, or C.

The metal hydride may include more than one metal hydride, e.g. 2, 3, 4, 5 or 6 metal hydrides. These metal hydrides may be present as a mixture, e.g.  $(\text{LiH} + \text{LiBH}_4)$ .

In one more specific embodiment, the metal hydride is LiH,  $\text{LiBH}_4$ ,  $\text{NaBH}_4$ , or a mixture thereof. These hydrides are preferred due to their ability of releasing hydrogen from metal halides at relatively low temperatures.

In one embodiment, the hydride is a non-metal hydride. The non-metal hydride may comprise one or more of the non-metallic elements, typically consisting of N, O, C and S. The non-metal hydride may comprise more than one of these elements, e.g. 2, 3, 4, 5 or 6 elements. The non-metal hydride may include more than one non-metal hydride, e.g. 2, 3, 4, 5 or 6 non-metal hydrides. These non-metal hydrides may be present as a mixture (e.g.  $\text{NH}_3 + \text{H}_2\text{O}$ ).

The hydride may be a mixture of one or more metal hydrides and one or more non-metal hydrides, e.g.  $(\text{LiH} + \text{NH}_3)$ .

The term "imide" refers to a compound comprising at least one imide group (NH) and one or more other elements or chemical groups that are more electropositive than the imide, including metal imides and non-metal imides.

In one embodiment, the imide is a metal imide. The metal imide may comprise one or more of the metals selected from the group consisting of alkali, alkaline earth, transition metals, and other metals, e.g. Li, B, Na, Mg, Al, Si, K and Ca. The metal imide may comprise more than one of these metals, e.g. 2, 3, 4, 5 or 6 metals. In this respect, the metal imide may be represented

by the formula  $M_1M_2(NH)_y$ , wherein  $y = 0.5$  to  $2$  and  $M_1$  and  $M_2$  are selected from the group consisting of alkali, alkaline earth, transition metals, and other metals, e.g. Li, B, Na, Mg, Al, Si, K and Ca.  $M_1$  and  $M_2$  may be the same or different.

The metal imide may include more than one metal imide, e.g. 2, 3, 4, 5 or 6 metal imides. These metal imides may be present as a mixture, e.g.  $(Mg(NH)_2 + Al(NH))_5$ .

The term "amide" refers to a compound comprising at least one amide group ( $NH_2$ ) and one or more other elements or chemical groups that are more electropositive than the amide, including metal amides and non-metal amides.

In one embodiment, the amide is a metal amide. The metal amide may comprise one or more of the metals selected from the group consisting of alkali, alkaline earth, transition metals, and other metals, e.g. Li, B, Na, Mg, Al, Si, K and Ca. The metal amide may comprise more than one of these metals, e.g. 2, 3, 4, 5 or 6 metals. In this respect, the metal amide may be represented by the formula  $MiM_2(NH_2)_y$ , wherein  $y = 1$  to  $4$  and  $Mi$  and  $M_2$  are selected from the group consisting of alkali, alkaline earth, transition metals, and other metals, e.g. Li, B, Na, Mg, Al, Si, K and Ca.  $Mi$  and  $M_2$  may be the same or different.

The metal amide may include more than one metal amide, e.g. 2, 3, 4, 5 or 6 metal amides. These metal amides may be present as a mixture, e.g.  $Li(NH_2) + B(NH_2)_3$ .

In one embodiment the further reactant is a ceramic compound (e.g. an oxide, a carbide or a nitride). Ceramic compounds include metal and non-metal ceramic compounds. Suitable oxide ceramic compounds include one or more metal oxides selected from the group consisting of  $Al_2O_3$ ,  $Ti_xO_y$ ,  $Zr_xO_y$ ,  $Fe_xO_y$ , and  $Nb_xO_y$  ( $x = 1, 2, \text{ or } 3$ ;  $y = 1, 2, \text{ or } 3$ ).

Suitable carbide ceramic compounds include one or more metal carbides and their derivatives selected from the group consisting of TiC, VC, ZrC, HfC, SiC, and NbC.

Suitable nitride ceramic compounds include one or more metal nitrides and their derivatives selected from the group consisting of TiN, VN, ZrN, NbN, AlN, LiN,  $Si_3N_4$ , and BN.

The further reactant may be a mixture of a hydride and/or an imide and/or an amide and/or a ceramic compound. This includes mixtures of one or more hydrides and/or one or more imides and/or one or more amides and/or one or more ceramic compounds.

In one embodiment of the present invention, at least one of the solid ammonium halide and the further reactant is present as one or more particles having a maximum diameter of about 5000 micrometers, alternatively about 500 micrometers, alternatively about 50 micrometers, alternatively about 5 micrometers, alternatively about 500 nanometers, alternatively about 50

nanometers, alternatively about 5 nanometers. This maximum diameter is advantageous because the particle size can be tailored to alter the kinetics of hydrogen release from the materials. It is likely that the smaller particles lead to faster kinetics, albeit at a higher cost. The minimum diameter of the one or more particles may be about 1 nanometer, alternatively about 10 nanometers, alternatively about 100 nanometers, alternatively about 1 micrometers, alternatively about 10 micrometers, alternatively about 100 micrometers. In another embodiment of the present invention, at least one of the solid ammonium halide and the further reactant is present as one or more films having a maximum thickness of about 5000 micrometers, alternatively about 500 micrometers, alternatively about 50 micrometers, alternatively about 5 micrometers, alternatively about 500 nanometers, alternatively about 50 nanometers, alternatively about 5 nanometers. This maximum thickness is advantageous because the film thickness can be tailored to alter the kinetics of hydrogen release from the materials. It is likely that the thinner films lead to faster kinetics, albeit at a higher cost. The minimum thickness of the one or more films may be about 1 nanometer, alternatively about 10 nanometers, alternatively about 100 nanometers, alternatively about 1 micrometers, alternatively about 10 micrometers, alternatively about 100 micrometers. The minimum thickness of the film used may be limited by cost.

In another embodiment of the present invention, at least one of the solid ammonium halide and the further reactant is present as fibres having a maximum diameter of about

5000 micrometers, alternatively about 500 micrometers, alternatively about 50 micrometers, alternatively about 5 micrometers, alternatively about 500 nanometers, alternatively about 50 nanometers, alternatively about 5 nanometers. This maximum diameter is advantageous because the fibre diameter can be tailored to alter the kinetics of hydrogen release from the materials. It is likely that the thinner fibres lead to faster kinetics, albeit at a higher cost. The minimum diameter of the one or more fibres may be about 1 nanometer, alternatively about 10 nanometers, alternatively about 100 nanometers, alternatively about 1 micrometers, alternatively about 10 micrometers, alternatively about 100 micrometers. The minimum diameter of the fibre used may be limited by cost.

In one embodiment, the solid ammonium halide and the further reactant are present in different forms. That is, the solid ammonium halide may be present as a particle, as described above, and the further reactant may be present as a film, as described above. Alternatively, the solid ammonium halide may be present as a particle, as described above, and the further reactant may be present as a fibre, as described above. Alternatively, the solid ammonium halide may be present as a film, as described above, and the further reactant may be present as a particle, as described above. Alternatively, the solid ammonium halide may be present as a film, as described above, and the further reactant may be present as a fibre, as described above. Alternatively, the solid ammonium halide may be present as a fibre, as described above, and

the further reactant may be present as a particle, as described above. Alternatively, the solid ammonium halide may be present as a fibre, as described above, and the further reactant may be present as a film, as described above.

In one embodiment, the solid ammonium halide may be of a different particle diameter, film thickness, and/or fibre diameter to the further reactant. In this embodiment, the ratios of the maximum diameters of the solid ammonium halide and the further reactant may be about 10:1, alternatively about 1 :1, alternatively about 1 :10. These ratios are advantageous because they allow for the control of hydrogen purity and kinetics in the relevant systems.

The solid ammonium halide and the further reactants used herein are either available commercially, e.g. from "Fisher Scientific" catalogues ([www.fisher.co.uk](http://www.fisher.co.uk)), and/or can be synthesised using known synthesis routes at relatively low costs. For instance,  $\text{NH}_4\text{Cl}$  can be readily synthesised by reacting  $\text{NH}_3$  with  $\text{HCl}$  (Egon Wiberg, Arnold Frederick Holleman, *Inorganic Chemistry*, Elsevier, 2001).

The solid ammonium halide and/or the further reactant may be milled to the required particle diameter. The person skilled in the art will appreciate that there are a number of methods known in the art which can be used to produce particles having a certain diameter. It is further known that particle diameter may be varied by adjusting certain milling process conditions such as:

i) Ball/powder weight ratio from about 1 : 1 to about 30: 1 ; ii) Length of milling time; iii) Diameter of milling balls from about 1 to about 30 mm; iv) Use of process control agents (e.g. methanol or ethanol); v) Nature of milling media (e.g. hardened steel or WC+Co); vi) Atmosphere (e.g.  $\text{H}_2$  or Ar); and vii) Use of cryogenic milling temperature from 0 to - 196 °C (77K); viii) Use of a high-pressure milling condition from 1 to 700 bars.

In the present invention, the ratio of the amount of solid ammonium halide to the further reactant may be about 10:1, alternatively about 1 :1, alternatively about 1 :10. This is advantageous because the ratio can be altered to control hydrogen purity and release kinetics.

In one embodiment, at least one of the solid ammonium halide and/or the further reactant is present on a support. The support may be any suitable support known in the art. In particular, the support may be selected from the group consisting of porous materials, honeycomb structures, zeolites, metal-organic frameworks, porous polymers and nanostructures of carbon or boron-nitride. The use of a support is advantageous because it improves the reaction conditions, reaction homogeneity, reaction kinetics and the management of reaction heat.

The material system of the present invention may contain a catalyst. As used herein, a "catalyst" is a material which enhances the hydrogen release properties of the aforementioned solid ammonium halide and the further reactant.

The catalyst may be selected from the group consisting of a transition metal, an alloy of one or more transition metals, a metal oxide, a metal carbide, a metal nitride and a metal halide and mixtures thereof.

Transition metal catalysts and catalysts comprising transition metal alloys may include one or more transition metals selected from the group consisting of Pt, Pd, Ni, Rh, Ru, Fe, Co, Ti, Zr, Nb, Mo, and V.

Metal oxide catalysts may include one or more metal oxides selected from the group consisting of  $\text{Al}_2\text{O}_3$ ,  $\text{Ti}_x\text{O}_y$ ,  $\text{Zr}_x\text{O}_y$ ,  $\text{Fe}_x\text{O}_y$ , and  $\text{Nb}_x\text{O}_y$  ( $x = 1, 2, \text{ or } 3$ ;  $y = 1, 2, \text{ or } 3$ ).

Metal carbide catalysts may include one or more metal carbides and their derivatives selected from the group consisting of TiC, VC, ZrC, HfC, SiC, and NbC. Metal nitride catalysts may include one or more metal nitrides and their derivatives selected from the group consisting of TiN, VN, ZrN, NbN, AlN,  $\text{Li}_5\text{N}$ ,  $\text{Si}_3\text{N}_4$ , and BN.

Metal halide catalysts may include one or more metal halides selected from the group consisting of  $\text{TiCl}_x$  (wherein  $x = 1 \text{ to } 3$ ),  $\text{FeCl}_3$ ,  $\text{AlCl}_3$ ,  $\text{ZnCl}_2$ ,  $\text{MgCl}_2$  and  $\text{BF}_3$ .

In one embodiment, the catalyst is present on a support. The support may be any suitable support known in the art. In particular, the support may be selected from the group consisting of porous materials, honeycomb structures, zeolites, metal-organic frameworks, porous polymers and nano structures of carbon or boron-nitride. The use of a support is advantageous because it improves the reaction conditions, reaction kinetics and the management of reaction heat, as well as reducing the cost of catalysts. The catalyst support may be the same support as that comprising the solid ammonium halide and/or the further reactant.

The material system of the present invention may be present in a device. The device may be a device for producing hydrogen.

The device of the present invention may provide the solid ammonium halide in a first compartment and the further reactant in at least a second compartment. Such a device may also comprise a means for mixing the solid ammonium halide and the further reactant.

The first and second compartments may be separate compartments.

The means for mixing the solid ammonium halide and the further reactant may be any suitable means known in the art. In particular, the means for mixing may be by a powder mixer, a blender, and ball mill under controlled speed and temperature, e.g. low or cryogenic temperatures.

The ammonium halide and the further reactant may be pre-packed in separate layers or compartments for easy storage and only allowed to mix at the point or time of use. The device of the present invention may be a fuel cell or a hydrogen combustion engine. In particular, the device may be a fuel cell for a mobile telephone, a portable electronic device, an emergency back-up power device or a fuel cell vehicle.

As mentioned previously, the present invention further provides a method for producing hydrogen by reacting solid ammonium halide and a further reactant selected from the group consisting of a metal, a hydride, an imide, an amide, a ceramic compound, and mixtures thereof.

As also mentioned previously, the present invention further provides a method for producing hydrogen using the material system or device of the present invention.

The methods of the present invention may produce hydrogen at a temperature of about 200°C or less, alternatively about 150°C or less, alternatively about 130°C or less, alternatively about 100°C or less, alternatively about 90°C or less, alternatively about 80°C or less, alternatively about 70°C or less, alternatively about 60°C or less, alternatively about 50°C or less, alternatively about ambient temperature (i.e. from about 20°C to about 23.5°C). These low temperatures are advantageous for practical applications such as for on-board fuel cell vehicles because they increase the safety of the hydrogen production device.

As also mentioned previously, the present invention further provides a method of hydrogen absorption, said method comprising the steps of subjecting the dehydrogenated product of the hydrogen production methods of the present invention to hydrogen at a pressure of from about 0.1 to about 70 MPa and a temperature of from about 20 to about 600°C to produce a solid ammonium halide and a further reactant selected from the group consisting of a metal, a hydride, an imide, an amide, a ceramic compound, and mixtures thereof. This reverses the hydrogen production process to hydrogenate the dehydrogenated products back into the ammonium halide and the further reactant for re-use if required. This provides easy recycling of the material systems and devices of the present invention resulting in less waste being produced. The pressure to which the dehydrogenated product is subjected is from about 0.1 to about 70 MPa, alternatively from about 0.2 to about 50 MPa, alternatively from about 0.2 to about 35 MPa, alternatively from about 0.2 to about 20 MPa, alternatively from about 0.2 to about 10 MPa, alternatively from about 0.2 to about 1.0 MPa.

The temperature to which the dehydrogenated product is subjected is from about 20 to about 600°C, alternatively from about 20 to about 400 °C, alternatively from about 20 to about 200 °C, alternatively from about 20 to about 100 °C, alternatively from about 20 to about 80 °C.



The methods of the present invention may be carried out in a fuel cell, in particular a fuel cell comprising a material system according to the present invention.

The present invention is now described, by way of illustration only, with reference to the accompanying figures, in which:

Figure 1 shows the hydrogen produced from a  $\text{NH}_4\text{Cl}$ ,  $\text{LiH}$  system from 0 to 300 °C (the horizontal axis is temperature) with

Figure 1(a); showing mass spectrometry analysis showing hydrogen and other residual gases; and

Figure 1(b) showing the sample weight-loss due to the release of hydrogen and other residual gases (temperature-programmed desorption) as a function of temperature;

Figure 2 shows the hydrogen produced from a  $\text{NH}_4\text{Cl}$ ,  $\text{LiBH}_4$  system from 0 to 300 °C

(the horizontal axis is temperature) with Figure 2(a) showing mass spectrometry analysis showing hydrogen and other residual gases; and

Figure 2(b) showing the sample weight-loss due to the release of hydrogen and other residual gases (temperature-programmed desorption) as a function of temperature;

Figure 3 shows the hydrogen produced from a  $\text{NH}_4\text{Cl}$ ,  $\text{LiBH}_4$ ,  $\text{LiH}$  system from 0 to 300 °C (the horizontal axis is temperature) with

Figure 3 (a) showing mass spectrometry analysis showing hydrogen and other residual gases; and Figure 3(b) showing the sample weight-loss due to the release of hydrogen and other residual gases (temperature-programmed desorption) as a function of temperature; Figure 4 shows the hydrogen produced from a  $\text{NH}_4\text{Cl}$ ,  $\text{NaBH}_4$  system from 0 to 300 °C (the horizontal axis is temperature) with Figure 4(a) showing mass spectrometry analysis showing hydrogen and other residual gases; and

Figure 4(b) showing the sample weight-loss due to the release of hydrogen and other residual gases (temperature-programmed desorption) as a function of temperature.

The invention is further illustrated by the following examples. It will be appreciated that the examples are for illustrative purposes only and are not intended to limit the invention as described above. Modification of detail may be made without departing from the scope of the invention.

#### Examples

#### Example 1 - $\text{NH}_4\text{Cl}$ and $\text{LiH}$

$\text{NH}_4\text{Cl}$  is milled for 1 minute with  $\text{LiH}$  by high energy milling in a stainless steel pot using a ball to power ratio of 10 to 1. The materials obtained after milling can release a large amount of hydrogen at a temperature as low as  $150^\circ\text{C}$  through thermolysis, as shown in Figure 1. The desorption of hydrogen is accompanied by the release of ammonia that can either be removed from the gas stream or further decomposed to produce hydrogen.

#### Example 2 - $\text{NH}_4\text{Cl}$ and $\text{LiBH}_4$

$\text{NH}_4\text{Cl}$  is milled for 1 minute with  $\text{LiBH}_4$  by high energy milling in a stainless steel pot using a ball to power ratio of 10 to 1. The materials obtained after milling can release a large amount of pure hydrogen ( $\sim 7 \text{ wt}\%$ ) at a temperature as low as  $60^\circ\text{C}$  through thermolysis, as shown in Figure 2. Further hydrogen can be released at higher temperatures ( $>100^\circ\text{C}$ ). The desorption of hydrogen above  $100^\circ\text{C}$  is accompanied by the release of a small amount of ammonia that can either be removed from the gas stream or further decomposed to produce hydrogen.

#### Example 3 - $\text{NH}_4\text{Cl}$ , $\text{LiBH}_4$ and $\text{LiH}$

$\text{NH}_4\text{Cl}$  is milled for 1 minute with  $\text{LiBH}_4$  and  $\text{LiH}$  (ratio 3:3:1) by high energy milling in a stainless steel pot using a ball to power ratio of 10 to 1. The materials obtained after milling can release pure hydrogen (3 wt%) at a temperature as low as  $50^\circ\text{C}$  through thermolysis, as shown in Figure 3. Further hydrogen is released from  $80^\circ\text{C}$ . The desorption of hydrogen above  $80^\circ\text{C}$  is accompanied by the release of a small amount of ammonia that can either be removed from the gas stream or further decomposed to produce hydrogen. The addition of  $\text{LiH}$  considerably reduces the release of ammonia in favour of hydrogen production.

#### Example 4 - $\text{NH}_4\text{Cl}$ and $\text{NaBH}_4$

$\text{NH}_4\text{Cl}$  is milled for 1 minute with  $\text{NaBH}_4$  by high energy milling in a stainless steel pot using a ball to power ratio of 10 to 1. The materials obtained after milling can release pure hydrogen (3 wt%) at a temperature of  $150^\circ\text{C}$  through thermolysis, as shown in Figure 4.

## PATENT CITATIONS

Cited Patent	Filing date	Publication date	Applicant	Title
<a href="#">JPS50148291A</a> *				<i>Title not available</i>
<a href="#">US3734863</a> *	11 Jun 1971	22 May 1973	Us Navy	Hydrogen generating compositions
<a href="#">US3977990</a> *	30 Oct 1974	31 Aug 1976	The United States Of America As Represented By The Secretary Of The Navy	Controlled generation of cool hydrogen from solid mixtures
<a href="#">US4341651</a> *	26 Aug 1980	27 Jul 1982	The United States Of America As Represented By The Secretary Of The Navy	Compositions and methods for generation of gases containing hydrogen or hydrogen isotopes
<a href="#">US20070084879</a> *	2 Oct 2006	19 Apr 2007	McLean Gerard F	Hydrogen supplies and related methods

\* Cited by examiner

## NON-PATENT CITATIONS

Reference	
1	BERG CHEM. COMMUN. vol. 6, 2008, page 668
2	* F.E. PINKERTON: " <a href="#">Decomposition kinetics of lithium amide for hydrogen storage materials</a> " JOURNAL OF ALLOYS AND COMPOUNDS, vol. 400, 10 May 2005 (2005-05-10), pages 76-82, XP002598854
3	* G. MEYER, TH. STAFFEL, S. DÖTSCH, TH. SCHLEID: " <a href="#">Versatility and Low Temperature Synthetic Potential of Ammonium Halides</a> " INORGANIC CHEMISTRY, vol. 24, 10 October 1985 (1985-10-10), pages 3504-3505, XP002598853
4	LAI-PENG MA ET AL. JOURNAL OF PHYSICAL CHEMISTRY C vol. 112, no. 46, 2008, pages 18280 - 18285

Reference	
5	P. CHEN, Z ET AL. NATURE vol. 420, 2002, pages 302 - 304
6	YUN HANG HU ET AL. JOURNAL OF PHYSICAL CHEMISTRY A vol. 107, no. 46, 2003, pages 9737 - 9739

\* Cited by examiner

## CLASSIFICATIONS

International Classification	<a href="#">C01B3/06</a> , <a href="#">C01B3/00</a>
Cooperative Classification	<a href="#">C01B3/001</a> , <a href="#">C01B3/00</a> , <a href="#">Y02E60/362</a> , <a href="#">C01B3/065</a> , <a href="#">Y02E60/324</a>
European Classification	C01B3/00, C01B3/00D2, C01B3/06C

## LEGAL EVENTS

Date	Code	Event	Description
19 Jan 2011	121	Ep: the epo has been informed by wipo that ep was designated in this application	<b>Ref document number:</b> 10724553 <b>Country of ref document:</b> EP <b>Kind code of ref document:</b> A1
29 Nov 2011	NENP	Non-entry into the national phase in:	<b>Ref country code:</b> DE
4 Jul 2012	122	Ep: pct app. not ent. europ. phase	<b>Ref document number:</b> 10724553 <b>Country of ref document:</b> EP <b>Kind code of ref document:</b> A1

## Appendix 2 Poster

# Hydrogen stores based on $\text{LiBH}_4$

**K.G. ANGUIE, K.F. AGUEY-ZINSOU\* and Z.X. GUO\***

School of Engineering and Materials, Queen Mary, University of London, LONDON, E1 4NS

\*Department of Chemistry, University College London, LONDON, WC1H 0AJ



g.k.anguie@qmul.ac.uk



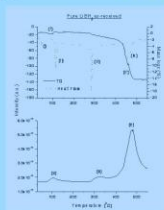
### Introduction

The primary aim of this project was the development of an inorganic  $\text{LiBH}_4$ -based material for effective use in hydrogen storage. To do so, we investigated  $\text{LiBH}_4$  and the possibility to destabilize this material in order to release a maximum of its hydrogen content. Why  $\text{LiBH}_4$ ? Lithium borohydride has one of the greatest hydrogen content among hydride materials: **18.5 wt.%**. However,  $\text{LiBH}_4$  only decomposes at temperatures above  $400^\circ\text{C}$ (\*) and the reaction is reversible(\*\*) (\*\*\*) under severe conditions of temperature ( $600^\circ\text{C}$ ) and pressure (155 bars). We tried to evaluate the impact of well chosen chemical additions to its thermostability.

### Materials and methods

To improve the thermodynamics, we added chlorides to substitute Li cation in order to weaken the bonds inside  $\text{BH}_4$  group.  
 $\text{LiBH}_4 + \text{MCl}_n \rightarrow \text{M}(\text{BH}_4)_n + \text{LiCl}$   
 Another strategy was to perform a direct substitution of H with elemental sulfur.  
 $\text{LiBH}_4 + n\text{S} \rightarrow \text{LiBH}_{4-2n}\text{S}_n + n\text{H}_2$   
 The desorption characteristics of the reactive mixtures prealably milled were comparatively studied by simultaneous TG, DTA and MS for further understanding of the destabilization of  $\text{LiBH}_4$  and some structural analysis such as XRD and FT-IR were carried out to elucidate the different steps of the decomposition.

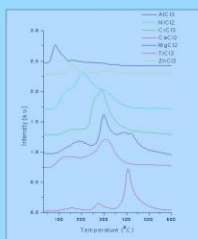
### Results



Thermal decomposition of  $\text{LiBH}_4$

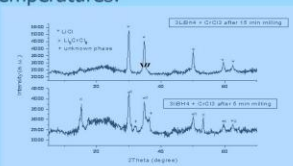
The main hydrogen desorption peak is around  $450^\circ\text{C}$ . There are 3 DTA peaks. 75% hydrogen content have been desorbed.

After 5 minutes of milling, we obtained for the main hydrogen desorption peak a temperature below  $400^\circ\text{C}$  except for the  $\text{CaCl}_2$  addition which has the same profile as pure  $\text{LiBH}_4$ . For  $\text{AlCl}_3$  and  $\text{ZnCl}_2$ , the main desorption peaks were below  $150^\circ\text{C}$ .



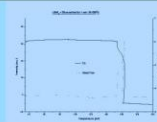
Hydrogen desorption profiles for different chlorides-added  $\text{LiBH}_4$

By mechanical milling, the reaction can be initiated with hydrogen liberated from  $\text{LiBH}_4$  at low temperatures.



After 5 minutes, the reaction has already started.  
After 15 minutes, the reaction is completed

We obtained a vigorous and exothermic reaction accompanied with a small  $\text{H}_2$  detection and many other by-products.



TG-DTA of  $\text{LiBH}_4 + 2\text{S}$

### Discussion

First, by using a metathesis route and by means of suitable chlorides,  $\text{LiBH}_4$  can be destabilised and hydrogen released at temperatures as low as  $100^\circ\text{C}$ . As a result, the main issue is that there is a trade-off between the storage capacity and the decrease in the release temperature. From 18.5 wt.%, we reached capacities comprised between only 4.5 and 6.1 wt.%. Also, for all sulfur-added systems, we found around  $150^\circ\text{C}$  an exothermic transformation that leads to a release of hydrogen but also other by-products such as hydrogen sulphide? This by-product is very detrimental to the fuel cells application.

### Conclusion

To conclude, further work on destabilisation strategies needs to be carried out but also on the reversibility of the most promising systems.

### References

- (\*) A. Zuttel et al, J. Alloy. Compds. 356-357 (2003) 515-520
- (\*\*) P. Mauron, J. Phys. Chem. B 112 (2007) 906-910
- (\*\*\*) O. Friedrichs, Acta Mater 56 (2008) 949-954

### Acknowledgements



EPSRC through UK-SHEC and SUPERGEN programs and networks

## **References**

**Chapter 1: General Introduction**

- [1] T. Riis *et al.*, Hydrogen production R&D: priorities and gaps, *OECD/IEA Publications*, 2006
  
- [2] D. L. Stojic, *et al.*, Hydrogen generation from water electrolysis – possibilities of energy saving, *Journal of Power Sources*, 2003, Vol. 118, pp. 315-319
  
- [3] H. I. Karunadasa, C. J. Chang and J. R. Long, A molecular molybdenum-oxo catalyst for generating hydrogen from water, *Nature*, 2010, Vol. 464, pp. 1329-1333

**Chapter 2: Literature review**

- [4] C. C. Elam, C. E. Gregoire Padro, G. Sandrock, A. Luzzi, P. Lindblad, E. F. Hagen, realizing the hydrogen future: the International Energy Agency's efforts to advance hydrogen energy technologies, *International Journal of Hydrogen Energy*, 2003, Vol. 28, pp. 601-607
  
- [5] Gary Sandrock, Overview of Hydrogen Storage: Gas. Liquid and solid, *DO-EERE/NIST Joint Workshop on Combinatorial Materials Science for Applications in Energy (MCMC-14)*, November 5, 2008
  
- [6] Li Zhou, Progress and problems in hydrogen storage methods, *Renewable and sustainable energy reviews*, 2005, Vol. 9, pp. 395-408

- [7] A.J. Kidnay and M.J. Hiza, High Pressure Adsorption Isotherm of Neon, Hydrogen and Helium at 76K, *Advances in Cryogenic Engineering*, 1967, Vol. 12, pp. 730
- [8] R. Chahine and T.K. Bose, Low-pressure adsorption storage of hydrogen, *International Journal of Hydrogen Energy*, 1994, Vol. 19, pp. 161-164
- [9] A.C. Dillon, K.E.H. Gilbert, P.A. Parilla, J.L. Alleman, G.L. Hornyak, K.M. Jones and M.J. Heben, Hydrogen storage in carbon single-wall nanotubes, *Proceedings of the 2002 U.S. DOE Hydrogen Program Review*, NREL/CP-610-32405
- [10] A.C. Dillon, K.M. Jones, T.A. Bekkedahl, C.H. Klang, D.S. Bethune and M.J. Heben, Storage of hydrogen in single-walled carbon nanotubes, *Nature*, 1997, Vol. 386, pp. 377-379
- [11] R. Strobel *et al.*, Hydrogen storage by carbon materials, *Journal of Power sources*, 2006, Vol. 159, pp. 781-801
- [12] A. R. Biris *et al.*, Hydrogen Storage in Carbon-Based Nanostructured Materials, *Particulate Science and Technology*, 2008, Vol. 26, issue 4, pp. 297 - 305



- [13] E. Poirier, R. Chahine and T.K. Bose, Hydrogen adsorption in carbon nanostructures, *International Journal of Hydrogen Energy*, 2001, Vol. 26, issue 8, pp. 831-835
- [14] Y. Ye *et al.*, Hydrogen adsorption and cohesive energy of single-walled carbon nanotubes, *Applied Physics Letters*, 1999, Vol. 74, p 2307
- [15] P. Guay, B.L. Stansfield and A. Rochefort, On the control of carbon nanostructures for hydrogen storage applications, *Carbon*, 2004, Vol. 42, pp. 2187-2193
- [16] E. Poirier, R. Chahine, P. Benard, D. Cossement, L. Lafi, E. Melancon, T.K. Bose and S. Desilets. Storage of hydrogen on single-walled carbon nanotubes and other carbon structures, *Applied Physics A: Materials Science and Processing*, 2004, Vol. 78, Issue 7, pp. 961-967
- [17] B.K. Pradhan, experimental probes of the molecular hydrogen-carbon nanotube interaction, *Physica B*, 2002, Vol.323, pp. 115-121
- [18] M. Hirscher *et al*, Hydrogen storage in carbon nanostructures, *Journal of Alloys and Compounds*, 2002, Vol. 330-332, pp. 654-658
- [19] A.D. Lueking and R.T. Yang, Hydrogen spillover to enhance hydrogen storage – study of the effect of carbon physicochemical properties, *Applied Catalysis A: General*, 2004, Vol. 265, pp. 259-268

- [20] S. A. Shevlin and Z. X. Guo, High-Capacity Room-Temperature Hydrogen Storage in Carbon Nanotubes via Defect-Modulated Titanium Doping, *Journal of Physical Chemistry C*, 2008, Vol. 112, pp. 17456-17464
- [21] Y. Xia *et al.*, Hydrogen Storage in High Surface Area Carbons: Experimental Demonstration of the Effects of Nitrogen Doping, *Journal of the American Chemical Society*, 2009, Vol. 13, pp. 16493-16499
- [22] A. Dyer, An introduction to Zeolite molecular sieves, Wiley, Chichester, 1988, pp. 87, ISBN 0-471-91981-0
- [23] J. Weitkamp, M. Fritz and S. Ernst, Zeolites as media for Hydrogen storage, *International Journal of Hydrogen Energy*, 1995, Vol. 20, Issue 12, pp. 967-970
- [24] H.W. Langmi *et al.*, Hydrogen adsorption in zeolites A, X, Y and RHO, *Journal of Alloys and Compounds*, 2003, Vol. 356-357, pp. 710-715
- [25] Y. Li and RT Yang, Hydrogen storage in low-silica type X Zeolites, *Journal of Physical Chemistry B*, 2006, Vol. 110, Issue 34, pp. 17175-17181
- [26] M. Hirscher, B. Panella and B. Schmitz, Metal-organic frameworks for hydrogen storage, *Microporous and Mesoporous Materials*, 2010, Vol. 129, pp. 335-339

- [27] H. Li *et al.*, Design and synthesis of an exceptionally stable and highly porous MOF, *Nature*, 1999, Vol. 402, pp. 276-279
- [28] N. L. Rosi *et al.*, Hydrogen storage in microporous MOF, *Science*, 2003, Vol. 300, pp. 1127-1129
- [29] B. Panella *et al.*, Hydrogen adsorption in metal-organic frameworks: Cu-MOFs and Zn-MOFs compared, *Advanced Functional Materials*, 2006, Vol. 16, pp. 520–524
- [30] A. Dailly, J. Vajo and C. Anh, Saturation of hydrogen sorption in Zn-Benzenedicarboxylate and Zn-naphtalenedicarboxylate, *Journal of Physical Chemistry*, 2006, Vol. 110, Issue 3, pp. 1099-1101
- [31] X. Lin *et al.*, High H<sub>2</sub> adsorption by coordination-framework materials, *Angewandte Chemie International Edition*, 2006, Vol. 45, issue 44, pp. 7358-7364
- [32] B. Xiao and Q. Yuan, Nanoporous metal organic framework materials for hydrogen storage, *Particuology*, 2009, Vol. 7, pp. 29-40
- [33] W. L. Mao *et al.*, Hydrogen clusters in clathrate hydrate, *Science*, 2002, Vol. 297, Issue 5590, pp. 2247-2249
- [34] H. Lee *et al.*, tuning clathrates for hydrogen storage, *Nature*, 2005, Vol. 434, pp. 743-746

- [35] G. Sandrock, A panoramic overview of hydrogen storage alloys from a gas reaction point of view, *Journal of Alloys and Compounds*, 1999, Vol. 293-295, pp. 877-888
- [36] L. Schlapbach and A. Züttel, Hydrogen-storage for mobile applications, *Nature*, 2001, Vol. 414, pp. 353-358
- [37] E. David, An overview of advanced materials for hydrogen storage, *Journal of Materials Processing Technology*, 2005, Vol. 162-163, pp. 169-177
- [38] G. Sandrock and G. Thomas, The IEA/DOE/SNL On-Line Hydride Databases, *Applied Physics A: Materials Science and Processing*, 2001, Vol. 72, Issue 2, pp. 153-155
- [39] B. Sakintuna, F. Lamari-Darkrim and M. Hirscher, Metal hydride materials for solid hydrogen storage: A review, *International Journal of Hydrogen Energy*, 2007, Vol. 32, pp. 1121-1140
- [40] B. Bogdanovic *et al.*, Thermodynamic investigation of the magnesium-hydrogen system, *Journal of Alloys and Compounds*, 1999, Vol. 288, pp. 84-92
- [41] Z.X. Guo, C. Shang and K.F. Aguey-Zinsou, Materials challenges for hydrogen storage, *Journal of the European Ceramic Society*, 2008, Vol. 28, Issue 7, pp. 1467-1473

- [42] B. Bogdanovic and M. Schwickardi, Ti-doped alkali metal aluminium hydrides as potential novel reversible hydrogen storage materials, *Journal of Alloys and Compounds*, 1997, Vol. 253-254, pp. 1-9
- [43] M. Fichtner, O. Fuhr *et al.*, Magnesium alanate - a material for reversible hydrogen storage? , *Journal of Alloys and Compounds*, 2003, Vol. 356-357, pp. 418-422
- [44] B. Bogdanovic, R. A. Brand, A. Marjanovic, M. Schwickardi and J. Tölle, Metal-doped sodium aluminium hydrides as potential hydrogen storage materials, *Journal of Alloys and Compounds*, 2000, Vol. 302, Issue 1-2, pp. 36-58
- [45] T.N. Dymova *et al.*, *Doklady Akademiia nauk SSSR*, 1974, Vol. 215, pp. 1369
- [46] I.P. Jain, Pragya Jain and Ankur Jain, Novel hydrogen storage materials: A review of lightweight complex hydrides, *Journal of Alloys and Compounds*, 2010, Vol. 503, pp. 303-339
- [47] A. Zaluska, L. Zaluski *et al.*, Sodium alanates for reversible hydrogen storage materials, *Journal of Alloys and Compounds*, 2000, Vol. 298, pp. 125-134
- [48] R.T. Walters and J.H. Scogin, A reversible hydrogen storage mechanism for sodium alanate: the role of alanes and the catalytic effect of the dopant, *Journal of Alloys and Compounds*, 2004, Vol. 379, pp. 135-142

- [49] K.J. Gross, G.J. Thomas *et al.*, Catalyzed alanates for hydrogen storage, *Journal of Alloys and Compounds*, 2002, Vol. 330-332, pp. 683-690
- [50] V. P. Balema *et al.*, Titanium catalysed solid-state transformations in  $\text{LiAlH}_4$  during high-energy ball-milling, *Journal of Alloys and Compounds*, 2001, Vol. 329, Issue 1-2, pp. 108-114
- [51] M. Resan *et al.*, Effects of various catalysts on hydrogen release and uptake characteristics of  $\text{LiAlH}_4$ , *International Journal of Hydrogen Energy*, 2005, Vol. 30, Issue 13-14, pp. 1413-1416
- [52] Y. Kojima, Y. Kawai, M. Matsumoto and T. Haga, Hydrogen release of catalysed lithium aluminium hydride by a mechanochemical reaction, *Journal of Alloys and Compounds*, 2008, Vol. 462, pp. 275-278
- [53] T. Sun *et al.*, The effect of doping  $\text{NiCl}_2$  on the dehydrogenation properties of  $\text{LiAlH}_4$ , *International Journal of Hydrogen Energy*, 2008, Vol. 33, Issue 21, pp. 6216-6221
- [54] J. Chen *et al.*, Reversible hydrogen storage via titanium-catalyzed  $\text{LiAlH}_4$  and  $\text{Li}_3\text{AlH}_6$ , *Journal of Physical Chemistry B*, 2001, Vol. 105, Issue 45, pp. 11214-11220

- [55] J. Wang, A.D. Ebner and J.A. Ritter, On the reversibility of hydrogen storage in novel complex hydrides, *Adsorption*, 2005, Vol. 11, pp. 811-816
- [56] H. Morioka *et al*, Reversible hydrogen decomposition of  $\text{KAlH}_4$ , *Journal of Alloys and Compounds*, 2003, Vol. 353, pp. 310-314
- [57] J.R. Ares, K-F Aguey-Zinsou *et al*, Hydrogen absorption/desorption mechanism in potassium alanate ( $\text{KAlH}_4$ ) and enhancement by  $\text{TiCl}_3$  doping, *Journal of Physical Chemistry C*, 2009, Vol. 113, pp. 6845-6851
- [58] R. Janot, Metallic amides and imides as new materials for reversible storage, *Annales de Chimie et de Science des Materiaux*, 2005, Vol. 30, Issue 5, pp. 505-517
- [59] K. Miwa, N. Ohba *et al.*, First principles on the thermodynamical stability of metal borohydrides:  $\text{Al}(\text{BH}_4)_3$ , *Journal of Alloys and Compounds*, 2007, Vol. 446-447, pp. 310-314
- [60] S.A. Shevlin and Z.X. Guo, Density functional theory simulations of complex hydride and carbon-based hydrogen storage materials, *Chemical Society Reviews*, 2009, Vol. 38, pp. 211-225
- [61] P. Chen, Z. Xiong, J. Luo, J. Lin and K.L. Tan, Interaction between lithium amide and lithium hydride, *Journal of Physical Chemistry B*, 2003, Vol. 110, Issue 13, pp. 7062-7067

- [62] Y.H. Hu and E. Ruckenstein, Ultrafast High reversible hydrogen capacity of  $\text{LiNH}_2/\text{Li}_3\text{N}$  mixtures, *Industrial and Engineering Chemistry Research*, 2005, Vol. 44, pp. 1510-1513
- [63] Y.H. Hu and E. Ruckenstein, Ultrafast reaction between  $\text{Li}_3\text{N}$  and  $\text{LiNH}_2$  to prepare the effective hydrogen storage material  $\text{Li}_2\text{NH}$ , *Industrial and Engineering Chemistry Research*, 2006, Vol. 45, pp. 4993-4998
- [64] T. Ichikawa, N. Hanada, S. Isobe, H. Leng and H. Fujii, Mechanism of novel reaction from  $\text{LiNH}_2$  and  $\text{LiH}$  to  $\text{Li}_2\text{NH}$  and  $\text{H}_2$  as a promising hydrogen storage system, *Journal of Physical Chemistry B*, 2003, Vol. 108, pp. 7887-7892
- [65] Y. Song and Z.X. Guo, Electronic structure, stability and bonding of the Li-N-H hydrogen storage system, *Physical Review B*, 2006, Vol. 74, p. 195120
- [66] K-F Aguey-Zinsou, J. Yao and Z.X. Guo, Reaction paths between  $\text{LiNH}_2$  and  $\text{LiH}$  with effects of nitrides, *Journal of Physical Chemistry B*, 2007, Vol. 111, Issue 43, pp. 12531-12536
- [67] L.L. Shaw *et al*, Effects of mechanical activation on dehydrogenation of the lithium amide and lithium hydride system, *Journal of Alloys and Compounds*, 2008, Vol. 448, Issues 1-2, pp. 263-271



- [68] Y. Nakamori, G. Kitahara, K. Miwa, N. Ohba, T. Noritake, S. Towata and S. Orimo, Hydrogen storage properties of Li-Mg-N-H systems, *Journal of Alloys and Compounds*, 2005, Vol. 404-406, pp. 396-398
- [69] P. Chen, Z. Xiong, L. Yang, G. Wu and W. Luo, Mechanistic investigations on the heterogeneous solid-state reaction of magnesium amides and lithium hydrides, *Journal of Physical Chemistry B*, 2006, Vol. 110, pp. 14221-14225
- [70] M. Aoki, T. Noritake, G. Kitahara, S. Towata and S. Orimo, Dehydriding reaction of  $\text{Mg}(\text{NH}_2)_2\text{-LiH}$  system under hydrogen pressure, *Journal of Alloys and Compounds*, 2007, Vol. 428, pp. 307-312
- [71] R. Janot, J.-B. Eymery and J.-M. Tarascon, Investigation of the processes for reversible hydrogen storage in the Li-Mg-N-H system, *Journal of Power Sources*, 2007, Vol. 164, pp. 496-502
- [72] Y. Chen, C.-Z. Wu, P. Wang and H-M. Cheng, Structure and hydrogen storage property of ball-milled  $\text{LiNH}_2/\text{MgH}_2$  mixture, *International Journal of Hydrogen Energy*, 2006, Vol. 31, pp. 1236-1240
- [73] Z. Xiong, J. Hu, G. Wu, P. Chen, W. Luo, K. Gross and J. Wang, Thermodynamic and kinetic investigations of the hydrogen storage in the Li-Mg-N-H system, *Journal of Alloys and Compounds*, 2005, Vol. 398, pp. 235-239

- [74] Y. Nakamori, G. Kitahara, and S. Orimo, Synthesis and dehydriding studies of Mg-N-H systems, *Journal of Power Sources*, 2004, Vol. 138, pp. 309-312
- [75] H.Y. Leng, T. Ichikawa, S. Isobe, S. Hino, N. Hanada, and H. Fujii, Desorption behaviours from metal-N-H systems synthesized by ball-milling, *Journal of Alloys and Compounds*, 2005, Vol. 404-406, pp. 443-447
- [76] H.Y. Leng, T. Ichikawa, S. Hino, N. Hanada, S. Isobe, and H. Fujii, Synthesis and decomposition reactions of metal amides in metal-N-H storage system, *Journal of Power Sources*, 2006, Vol. 156, pp. 166-170
- [77] J. Lu, Z. Z. Fang and H. Y. Sohn, A dehydrogenation mechanism of metal hydrides based on interactions between  $H^{\delta+}$  and  $H^-$ , *Inorganic Chemistry*, 2006, Vol. 45, Issue 21, pp. 8749-8754
- [78] W. Luo and S. Sickafoose, Thermodynamic and structural characterization of the Mg-Li-N-H hydrogen storage system, *Journal of Alloys and Compounds*, 2006, Vol. 407, Issues 1-2, pp. 274-281
- [79] S.V. Alapati *et al*, Identification of destabilized metal hydrides for hydrogen storage using first principles calculations, *Journal of Physical Chemistry B*, 2006, Vol. 110, Issue 17, pp. 8769-8776
- [80] Z. Xiong *et al.*, Investigations into the interaction between hydrogen and calcium nitride, *Journal of Materials Chemistry*, 2003, Vol. 13, pp. 1676-1680

- [81] K. Tokyohada, S. Hino *et al.*, Hydrogen desorption/absorption properties of Li-Ca-N-H system, *Journal of Alloys and Compounds*, 2007, Vol. 439, Issues 1-2, pp. 337-341
- [82] J. Lu and Z. Z. Fang, Dehydrogenation of a combined  $\text{LiAlH}_4/\text{LiNH}_2$  system, *Journal of Physical Chemistry B*, 2005, Vol. 109, pp. 20830-20834
- [83] Y. Kojima, M. Matsumoto, Y. Kawai, T. Haga, N. Ohba, K. Miwa, S. Towata, Y. Nakamori and S. Orimo., Hydrogen absorption and desorption by the Li-Al-N-H system, *Journal of Physical Chemistry B*, 2006, Vol. 110, pp. 9632-9636
- [84] Z. Xiong, G. Wu and J. Hu and P. Chen Y, Investigation on chemical reaction between  $\text{LiAlH}_4$  and  $\text{LiNH}_2$ , *Journal of Power Sources*, 2006, Vol. 159, pp. 167-170
- [85] F. E. Pinkerton, G. P. Meisner *et al.*, Hydrogen Desorption exceeding ten weight percent from the new quaternary hydride  $\text{Li}_3\text{BN}_2\text{H}_8$ , *Journal of Physical Chemistry B*, 2005, Vol. 109, Issue 1, pp. 6-8
- [86] F. E. Pinkerton, M. S. Meyer *et al.*, Improved hydrogen release from  $\text{LiB}_{0.33}\text{N}_{0.67}\text{H}_{2.67}$  with noble metal additions, *Journal of Physical Chemistry B*, 2006, Vol. 110, Issue 15, pp. 7967-7974

- [87] G. P. Meisner, M. L. Scullin, M. P. Balogh, F. E. Pinkerton and M. S. Meyer, Hydrogen release from mixtures of Lithium borohydride and Lithium amide: A phase diagram study, *Journal of Physical Chemistry B*, xxxx, Vol. 110, Issue 9, pp. 4186-4192
- [88] M. Aoki, K. Miwa *et al.*, Destabilization of  $\text{LiBH}_4$  by mixing with  $\text{LiNH}_2$ , *Applied Physics A-Materials Science & Processing*, 2005, Vol. 80, Issue 7, pp. 1409-1412
- [89] A. Stock, The hydrides of boron and silicon, *Cornell University Press*, 1933
- [90] J. S. Kasper *et al.*, Sodium Borohydride-Disodium Diborane, *Journal of the American Chemical Society*, 1949, Vol. 71, Issue 7, pp. 2583
- [91] H.I. Schlesinger, R.T. Sanderson and, Metallo borohydrides III. Aluminium borohydride, *Journal of the American Chemical Society*, 1940, Vol. 62, pp. 3421-3424
- [92] A.B. Burg and H.I. Schlesinger, Metallo borohydrides III. Beryllium borohydride, *Journal of the American Chemical Society*, 1940, Vol. 62, pp. 3425-3428
- [93] H.I. Schlesinger and H.C. Brown, Metallo borohydrides III. Lithium borohydride, *Journal of the American Chemical Society*, 1940, Vol. 62, pp. 3429-3435

- [94] E. Wiberg and R. Bauer, in German, *Z. Naturforsch B (Chemical Sciences)*, 1950, Vol. 5, pp. 397-398
- [95] H. I. Schlesinger *et al.*, Reactions of diborane with alkali metal hydrides and their addition compounds. New syntheses of borohydrides. Sodium and potassium borohydrides, *Journal of the American Chemical Society*, 1953, Vol. 75, pp. 199-204
- [96] B.D. James and M.G.H. Wallbridge, Metal borohydrides, *Progress in Inorganic Chemistry*, 1979, Vol. 11, pp. 99-230
- [97] B. M. Bulychev, Alumino- and borohydrides of metals: history, properties, technology and applications, *NATO Science series II: Mathematics, Physics and Chemistry*, 2004, 105
- [98] T. J. Marks and J. R. Kolb, *Chemical reviews*, 1977, Vol. 77, Issue 2, pp. 263-293
- [99] Transition metal hydroborate complexes, series in *Inorganic Chemistry* and *\*Journal of American Chemical Society* :
1. The solid-state structure of borohydridobis(triphenylphosphine)-copper(I), S. J. Lippard and K. M. Melmed, 1967, Vol. 6, issue 12, pp. 2223-2228
  2. The reaction of copper (I) compounds with boron hydride anions, S. J. Lippard and D. Ucko, 1968, Vol. 7, Issue 6, pp. 1051-1056

3. Structure of octahydrotriboratobis(triphenylphosphine)copper (I), S. J. Lippard and K. M. Melmed, 1969, Vol. 8, Issue 12, pp. 2755
  4. Cyanotrihydroborate complexes of the Group Ib metals, S. J. Lippard and P. S. Welcker, 1972, Vol. 11, Issue 1, pp. 6-11
  5. Crystal structure of tetrahydroboratobis(cyclopentadienyl)titanium(III), K.M. Melmed, D. Coucouvanis and S. J. Lippard, 1973, Vol. 12, Issue 1, pp. 232-236
  6. \*Solid-state structure of  $\mu$ -bis(cyanotrihydroborato)-tetrakis(triphenylphosphine)dicopper (I), K.M. Melmed, J.J. Mayerle and S. J. Lippard, 1974, Vol. 96, Issue 1, pp. 69-75
  7. Preparation, properties, and structure of bis(cyanotrihydroborato)-1,1,4,7,7-pentamethyldiethylenetriaminecopper(II), B. G. Segal and S. J. Lippard, 1974, Vol. 13, Issue 4, pp 822-828
  8. Structure of  $\mu$ -decahydrodecaboratotetrakis(triphenylphosphine)dicopper(I)-chloroform. Bonding analogies between boron hydrides and nido-metalloboranes, J.T. Gill and S.J. Lippard, 1975, Vol.14, Issue 4, pp. 751-761
  9. Preparation, properties, and structure of di- $\mu$ -cyanotrihydroborato-bis(2,2',2''-triaminotriethylamine) dinickel(II) tetraphenylborate, B. G. Segal and S. J. Lippard, 1977, Vol. 16, Issue 7, pp 1623–1629
  10. Crystal and molecular structure of tris-(tetrahydroborato)tris-(tetrahydrofuran)yttrium(III), B.G. Segal and S.J. Lippard, 1978, Vol.17, Issue 4, pp. 844-850
- [100] V. D. Makhaev, Structural and dynamic properties of borohydride complexes, *Russian chemical reviews*, 2000, Vol. 69, pp. 727-746

- [101] D. Goerrig, 1960, German patent n<sup>o</sup>: 1,077,644
- [102] P. Mauron, Stability and reversibility of LiBH<sub>4</sub>, *Journal of Physical Chemistry B*, 2008, Vol. 112, pp. 906-910
- [103] O. Friedrichs, Direct synthesis of Li[BH<sub>4</sub>] and Li[BD<sub>4</sub>] from the elements, *Acta Materialia*, 2008, Vol. 56, Issue 5, pp. 949-954
- [104] H. I. Schlesinger *et al*, New Developments in the chemistry of diborane And Of The Borohydrides .7. The Preparation Of Other Borohydrides By Metathetical Reactions Utilizing The Alkali Metal Borohydrides, *Journal of The American Chemical Society*, 1953, Vol.75, Issue 1, pp. 209-213
- [105] K. Chlopek, Synthesis and properties of magnesium borohydride, Mg(BH<sub>4</sub>)<sub>2</sub>, *Journal of Materials Chemistry*, 2007, Vol. 17, Issue 33, pp. 3496-3503
- [106] P. Zanella, Facile high-yield synthesis of pure, crystalline Mg(BH<sub>4</sub>)<sub>2</sub>, *Inorganic Chemistry*, 2007, Vol. 46, pp. 9039-9041
- [107] V. I. Mikheeva and L.V. Titov, Calcium borohydride, *Russian Journal of Inorganic Chemistry*, 1964, Vol. 9, Issue 4, pp. 437-440
- [108] S. Narashimhan and R. Balakumar, Synthetic applications of zinc borohydride, *Aldrichimica Acta*, 1998, Vol. 31, Issue 1, pp. 19-26

- [109] S. Srinivasan, Effects of catalysts doping on the thermal decomposition behavior of  $\text{Zn}(\text{BH}_4)_2$ , *International Journal of Hydrogen Energy*, 2008, Vol. 33, Issue 9, pp. 2268
- [110] Scifinder Scholar Software subscribed by UCL Chemistry
- [111] G. Renaudin, Structural and spectroscopic studies on the alkali borohydrides  $\text{MBH}_4$  ( $\text{M} = \text{Na}, \text{K}, \text{Rb}, \text{Cs}$ ), *Journal of Alloys And Compounds*, 2004, Vol. 375, Issue 1-2, pp. 98-106
- [112] A. Zuttel, Borohydrides as new hydrogen storage materials, *Scripta Materialia*, 2007, Vol. 56, Issue 10, pp. 823-828
- [113] R. L. Davis, Structure of Sodium Tetradeuteroborate,  $\text{NaBD}_4$ , *Journal of Solid State Chemistry*, Vol. 9, Issue 3, pp. 393-396
- [114] P. Fischer, Order-disorder phase transition in  $\text{NaBD}_4$ , *European Powder Diffraction Conference (Epdic)* 8, 2004, Vol. 443-444, pp. 287-290
- [115] A. V. Talyzin, High pressure phase transition in  $\text{LiBH}_4$ , 2004, *Journal of Solid State Chemistry*, Vol. 180, pp. 510-517
- [116] Y. Filinchuk, High-pressure phase of  $\text{NaBH}_4$ : Crystal structure from synchrotron powder diffraction data, *Physical Review B*, 2007, Vol. 76, pp. 092104



- [117] Cw. Pistorius, Melting and polymorphism of  $\text{LiBH}_4$  to 45 Kbar, *Zeitschrift Fur Physikalische Chemie-Frankfurt (International Journal of Research in Physical Chemistry and Chemical Physics)*, Vol. 88, Issue 5-6, pp. 253-263
- [118] B. Sundqvist, Phase transitions in hydrogen storage compounds under pressure, *Journal of Physics - Condensed Matter*, Vol. 19, Issue 42, pp. 425201
- [119] V. N. Konoplev and V.M. Bakulina, Some properties of magnesium borohydride, *Izvestiya Akademii Nauk Sssr-Seriya Khimicheskaya (Russian Chemical Bulletin)*, 1971, Vol.20, pp. 136-138
- [120] J. H. Her, Structure of unsolvated magnesium borohydride  $\text{Mg}(\text{BH}_4)_2$ , *Acta Crystallographica, Section B-Structural Science*, 2007, Vol. 63, pp. 561-568
- [121] M. D. Riktor, In situ synchrotron diffraction studies of phase transitions and thermal decomposition of  $\text{Mg}(\text{BH}_4)_2$  and  $\text{Ca}(\text{BH}_4)_2$ , *Journal of Materials Chemistry*, 2007, Vol. 17, pp. 4939-4942
- [122] R. Cerny, Magnesium borohydride: Synthesis and crystal structure, *Angewandte Chemie-International Edition*, 2007, Vol. 46, Issue 30, pp. 5765-5767
- [123] N. S. Kedrova and N.N. Maltseva, Synthesis and properties of borohydrido-zincates of II group metals, *Russian Journal of Inorganic Chemistry*, 1977, Vol. 22, Issue 7, pp. 1791-1794

- [124] K. Miwa *et al*, Thermodynamical stability of calcium borohydride  $\text{Ca}(\text{BH}_4)_2$ , *Physical Review B*, 2006, Vol. 74, Issue 15, pp. 155122
- [125] Y. Filinchuk, E. Ronnebro and D. Chandra, Crystal structures and phase transformations in  $\text{Ca}(\text{BH}_4)_2$ , *Acta Materialia*, 2009, Vol. 57, Issue 3, pp. 732-738
- [126] S. Aldridge *et al*, Some borohydride derivatives of aluminium: Crystal structures of dimethylaluminium borohydride and the alpha and beta phases of aluminium tris(borohydride) at low temperature, *Journal of The Chemical Society-Dalton Transactions*, 1997, Issue 6, pp. 1007-1012
- [127] K. Miwa *et al*, First-principles study on thermodynamical stability of metal borohydrides: Aluminum borohydride  $\text{Al}(\text{BH}_4)_3$ , *Journal of Alloys And Compounds*, 2007, Vol. 446, pp.310-314
- [128] V. Barone *et al*, Transition metal borohydride complexes as catalysts 1. Non-empirical determination of static, dynamic, and chemical properties of the model Compounds  $\text{NaBH}_4$  and  $\text{AlH}_2\text{BH}_4$ , *Inorganic Chemistry*, 1981, Vol. 20, Issue 6, pp. 1687-1691
- [129] J. Seyden-Penne, Reductions by the alumino- and borohydrides in organic synthesis, *Wiley Chichester*, 2<sup>nd</sup> edition

- [130] J.A. Jensen *et al.*, Titanium, zirconium, and hafnium borohydrides as "tailored" CVD precursors for metal diboride thin films, *Journal of the American chemical society*, 1988, Vol. 110, Issue 5, pp. 1643-1644
- [131] A. Muller, 1980, US patent n<sup>o</sup>: 4,193,978
- [132] E. M. Fedneva, V.L. Alpatova, V.I. Mikheeva, Thermal stability of lithium borohydride, *Russian Journal of Inorganic Chemistry*, 1964, Vol. 9, Issue 6, pp. 826-827
- [133] D.S. Stasinevich, G.A. Egorenko, Thermographic investigation of alkali metal and magnesium borohydrides at pressures up to 10 am, *Russian Journal of Inorganic Chemistry*, 1968, Vol.13, Issue 3, pp. 341-343
- [134] Y. Nakamori, K. Miwa *et al.*, Correlation between thermodynamical stabilities of metal borohydrides and cation electronegativities: First-principles calculations and experiments, *Physical Review B*, 2006, Vol. 74, pp. 045126
- [135] A. Züttel, P. Wenger *et al.*, LiBH<sub>4</sub> a new hydrogen storage material, *Journal of Power Sources*, 2003, Vol. 118, Issue 1-2, pp. 1-7
- [136] M. Au and A. Jurgensen, Modified lithium borohydrides for reversible hydrogen storage, *Journal of Physical Chemistry B*, 2006, Vol. 110, Issue 13, pp. 7062-7067

- [137] J. J. Vajo, S. L. Skeith *et al.*, Reversible storage of hydrogen in destabilized  $\text{LiBH}_4$ , *Journal of Physical Chemistry B*, 2005, Vol. 109, Issue 9, pp. 3719-3722
- [138] X.D. Kang *et al.*, Reversible hydrogen storage in  $\text{LiBH}_4$  destabilised by milling with Al, 2007, Vol. 89, pp. 963-966
- [139] Z.Z. Fang, X.D. Kang *et al.*, Reversible dehydrogenation of  $\text{LiBH}_4$  catalyzed by as-prepared single-walled carbon nanotubes, *Scripta Materialia*, 2008, Vol. 58, pp. 922-925
- [140] M. Au and R.T. Walters, Reversibility aspect of lithium borohydrides, *International Journal of Hydrogen Energy*, 2010, Vol. 335, p. 10311-10316
- [141] Y. Nakamori and S. Orimo, Destabilization of Li-based complex hydrides, *Journal of Alloys and Compounds*, 2004, Vol. 370, Issues 1-2, pp. 271-275
- [142] E. Ronnebro and E.H. Majzoub, Calcium borohydride for hydrogen storage: catalysis and reversibility, *Journal of Physical Chemistry B*, 2007, Vol. 111, Issue 42, pp. 12045-12047
- [143] M.D. Riktor *et al.*, The identification of a hitherto unknown intermediate phase  $\text{CaB}_2\text{H}_x$  from decomposition of  $\text{Ca}(\text{BH}_4)_2$ , *Journal of Materials Chemistry*, 2009, Vol. 19, pp. 2754-2759

- [144] T.J. Frankcombe, Calcium borohydride for hydrogen storage: a computational study of  $\text{Ca}(\text{BH}_4)_2$  crystal structures and the  $\text{CaB}_2\text{H}_x$  intermediate, *Journal of Physical Chemistry C*, 2010, Vol. 114, Issue 20, pp. 9503-9509
- [145] L.L. Wang *et al.*, On the reversibility of hydrogen storage reactions in  $\text{Ca}(\text{BH}_4)_2$ : characterization via experiment and theory, *Journal of Physical Chemistry C*, 2009, Vol. 113, Issue 46, pp. 20088-20096
- [146] J. Mao *et al.*, Study on the dehydrogenation kinetics and thermodynamics of  $\text{Ca}(\text{BH}_4)_2$ , *Journal of Alloys and Compounds*, 2010, Vol. 500, Issue 2, pp. 200-205
- [147] J.-H. Kim *et al.*, Thermal decomposition behavior of calcium borohydride  $\text{Ca}(\text{BH}_4)_2$ , *Journal of Alloys and Compounds*, 2008, Vol. 461, Issues 1-2, pp. L20-L22
- [148] J.-H. Kim *et al.*, Reversible hydrogen storage in calcium borohydride  $\text{Ca}(\text{BH}_4)_2$ , *Scripta Materialia*, 2008, Vol. 58, Issue 6, pp. 481-483
- [149] H.W. Li *et al.*, Formation of an intermediate compound with a  $\text{B}_{12}\text{H}_{12}$  cluster: experimental and theoretical studies on magnesium borohydride  $\text{Mg}(\text{BH}_4)_2$ , *Nanotechnology*, 2009, Vol. 20, pp. 204013
- [150] G.L. Soloveichik, Y. Gao, J. Rijssenbeek, M. Andrus, S. Kniajanski, R.C. Bowman and S.J. Hwan, Magnesium borohydride as a hydrogen storage material:

properties and dehydrogenation pathway of unsolvated  $\text{Mg}(\text{BH}_4)_2$ , *International Journal of Hydrogen Energy*, 2009, Vol. 34, Issue 2, pp. 916-928

[151] G. Severa *et al*, Direct Hydrogenation Magnesium Boride to Magnesium Borohydride: Demonstration of >11 Weight Percent Reversible Hydrogen Storage, *Chemical Communications*, 2010, Vol. 46, Issue 3, pp. 421-423

[152] S.G. Shore and R.W. Parry, The crystalline compound ammonia-borane  $\text{H}_3\text{NBH}_3$ , *Journal of American Chemical Society*, 1955, Vol. 77, pp. 6084-6085

[153] S.G. Shore and R.W. Parry, Chemical evidence for the structure of the “diammoniate of diborane”. II. The preparation of ammonia-borane, *Journal of American Chemical Society*, 1958, Vol. 80, pp. 8-12

[154] S.G. Shore and R.W. Parry, Chemical evidence for the structure of the “diammoniate of diborane”. III. The reactions of borohydride salts with lithium halides and aluminium chloride, *Journal of American Chemical Society*, 1958, Vol. 80, pp. 12-15

[155] S.G. Shore, P. R. Girardot and R.W. Parry, Chemical evidence for the structure of the “diammoniate of diborane”. V. A tracer study of the reaction between sodium and the “diammoniate of diborane”, *Journal of American Chemical Society*, 1958, Vol. 80, pp. 20-24

- [156] D.J. Heldebrant *et al*, Synthesis of ammonia borane for hydrogen storage applications, *Energy and Environmental Science*, 2008, Vol. 1, pp. 156-160
- [157] F.H. Stephens *et.al.*, Ammonia-borane: the hydrogen source par excellence?, *Dalton transactions*, 2007, pp. 2613-2626
- [158] C.W. Hamilton, R.T. Baker *et al*, BN compounds for chemical hydrogen storage, *Chemical Society Reviews*, 2009, Vol. 38, pp. 279-293
- [159] P. Wang and X. Kang, Hydrogen-rich boron-containing materials for hydrogen storage, *Dalton Transactions*, 2008, pp. 5400-5413
- [160] G. W. Schaeffer, R. Schaeffer and H. I. Schlesinger, The preparation of Borazole and its reactions with boron halides , *Journal of American Chemical Society*, 1951, Vol. 73, pp. 1612-1614
- [161] V. I. Mikheeva and V. Yu Markina, Synthesis of Borazole by the reaction between lithium borohydride and ammonium chloride, *Russian Journal of Inorganic chemistry*, 1956, Vol. 1, Issue 12, pp. 2700-2707
- [162] V. V. Volkov, G. I. Bagryantsev and K.G. Myakishev, Preparation of borazine by the reaction of sodium tetrahydroborate with ammonium chloride, *Russian Journal of Inorganic chemistry*, 1970, Vol. 15, Issue 11, pp. 1510-1513

- [163] M.G. Hu, R.A. Geanangel and W.W. Wendlandt, The thermal decomposition of ammonia borane, *Thermochimica Acta*, 1978, Vol. 23, Issue 2, pp. 249-255
- [164] R.W. Parry and S.G. Shore, Chemical evidence for the structure of the “diammoniate of diborane”. IV. The reaction of sodium with Lewis acids in liquid ammonia, *Journal of American Chemical Society*, 1958, Vol. 80, pp. 16-19
- [165] S. G. Shore and K.W. Boddeker, Large scale synthesis of  $\text{H}_2\text{B}(\text{NH}_3)_2^+\text{BH}_4^-$  and  $\text{H}_3\text{NBH}_3$ , *Inorganic Chemistry*, 1964, Vol. 3, pp. 914-915
- [166] M. Bowden *et al.*, The diammoniate of diborane: crystal structure and hydrogen release, *Chemical Communications*, 2010, Vol. 46, pp. 8564-8566
- [167] G. Wolf *et al.*, Calorimetric process monitoring of thermal decomposition of B-N-H compounds, *Thermochimica Acta*, 2000, Vol. 343, pp. 19-25
- [168] N.C. Smythe and J.C. Gordon, Ammonia borane as a hydrogen carrier: dehydrogenation and regeneration, *European Journal of Inorganic Chemistry*, 2010, Issue 4, pp. 509-521

### **Chapter 3: Experimental methods**

- [169] G. Widmann, Manual for users of Mettler Toledo thermal analysis systems, 2001



- [170] S. Orimo *et al*, Experimental studies on intermediate compound of  $\text{LiBH}_4$ , *Applied Physics Letters*, 2006, Vol. 89, pp. 021920
- [171] B.J. Zhang and B.H. Liu, Hydrogen desorption from  $\text{LiBH}_4$  destabilised by chlorides of transition metal Fe, Co, and Ni, *International Journal of Hydrogen Energy*, 2010, Vol. 35, Issue 14, pp. 7288-7294
- [172] Z-Z. Fang, X-D. Kang and P. Wang, Improved hydrogen storage properties of  $\text{LiBH}_4$  by mechanical milling with various carbon additives, *International Journal of Hydrogen Energy*, 2010, Vol. 35, Issue 14, pp. 8247-8252
- [173] J.Y. Lee *et al*, Metal halide doped metal borohydrides for hydrogen storage: the case of  $\text{Ca}(\text{BH}_4)_2\text{-CaX}_2$  ( $\text{X}=\text{F}, \text{Cl}$ ) mixture, *Journal of Alloys and Compounds*, 2010, Vol. 506, Issue 2, pp. 721-727

#### **Chapter 4: Results**

- [174] H.-W. Li *et al.*, Materials designing of metal borohydrides: Viewpoints from thermodynamical stabilities, *Journal of Alloys and Compounds*, 2007, Vol. 446-447, pp. 315-318
- [175] L. Pauling, The nature of the chemical bond. IV. The energy of single bonds and the relative electronegativity of atoms, *Journal of the American Chemical Society*, 1932, Vol. 54, Issue 9, pp. 3570-3582
- [176] L. Pauling, Nature of the Chemical Bond, Cornell University Press, 1960, pp. 88–107, ISBN 0801403332

---

**Chapter 5: General Discussion**

- [177] A. Zuttel et al, Hydrogen density in nanostructured carbon, metals and complex materials, *Materials Science and Engineering B*, 2004, Vol. 108, pp. 9 -18
- [178] S. Gomes et al, x, *Journal of Alloys and Compounds*, 2002, Vol. 346, pp. 206-x
- [179] J-Ph. Soulie et al, x, *Journal of Alloys and Compounds*, 2002, Vol. 346, pp. 200-x
- [180] H. Hagemann et al, x, *Journal of Alloys and Compounds*, 2004, Vol. 363, pp. 129-x
- [181] S.K. Callear et al, Order and disorder in  $\text{LiBH}_4$ , *Journal of Materials Science*, 2010, Vol. 46, Issue 2, pp. 566-569
- [182] P. Martelli et al,  $\text{BH}_4^-$  self-diffusion in liquid  $\text{LiBH}_4$ , *Journal of Physical Chemistry C*, 2010, Vol. 114, Issue 37, pp. 10117-10121
- [183] J. Kotska et al, Diborane release from  $\text{LiBH}_4$ /silica gel mixtures and the effect of additives, *Journal of Physical Chemistry C*, 2007, Vol. 111, pp. 14026-14029

- [184] J.K. Kang et al, A candidate  $\text{LiBH}_4$  for hydrogen storage: crystal structures and reaction mechanisms of intermediate phases, *Applied Physics Letters*, 2005, Vol. 87, Issue 11, pp. 111904-111906
- [185] N. Ohba et al, First principles study on the stability of intermediate compounds of  $\text{LiBH}_4$ , *Physical Review B*, Vol. 74, Issue 7, pp. 075110
- [186] J-H. Her et al, Crystal structure of  $\text{Li}_2\text{B}_{12}\text{H}_{12}$ : a possible intermediate species in the decomposition of  $\text{LiBH}_4$ , *Inorganic Chemistry*, 2008, Vol. 47, pp. 9757-9759
- [187] O. Friedrichs et al, A role of  $\text{Li}_2\text{B}_{12}\text{H}_{12}$  for the formation and decomposition of  $\text{LiBH}_4$ , *Chemical materials*, 2009, Vol. 22, pp. 3265-3268
- [188] Material Safety Data Sheet of pure diborane
- [189] K.C. Kim et al, Predicting impurity gases and phases during hydrogen evolution from complex metal hydrides using free minimization enabled by first-principles calculations, *Physical Chemistry Chemical Physics*, 2010, Vol. 12, pp. 9918-9926
- [190] W.B. Jensen, The place of zinc, cadmium and mercury in the periodic table. *Journal of Chemical Education*, 2003, Vol. 80, Issue 8, pp. 952-961

- [191] M. Au et al, Stability and reversibility of lithium borohydrides doped by metal halides and hydrides, *Journal of Physical Chemistry C*, 2008, Vol. 112, Issue 47, pp. 18661-18671
- [192] E. Jeon and YW. Cho, mechanochemical synthesis and thermal decomposition of zinc borohydride, *Journal of Alloys and Compounds*, 2006, Vol. 273-275, p.422-xxx
- [193] D.A. Lesch et al, Discovery of Novel complex metal hydrides for hydrogen storage through molecular modelling and combinatorial methods, *FY 2007 Annual Progress Report, DOE Hydrogen Program*, pp.345-349
- [194] L. Moosegard et al, Reactivity of  $\text{LiBH}_4$ : In situ synchrotron powder X-Ray Diffraction study, *Journal of Physical Chemistry C*, 2008, Vol. 112, pp. 1299-1303
- [195] L.M. Arnberg et al, Structure and dynamics for  $\text{LiBH}_4$ - $\text{LiCl}$  solid solutions, *Chemical Materials*, 2009, Vol. 21, pp. 5772-5782
- [196] Z.Z. Fang et al, In situ formation and rapid decomposition of  $\text{Ti}(\text{BH}_4)_3$  by mechanical milling  $\text{LiBH}_4$  with  $\text{TiF}_3$ , *Applied Physics Letters*, 2009, Vol. 94, pp. 044104

- [197] H.R. Hoekstra and J.J. Katz, The preparation and properties of the Group IV-B metal borohydrides, *Journal of American Chemical Society*, 1949, Vol. 71, pp. 2488-2492
- [198] S.E. Kravchenko et al, Preparation of titanium diboride nanopowder, *Inorganic Materials*, 2010, Vol. 46, Issue 6, pp. 614-616
- [199] J.W. Kim et al, Mechanochemical synthesis and characterisation of TiB<sub>2</sub> and VB<sub>2</sub> nanopowders, *Materials Letters*, 2008, Vol. 62, pp. 2461-2464
- [200] B. J. Zhang and B.H. Liu, Hydrogen desorption from LiBH<sub>4</sub> destabilised by chlorides of transition metal Fe, Co and Ni, *International Journal of Hydrogen Energy*, 2010, Vol. 35, pp. 7288-7294
- [201] H.C. Brown and C.A. Brown, New highly active metal catalysts for the hydrolysis of borohydride, *Journal of American Chemical Society*, 1962, Vol. 84, pp. 1493-1494
- [202] N.T. Kuznetsov et al, Thermal reactions of alkaline metal borohydrides: synthesis of borides, *Journal of The Less Common Metals*, 1986, Vol. 117, Issues 1-2, pp. 41-44
- [203] V.V. Volkov et al, Interaction of chromium trichloride with tetrahydroborates of alkali-metals, *Russian Journal of Inorganic Chemistry*, 1985, Vol. 30, Issue 3, pp. 593-597

- [204] V.I. Mikheeva et al, Preparation and properties of zinc tetrahydridoborate and some of its derivatives, *Russian Journal of Inorganic Chemistry*, 1979, Vol. 24, Issue 2, pp. 408-413
- [205] N.N. Maltseva et al, Synthesis of zinc borohydride and its derivatives by mechanoactivation of mixtures of alkali-metal borohydrides with zinc chloride, *Russian Journal of Inorganic Chemistry*, 1989, Vol. 34, Issue 6, pp. 1430-1434
- [206] V.V. Volkov and K.G. Myakishev, Synthesis of Titanium (III) tetrahydroborate from  $\text{TiCl}_3$  and  $\text{LiBH}_4$ , *Bulletin of the Institute of Inorganic Chemistry, Siberian Division, Academy of Sciences of the USSR, Division of Chemical Science*, 1987, Vol. 36, Issue 2, p. 1321
- [207] V.V. Volkov and K.G. Myakishev, Mechanochemical Technology of borane Compounds and Their Application, *Chemistry for Sustainable Development*, 2002, Vol. 10, pp. 221-233
- [208] A. Karkamkar et al., Thermodynamic and structural investigations of ammonium borohydride, a solid with a highest content of thermodynamically and kinetically accessible hydrogen, *Chemistry of Materials*, 2009, Vol. 21, Issue 19, pp. 4356-4358
- [209] Z. Xiong et al., High-capacity hydrogen storage in lithium and sodium amidoboranes, *Letters to Nature Materials*, 2008, Vol. 7, pp. 138-141
- [210] D.J. Heldebrant et al., The effects of chemical additives on the induction phase in solid-state thermal decomposition of ammonia borane, *Chemistry of Materials*, 2008, Vol. 20, Issue 16, pp. 5332-5336

## WEB REFERENCES

## Chapter 1: General Introduction

- [Web 1] <http://www.eia.doe.gov>
- [Web 2] [http://ec.europa.eu/research/energy/pdf/hydrogen-report\\_en.pdf](http://ec.europa.eu/research/energy/pdf/hydrogen-report_en.pdf)
- [Web 3] <http://www.hydrogenambassadors.com/background/worldwide-hydrogen-production-analysis.php>
- [Web 4] National Hydrogen Association:  
<http://www.hydrogenassociation.org/general/faqs.asp#howmuchproduced>
- [Web 5] Wikipedia article on Hydrogen Production :  
[http://en.wikipedia.org/wiki/Hydrogen\\_production](http://en.wikipedia.org/wiki/Hydrogen_production)
- [Web 6] Wikipedia article on Electrolysis of water:  
[http://en.wikipedia.org/wiki/Electrolysis\\_of\\_water](http://en.wikipedia.org/wiki/Electrolysis_of_water)
- [Web 7] Wikipedia article on Hydrogen Economy:  
[http://en.wikipedia.org/wiki/Hydrogen\\_economy](http://en.wikipedia.org/wiki/Hydrogen_economy)
- [Web 8] Article on the Global Energy Network Institute (GENI) website:  
<http://www.geni.org/library>
- [Web 9] Wikipedia article on Fuel Cell: [http://en.wikipedia.org/Fuel\\_cell](http://en.wikipedia.org/Fuel_cell)
- [Web 10] Wikipedia article on Fuel Cell cars:  
[http://en.wikipedia.org/List\\_of\\_fuel\\_cell\\_vehicles](http://en.wikipedia.org/List_of_fuel_cell_vehicles)
- [Web 11] TFL corporate article on Hydrogen vehicles:  
<http://www.tfl.gov.uk/corporate/projectsandschemes/environment/8444.aspx>
- [Web 12] BBC article on Hydrogen Black cabs:  
<http://www.bbc.co.uk/news/business-10836132>

[Web 13] UK SHEC consortium website: <http://www.uk-shec.org.uk>

## Chapter 2: Literature review

[Web 14] [http://www.eere.energy.gov/hydrogenandfuelcells/pdfs/freedomcar\\_targets\\_explanations.pdf](http://www.eere.energy.gov/hydrogenandfuelcells/pdfs/freedomcar_targets_explanations.pdf)

[Web 15] The IEA HIA website : <http://www.iehia.org>

[Web 16] <http://automobiles.honda.com/fcx-clarity/>

[Web 17] Wikipedia article on Hydrogen Storage:  
[http://en.wikipedia.org/wiki/Hydrogen\\_storage](http://en.wikipedia.org/wiki/Hydrogen_storage)

[Web 18] J. Shelby and M. Hall, Glass microspheres for hydrogen storage, May 25, 2005: [http://www.hydrogen.energy.gov/pdfs/review05/stp\\_47\\_hall.pdf](http://www.hydrogen.energy.gov/pdfs/review05/stp_47_hall.pdf)

[Web 19] Andrew Haaland, High-pressure conformable hydrogen storage for fuel-cell vehicles, Proceedings of the 2000 Hydrogen Program Review,  
<http://www1.eere.energy.gov/hydrogenandfuelcells/pdfs/28890cc.pdf>

[Web 20] Conformable tanks,  
<http://www1.eere.energy.gov/hydrogenandfuelcells/storage/basics.html>

[Web 21] Liquid Hydrogen tanks,  
[http://www1.eere.energy.gov/hydrogenandfuelcells/storage/hydrogen\\_storage.html](http://www1.eere.energy.gov/hydrogenandfuelcells/storage/hydrogen_storage.html)

[Web 22] BMW website section on Hydrogen 7:  
[http://www.bmw.com/com/en/insights/technology/efficient\\_dynamics/phase\\_2/clean\\_energy/bmw\\_hydrogen\\_7.html](http://www.bmw.com/com/en/insights/technology/efficient_dynamics/phase_2/clean_energy/bmw_hydrogen_7.html)

[Web 23] Current status of hydrogen technologies on the DOE website:  
[http://www.eere.energy.gov/hydrogenandfuelcells/pdfs/freedomcar\\_targets\\_explanations.pdf](http://www.eere.energy.gov/hydrogenandfuelcells/pdfs/freedomcar_targets_explanations.pdf)



- [Web 24] D. Brampton, e-thesis, University of Birmingham
- [Web 25] H.W. Li *et al*, Improved hydrogen storage properties of magnesium borohydride  $\text{Mg}(\text{BH}_4)_2$  with additives, Online poster version:  
[http://nsm.raunvis.hi.is/~nsm/abstracts/M1-ydrBulk%2091/Poster/lihw\\_imr.tohoku.ac.jp.pdf](http://nsm.raunvis.hi.is/~nsm/abstracts/M1-ydrBulk%2091/Poster/lihw_imr.tohoku.ac.jp.pdf)

### **Chapter 3: Experimental methods**

- [Web 26] Sigma Aldrich website [www.sigma-aldrich.com](http://www.sigma-aldrich.com)
- [Web 27] <http://www.hkbu.edu.hk/~matsci/thermoanal/thermoanal.htm>
- [Web 28] <http://www.anasys.co.uk/library/dsc2.htm>
- [Web 29] <http://www.chemguide.co.uk/analysis/masspec/howitworks.html>
- [Web 30] <http://www.pemtron.com/eng/page.php?Main=3&sub=3>
- [Web 31] <http://www.chem.orst.edu/courses/ch361-464/ch362/irinstrs.htm>

### **Chapter 4: Results**

- [Web 32] [http://sfscience.files.wordpress.com/2011/03/periodic\\_table.gif](http://sfscience.files.wordpress.com/2011/03/periodic_table.gif)
- [Web 33] <http://en.wikipedia.org/wiki/Electronegativity>